PROCESSING OF SIGNALS IN THE PERIPHERAL AUDITORY SYSTEM IN RELATION TO AURAL PERCEPTION

a thesis submitted
for the degree of doctor of philosophy
of the university of London
by

Paul Antony Lynn
BSc(Eng.), ACGI

department of electrical engineering
imperial college of science and technology
London SW7

january 1969

ABSTRACT

This work is concerned with the nature of amplitude coding in the cochlea and, in particular, with the main perceptual effects of interaural amplitude difference in binaural hearing. After an initial review of aspects of cochlear structure and function, some new binaural listening experiments are described. These utilise single and double acoustic pulse trains, filtered to eliminate confusion caused by multiple binaural images. It is concluded that the major perceptual effects can be explained if the temporal centre of gravity of neural responses, ensemble-averaged over many neural units in the relevant cochlear region, is assessed in auditory perception. Quantitative support for this view is available if neural activity recorded in the cat is paralleled in the human.

It is thus argued that fine details of the peripheral neural response are closely related to aural perception phenomena. Existing models of the cochlear neural transduction have been found inadequate for the description of such details, and new models are therefore proposed and studied.

Digital computer simulations of stochastic threshold systems and of the superposition of a number of random point sequences suggest that the statistics of spontaneous activity in eighth nerve fibres may be most satisfactorily explained on the latter basis; the possible causes of such an effect are explored. Electrical and chemical transmitter models of stimulated activity at the single afferent hair cell synapse are then investigated, in an attempt to

reproduce the neural responses of interest. The difficulties of such an approach suggest a further proposition, which specifies a controlling action by outer hair cells and spiral afferent fibres on radial afferent fibre activity. This scheme receives support both from recent anatomical evidence and from digital computer studies, and suggests the importance of the cochlear innervation pattern in peripheral signal processing.

CONTENTS

	Page No.
Acknowledgements	8
1. INTRODUCTION	9
2. A BRIEF REVIEW OF COCHLEAR STRUCTURE AND FUNCTION	
2.1 Mechanical properties of the ear.	13
2.2 The effective stimulus for the hair cells of the organ of Corti.	16
2.3 Cochlear hair cell arrangement and structure	18
2.4 Electric potentials of the cochlea.	22
2.5 Cochlear innervation.	25
2.6 The hair cell-nerve ending junction.	29
2.7 Activity in first order auditory neurons in cat.	
2.7.1. Recordings of spontaneous activity.	33
2.7.2. Driven activity.	36
2.7.3. Statistical analysis.	42
2.8 Discussion.	47
3. ASPECTS OF AUDITORY PERCEPTION	
3.1 Review of some binaural listening phenomena.	51
3.2 Further problems in binaural listening; interaural amplitude difference (IAD).	55
3.3 Time-intensity trading: experimental results	57
3.4 A proposition about amplitude effects.	60
3.5 Further discussion.	67
4. PREVIOUS MODELLING OF THE PERIPHERAL AUDITORY SYSTEM	
4.1 van Bergeijk: model of cochlear spiral innervation.	70
4.2 Siebert and Gray: analysis of nonstationary neural activity.	71

4. (continued) Page No.

4.3 Weiss: a model of the peripheral auditory system. 73

4.3.1. Spontaneous activity. 75

4.3.2. Response to stimuli. 76

4.4 Geisler: neural responses to pure tones. 78

4.5 Discussion. 79

5. MODELS FOR THE SPONTANEOUS ACTIVITY OF COCHLEAR NERVE FIBRES

5.1 Introductory comments. 83

5.2 Previous chemical models for random neural activity.

5.2.1. Stein's model 86

5.2.2. Gerstein and Mandelbrot's random walk model. 89

5.2.3. Fetz and Gerstein: digital computer simulations. 91

5.3 New modelling of spontaneous synaptic activity.

5.3.1. Theoretical analysis by Johannesma. 92

5.3.2. Comments on Johannesma's analysis. 96

5.3.3. Computer simulation of Johannesma's model. 98

5.3.4. Comparisons between analysis and simulation. 102

5.3.5. Applicability of the model to spontaneous activity in first order auditory neurons. 115

5.4 Cochlear innervation and spontaneous neural activity.

5.4.1. A proposition. 120

5.4.2. Computer simulations and results. 124

5.5 Discussion. 131

6. BASILAR MEMBRANE ACTIVITY AND PERIPHERAL AUDITORY PROCESSING

6.1 Calculation of basilar membrane response.

6.1.1. Computer programme. 134

6. (continued) Page No.

6.1.2. Results. 137

6.2 Signal processing by cochlear nerve fibres.

6.2.1. Introductory comments. 144

6.2.2. Computer simulation of spiral cochlear fibres. 146

6.2.3. Results. 148

6.2.4. Discussion. 152

7. ELECTRICAL MODELS FOR COCHLEAR NEURAL TRANSDUCTION

7.1 Electrical synaptic transmission. 156

7.2 Nonlinear effects in nerve. 159

7.3 Lewis' electronic model of nerve membrane.

7.3.1. General description. 161

7.3.2. Response of the model to voltage clamps. 163

7.3.3. Detailed circuit operation. 166

7.4 The ionic theory in relation to cochlear neural transduction. 169

7.5 Discussion. 175

8. CHEMICAL TRANSMITTER MODELS FOR COCHLEAR NEURAL TRANSDUCTION

8.1 Introductory comments. 176

8.2 Evidence from other chemical synaptic systems 178

8.3 Digital computer simulations.

8.3.1. Simple relationships between stimulus and chemical release. 181

8.3.2. More complex effects. 190

8.4 Discussion. 200

9. STIMULATED NEURAL ACTIVITY AND COCHLEAR INNERVATION

9.1 A proposition. 202

9.2 Filtering properties of spiral cochlear fibres 207

9.3 Digital computer simulations 211

9. (continued) Page No.

9.4 Discussion. 218

10. DISCUSSION AND CONCLUSIONS

10.1 Modelling the peripheral auditory system; a reappraisal. 225

10.2 The significance of time-intensity trading in binaural listening. 230

10.3 The prediction of effects due to more complex acoustic signals; suggestions for further work. 240

11. A FINAL REVIEW 250

APPENDIX A 259

BIBLIOGRAPHY 264

ACKNOWLEDGEMENTS

I wish to acknowledge with gratitude the advice and encouragement of my supervisor, Professor B.McA. Sayers, and also to express appreciation of the friendly and purposeful atmosphere in the Engineering in Medicine Section of the Electrical Engineering Department at Imperial College.

Amongst others who have helped me during the course of research described here, my special thanks are due to P.I. Johannesma, of the University of Nijmegen in Holland, who, during a year's work at Imperial College, introduced me to many concepts in neural modelling. Not least I am grateful for the many interesting discussions which arose out of his theoretical studies of stationary neural activity, without which much of Section 5 of this work would not have been written.

I also wish to record with thanks the help of R.F.N. Curry who, during a final-year undergraduate project, assisted with some of the binaural listening experiments reported in Section 3.

Finally, I gratefully acknowledge permission granted by the following publishers and authors for the reproduction of various figures, for inclusion in this work:-

McGraw Hill Publications, London, W.1.: Figures 1, 2.

Almqvist and Wiksell, Stockholm: Figures 5, 6, 8, 9.

Journal of Laryngology and Otology, London, W.C.2.: Figure 7.

MIT Press, Cambridge, Mass., U.S.A.: Figures 10, 11, 12, 13, 14.

Dr. P.R. Gray: Figures 15, 16, 17, 18.

Mr. D. Stagg: Figure 43.

1. Introduction

Recent advances in the understanding of peripheral auditory processes stem from research in a number of parallel fields. Most obviously, such techniques as electron microscopy and chemical staining have permitted more and more accurate anatomical descriptions of the inner ear, although the relationships between structure and function have always been much more problematical. However, the relatively recent work of von Békésy[1] in measuring the mechanical properties of the basilar membrane in the cochlea of several species has greatly clarified the situation. Partly as a result of such work it is possible to claim that the main aspects of signal processing by the mechanical structures of the mammalian ear are now quantitatively understood. Further confidence in this claim is possible because of advances in the closely-related field of electrophysiology; in the last five years or so it has become feasible to measure the discharges of single nerve fibres in the auditory nerve of anaesthetised animals, and there are striking parallels between such records and the presumed vibrations of the basilar membrane (calculated on the basis of von Békésy's data). It therefore seems probable that to deny the quantitative evidence on the mechanical filtering properties of the mammalian cochlea is also to challenge a considerable body of supporting electrophysiological evidence. The other disciplines which have been increasingly brought to bear on the study of the ear in recent years are those which fall under the heading of communications engineering; these include signal analysis and statistics, electronic circuits and computer techniques, all

of which have contributed significantly to auditory research.

Now that the main mechanical properties of the mammalian ear have been quantitatively investigated and the broad features of the neural transduction from mechanical vibration to neural firing patterns clarified, much research tends to be concentrated on the higher centres of the auditory pathway. Such work is indeed vital to further understanding of the hearing process, but there are important reasons for continuing study of the peripheral system. Firstly, the nature of the cochlear neural transduction is only understood in the broadest terms, and there is little information about the detailed roles played by the various cells and structures of the organ of Corti. This matter is of great interest not only in its own right, but also because it almost certainly reflects importantly on other sensory receptor systems. Also, without a quantitative description of the transduction process it is difficult to appreciate the extent of signal processing in the peripheral system, or adequately to specify the signals which form inputs to the higher centres. Finally there is evidence that cochlear mechanics and transduction are closely involved in certain detailed aspects of aural perception, and it seems important to explore the matter as thoroughly as possible.

One of the most powerful ways of examining the relationships between peripheral auditory mechanisms and sound perception is by binaural listening experiments, in which use is made of a subject's ability to fuse the acoustic images from the two ears into one intracranial image having spatial properties. In the normal hearing environment this ability

allows a listener to assign directional properties to a sound and to discriminate effectively between two spatially-separated sources. The subjective spatial properties of such binaural images may be explored by objective measurements, and it is possible to relate some of the results of carefully devised listening experiments to cochlear mechanisms, if some simple assumptions are made about the overall nature of the neural transduction process, and about the fusion of neural signals from the two ears which must occur in higher centres of the brain.

On the other hand there are some important unanswered questions; one of these concerns the effects of interaural amplitude difference (IAD) in binaural listening and the way in which this affects the perceived position of fused binaural images. If it could be shown that the main effects of IAD may be accounted for in terms of cochlear mechanisms, this would help to clarify the way in which signal amplitude is coded at the periphery. This is not such a straightforward issue as it might appear. It seems quite clear from listening experiments that signal amplitude is not only coded in terms of (say) the firing rates of a variable population of responding neurons, but that there is a complex interaction between intensity and latency of neural response in the individual ear. Such effects may usefully be explored in binaural listening experiments, thereby reflecting the fact that binaural phenomena are not only important in their own right but can also give valuable clues to the monaural situation. It is indeed often convenient to regard the signal presented to one ear (and the neural activity arising from it) as a probe

with which to explore the effects of parameter changes in a signal applied to the other, by investigating the subjective properties of the resulting fused image.

There are other important points needing clarification, such as the extent to which signals are transformed by the cochlear transducer and by the distinctive pattern of nerve fibre termination. Furthermore, if significant processing is occurring in these regions, it may be possible to explain it in terms of known physiological mechanisms. These are questions which have not so far been quantitatively investigated in the literature, although it is possible that there are clues in published neurophysiological recordings from experimental animals. Such matters form the main material of the present work.

2. A BRIEF REVIEW OF COCHLEAR STRUCTURE AND FUNCTION

2.1 Mechanical properties of the ear

The characteristics of sound transmission through the outer and middle ear, and the subsequent vibrations of the cochlear partition, have been quantitatively investigated. In particular, the work of von Békésy[1] in measuring the frequency response of the mammalian cochlea has been widely reviewed and discussed, and it seems fair to claim that signal processing by the mechanical structures of the ear is now well understood (for example, see reviews by Weiss[67] or, in more detail, Sayers[54] or Whitfield[71]). Briefly, von Békésy succeeded in measuring the response of the basilar membrane to sinusoidal inputs of displacement at the oval window, for several species including man, and showed that the membrane behaves as a graded mechanical filter. Any one membrane point shows a broadly peaked response curve of displacement amplitude with frequency, as shown in Figure 1. Conversely, the magnitude of the membrane displacement at any one frequency, as a function of distance from the stapes, is also a peaked curve, with the phase lag increasing more or less linearly with distance (see Figure 2).

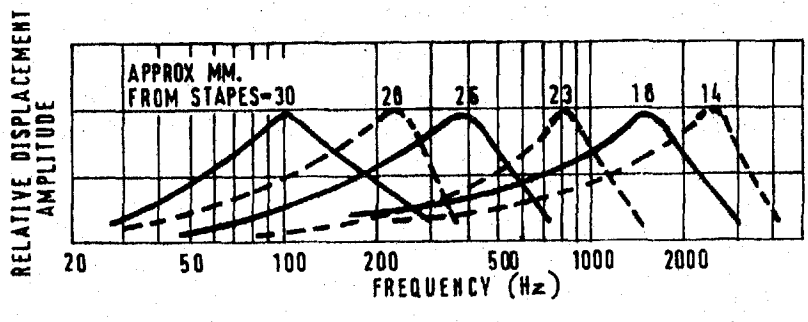

Figure 1. Relative amplitude of membrane displacement as a function of frequency, for different points along the basilar membrane. The stapes is driven with constant displacement amplitude (after Békésy[1]).

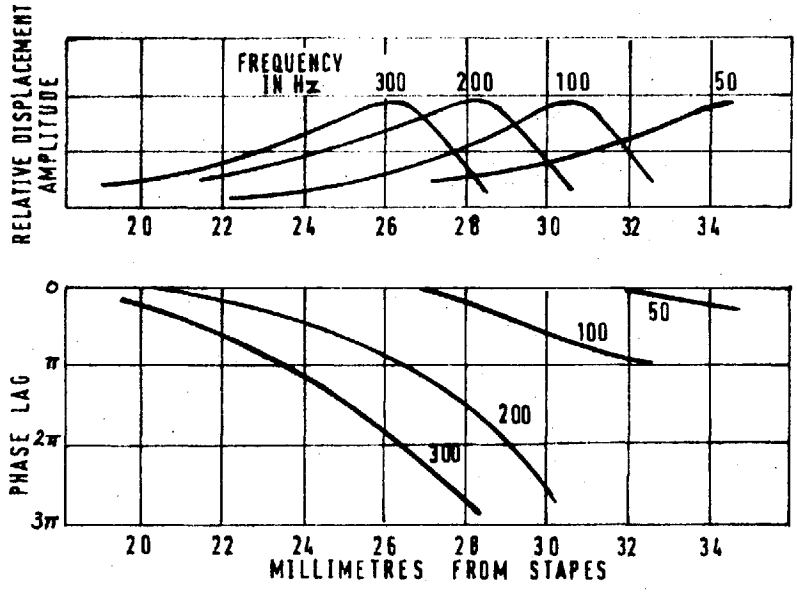

Figure 2. Relative amplitude and phase of basilar membrane displacement as a function of distance from the stapes (after Békésy[1]).

From such results it appears that the basilar membrane performs an initial frequency analysis of acoustic signals, in which high and low frequency components are optimally represented in basal and apical cochlear regions respectively. Such filtering action causes any wideband signal to be arrayed along the length of the cochlear partition, and is now seen as an elaborate first step in the peripheral processing.

From this original data, Flanagan[16] obtained analytic expressions for the response of the basilar membrane to an impulsive stimulus at the oval window, using the Fourier Transform technique. This derived impulse response, for any one point on the membrane, has the form of a decaying oscillation as shown in Figure 3, with the period of oscillation closely equal to the inverse of the characteristic frequency (C.F.) of the point considered. This frequency is the sinusoid frequency to which the point on the membrane responds

maximally, already indicated by the tuning curves of Figure 1.

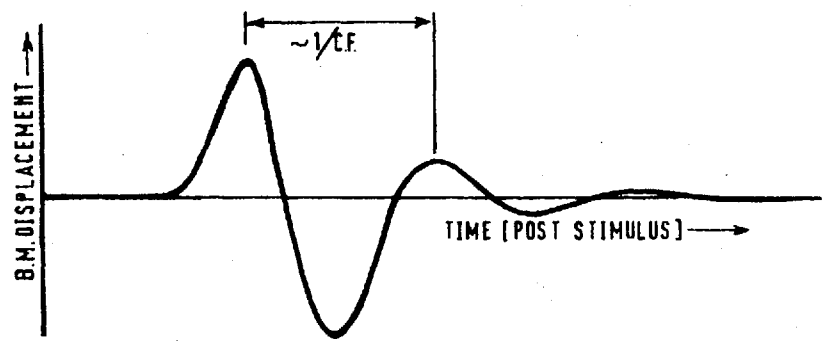

Figure 3. Form of the impulse response of a point on the basilar membrane, derived by Flanagan[16].

2.2 The effective stimulus for the hair cells of the organ of Corti

That the displacement pattern of the basilar membrane is the initial event leading to the stimulation of the hair cells of the organ of Corti, and to the subsequent stimulation and firing of the nerve fibres of the acoustic nerve, is now widely accepted. The work of von Békésy and Flanagan on the description of basilar membrane mechanics, and its close relationship to the physiological measurement of the firing patterns of individual auditory nerve fibres in cat by Kiang[37] and others (to be described in Section 2.7.2), makes it very difficult to exclude basilar membrane activity from a central role in fibre excitation. How this initial event becomes an effective stimulus for the hair cells is a more controversial matter, although it is generally believed that the tectorial membrane plays an important part. This latter membrane, which is in intimate contact with the ends of the hairs protruding from the upper surface of the hair cells, is thought to exert shearing forces on the hairs as a result of its motion relative to the basilar membrane[1,71]. The relationships between these various structures and the hair cells of the organ of Corti are shown in Figure 4. In other species, and notably goldfish[20], inner ear hair cells and nerve fibres have been found which are sensitive to a mechanical stimulus applied in one direction, and inhibited by a stimulus of opposite polarity. There is also powerful supporting evidence from similar cell types in the vestibular system[2,64].

Like other hypotheses enjoying less support, the one which invokes the bending of hairs as the final mechanical event in

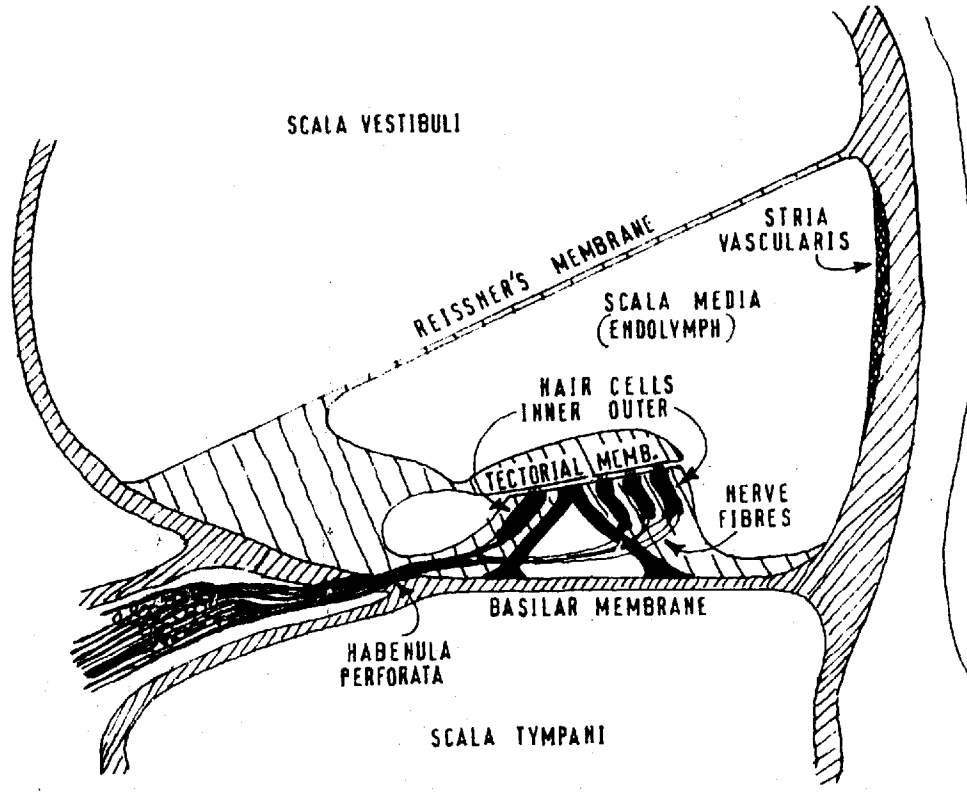

Figure 4. Diagrammatic view of a section through a turn of the mammalian cochlea, showing the disposition of the main cochlear structures and the hair cells of the organ of Corti.

the cochlea does little to counteract the objection that, at the threshold of hearing, extremely small basilar membrane displacements seem to be involved. It has been argued[7] from extrapolation of von Bekesy's measurements of membrane displacement at high stimulus intensities, that movements considerably less than the diameter of the hydrogen atom are implied. However, Whitfield[71], arguing that nonlinearities in the system at high intensities make such extrapolation invalid, has used the relative magnitudes of measured cochlear electrical activity at low and high intensities to infer the magnitude of basilar membrane movement near threshold. His result, though still remarkable, is some orders of magnitude greater.

2.3 Cochlear hair cell arrangement and structure

A section through the mammalian organ of Corti (see Figure 4) reveals the orderly arrangement of hair cells, normally into 1 or 2 inner and 3 outer rows which stretch the length of the cochlea. This order is so striking that Engstrom et al[11], and Bredberg[3], have recently been able to map hair cell damage due to drugs or intense sound by means of what they call a "cochleogram", showing the individual cells in their well-defined rows. It seems however that this precision of arrangement tends to be lost in the developing human foetus and more particularly in the adult, whereas in most mammals the order is maintained throughout life.

There is persistent speculation as to the significance of the various hair cell rows. It is widely believed that the outer rows are more sensitive to sound than the inner, and this view is supported by the selective destruction caused by very high level sounds and by ototoxic drugs[3]. Flanagan[17] and von Békésy[1] have suggested that the inner hair cells respond to the local spatial derivative of basilar membrane displacement, whereas they consider the outer cells to be sensitive to the displacement itself. Such hypotheses seem controversial in view of the fact that no systematic groupings have been reported in single unit neural activity under stimulus conditions. In addition to a difference in sensitivity between inner and outer cells, there is strong evidence for a systematic variation in sensitivity between the 3 outer rows, both to drugs and to acoustic trauma[3]. These effects may merely reflect the well-documented evidence[57,58] for graded differences in the innervation density of the various

outer hair cell rows. Finally, there is evidence of groupings in the rates of spontaneous firing in individual fibres of the acoustic nerve which has been suggested[37] to reflect their connection to one or other hair cell rows.

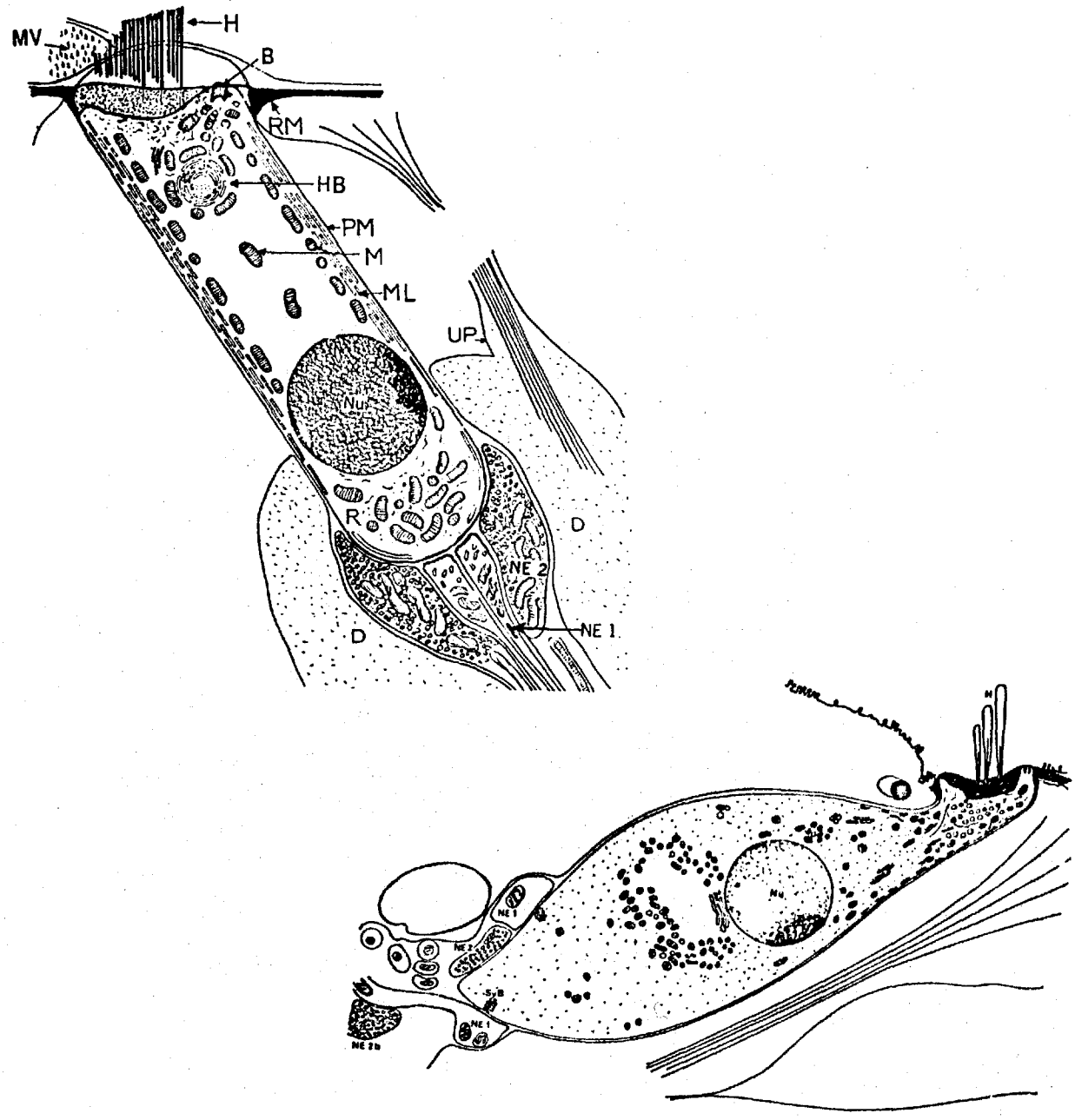

Figure 5 Schematic drawings of an outer hair cell (above) and an inner hair cell. Prominently shown are the cell nuclei and various inclusions, the hairs imbedded in the cuticular plate, and the afferent and efferent nerve endings clustered around the base of the cells (after Engstrom[13])

In Figure 5 are shown diagrammatic pictures of a mammalian outer and inner hair cell. In the outer hair cell the large number of hairs (H) are embedded in a cuticular plate and, when viewed from above, they reveal a characteristic distribution in a curved form, earlier described as being like a "W", but more recently[13] as a "U". In the inner hair cells, the hairs are arranged in a straight line parallel to the long axis of the basilar membrane[71]. Whatever the precise form of the arrangements, the fact that there is directional organisation of the hairs gives some justification for the assertion that particular shearing movements of the tectorial membrane act as the most effective stimuli. Perhaps also significant is the gradation in length of the hairs; for if it can be assumed that higher sound levels cause progressively more of the shorter hairs to be activated by the tectorial membrane, this may provide a clue to the large cochlear dynamic range. The function of the cuticular plate, in which the roots of the hairs are firmly embedded, remains uncertain, but in the case of the outer cell it seems to be closely connected with the presence of the so-called basal body (B) which lies close to the cell's upper surface. Such basal bodies are also present in the hair cells of the vestibular system and have in that system a mobile hair protrusion, or kinocilium, which is absent in the cochlear cells[18]: similar structures are now known to be present in other sensory systems including vision and olfaction, and they have been described by Wolken[72] as the "most elementary nervous system". Indeed, Engstrom et al.[10] have put forward the view that the basal body should be regarded as the essential excitable structure of the hair cell, and describe the kinocilium which

projects from it in other sensory systems as being extraordinarily sensitive to many different kinds of stimulation. Further investigation of this region should provide interesting clues about this link in the chain of events leading to the stimulation of the nerve fibres, whose terminal branches cluster round the base of the hair cells.

2.4 Electric potentials of the cochlea

In a recent review article, Wever[69] has described the various theories put forward to explain the different electric signals which may be picked up by a microelectrode inserted into the cochlea. His review clearly demonstrates the controversy surrounding the generation and function of these potentials, which are generally believed to be closely involved in the cochlear transduction process.

The endolymphatic potential, recorded by a microelectrode as a d.c. resting potential in the scala media, is biologically unusual in being electrically positive. Most recent authors have put the site of generation of the potential at the stria vascularis, on the basis that its healthy state appears necessary for the proper generation of the potential. Although the potential reaches some 80 mV. in mammals, it is much smaller in birds and almost absent in reptiles[71].

Resting negative potentials, variously reported as being between - 40 mV. and - 90 mV., may be recorded inside the various cells of the organ of Corti, as indeed is the case in most living cells, including nerve fibres.

The cochlear microphonic potential is an alternating potential, conveniently picked up by an electrode in the scala media, which faithfully reproduces the acoustic pressure waveform of pure sinusoidal (tone) stimuli. It is remarkable for the extremely linear variation of its amplitude with stimulus intensity over a wide dynamic range from threshold to some 70dB above threshold. As intensity is raised towards a value which causes noise damage in the cochlea, its magnitude levels off and then falls, although there is no noticeable distortion of the measured sinusoidal

waveform. Various explanations of this potential have been put forward, most of which stipulate the endolymphatic and/or the negative intracellular hair cell potentials as d.c. supplies, with the upper surface of the hair cells performing some sort of current or resistance modulation (in sympathy with basilar membrane vibrations). There have also been various more complicated electrochemical theories involving the movement of charges or ions in the hair cell region. In any case the correlation between the number of healthy hair cells and the magnitude of the microphonic potential does much to support the view that this electrical signal is the result of hair cell activity. Furthermore, the reversal in polarity of the microphonic as a recording electrode penetrates the cuticular plate is strong evidence that the site of microphonic generation is close to the hair-bearing surface of the hair cells[60].

Perhaps the most perplexing electrical signal in the cochlea is the summating potential, a d.c. signal which may be recorded during the application of high level stimuli. The signal seems to be related to some sort of running average of basilar membrane activity, and dies away rapidly when the sound ceases. Some strange theories have been advanced for its presence, but one of the most simple, and therefore attractive, ones (not mentioned by Wever) is that of Whitfield and Ross[70]. These authors have ascribed both the appearance of the summating potential and the decline in the level of the cochlea microphonic at high sound levels to a distortion and limiting effect in the output of individual hair cells. They contend that distortion in the microphonic fails to be detected by the normal recording electrode, because

the placing of the latter in the scala media causes it to pick up the averaged response of many hair cells. Such averaging essentially performs a low-pass filtering of the individual hair cell output waveform, discriminating effectively against the various harmonics produced by the distortion. It does however allow the fundamental and d.c. component of the waveform to be recorded as the microphonic and summating potential respectively.

2.5 Cochlear innervation

The nerve fibres of the acoustic nerve, which enter the organ of Corti through the habenula perforata (see Figure 4) and there lose their myelin sheaths, put out terminations to the hair cells in two rather distinct ways. Some fibres are essentially radial in their connections to the hair cells, but others travel along the cochlea for considerable distances (up to $\frac{1}{4}$ or $\frac{1}{2}$ of a cochlear turn) before terminating. This so-called spiral innervation of the cochlea is perhaps the most distinctive aspect of its neuroanatomy. It is clearly visible when the nerve fibre distribution is clarified by staining techniques[11,12]. Such techniques may also be used to distinguish between afferent and efferent nerve fibres, and show that both systems are well-developed in the cochlea. The other established rule of cochlear innervation is that it tends to be multiple, i.e. nerve fibres appear to make contact with several, or many, hair cells and hair cells are innervated by several, or many, nerve fibres.

Beyond these central facts of cochlear innervation, the subject becomes rather confused. A number of authors have described the main routes of the fibres from the acoustic nerve trunk to the hair cells and have described the various fibre bundles in the organ of Corti[58,68]. It is generally agreed that the innervation of the inner hair cells is predominantly radial, and that of the outer hair cells predominantly spiral. The details of the method of termination of the spiralling fibres, an issue which seems of some importance from the signal processing viewpoint, has long been the subject of discussion, and until the last year or two it was generally believed that spiralling fibres might

turn either apically, or basally, or both, and that they put out many terminations to hair cells lying along their course.

The controversy surrounding these details of cochlear innervation seems to have been resolved to a considerable extent in the last few years by advances in microscopic and chemical staining techniques. Engstrom et al.[11] have in this way managed to categorise the various fibre bundles into afferent and efferent groups, and have estimated both the relative numbers of fibres and the innervation density of the various hair cell rows in various regions of the cochlea. One of their most interesting assertions is that the spiral fibres put out terminations only towards the end of their spiral course as shown in Figure 6, and not all the way along it as has often been supposed. Furthermore, spiralling occurs in a mainly, or even exclusively, basalward direction.

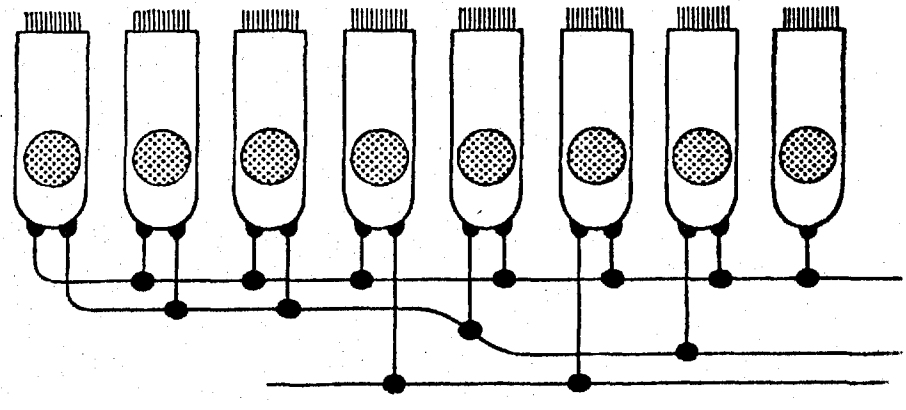

Figure 6 Diagram to illustrate typical modes of termination of spiral fibres on the third outer hair cell row in guinea pig. Such termination appears to occur only after rather long spiral runs by the fibres (after Engstrom et al.[11])

In another recent article, Spoendlin[58] has described the results of investigations which broadly support those of Engstrom. His diagram of the overall innervation pattern,

reproduced in Figure 7, forms a useful summary of current views on this complicated subject.

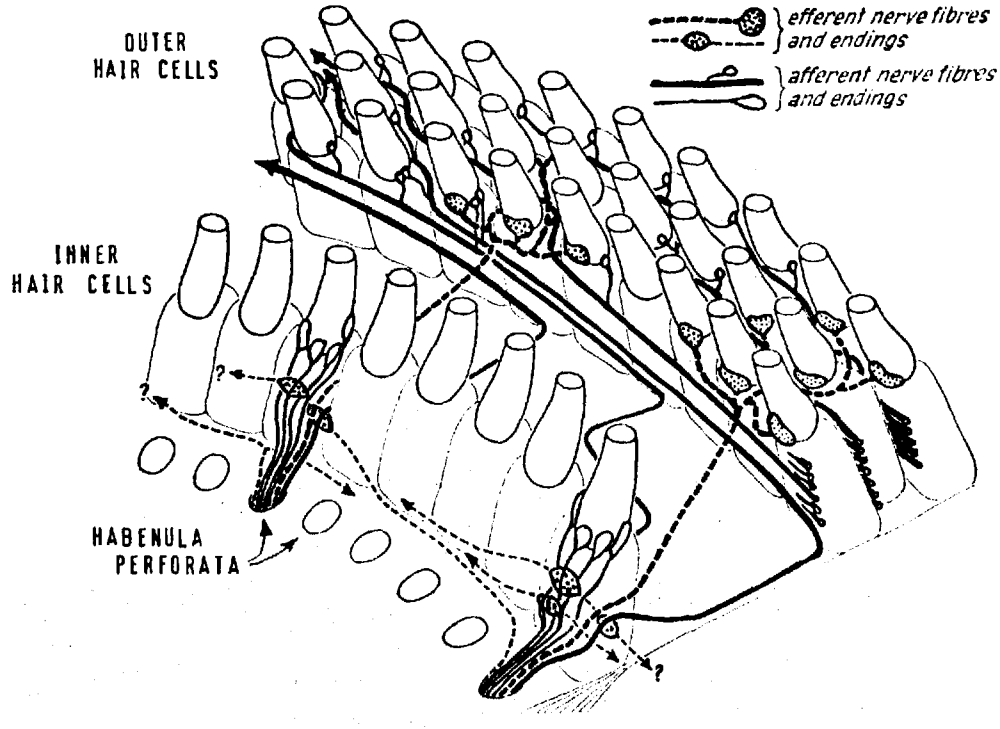

Figure 7 Schematic diagram of cochlear innervation in mammals. The full extent of basalward spiralling is not shown, nor do the indicated fibres and endings correspond to their actual numbers (after Spoendlin[58])

In this diagram it may be seen that:-

(a) Afferent innervation of the inner hair cells is predominantly radial, efferent spiral.

(b) Afferent innervation of the outer hair cells is predominantly spiral, efferent radial.

Spoendlin also makes the following points which seem relevant to the present study:-

(c) The majority of afferent fibres innervate the inner hair cells.

(d) Multiple innervation of hair cells by afferent fibres is much more obvious in the case of the outer hair cells.

(e) There are synaptic contacts between all hair cells and afferent dendrites, between the efferent endings and the outer hair cells, and between the efferent terminal fibres and the afferent dendrites, predominantly in the region beneath the inner hair cells.

(f) Afferent and efferent unmyelinated fibres are in very close relationships in the area below the inner hair cells.

Finally the following points concern the efferent system:-

(g) Degeneration studies reveal that efferent fibres derive mainly from the so-called olivocochlear bundle of Rasmussen. There are only about 500 fibres in this bundle, and their extensive branching in the organ of Corti is proved by the presence of some 40,000 efferent endings on the hair cells in cat. (There is some evidence[30] of further efferent fibres in the main trunk of the acoustic nerve which are not part of the bundle of Rasmussen).

(h) There is a systematic decrease in efferent innervation density of the outer hair cells, from base to apex of the cochlea and from the innermost to outermost row[11].

2.6 The hair cell-nerve ending junction

One of the most interesting, and in the case of the afferent fibres also the most problematical, aspects of the individual peripheral fibre is the detail of its connection to the base of a hair cell, and of the mechanisms which operate at this critical junction. In the case of the efferent fibres, electron micrographs of the hair cell junction suggest that it conforms to the more or less standard structure of a nervous system synapse. The efferent nerve endings are described by Engstrom[9,11] as being richly granulated and containing large quantities of synaptic vesicles, which are thought to play an important role in the release of a chemical transmitter substance across the synaptic cleft. The generally accepted view[33,42] is that the chemical transmitter, released in quantal packets from the presynaptic terminal (in this case the efferent nerve ending), subsequently causes a change in the polarisation of the postsynaptic membrane (in this case the hair cell membrane). Further evidence for chemical transmission in the efferent system is provided by the presence of a multilayered membrane boundary[13], across which direct electrical transmission would appear to be very unlikely, and also by evidence[30,43] for the presence of acetylcholine in the organ of Corti.

In the case of junctions between hair cells and afferent fibres, which are of more direct interest in the present study, the evidence for chemically-transmitting synapses seems much less clear, although most recent authors use the term "synapse" quite freely. In Figure 8 are reproduced two electron micrographs of the critical junction, this time in guinea pig and squirrel monkey. The two types of nerve ending

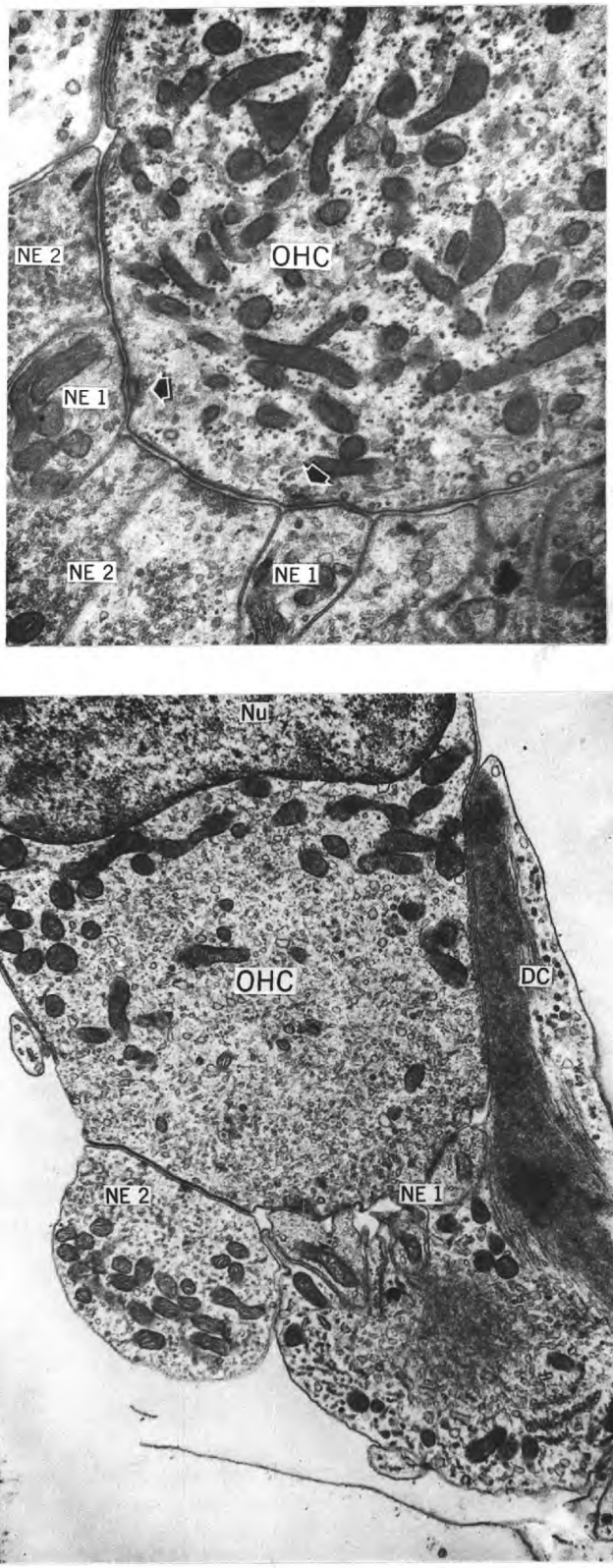

Figure 8 Electron micrographs of junctions between nerve endings and outer hair cells. Above: guinea pig. Below: squirrel monkey. In both cases efferent (NE2) and afferent (NE1) nerve endings are visible, and, in the upper picture, so-called "synaptic bars" are shown arrowed at each afferent junction (after Engstrom[13])

(NE1 and NE2), afferent and efferent respectively, are clearly visible. Engstrom[13] notes that the presence of synaptic bars in the hair cells, adjacent to the afferent boundaries, is very problematical. It is also interesting to note the intimate contact between afferent and efferent endings shown by this figure, which supports the comments of Spoendlin[58]. The junction region is again shown in Figure 9, this time with greater magnification. Both halves of the figure show afferent synaptic contacts between nerve and inner hair cell in squirrel monkey, with synaptic bars clearly visible. In this case there seems somewhat more evidence for inclusions in the presynaptic (hair cell) terminal which might be thought to suggest chemical transmission. An electron micrograph in another paper by Engstrom[9] (not reproduced here) shows a multilayered synaptic boundary which is considered highly suggestive of chemical transmission effects, although in none of these cases has a chemical transmitter been positively identified.

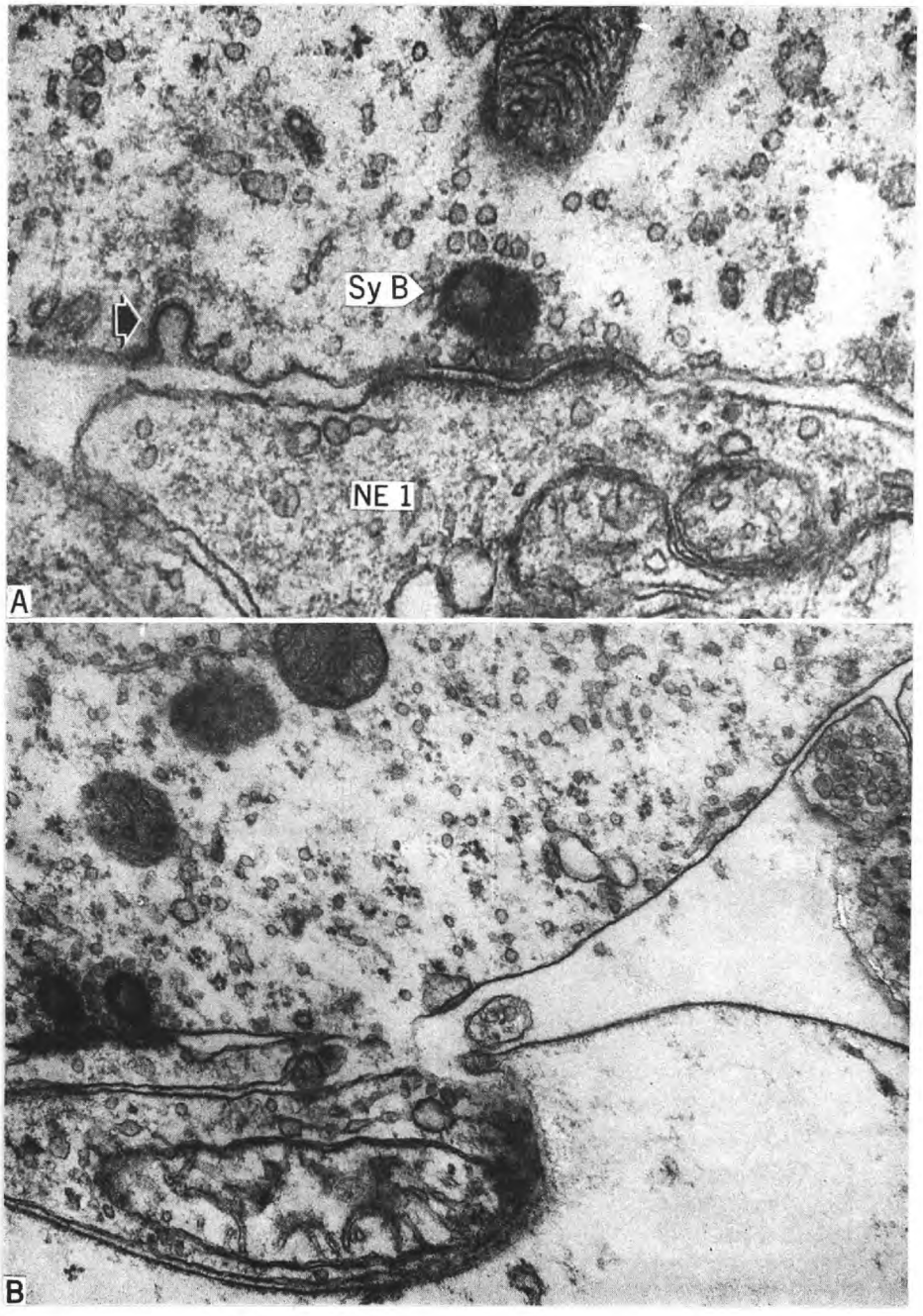

Figure 9 Two electron micrographs at higher magnification, showing afferent synapses between nerve endings and inner hair cells in squirrel monkey (after Engstrom[13])

2.7 Activity in first order auditory neurons in cat

2.7.1 Recordings of spontaneous activity

Recent electrophysiological recordings of the response of single nerve fibres in the acoustic nerve of cat, to a variety of simple acoustic stimuli, have greatly enhanced the possibilities for modelling of the peripheral auditory system. Kiang[37] and his colleagues have collected a large amount of data on the firing patterns of single units in the auditory nerve, and in a more recent work Gray[25] has carried out some detailed statistical analysis of such recordings. It is here proposed to outline those of their results which seem to reflect most directly on the present work.

Spontaneous activity

The majority of first order auditory neurons display spontaneous activity in the absence of controlled acoustic stimulus. Rates of spontaneous firing vary between zero and about 120 spikes per second, and there is some evidence[37] for clustering about certain preferred values. Figure 10 shows the spontaneous activity of two typical units plotted as interval histograms, and Figure 11, also typical, shows a joint interval scatter diagram in which successive intervals between firings are plotted against one another. Apart from the lack of very short intervals, presumably due to refractory properties of the nerve fibres, these figures suggest that the spontaneous activity is typical of a stochastic Poisson process, having no substantial correlation between successive intervals. In Figure 12 is shown the variation of interval histogram mode with rate of spontaneous discharge, for a large number of different units. The mode lies mainly between 4

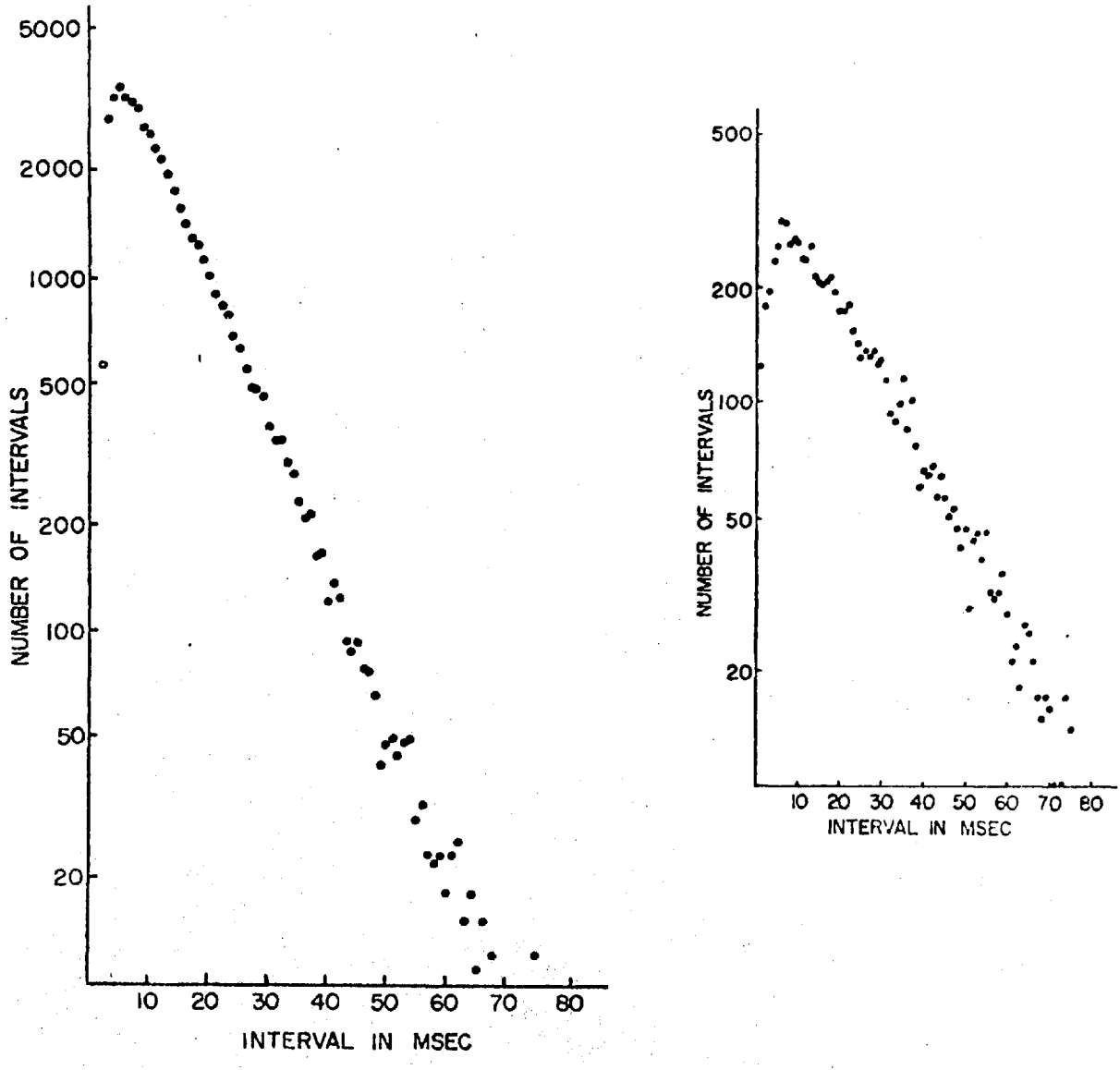

Figure 10 Two typical interval histograms of spontaneous activity in first order auditory neurons in cat. Left: fibre of C.F.=7.3 KHz., mean spontaneous rate = 76 spikes/second. Right: fibre of C.F. = 0.58 KHz., mean rate = 45 spikes/second (after Kiang[37])

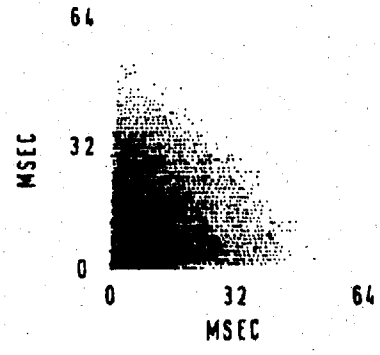

Figure 11 A typical joint interval scatter diagram for the spontaneous activity of a first order auditory neuron in cat (after Kiang[37])

and 7 msec and does not appear to be very dependent on the firing rate.

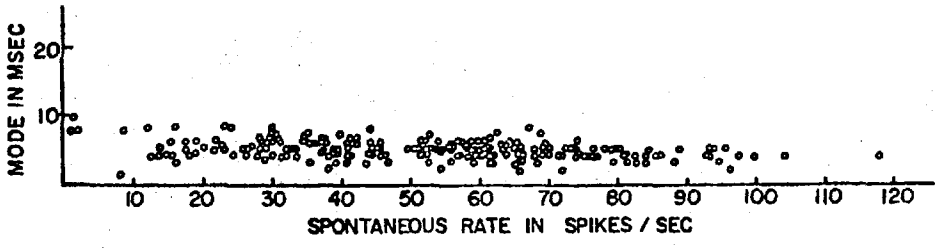

Figure 12 The mode of the spontaneous interval histogram plotted against the mean rate of discharge, for a number of first order auditory neurons in cat (after Kiang[37])

2.7.2 Driven activity

Response to click stimuli

A single nerve fibre in the auditory nerve is generally described by its characteristic frequency, which is that sinusoidal frequency (applied as an acoustic stimulus) to which the fibre is most sensitive in terms of its detectable firing response. It is assumed that this maximum sensitivity to a particular frequency merely reflects the fact that the fibre innervates a region of the basilar membrane of the same C.F. Strong supporting evidence for this view is provided by fibre responses to click stimuli, which parallel in certain obvious ways the presumed relevant basilar membrane impulse responses.

Typical neural responses of individual acoustic nerve fibres to acoustic clicks, which are shown in Figure 13 in the form of post-stimulus-time (PST) histograms, show some striking resemblances to the Basilar Membrane impulse response (see Figure 3), and, on closer inspection, also reveal some interesting differences.

The following generalisations seem possible from these recordings:-

(a) Individual histogram peaks are separated by a time approximately equal to the inverse of the C.F. of the unit considered, paralleling in an important way the presumed basilar membrane impulse response in the relevant cochlear region.

(b) Many more peaks are generally visible in the PST histograms than in the basilar membrane impulse response waveform, when both are plotted on linear scales. However the response of units of C.F. above about 4 KHz does not

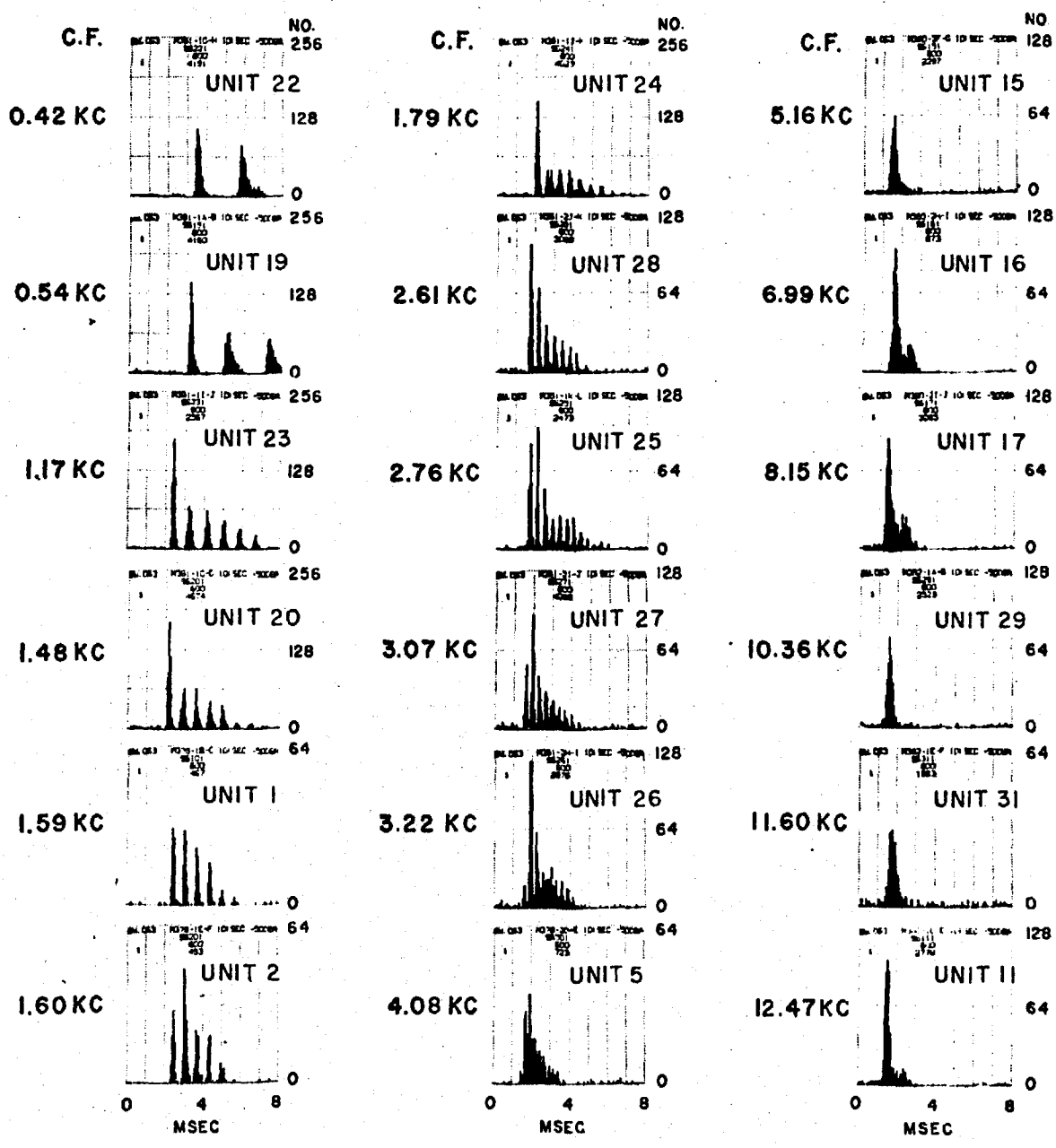

Figure 13 PST histograms of the responses to rarefaction click stimuli of 18 first order auditory neurons in a single cat. 600 stimuli presentations were used to obtain each histogram, at a rate of 10 per second (after Kiang[37])

show multiple peaks, as a result of lack of resolution either in the neural system or in the recording apparatus. To a first approximation, the number of peaks visible (in the response of units having a C.F. lower than about 4 KHz) is independent of the actual value of the C.F.

(c) The first visible peak in the histogram is not always the greatest, unlike the first peak of the presumed basilar membrane impulse response.

Although typical responses to condensation (as opposed to rarefaction) clicks are not shown here, in fact the positions of peaks and troughs in the neural histograms are reversed, in a manner which is consistent with the view that rarefaction movements of the basilar membrane (towards scala vestibuli) cause increased neural firing probability, and vice versa. In the response of a unit with a relatively high rate of spontaneous firing to a condensation click, it is sometimes possible to detect a trough as the first part of the PST response. This suggests that condensation movements of the basilar membrane cause a genuine reduction in firing probability, and therefore that the troughs between successive peaks of the PST histograms are not merely due to neural refractory effects.

Figure 14 shows the effect on the PST histogram of changes in click stimulus intensity, for a typical unit. Starting with a stimulus near threshold, two or three peaks may typically be seen emerging out of the background noise (spontaneous activity) of the histogram. As intensity is raised, the earlier peaks tend to increase in height relative to later ones, and at perhaps 20 or 30 db above the threshold a new peak of smaller latency becomes apparent. As intensity is further raised, the new peak grows and finally dominates. The effect seems to be maintained throughout the large dynamic range investigated, and the picture is typical of nerve fibres studied by Kiang, and does not seem to reflect individual fibre connections. The other point of interest is that

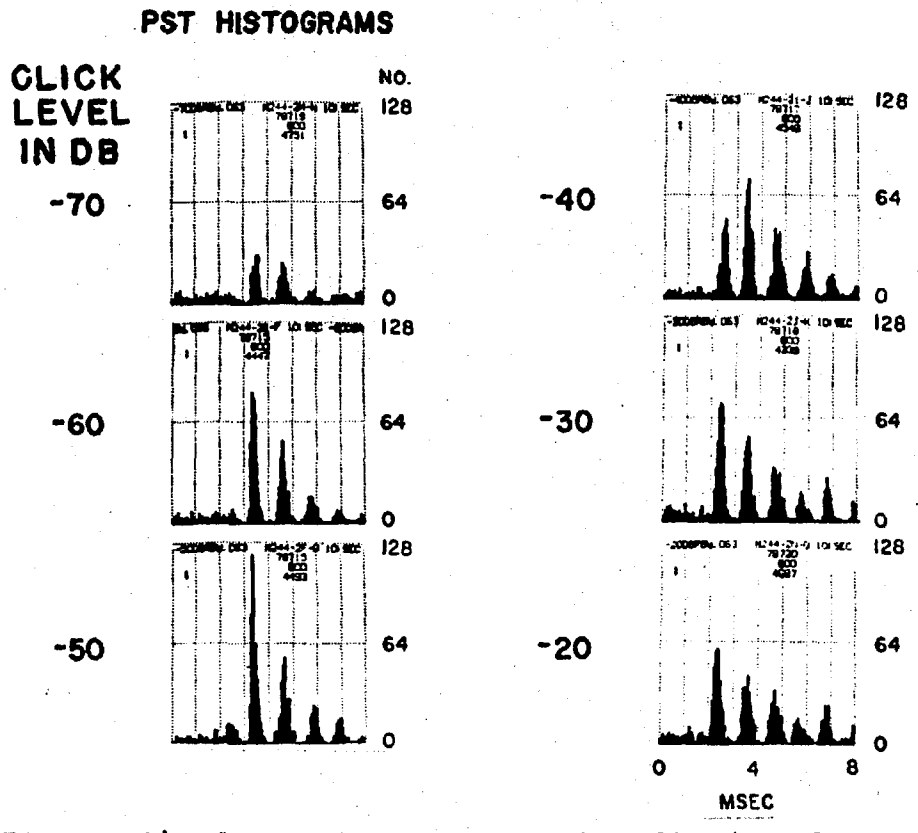

Figure 14 Typical response of a first-order unit to changes in rarefaction click level. C.F. of unit = 0.65 KHz (after Kiang[37])

there is negligible change in the latency of individual peaks with increasing intensity; the maximum shift observed over the whole intensity range is in all cases less than $\frac{1}{4}f_o$, where f_o is the characteristic frequency.

Responses to other types of stimuli

Single unit recordings have also been obtained[25,37] for other types of acoustic stimulus, including continuous tones (mainly at the C.F. of the unit), tone and noise bursts, and for various more complicated signals such as tone combinations and clicks in the presence of noise. In Figure 15 are shown some typical PST responses of an auditory nerve fibre to tone bursts of various durations at the C.F. Also shown, on a finer time scale, are the start-up effects which occur during the first few cycles. The overall envelope of

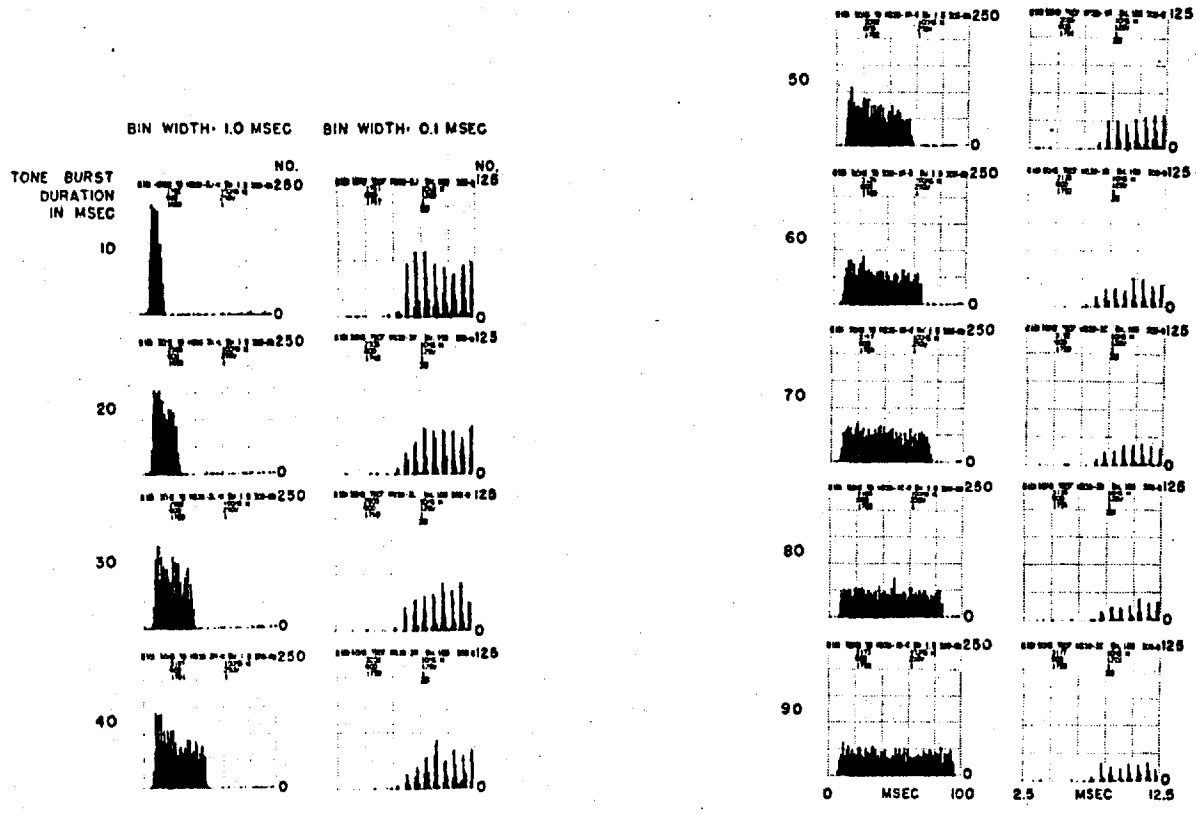

Figure 15 Typical PST histograms for tone bursts (600 stimuli at 10 per second) at the C.F. of the unit. The first few peaks of the response are shown on the right in each case, to an expanded time scale. C.F. of unit = 1.45 KHz (after Gray[25])

such responses is remarkably similar in different units having a wide range of C.F. values, the main difference being that a fine structural pattern representing the response to individual cycles of the stimulus is only visible when the C.F. is below about 4 KHz. The envelope is also strikingly similar in the case of noise bursts, but here, as might be expected, the fine structure of the PST histogram is lost.

The PST responses are not so straightforward for all of these "simple" stimuli. Kiang reports[37] a two-tone inhibition effect in which the response to a continuous tone at the C.F. is actually inhibited by a tone burst at a

different frequency. Although such effects are not yet well documented,it seems unlikely that they involve efferent mechanisms because sectioning of the auditory nerve appears not to modify the result.

2.7.3 Statistical analysis

In a more detailed analysis of such recordings, Gray[25] has shown that there is much information to be extracted which is not available in the normal PST histograms. Much of his work is concerned with the analysis of conditional firing probabilities (the normal PST histogram displaying unconditional probability). From a conceptual point of view his analysis of recovered probability is perhaps the most valuable, since by concentrating on probability of firing, on condition that a unit has not fired for a long time (i.e. it has "recovered"), the complications introduced by refractory effects are effectively eliminated. Gray has estimated the recovery time of typical auditory neurons from an analysis of their spontaneous activity, showing that the probability of a spontaneous firing during a small time increment reaches a constant level some 20 msec. after the previous firing. Subsequent recovered probability estimates during stimulus conditions are then made by discounting any firing which occurs less than (say) 20 msec. after the previous one.

The estimates of recovered probability for click stimuli as a function of intensity are possibly the most interesting statistics. Figure 16 shows normal PST histograms and recovered probability histograms for a typical unit stimulated at three different intensity levels, and makes it clear how much effect the refractory properties have in suppressing firing during later basilar membrane movements. A useful summary of these effects is given in Figure 17 which shows the intensity effects in four different, but typical, units of various C.F. values and spontaneous rates.

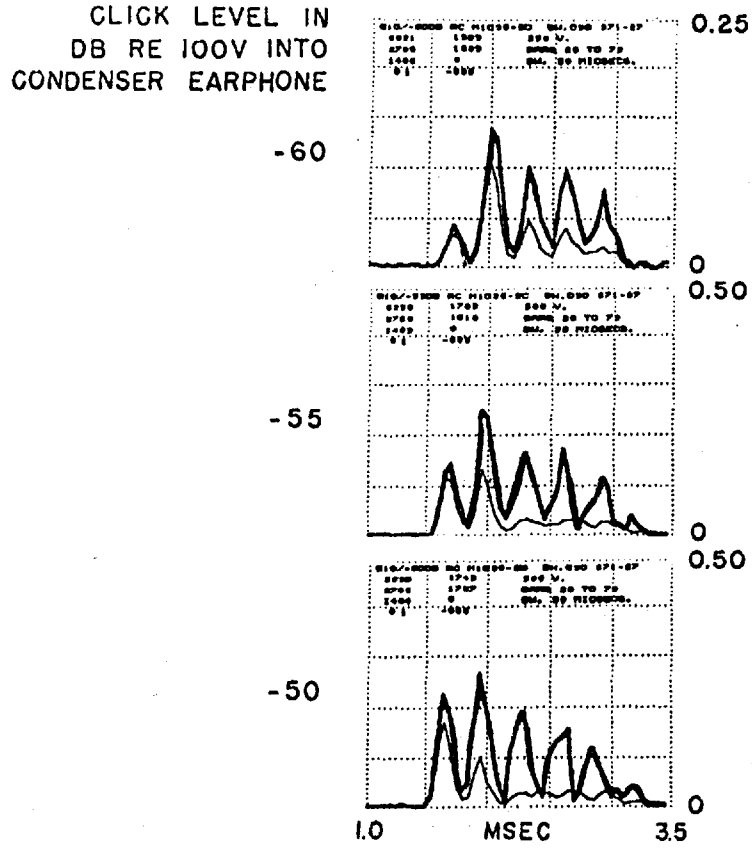

Figure 16 Recovered probability histograms (heavy lines) and normal PST histograms (light lines) for rarefaction clicks presented at a rate of 10 per second and at 3 intensity levels. C.F. of unit = 4 KHz. Total no. of stimuli = 600 (after Gray[25]).

In Figure 17 are plotted recovered probabilities of firing during whole peaks of the relevant PST histogram. In the case of a rarefaction click, the first, third, fifth, etc. half-cycles are the ones during which firing probability increases; for a condensation click, the even-numbered half-cycles are relevant. In the figure a redundant "C" or "R" is used to make clearer which click polarity is involved.

Although all units do not show identical effects, some generalisations seem possible:-

(a) In all units, at all intensities, there is an increase in recovered probability during successive click

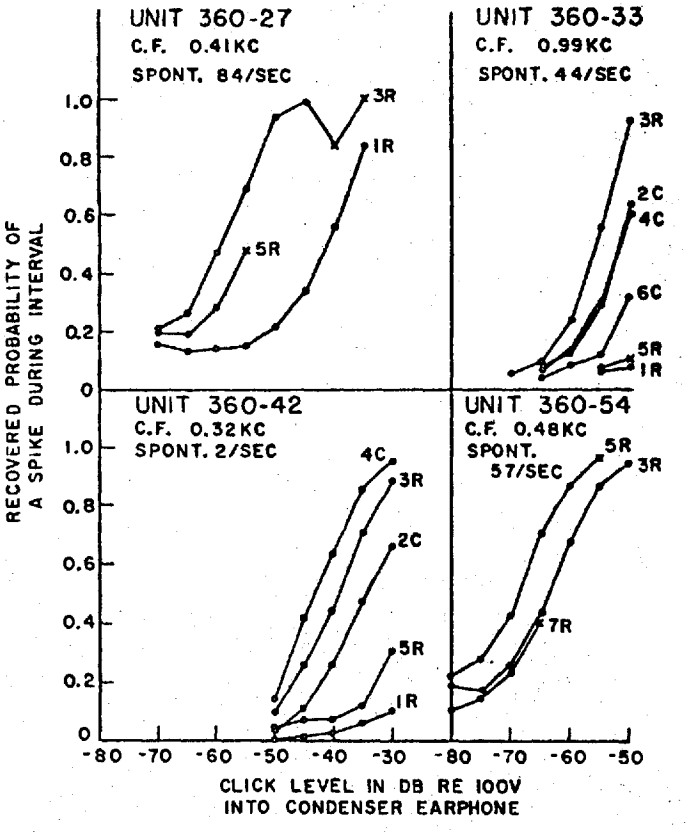

Figure 17 Recovered probabilities associated with peaks of the PST histograms for four units as a function of intensity. A redundant C or R is used to indicate condensation or rarefaction stimuli (after Gray[25]).

histogram peaks, up to about "4C" or "5R". This is in marked contrast to the rather drastic reduction in the heights of the peaks of the presumed basilar membrane displacement waveform (see Figure 3).

(b) There seems definite evidence that the recovered probability associated with peak 2C is always greater than that of peak 1R, at the same intensity.

(c) The recovered probability for any histogram peak is

rather simply related to the logarithm of the stimulus level.

At the higher stimulus intensities, evidence of a further effect is revealed by assessing recovered probability during smaller time intervals than whole peaks of the click histogram - appropriate time bin-widths are of the order 0.1 msec. When this is done there is evidence that recovered probability is reduced immediately following previous high values of itself. As Gray has pointed out, this cannot be a refractory mechanism, and he prefers to call it a "depletion effect", although he is careful to avoid any direct physiological implications.

Also studied by Gray are recovered probability histograms for tone burst stimuli. Typical results for two units are shown in Figure 18, together with the normal PST histograms.

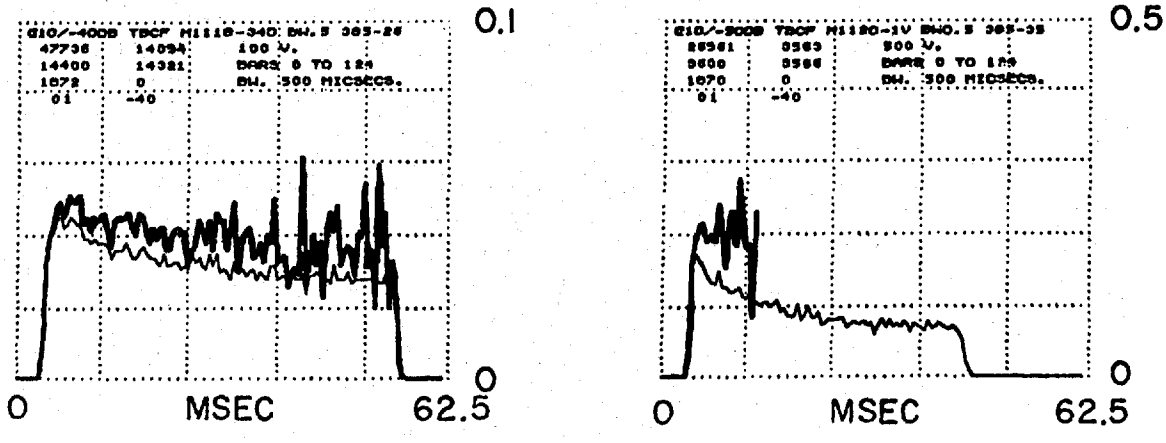

Figure 18 Typical recovered probability histograms (heavy lines) and normal PST histograms (light lines) for tone bursts presented at the C.F. (17.5 KHz, left; and 9.5 KHz, right). Burst frequency = 10 per second (after Gray[25]).

These results suggest that most of the progressive reduction in firing probability seen in the PST histograms is due to

the refractory properties of the neurons; there is, however, some evidence in the left-hand diagram of a reduction in recovered probability during the course of the tone burst, tending to confirm the presence of a "depletion effect".

2.8 Discussion

Having reviewed what seem to be the most relevant aspects of cochlear anatomy, innervation and neural activity, it seems appropriate to discuss briefly the overall operation of the peripheral system. Although many papers have recently appeared concerning the fine details of cochlear structure and neural activity, few authors have speculated about the possible relationship between structure and function. This is particularly true of the neural transduction process in the cochlea.

In discussing the detailed transformation between acoustic pressure waveform and firings in individual fibres of the acoustic nerve, it is assumed that the vibrations of any point on the basilar membrane resulting from a given acoustic stimulus may be calculated using Flanagan's formula (see Figure 3) for the impulse response, and taking due account of middle and outer ear transmission. In such computations it is usual to assume a linear mechanical system, and this seems justifiable, at least over a limited dynamic range. The next step is less easy, since it involves making some assumptions about the action of the hair cells. However it is becoming generally accepted that the high resting potential difference across the upper membrane surface of the hair cells and the existence of the cochlear microphonic potential are firm evidence of hair cell electrical activity. It further seems reasonable to implicate the cuticular plate and basal body region of the hair cell, which, perhaps acting rather like a variable resistance which controls a current into the hair cell body, also controls the cell's polarisation, causing it to change in sympathy with the local vibrations of the basilar membrane. This view is broadly supported

by Flock et al.[18] and by Engstrom[13], who says, "The depolarisation and/or hyperpolarisation of the sensory cell influence the activity at the synaptic areas at the base of the hair cells, thus modulating the action potentials in the nerve fibres of the acoustic nerve . . ." If the cochlear microphonic potential is accepted as evidence of such action, then it becomes rather difficult to accept any severe nonlinearity in the system over moderate dynamic ranges, at least as far as the stage of hair cell polarisation.

The next question concerns the way in which a change in hair cell polarisation might affect the nerve fibres and cause discharge. The evidence already reviewed suggests that an intermediate liberation of chemical transmitter substance may be involved, in which case it would be appropriate to examine any available evidence on such systems, to see whether or not some of the effects visible in neural PST histograms may be accounted for in terms of known physiology. It seems quite possible that changes in polarisation of a hair cell about some resting level could give rise to increased or reduced liberation of a transmitter substance; these changes in hair cell polarisation might presumably arise as a result either of basilar membrane activity or of activity in the efferent nervous system, the latter giving rise to a chemical transmission from the "type 2" nerve endings to the hair cell.

Although known synaptic mechanisms may provide clues to some of the more puzzling aspects of the neural PST histograms, it also seems quite possible that the complex pattern of cochlear innervation is responsible. The whole question of signal processing in cochlear nerve fibres has been largely

ignored in the literature, although it seems a question of great interest. Previous attempts at modelling the peripheral auditory system have almost all considered a nerve fibre travelling radially to innervate a single hair cell, and possible effects of multiple and spiral innervation have not been investigated. One of the main reasons for this is perhaps that there have not so far been reported any systematic groupings in measured neural activity, which might reasonably be attributed to differences in innervation of the various fibre groups.

As far as efferent innervation in the cochlea is concerned it seems both from anatomical considerations and from adaptation phenomena in auditory nerve fibres that this system must have a considerable latency. It therefore seems fair to discount the possibility that the efferent system has any substantial effects on the firing patterns of primary afferent fibres, at least for low repetition rate transient stimuli such as clicks, and at low and medium stimulus intensities.

To embark on a detailed study of cochlear transduction would be impossible without some knowledge of the firing patterns of individual acoustic nerve fibres. The work of Kiang and Gray, extracts of which have already been presented, gives important clues and shows that stochastic models are almost certainly necessary to reproduce any of the finer effects visible in the neural PST histograms. It is proposed to concentrate here largely on the acoustic click response, not least because it is fully documented and because it shows a number of complex effects. If these can be explained, it seems probable that the relatively

straightforward neural responses of first order fibres to other simple acoustic stimuli such as noise and tone bursts, and continuous tones, could be predicted.

3. ASPECTS OF AUDITORY PERCEPTION

3.1 Review of some binaural listening phenomena

The main characteristic of binaural headphone listening is that a subject can, under certain circumstances, fuse the sound images from the two ears into one intracranial image with subjective spatial properties. Although there are certain differences between perceptual effects in headphone and loudspeaker (free space) experiments, it is clear that this fusion mechanism accounts for the ability of a person to assign direction to a sound source, a matter sometimes discussed under the heading of "the cocktail party problem". In headphone listening experiments the fusion mechanism operates for a wide variety of similar signals presented to the two ears. The main experimental parameters have generally been interaural time difference (ITD) and interaural amplitude difference (IAD), and the perceived movements of the intracranial image under the influence of changes in these two parameters have been the subject of considerable study in the literature. Such effects are of interest for two main reasons. Firstly, consider two sound sources spatially separated, one being the signal to which the listener wishes to attend, the other being an interfering noise. In a binaural listening situation, with optimum positioning of the two sound sources in space, a subject can achieve some 15-20 dB improvement in his signal to noise discrimination, compared with a monaural listening situation. Such an effect represents an improvement which the communications engineer would like to copy. The other reason for interest in binaural listening phenomena is that, with suitably devised experiments, considerable insight can be obtained into the relationships

between auditory perception and cochlear activity. In a series of articles, Sayers and Toole[52,53,62,63] have investigated binaural effects with simple stimuli such as tones and impulses. It is now proposed to review their work, which seems to provide some satisfactory explanations of a perceptual situation which, from a review of the literature as a whole, appears complex and unresolved.

One of the most important issues concerns the way in which subjects are asked to report the perceived position of the intracranial image in binaural listening experiments. Other experimenters have often relied solely on the image centring technique, whereby a movement of the fused image away from subjective centre caused by a change in one parameter (say ITD) outside the control of the subject, may be offset by him by adjustment of, say, an IAD control. Although this method is valid for some situations, Sayers and Toole have found that many binaural images, within certain ranges of experimental parameters, cannot be centred in this way, and that they are always perceived to one side or other of the subject's auditory space. In this case, the use of an image centring technique may erroneously suggest that such images do not exist, because they cannot be centred. In such situations Sayers and Toole have instead asked listeners to describe the position of an image in terms of a subjective lateral scale; this task may be made easier by using an actual scale marked in, say, 10 divisions, mounted in front of the listener. Using such methods of lateralisation judgement, highly consistent results may be obtained with different subjects in a variety of listening situations.

Tone stimuli

In the case of equal-level pure tones, they have shown typical results in which subjects report a more or less linear variation of perceived lateral image position with ITD. As ITD approaches and then exceeds half the period of the waveform, the subject begins to attend to a new image perceived on the other side of his auditory space. This effect can be clearly demonstrated for tones between about 200 Hz and 1200 Hz. On the basis of such results, it is suggested that the behaviour of subjects making lateralisation judgements can be described as if the images arise from a type of running cross-comparison performed on the neural signals arising in similar cochlear regions of the two ears. When IAD is introduced with pure tones, there is evidence that the image trajectory judgements are simply shifted towards the louder side.

Transient stimuli

The use of repetitive click stimuli (also referred to as impulses, or wideband transients) is probably more illuminating, although the listening situation becomes very confusing unless certain precautions are taken. In particular it appears that with wideband signals, a subject generally perceives two or more co-existing binaural images with different lateralisation characteristics, which Sayers and Toole have inferred to arise from cross-comparisons of neural activity originating in various corresponding regions of the two cochleae; arbitrary attention by the subject to one or other of these images can cause considerable confusion in the interpretation of results. The difficulty seems, however, to be much reduced by the use of high-pass filtered masking

noise applied to one or both headphones, which effectively eliminates significant neural cross-comparisons between the more basal cochlear regions. This has the effect of allowing only binaural images of low-pitched character to be perceived. Similar effects are achieved by the use of low-pass filtered transients.

Having established an experimental technique, Sayers and Toole then considered in some detail the lateralisation characteristics of images arising from the use of low-pass filtered transients, as a function of ITD. They were also able to clarify the situation with wideband transients, and to investigate the different lateralisation characteristics of the two main impulsive images arising, presumed to originate in different cochlear regions. They afterwards investigated the more complicated case of a single filtered transient train in one ear and filtered double-pulse train in the other, again with ITD as the main variable. By a consideration of basilar membrane activity in these various cases which, on the basis of Flanagan's work[15,16] they assumed to arise in the cochlear regions of interest, they showed that the image lateralisation phenomena could again be accounted for on the basis of neural cross-comparisons performed on the signals from the two ears. For this purpose, they found it unnecessary to implicate any fine details of neural activity, but merely to assume that enhanced neural firing occurs during rarefaction half-cycles of local basilar membrane vibration. In this way Sayers and Toole succeeded in showing that presumed peripheral neural activity is directly implicated in the perceived movements of binaural images as a function of ITD.

3.2 Further problems in binaural listening; interaural amplitude difference (IAD)

Accepting that a framework now exists for the description of the main effects of ITD on the perceived position of fused binaural images, it would also be very attractive to be able to explain the major effects of IAD in terms of peripheral mechanisms.

It has been known for some time that, in a wide variety of headphone listening situations, a perceived lateral shift of a binaural image caused by ITD can be corrected by introducing an appropriate amplitude difference between the two ears. Wideband or filtered transient signals are particularly suitable for exploring such effects, although the former signals tend to suffer from the difficulties already mentioned - namely, that the presence of two or more co-existing images confuses results. If running speech, or indeed, any continuous (rather than transient) wideband signal is used instead, the same effects are generally reported as being accompanied by a perceived broadening of the image, which can be detected by objective measurements. Although the offsetting of the effects of ITD by introducing IAD is only possible over limited ranges of the two variables, the phenomenon has given rise to the concept of an equivalence, or "trading ratio", between them. It need hardly be added that an explanation of such effects should help to clarify the manner in which amplitude is coded at the neural level.

The available literature on the subject is somewhat inconsistent. It is felt that this is largely due to the fact that wideband transient signals have generally been used, and that subjects have often been confused by the presence

of several binaural images, arbitrarily attented to. Accordingly the magnitude of the trading ratio between IAD and ITD is variously reported as being between about 5 and 250 μsec/dB, with a tendancy for continuous tone stimuli to produce the lower values and for repetitive impulsive stimuli to give rise to the higher values of the ratio. Some experiments will now be described which attempt to clarify the situation for the latter type of signal.

3.3 Time-intensity trading: experimental results

The trading ratio between IAD and ITD has been determined using low-pass filtered binaural transients of known waveform under conditions in which no ambiguity due to multiple images should arise. Signals which produce maximum basilar membrane activity in medial and apical cochlear regions have been used, thus eliminating high pitched impulsive images which have different lateralisation characteristics.

Binaural, repetitive acoustic transients, low-pass filtered with various filter cut-off frequencies, have been used to determine the IAD/ITD trading ratio as a function of the absolute sound level at which the test was conducted. Rarefaction pulses of duration 0.1 msec. and repetition frequency approximately 30/second, were low-pass filtered by Allison 2A passive filters, set to the given cut-off frequency, here 800 Hz.* The experiments were conducted in a quiet room environment using Sharpe HA-10 headphones, and the listener was able to control the ITD between the filtered pulse trains in the two ears. Arbitrary values of IAD were introduced by the experimenter, the signals to the two headphones were then switched on and the subject was asked to centre the fused binaural image.

Six subjects were tested, using various values of mean absolute sensation level between 5 dB and 45 dB above threshold (in the test environment, threshold corresponded to approximately 0.1 mV peak signal into the headphones). Results for four subjects are reported, two (BMcAS, PAL) with considerable listening experience, and two untrained. The results, closely representative of all other measurements, are shown in Figure 19, each line representing an approximate best straight line,

* These filters give an attenuation of about 6 dB at the nominal cut-off frequency, with a slope of approximately 30 dB/octave.

fitting some 50 separate judgements.

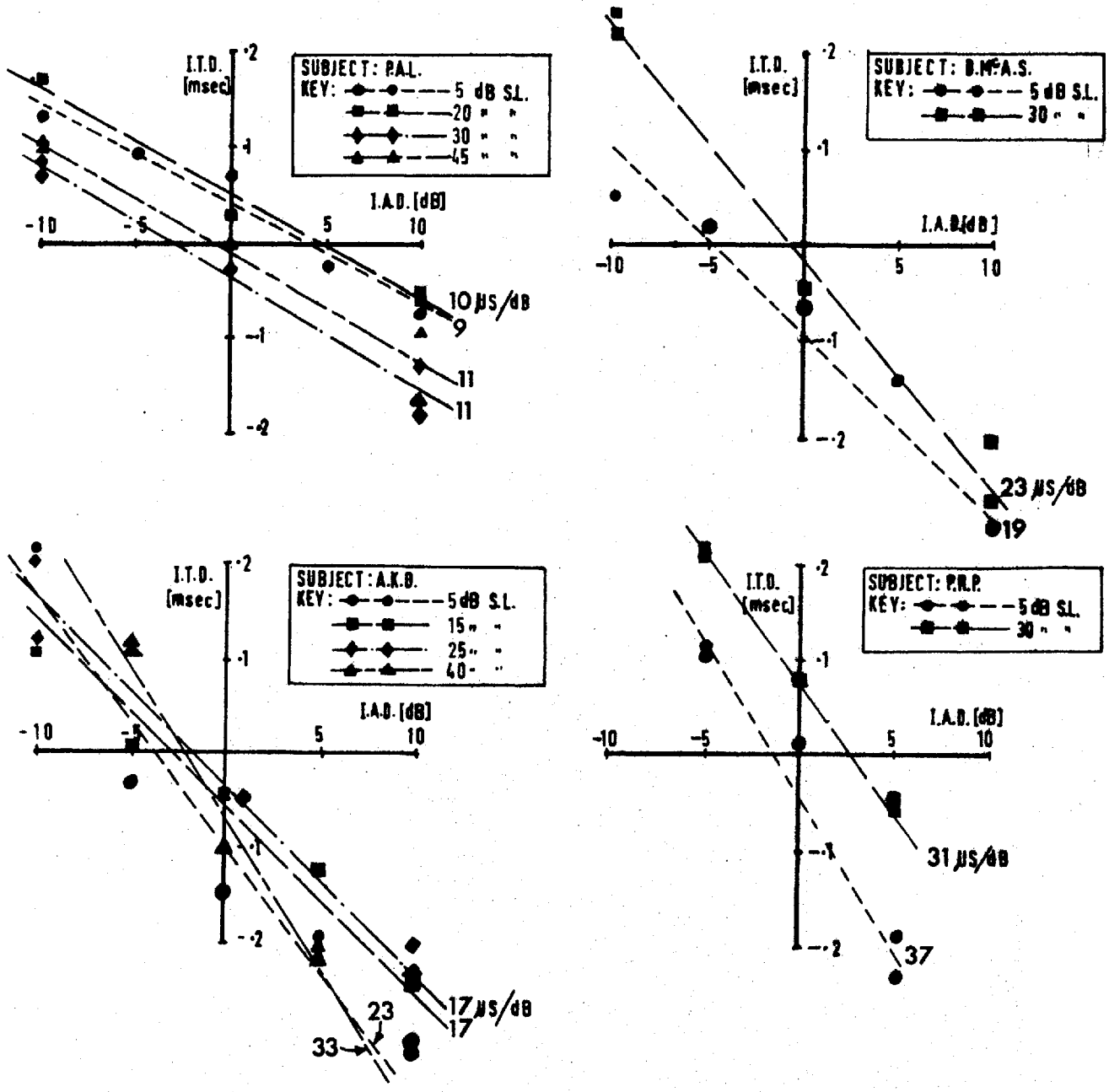

Figure 19 Curves for four listeners of the ITD required to return a binaural image to judged central location after displacement by IAD imposed by the experimenter. Low-pass (800 Hz) filtered waveforms from 0.1 msec. rarefaction transients repeated 30/sec. at various signal levels. The figure shown against each curve represents the slope of the approximate best straight line, fitted to 50 judgements.

The results of this simple but important measurement show considerable consistency between the various subjects, with no apparent dependence of the ITD/IAD trading ratio on the absolute sound level of the test, at least for this type of signal. Although these measurements cannot rule out the possibility that the extent of the trading relationship is altered at lower and higher sound intensities, the results do seem to suggest that the ratio is approximately constant in the normal hearing environment, at least for signals of a type which give a fused binaural image of a predominantly low-pitched, impulse character.

3.4 A proposition about amplitude effects

It is believed that the perceived relationships between IAD and ITD, reported in the previous section, can be accommodated by currently understood peripheral mechanisms. In particular it is proposed that, if neurophysiological activity observed in the cat is also relevant to the human, a straightforward explanation of the main effects of IAD/ITD trading is available in terms of cochlear neural activity.

In more detail, the present proposition is that the effective centre of gravity of the averaged neural responses to a repeated transient stimulus, specifies in neural terms the basic temporal features of that signal for binaural lateralisation purposes. It is assumed that the post-stimulus-time histogram for a particular fibre, responding to many repetitions of a stimulus, represents equally well the ensemble average of neural activity over many fibres with sensory endings in the same cochlear region, responding to a single stimulus. Thus the form of the single unit PST histogram seems relevant to a discussion of image lateralisation judgements made on the basis of even relatively few stimulus presentations.

By specifying the centre of gravity of the neural PST histogram as the important parameter, it is implied that it is the average time, post-stimulus, of generation of stimulated neural activity in the two ears which is used to form binaural lateralisation judgements. This seems appropriate for the type of listening experiment just reported, where the subject is not asked to separate out multiple images presumed to be due to the individual peaks of the PST histogram. Even if he did so (so that his judgements tended to fall into groups reflecting such multiple images), the averaging of the

results by the experimenter must ensure that only some mean effect is finally recorded.

Assuming that neurophysiological recordings on cat (reviewed in Section 2.7.2) are relevant to the human cochlea, it is clear that the relative increase in size of the earlier peaks of a click PST histogram with increasing intensity may well provide just such a shift in the centre of gravity of the histogram, even though there may be no change in the latencies of individual peaks. It is therefore interesting to check whether such a proposition is quantitatively supported by the neural data, and an attempt has been made to estimate the order of centre of gravity shift in histograms measured by Kiang[37], as a result of change in signal level. If the effect is indeed relevant to the human binaural situation, an increase in signal level at one ear would be expected to result in a time advance of the PST histogram centre of gravity for first order cochlear nerve fibres emanating from the maximally active basilar membrane region, even though no change in latency results for the individual PST peaks. The effect would give rise to an apparent lateral displacement of the binaural image towards the side receiving the earlier neural signals, which could be compensated by time advancing the contralateral signal. Thus such a mechanism could provide a source for the IAD/ITD trading relationship observed.

In Figure 20 are shown some estimates made from the recordings of Kiang[37], of centre of gravity shifts as a function of stimulus intensity for a number of first order units. The best method of calculation is debatable for units exhibiting spontaneous activity, since a reduction of neural

activity during condensation movements of the basilar membrane can be argued to be as much a stimulus-locked response as the peaks of the PST histogram themselves. In cases where an attempt has been made to allow for this effect, it has been found to cause little change in magnitude of the estimated shift. The calculations are therefore based on the relative size and latency of the PST histogram peaks only, which provide estimates accurate enough for the present purpose.

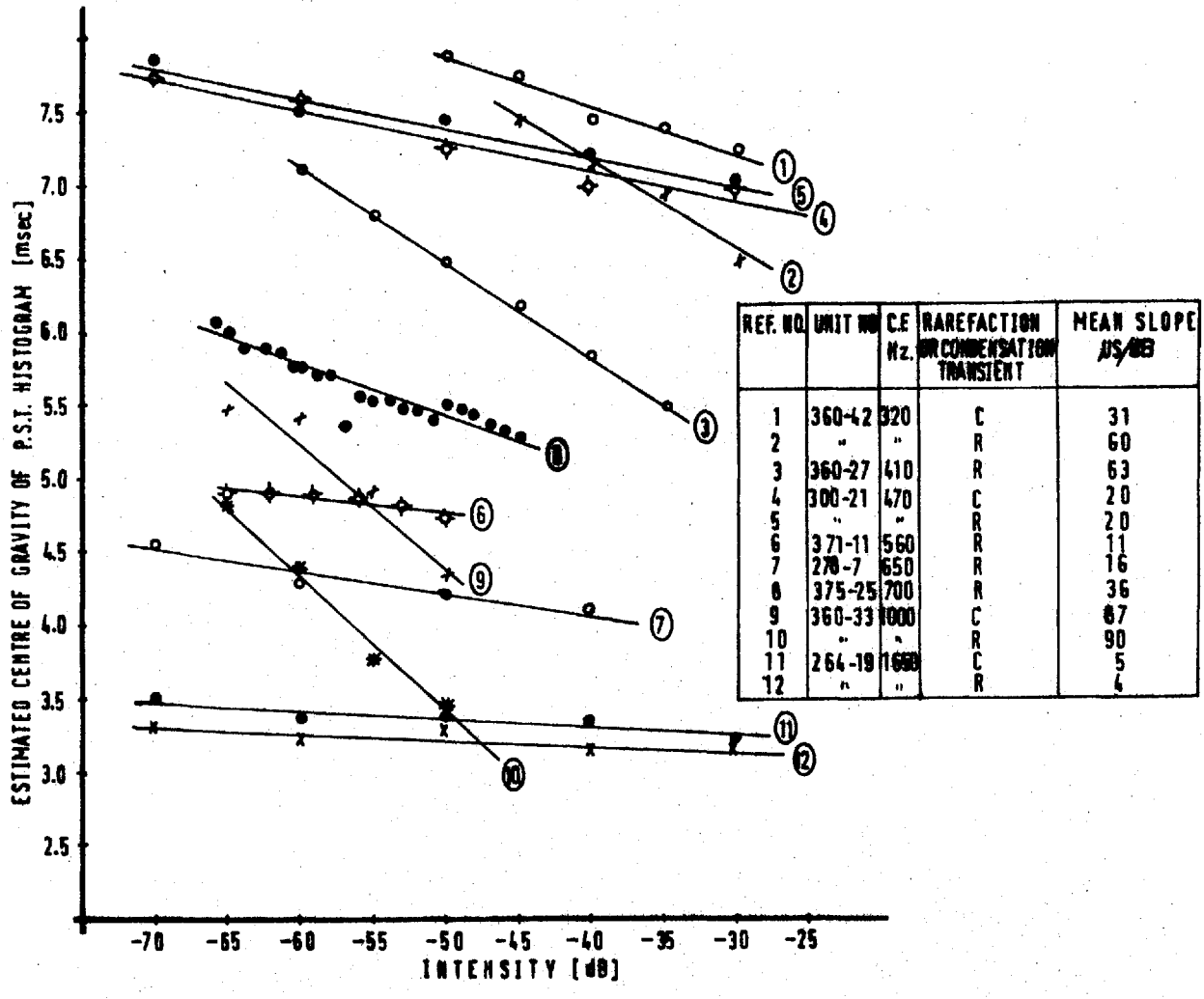

REF. NO.	UNIT NO.	C.F. Hz.	RAREFACTION OR CONDENSATION TRANSIENT	MEAN SLOPE µs/dB
1	360-42	320	C	31
2	"	"	R	60
3	360-27	410	R	63
4	300-21	470	C	20
5	"	"	R	20
6	371-11	560	R	11
7	270-7	650	R	16
8	375-25	700	R	36
9	360-33	1000	C	87
10	"	"	R	90
11	264-19	1600	C	5
12	"	"	R	4

Figure 20 Estimated centre of gravity of a number of PST histograms as a function of click signal level; the fibres are described by their C.F., and their code numbers are those used by Kiang[37]. The last column in the table shows the average slope of time shift with amplitude level, proposed to be relevant to binaural time-amplitude trading.

Two observations which are felt to be significant are that the centre of gravity shift in the PST histograms seems to be maintained throughout the dynamic range studied, and that the effect seems to be not noticeably dependent on the stimulus level. Also, the time-shift/intensity ratio seems to bear no obvious relation to the C.F. of the fibre considered. The actual magnitude of the ratio is some 37 μsec/dB over all the units for which calculations were possible, and which may be presumed, on the basis of their C.F. values, to innervate medial and apical cochlear regions.

It is extremely interesting that in the reported experiments with low-pass filtered binaural transients, the time-intensity ratio seemed to be independent of signal level and for all subjects fell in the range 10 - 35 μsec/dB. It is also true that as far as experiments have gone, this ratio appears not to be clearly related to the low-pass filter cut-off frequency used to generate the filtered transients. All of these features thus parallel effects observed in the experimental animal, if the above interpretation is correct.

The proposition suggests certain other types of relevant experiment; in those discussed so far, presumed shifts in the centre of gravity of neural PST histograms have been produced by changes in signal level. There is however another way in which centre of gravity shifts might be imposed, by utilizing a masking effect presumed to be due to neural refractory properties. Consider, for example, a monaural double pulse train (pulse C following pulse B in each pair with suitable spacing). If a cochlear neuron has fired in response to the first pulse (B) of the pair, it may well be in a refractory condition when the second pulse (C) arrives; it might

reasonably be expected, therefore, that there will be a significant reduction in the size of the earlier peaks of the PST histogram for C. The effect would be expected to increase with the level of B and to be broadly similar to a reduction in the amplitude of C, in terms of centre of gravity time-shift. Therefore, a contralateral probe pulse train (A) could be used in a binaural experiment to detect such timing shifts in respect of pulse C. Some experiments of this type are now reported.

Rarefaction transients (from trains of 0.1 msec. electrical pulses low-pass filtered, 0-800 Hz transmission band, as in the previous experiments, and applied to HA-10 headphones) were used to produce pulse trains A, B, C (A at one ear, B and C at the other, with relative levels specified as A:B:C), with a repetition rate of 30 per second and, where appropriate, BC spacing of 7 msec. Any one diagram in the two following figures shows results taken at one sitting. With levels 1:0:1, the listener was required to judge and report the lateral position of the binaural AC image for various ITD values set randomly in a continuous range by the experimenter. After establishing that the complete trajectory was symmetrical about the subjective centre position, particular attention was directed to ITD values giving lateralisation judgements of the AC image near subjective centre (since a near-central image is most reliably reported).

Figure 21 shows some results for three subjects. Much less importance is attached to the slopes of the curves than to the ITD position for a centralised image, since the latter was much more extensively investigated.

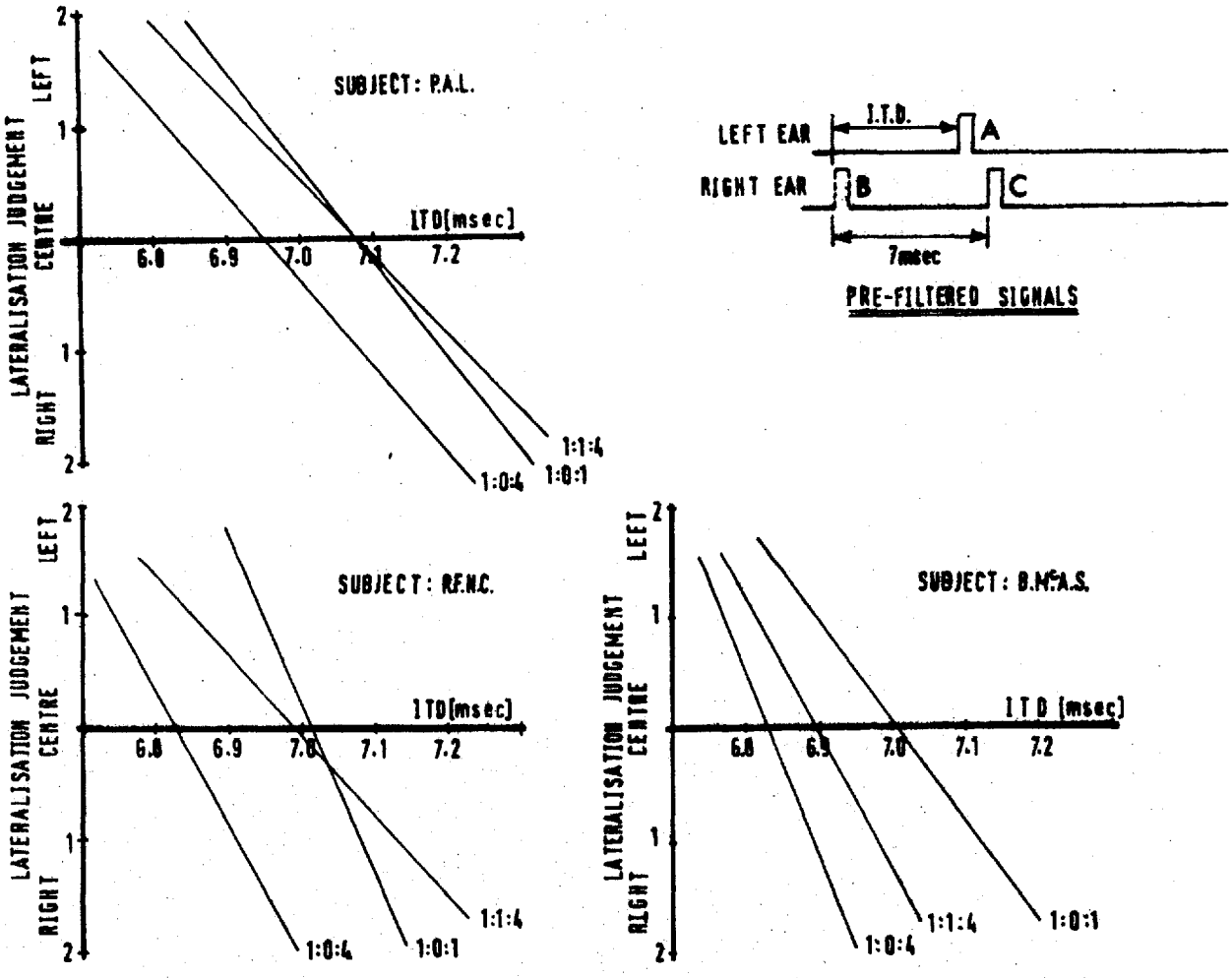

Figure 21 Lateralisation judgements for 3 listeners for the (AC) image formed between a single low-pass filtered pulse C which may be preceded by a pulse B, 7 msec. earlier in time. Relative amplitude levels as indicated. Each line represents a fit to some 40 judgements, with a typical standard deviation of between 20 and 40 microseconds.

Initially pulse B was removed, and pulses A and C were set to equal level of about 35 dB S.L. The curves for this case are labelled 1:0:1. When the level of pulse C was increased by 12 dB (i.e. A:B:C: becomes 1:0:4), the results showed a trajectory shift of the AC image in the usual manner and to an extent (10-20 μsec/dB) consistent with previous observations in the same, single-image, situation. Pulse B was then introduced at the same level as A (A:B:C becomes 1:1:4), B preceding C by 7 msec.; the AC image trajectory was found

to be displaced back towards its original position.

Since in this experiment no attempt was made to resolve the AC image into components which might be separately associated with the individual peaks of the click response PST histogram in respect of pulse C, these judgements should also reflect simply a change of centre of gravity in the histogram, if this occurs. The proposition that a change of centre of gravity of the PST responses in respect of the C pulse results from the masking imposed by introducing the B pulse would seem to provide a simple explanation of these results.

It can be shown that the effect is, as would be predicted, progressive in that the larger B, the greater the effect on C. Figure 22 shows the lateralisation characteristics for the same type of experiment when the B pulse is present at one of several levels (A:B:C thus 1:$\frac{1}{2}$:4, 1:1:4 and 1:2:4), in which this progressive shift is confirmed.

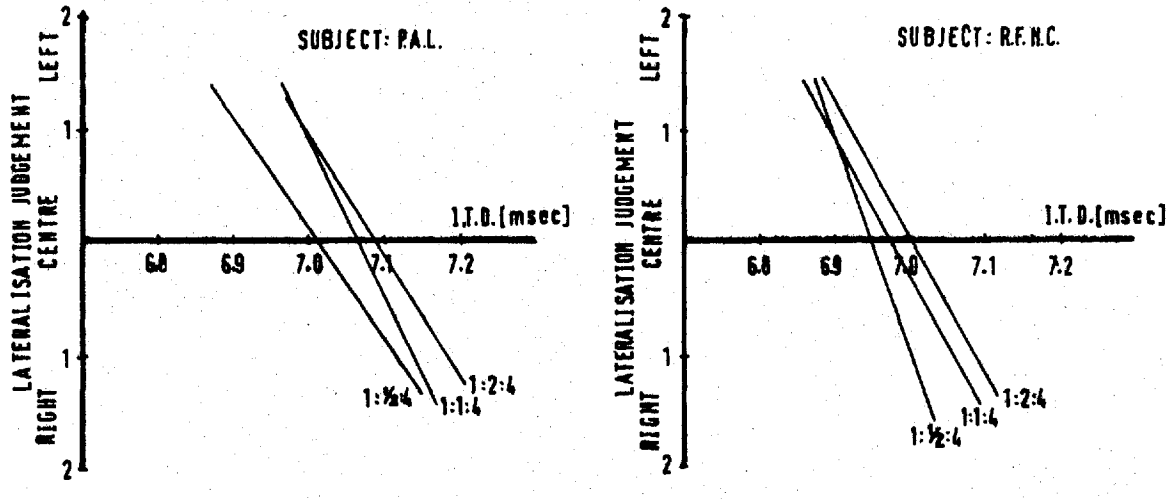

Figure 22 Effect of B pulse level on the lateralisation characteristics of the image AC. Each line again represents a fit to some 40 judgements, with a typical standard deviation of between 20 and 40 microseconds.

3.5 Further discussion

The simplicity with which the perceptual effects discussed here can be interpreted, if neurophysiological mechanisms observed in the cat are also relevant in the human, is striking. In the nature of the listening experiments no attempt has been made to resolve the perceived complex images due to filtered clicks into separate images which could perhaps be associated with peaks of the PST click histogram of neural firings; indeed, if the proposition is correct, there should be no appreciable latency change in each of these resolved images when the sound level changes, since there is little or no shift in the latencies of the individual histogram peaks due to intensity changes.

It should be possible to test this hypothesis by investigations using a situation in which multiple binaural images can be identified, provided that these can be presumed to arise from successive peaks of the averaged neural response. One of the simplest situations of this type occurs with a train of single low-pass filtered pulses presented binaurally in antiphasic mode (condensation pulses at one side, identical rarefaction pulses at the other), both left and right ear signals being low-pass filtered to, say, 800 Hz. In this case, while judgements are difficult, two images can be separated, one of which is more clearly defined than the other; the trajectory of this image, and the ITD at which it is centred for various IAD values, can be determined. This image trajectory with ITD is found to be unaltered by IAD and the image is centred at the same location (provided that the rarefaction transient is not smaller than the condensation transient), over the range of 15 dB change in IAD which has been tested. The second

image does seem to show some changes with IAD and this effect may perhaps be attributed to an inability to separate the contributions due to later peaks of the averaged neural responses, so perhaps allowing the centre of gravity of remaining peaks to dominate judgements.

The apparent time-shift introduced by change of signal level seen in the main experiments reported above, is thus envisaged as a product of the present experimental technique. Thus while it is proposed that the effects of changing signal level are indeed very real when viewed in the click PST histograms of fibres emanating from the most important cochlear region (or any other), the effects expressed in trading relations between ITD and IAD in, say, a binaural situation, are thought to exist only when judgement averaging by listener or experimenter takes place.

It would seem to be a salient feature of the way the PST click-histogram changes with signal level, that the average number of spikes per stimulus changes relatively little over the signal amplitude range, except near threshold for units with low rates of spontaneous firing. Increasing signal level therefore would be represented by an increase in the number of units responding, as expected from other evidence. It is difficult to rule out the possibility that the total number of units producing signal-synchronized firings at each cochlea is in some sense assessed by mechanisms in higher centres of the auditory pathway and that this affects lateralisation judgements. Time shifts would not be expected to arise in this way, but a bias on the lateralisation judgements might result. Some such mechanisms may be relevant to the vertical displacement, without time shifts, of lateralisation trajectories seen with pure tones when an IAD is introduced

(Sayers[52]). Since imposing an IAD with a continuous repetitive waveform seems dominantly to result in a position bias of lateralisation trajectories (i.e. towards one side), while with transient type signals a time-shift of lateralisation trajectories seems most important, it might be concluded that separate mechanisms are involved. The proposition put forward here is envisaged as relevant for transient-type waveforms, but, by its nature, would not apply to, say, sinusoids.

It is believed that the existing framework for the description of certain perceptual effects in binaural hearing has now been extended to cover the main effects of interaural amplitude difference. If the present proposition is accepted, then it follows that the amplitude of transient signals is almost certainly coded at the most peripheral neural levels in two distinct ways. Firstly, the number of first order neurons responding to a particular stimulus will increase with signal amplitude, and individual neurons may or may not show a significant increase in total stimulated activity, reflected in increased firing probability. This much has been generally recognised. The other interesting effect of amplitude is that of a timing shift, reflected not in a latency shift of averaged neural activity due to individual basilar membrane oscillations, but in a change in the mean centre of gravity of the total neural response. Complex effects in the neural transduction of the cochlea, as seen in microelectrode recordings from cat, are of great interest in their own right, and must reflect importantly on the mechanisms involved; the proposed relationships between such complexities and binaural perception give, however, a powerful additional motive for their exploration.

4. PREVIOUS MODELLING OF THE PERIPHERAL AUDITORY SYSTEM

4.1 Van Bergeijk: model of cochlear spiral innervation

Van Bergeijk[65] has attempted to explain the large dynamic range of the cochlea in terms of its innervation. He considered effects at a node of converging fibres, such as would occur in a spiralling fibre which puts out a large number of terminations to the outer hair cells. Assuming that these terminations act as independent spike generators and that the fibres have refractory properties, Van Bergeijk argued that, at low stimulus intensities, neural spikes arriving at the node would be unlikely to interfere because of their infrequent arrival along different terminal paths. At higher intensities, however, the refractory properties of the nodal fibre would cause increasing interference between approximately coincident spikes. The postnodal portion of the fibre would therefore saturate slowly with intensity.

Such a situation was simulated using artificial neurons, or neuromimes, demonstrating that the more terminal branches each spiralling fibre had, the greater the effective dynamic range of the system.

4.2 Siebert and Gray: analysis of nonstationary neural activity

Although the peripheral auditory system may not have been the prime motivation for an analysis of nonstationary neural activity by Siebert and Gray[55], they suggested that the measured activity of first order auditory neurons should form a good test of their results. In attempting to derive an analytically manageable model of nonstationary neural processes, they defined the conditional probability p' of a neural spike in a small time increment δt :-

$$p'[1 \text{ spike in } (t,t+\delta t), \text{ previous spikes at } t_1, t_2, t_3 \ldots]\delta t$$

$$= g[r(t), t_1, t_2, t_3 \ldots.].\delta t$$

Thus the probability is assumed to depend upon previous firing times (t_1, t_2, t_3 ....) and upon the instantaneous value of an Intensity Function r(t). They then considered a particular case in which p' may be defined as the product of the Intensity Function, r, and a Recovery Function, s. Thus:-

$$p'[1 \text{ spike in } (t,t+\delta t), \text{ previous spikes at } t_1, t_2, t_3 \ldots]\delta t$$

$$= r(t).s(\int_{t_1}^{t} r(u).du).\delta t$$

In this simplified case, the recovery of the neuron is assumed to be dependent only on the time since the previous firing (t_1), and is effectively speeded up by the application of a high level stimulus, since it now depends on the time integral of the intensity function between t_1 and t. Siebert and Gray then showed that this last equation may be transformed to:-

$$p'[1 \text{ event in } (\tau,\tau+\delta\tau), \text{ past events at } \tau(t_1), \tau(t_2) \ldots]\delta t$$

$$= s(\tau(t) - \tau(t_1)).\delta t$$

where τ is a new time variable given by:-

$$\tau(t) = \int_{-\infty}^{t} r(u).du$$

In terms of the new clock τ, the process is stationary, p' no longer being a function of the stimulus. If the Recovery Function is unity, the process reduces to a stationary Poisson process. However in the general case when the neuron has not fully recovered from its previous firing, a second clock time may be defined (which now depends on previous output firing times), in terms of which the process is again stationary.

Using such an approach, Siebert and Gray then derived the inter-event distribution (interval histogram) for the case of a constant value of the Intensity Function. They also showed the unconditional firing probability in a small time increment to be proportional to the Intensity Function, thereby giving this function a simple interpretation in terms of a neural PST histogram. Finally, they derived an analytic expression for the interval histogram for a periodic Intensity Function, although they did not apply such results to any specific system.

4.3 Weiss: a model of the peripheral auditory system

Weiss' digital computer model[67] for the firing patterns of auditory nerve fibres represents perhaps the most complete attempt yet made to model the peripheral auditory system, and in particular to reproduce its neural responses to a variety of simple acoustic stimuli. Unlike Siebert and Gray's work, which is predominantly mathematical and not specifically related to the cochlea, Weiss' model takes some account of peripheral anatomy and physiology. Figure 23 shows the main elements of his model.

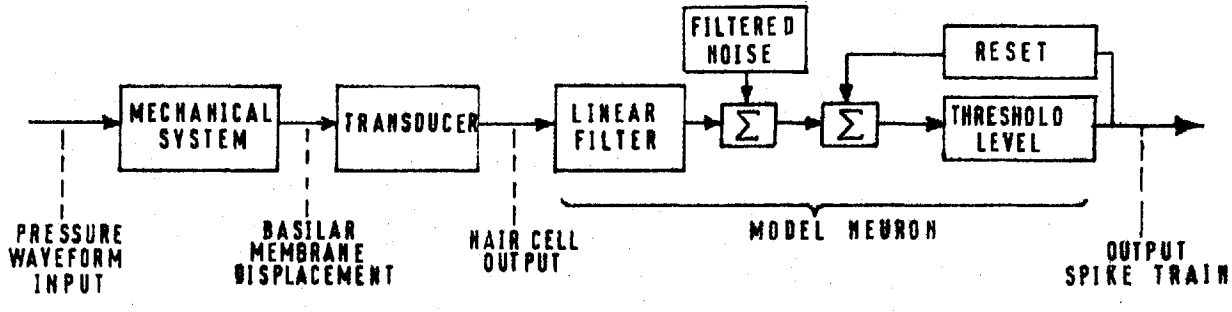

Figure 23 Block diagram of Weiss' model of the peripheral auditory system.

A linear mechanical system, the output of which is the displacement of a point on the basilar membrane computed by using Flanagan's formula (see Section 2.1), forms the input to a transducer representing the action of the hair cells. The transducer output is added to a low-pass filtered noise signal to produce the simulated membrane potential of a first order auditory neuron. This latter potential is compared with a firing threshold, and, whenever the threshold is exceeded, an output spike is generated and the threshold reset to some high level. The subsequent decay of the threshold

towards an equilibrium value represents the refractory properties of the neuron. These points are illustrated by Figure 24.

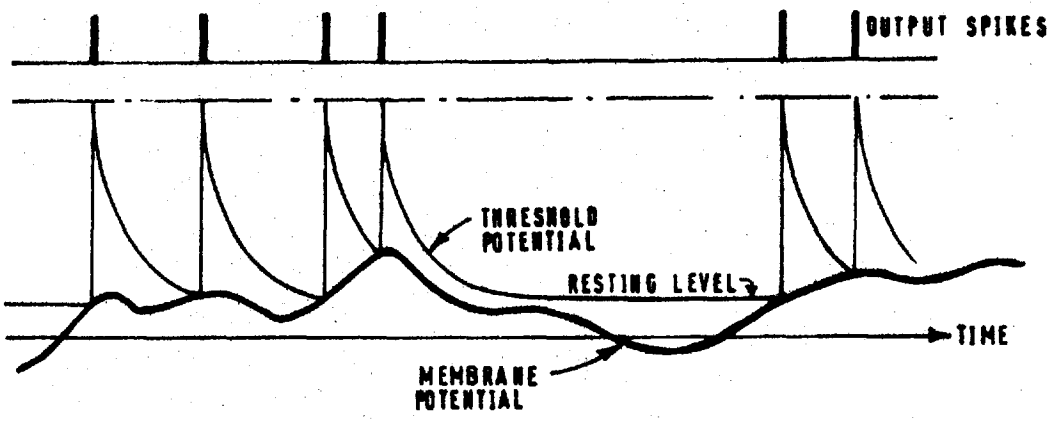

Figure 24 Diagram showing typical time courses for the membrane potential, threshold potential and spike activity of Weiss' model.

The main assumptions of Weiss' model may be summarised as follows:-

(a) The mechanical system is linear over the dynamic range of interest.

(b) The frequency response of the outer and middle ear is flat in the frequency range 100 Hz. to 2KHz.

(c) A particular neural fibre is excited by hair cell(s) responding to the displacement waveform of a single point on the basilar membrane.

(d) Efferent effects are ignored.

4.3.1 Spontaneous Activity

Spontaneous firing by the model is caused by random fluctuations of the membrane potential sufficient to exceed threshold. As Figure 24 shows, the threshold is reset to some high value when a firing occurs and subsequently decays exponentially towards its resting level. Because the membrane voltage is not reset when the neuron fires, there tends to be serial correlation in the output interval sequence. This is particularly the case when the noise, which is low pass filtered, has a limited bandwidth (in which case a particular value of the noise waveform tends to be preserved during several output spike intervals, giving rise to groups of successive intervals either longer or shorter than the mean). The fact that no significant serial correlation has been detected in the records of spontaneous activity of first order auditory neurons in cat (see Section 2.7.1) suggests that the passband of the noise must extend at least up to about 3KHz. This is corroborated by the form of the interval histograms generated by the model, which are too long-tailed (i.e. there are more long intervals than are observed experimentally) if the noise bandwidth is reduced.

Weiss also showed that the rate of spontaneous activity generated by his model was critically dependent on the ratio between the standard deviation of the noise and the resting threshold level. A 50°/o change in the ratio can produce a 500°/o change in spontaneous firing rate, and rates of 500 spikes per second can easily be achieved with a threshold resetting time constant of the order of 1 millisecond.

4.3.2 Response to stimuli

When considering the model's response to sinusoids, Weiss concentrated not so much on the fine details of PST or interval histograms as on the mean rate of firing as a function of stimulus frequency and intensity. By comparing firing threshold data for a large number of first order auditory neurons in cat with the mechanical sensitivity characteristics of the basilar membrane, he inferred that the transducer-neuron system must somehow contribute a change in sensitivity of the order 15 dB/decade in the frequency range 200 Hz. - 2KHz. By testing the model with sinusoids of different frequencies, and assuming a linear transducer, he showed that such an effect was present, although not perhaps to such an extent as 15 dB/decade.

In the case of click stimuli, the model failed to provide more than two peaks in its simulated click PST histograms unless a nonlinear transducer function was assumed. A function of the form:-

$$F(y) = \frac{k_1 y}{k_2 + y}$$

where $F(y)$ = transducer output

y = transducer input

k_1, k_2 = constants

gave a number of peaks in the click PST histogram, but there was no suppression of the earlier peaks at low stimulus intensities. Further, an input dynamic range of some 100 dB was required to obtain the full range of PST histogram shapes (i.e. before the response became stereotyped), which is some 40 dB more than is required by a typical auditory neuron.

Weiss considered the lack of suppression of early PST histogram peaks at low intensities to be a trivial issue, and probably due to an error in the form of basilar membrane impulse response which he used (that of Flanagan[16]). A different class of nonlinear transducer functions, of sigmoid form, was suggested for solving the dynamic range problem, but the matter was not further investigated by computer simulations.

4.4 Geisler: neural responses to pure tones

Geisler[22] has used a model essentially similar to that of Weiss in an attempt to reproduce some pure tone interval histogram data from cochlear neurons. His method was to simulate a single neuron's activity in response to a range of sinusoidal frequencies by driving the model at such a level that its output rate variation was similar to that measured in a real neuron. In order to account for the observed dynamic range and for variations in mean firing rate with intensity, he, like Weiss, had to incorporate a nonlinear transducer function. In this case, however, a simple logarithmic transformation was used for rarefaction displacements of the basilar membrane, with high intensity limiting. Apart from a rather unrealistic high intensity performance, the model produced interval histograms broadly similar to those observed experimentally. No attempt was however made at further statistical analysis.

4.5 Discussion

In this chapter, previous work which is specifically related to the peripheral auditory system has been briefly reviewed. Much other work has been done in recent years on neural models, either of a general kind, or of other specific systems (see, for example, a review by Harmon and Lewis[27]). Some of these latter investigations may have important implications for research into peripheral auditory mechanisms; reference to them will however be reserved for the particular sections to which they are most relevant.

Van Bergeijk's model of cochlear spiral innervation is unusual in that it takes account of the cochlear innervation pattern. However, it considers no details of the generation of spike activity and ascribes an increase in dynamic range to the presumed refractory properties of cochlear nerve fibres. It makes the assumption that action potentials are initiated in the extreme terminal branches of a spiralling fibre, which is a point of some debate; for example, Spoendlin[58] considers the action potentials to be generated where the fibres enter the habenula perforata, and where they first become myelinated (see Section 2.6).

Although Van Bergeijk considers the large cochlear dynamic range to be the result of the spiral innervation, it seems that multiple innervation would also be sufficient to support the same general conclusions. His argument relies upon the convergence of a number of dendritic terminations at one node, a situation which would also exist in a radial fibre innervating more than one hair cell. Recent work by Engstrom (see Section 2.5) suggests that a spiral fibre puts out terminations to hair cells only towards the end of its

spiral course, so that extensive branching along its length no longer seems likely. It may be that some other functional significance is reserved for the spiral innervation pattern.

Siebert and Gray's work suffers from the present disadvantage of all attempts at analytical description of non-stationary neural activity - that of great complexity. By assuming the probability of firing of a neuron to be the product of two functions, one dependent on instantaneous stimulus intensity and the other on the recovery characteristics of the neuron, and by effecting a time transformation, they achieved some analytical simplification. It is, however, difficult to see how their model can make realistic predictions of neural responses to, say, click stimuli, even with the considerable assumptions which they have made, bearing in mind the complex effects which appear in the published electrophysiological recordings in cat. As has already been pointed out in Section 3.5, it is these fine effects which are the ones of present interest because of their postulated correlates in aural perception, and because of the clues they probably give to the detailed nature of cochlear transduction. For this reason it seems impossible to avoid computer modelling of the neural transduction process.

Weiss' computer model is of greater direct interest, although the assumption of a simple radial innervation scheme is at variance with the known neuroanatomy. Although he does not discuss this issue in any detail, it must be likely that some of the less satisfactory results from the model are due to this over-simplification. The spontaneous activity of the model may be made to parallel that of real auditory neurons provided certain assumptions are made about the filtered

noise presumed to generate it. One difficulty is that spontaneous rates in excess of 500 spikes per second may readily be generated when an otherwise appropriate value of threshold time constant is used; such rates are not observed in the experimental animal. The proposition that such activity is due to random nerve membrane potential fluctuations may well be sound. On the other hand, the very great sensitivity of the ear makes it seem probable that the mechanical and transducer systems are involved in the production of noise.

The response of Weiss' model to click stimuli clearly demonstrates that a nonlinear transducer characteristic is necessary to represent hair cell activity, at least if the other assumptions of the model are valid. However, the empirical selection of a function to fit the data is one of the more unsatisfactory aspects of the model. Weiss' contention that the suppression of the first peaks of click PST histograms at low intensities is a trivial issue and that it probably reflects an error in the form of the impulse response used, seems unsupportable. At low intensities, the third peak of such a PST histogram is generally the greatest, in spite of refractory effects. The third peak of presumed basilar membrane displacement is perhaps 1 or 2% of the size of the first peak, so that any such contention must imply that the impulse response waveform used is radically in error. It further seems clear that if the response waveform were altered empirically in order to fit the data, then it could no longer be characteristic of a damped linear system.

Some of the statistical results reported by Gray (see Section 2.7.3) cannot be reproduced by Weiss' model. For

example, the recovered probability of firing during the first rarefaction half cycle (2C) due to a condensation click is always greater than that during the first half cycle (1R) when a rarefaction click of the same intensity is used. This suggests that previous basilar membrane activity affects subsequent nerve fibre activity even when it does not cause firing. Weiss' model holds no memory of previous stimulus conditions apart from refractory properties, and cannot therefore produce such effects. It seems quite possible that a model based more firmly on known cochlear structure and function (particularly the innervation details) would solve some of these difficulties.

Problems of the same kind occur in Geisler's model for tone responses, which is essentially similar to that of Weiss. Once again an arbitrary nonlinear transducer function was invoked to reproduce interval histogram data for pure tones.

The work reviewed here provides some valuable clues and suggests some important questions. The failure of Weiss' model to match actual click PST histograms in important respects seems to suggest that such data hold significant clues to the neural transduction process. It seems that a model based on physiological concepts which reproduced such recordings would probably also explain the detailed responses of cochlear neurons to other simple stimuli.

5. MODELS FOR THE SPONTANEOUS ACTIVITY OF COCHLEAR NERVE FIBRES

5.1 Introductory comments

Although the matter is still finally unresolved, recent anatomical work tends on balance to support the idea of chemical transmitter activity at the afferent hair cell - neuron junction in the cochlea (see Section 2.6). Such a system has never been investigated in detail in a peripheral sensory mechanism, but there has been much investigation of chemical transmitter effects at central nervous synapses, and a considerable body of knowledge also exists in the case of the neuromuscular junction[8,33,35,41,49]. In the latter system it is clear that there is generally random emission of quantal packets of chemical transmitter across the synaptic junction, giving rise to spontaneous miniature postsynaptic potentials (psp's) which may be measured by a microelectrode in the post-synaptic terminal.

The danger of drawing parallels between two very different systems such as the neuromuscular junction and the sensitive auditory receptor must not be underestimated. However, if there is measurable random chemical release in the neuro-muscular junction, then the much greater sensitivity of a hair cell receptor would lead one to expect it there also. Such a scheme would seem to provide an attractive proposal for the generation of spontaneous activity in first order auditory neurons. As far as stimulus conditions are con-cerned, it might be proposed that local basilar membrane movements cause a modulation of the ongoing (spontaneous) release of chemical transmitter. Thus stimulus activity would become a controlled modulation of a noise process

which is at all times active. Although there is no direct evidence for such a scheme, it seems intuitively attractive in that it assumes spontaneous and stimulated activity to be closely related phenomena. A chemical transmitter model for stimulus activity has the further attraction that there are a number of complex effects in documented chemical systems (such as delayed mobilisation of transmitter and its subsequent migration up to the synaptic boundary, discussed later in Section 8) which might perhaps explain the complex effects visible in the neural PST histograms.

Although spontaneous activity is sometimes dismissed as a noise process of no great interest, a close inspection of it poses some interesting questions. Because observed spontaneous activity in first order auditory neurons has well defined characteristics (see Section 2.7.1), constraints must presumably be imposed on the values of parameters used in any simulation. However, before discussing such matters in detail, it seems appropriate to consider work which has already been done on the general characteristics of chemical transmitter models; these have in fact received considerable attention in the literature. Much of this work assumes a random release of quanta of a chemical transmitter substance across a synaptic boundary, although the theoretical analysis of even simple systems of this type is far from complete.

It might seem quite reasonable to ascribe spontaneous spike generation in neurons to other factors, such as chance fluctuations in the potential of the nerve membrane. Weiss' model of the peripheral auditory system (see Section 4.3) assumes spontaneous activity to be due to membrane noise of this type, occasionally sufficient to exceed firing threshold.

He quotes evidence that such fluctuations are more significant in nerve fibres of small diameter, and, since cochlear fibres are very fine, he considers them suitable candidates for such an effect. There might even be a combination of chemical and membrane noise.

The section which follows is not therefore intended to imply that spontaneous activity in cochlear fibres is necessarily of chemical origin, but rather that it seems interesting to investigate the possibility more quantitatively than has so far been attempted.

5.2 Previous chemical models for random neural activity

5.2.1 Stein's model

One of the most complete treatments of the general chemical synaptic system is that of Stein[59], whose model is represented diagrammatically in Figure 25.

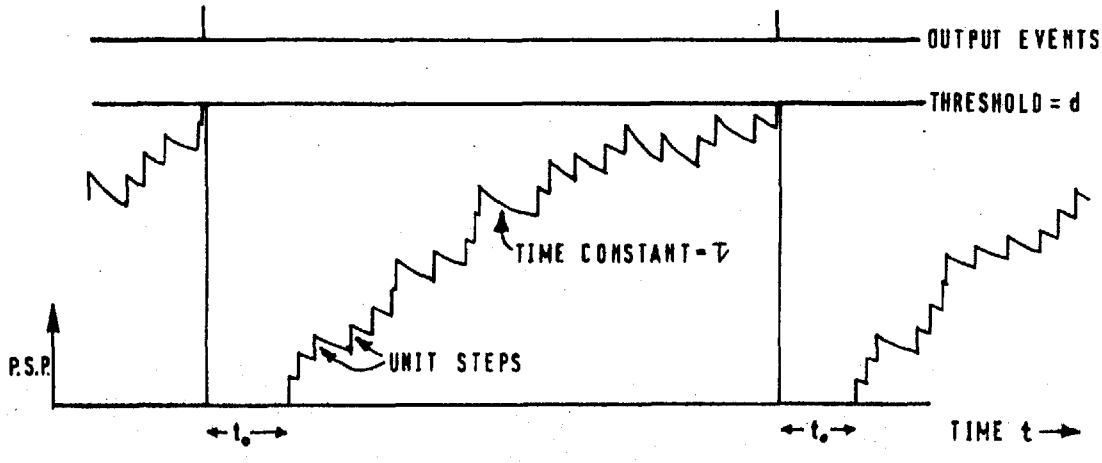

Figure 25 Typical time course of the postsynaptic potential and output spike sequence in Stein's model of a neuron.

The random liberation of chemical quanta from the presynaptic terminal is assumed to be a Poisson process of rate n_e. These quanta have an excitatory effect on the postsynaptic membrane, each causing a unit step change in its polarisation, which then decays with time constant τ. This decay is generally considered to represent the destructive action of an enzyme present in the postsynaptic terminal. If the depolarisation of the nerve membrane (from its typical resting value of about - 70 mV.) reaches a critical threshold value (d), an action potential occurs and the membrane potential is reset. For a short time (t_o) after resetting further quanta have no effect; this corresponds to an absolute refractory period during which no firing can occur.

This model is a simplification of the usual physical situation. For example, it assumes all quanta to have the

same effect on the postsynaptic membrane, regardless of the latter's instantaneous level of polarisation. Furthermore, in assuming that the state of the membrane may be characterised by one variable, it excludes spatial summation effects in a dendritic tree, as discussed by Rall[48]; such effects might presumably be important in a spiral cochlear nerve fibre, (a matter to be investigated later in Section 6.2.) In spite of such simplifications, its theoretical analysis presents difficulties. Only in the special case of negligible decay of transmitter ($\tau \rightarrow \infty$) has the distribution of output events (spikes) been expressed analytically; in this latter case Stein shows the output interval distribution to be of gamma form:-

$$f(x) = n_e^{\,d}(x-t_o)^{d-1}.e^{-n_e(x-t_o)}$$

The two extreme cases of this generalised distribution are the Poisson distribution, which occurs when $d < 1$ (i.e. every input quantum causes an output spike), and the Gaussian, or normal, distribution, which results when the distance to threshold is much larger than the unit depolarisation step size (i.e. $d >> 1$).

In the case of a substantial decay, Stein has described the average time course of the P.S.P. waveform after resetting, assuming no firing, in terms of its mean μ and variance σ^2:-

$$\mu = n_e.\tau(1 - e^{-t/\tau})$$

$$\text{and} \quad \sigma^2 = (n_e\tau/2)(1 - e^{-2t/\tau})$$

Although there exists no simple analytic result for the form

of the output interval distribution in this case, certain deductions about it can be made from a consideration of the two above equations. For example, the fact that both mean and variance of the postsynaptic potential settle towards steady values after a few time constants suggests that the probability of firing during each subsequent small time interval is constant. This is a characteristic of the Poisson process, which implies that the tail of the output distribution must be exponential.

When inhibition is included, Stein shows that the climb of the PSP towards its equilibrium level after resetting may again be expressed analytically. Once again the mean and variance tend to settle towards constant values, allowing similar deductions to be made about the tail of the resulting output interval distribution in this case also.

In spite of the lack of analytic expressions for the output sequence in these more realistic cases of non-negligible decay of the PSP, Stein nevertheless succeeded in showing that a variety of spontaneous interval distributions, as measured in central and peripheral nervous systems, could be fitted empirically by gamma distributions.

5.2.2 Gerstein and Mandelbrot's random walk model

Using a somewhat different approach, Gerstein and Mandelbrot[24] paid particular attention to the measured spontaneous activity of certain neurons, in which the "scaling" of the interval histogram produces no change in histogram form, but only a simple change in scale. (An "n-scaled" histogram is one composed of intervals obtained by taking two events separated by (n-1) intermediate events). Such distributions are known as "stable", and amongst these are the Gaussian and Cauchy distributions, and the so-called stable distribution of order $\frac{1}{2}$. Since the particular form of interval distribution of the neurons in which they were interested could clearly not be described by either of the two first-mentioned distributions, they concentrated on the stable distribution of order $\frac{1}{2}$, showing that it is equivalent to a certain type of random walk model. In this model a particle starts from a certain point and moves towards or away from an absorbing barrier in a random series of positive and negative steps, meeting a reflecting barrier if it strays too far in the negative direction. Whenever the particle reaches the absorbing barrier an output event is recorded and the particle is reset to its starting position. Such a random walk process is analogous to a game of coin-tossing, in which, for example, the excess of "heads" over "tails" is recorded, the game starting again after a certain score has been reached. The fact that the system has an infinitely long memory accounts for some curious aspects of the stable distribution of order $\frac{1}{2}$; it has a very long tail because infinitely long output intervals are possible (the game may never end); and the moments of

the distribution do not exist (in the sense that they do not tend towards limiting values as the game proceeds).

Gerstein and Mandelbrot simulated such random walk models on a digital computer and found that by introducing a drift term (an excess of positive steps over negative steps in the random walk) they could simulate the spontaneous activity of such neurons with some accuracy. They further found that by introducing periodic changes in the drift parameter they could imitate interval histograms of a unit in the cochlear nucleus stimulated by clicks. It is not difficult to see that such a random walk model is closely analogous to the model of Stein, if no decay is assumed. Steps in the random walk correspond to the release of quanta, with the absorbing barrier acting as threshold. The main difference is that Stein did not consider cases in which excitatory and inhibitory inputs were both present to approximately the same degree.

5.2.3 Fetz and Gerstein: digital computer simulations

Fetz and Gerstein[14] used a digital computer to examine a model of the same kind with excitatory and inhibitory inputs, and also with decay. They were, like the other authors, unable to treat such a model analytically, but they did describe the general differences in the output interval distribution when the equilibrium level of the P.S.P. was either above or below the threshold, (the equilibrium value being the mean value to which the P.S.P. would settle if there were no firing). They showed that all such simulations tend to produce distributions with an exponential tail, although there was some slight evidence for longer tails if the mean excitation and inhibition levels were roughly equal. Apart from the inclusion of decay, such a situation is parallel to the Gerstein and Mandelbrot simple random walk with no drift, which also produces a long tail. Fetz and Gerstein concluded that their simulations could reproduce many forms of unimodal spontaneous interval distributions by suitable choice of parameters, and that revision of some of their assumptions (e.g. that quantal release conforms to a Poisson process) might produce further shapes of output distribution. However they failed to give any clear quantitative indications of the shape of the output distribution as a function of the input parameters, and their work was largely descriptive.

5.3 New modelling of spontaneous synaptic activity

5.3.1 Theoretical analysis by Johannesma

Models of chemically transmitting synapses which do not allow for decay of the postsynaptic potential have been analysed in detail,and the resulting distributions of the output events expressed analytically. It is however impossible to escape the fact that the decay of P.S.P. level, due to the selective destruction of chemical transmitters by enzymes, is well established, and so far no proper analytical framework has existed for the accurate description of this more realistic situation. Various computer simulations have been carried out, and although some idea of the influence of the input parameters on the output distribution has been obtained, this is still much too qualitative. From the point of view of spontaneous activity in first order auditory neurons, it is still unclear what range of input parameters is possible if the measured results of Kiang et al.[37] are to be reproduced.

In a recent paper, Johannesma[32] has used a new approach to analyse the input-output relations of spontaneous synaptic activity. By a collaborative effort in which the present author carried out simulations of the model on a digital computer, it has been possible to verify some of the main aspects of the theoretical work and to obtain considerable insight into the effects of changes of the various input parameters on the form of the output interval distribution. The main steps in Johannesma's analysis will now be outlined and his predictions presented, together with the results of the parallel computer simulations. Later sections will deal more specifically with the spontaneous activity of

cochlear neurons.

The model analysed by Johannesma is shown in Figure 26.

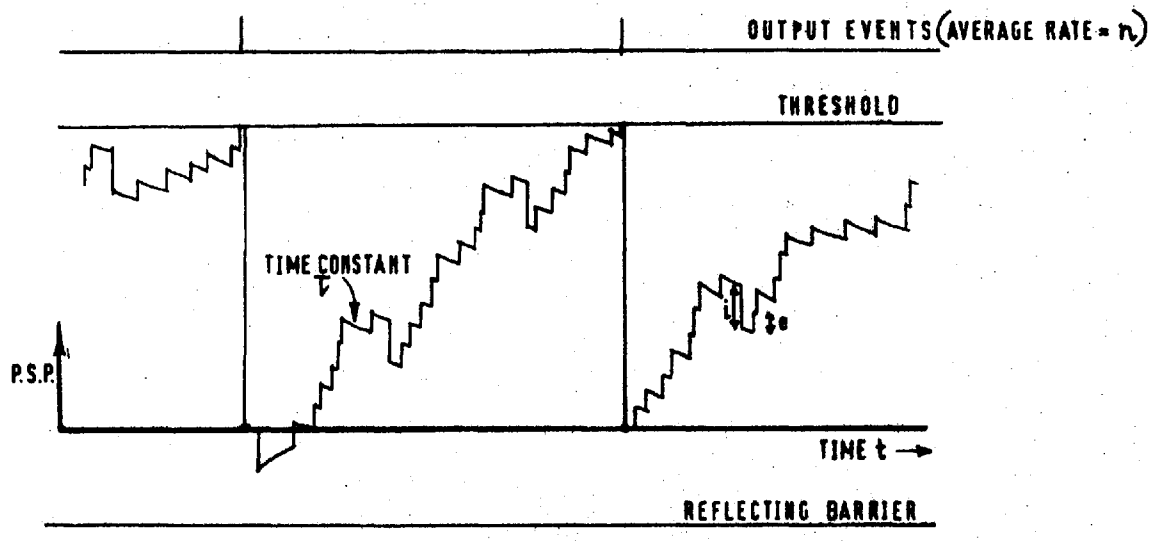

Figure 26 Johannesma's model of a neuron. Typical time course of the P.S.P. and output spike sequence.

It is more general than that of Stein in that both excitation and inhibition may occur with different step sizes and at different mean quantal rates. The P.S.P. decays towards zero with a time constant τ. Threshold refractory properties are not at this stage considered. Like all models in which the system is reset after each firing, this model generates an output sequence which is a renewal process; in other words the size of one interval between successive spikes cannot affect the next, so that there can be no serial correlation in the output interval sequence.

The important first step in Johannesma's analysis is the derivation of the transition probability, which is the probability that the P.S.P. reaches a particular value y at time t given that it started at a value x at a given instant (the time of the last output event). This is done by considering the various ways in which excitatory and inhibitory steps might effect such a transition. A simplifi-

cation of the resulting expression is made which is only valid if the step sizes due to excitatory and inhibitory quanta are small compared with the distance from starting point to threshold, the latter assumption now becoming important for the subsequent mathematical derivation of the model. Using this assumption, the expression for the transition probability simplifies and the following two input parameters appear:-

$$m = n_e.e + n_i.i \quad \text{(average or d.c. input)}$$

$$s^2 = n_e.e^2 + n_i.i^2 \quad \text{(a.c. component of input)}$$

where n_e = mean rate of excitatory quanta

n_i = " " " inhibitory "

e = step size of excitatory quanta

i = " " " inhibitory "

Furthermore, the equation now assumes the form of a diffusion equation with dispersion and drift terms.

The introduction of an absorbing barrier, or threshold, into the analysis converts the problem into one of finding the first passage time of the P.S.P. from its reset level to the threshold, and the solution exists in closed analytic form only in the case when the drift and diffusion terms are independent of the instantaneous P.S.P. value. In this case the so-called Weiner-Einstein equation results. In the more general case, however, Johannesma shows that a Laplace transform operation on the first-passage-time equation

allows any moment of the output interval distribution to be calculated in terms of the lower order moments, using an iterative procedure. Alternatively the use of the characteristic function of the distribution allows an iterative expression to be derived for the cumulants (see Appendix A). Finally, Johannesma discusses the possibility that the output interval distribution be expressed in various other forms such as by Pearson or gamma functions, or by a set of orthogonal polynomials; he also derives relations between such polynomials and the previously found moments and cumulants. Using these results Johannesma is able to predict the effect of input paramters on the output distribution of spike intervals, expressed in terms of its moment and cumulants. This work involves lengthy numerical approximations on a digital computer, and is not yet complete.

5.3.2 Comments on Johannesma's analysis

Johannesma's work yields interesting and simplifying results. The first, which is a result of assuming the effect of any one chemical quantum on the postsynaptic membrane to be small, is that the actual time distribution of quantal impulses is unimportant. Thus it is no longer necessary to assume that these impulses are Poisson-distributed, the input being completely described in terms of its mean level and a.c. component (if a constant membrane depolarising current is considered, this is added directly to the mean input but does not affect the a.c. term). Such a simplification is tantamount to saying that all input information is conveyed by mean and variance terms.

A further simplification is suggested by the form of the analytical results. If input and output parameters are normalised, where appropriate, by the time constant τ, direct comparisons are possible between simulations using different time constant values. This may be intuitively understood by reference to Figure 27.

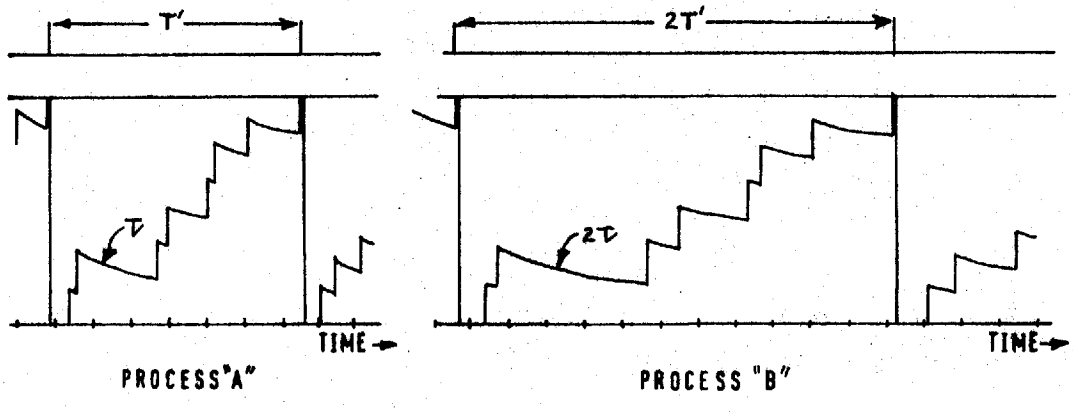

Figure 27 Typical time course of P.S.P. level and spike generation in two versions of Johannesma's model, identical except for their time scale.

Process A shows a number of input events and output events. The time constant of decay is τ. Process B is identical except that the time axis has been expanded by some factor, say 2. In this case it is clear that the mean input and output rates are halved and that the time constant has become 2τ; the output interval distribution will be identical in shape but changed in scale. If input and output quantities are normalised, where appropriate, by the time constant, then the two processes are directly comparable and a considerable simplification results. Similar considerations show that it is only the relative sizes of input steps and distance to threshold which are important, so that normalisation of relevant parameters by the latter quantity produces further simplification.

5.3.3 Computer simulation of Johannesma's model

The programme, written by the present author in Fortran IV for use on the IBM 7090/7094 digital computer series, aims to provide as much information about the output spike sequence as possible and generates not only the interval distribution but also its moments and cumulants, for direct comparison with the analytical results.

Although Johannesma's analysis shows the precise time-ordering of the input (quantal release of transmitter) to be unimportant, some form of stochastic input is required. Poisson processes were chosen for the excitatory and inhibitory inputs in the simulations because such processes assume a minimum of knowledge about the input, being completely specified by one parameter (their mean rate). The programme generates such sequences by calling on the machine-store of evenly distributed random numbers, and using them to test for the number of excitatory or inhibitory events in each programme sampling interval. The P.S.P. value is then updated and if threshold is reached an output event occurs. The time lapse since the last firing is used to generate a contribution to the various moments and cumulants of the output interval histogram. It was decided in all cases to simulate 15 seconds of neural activity, and sampling errors in the results are therefore more significant when low output rates occur. A simplified block diagram of the computer programme is shown in Figure 28. This diagram shows a number of features, such as the calculation of PST histograms and recovered probabilities, which are not of interest in the present context, but which were included for the simulation of stimulated activity (to be described in later sections).

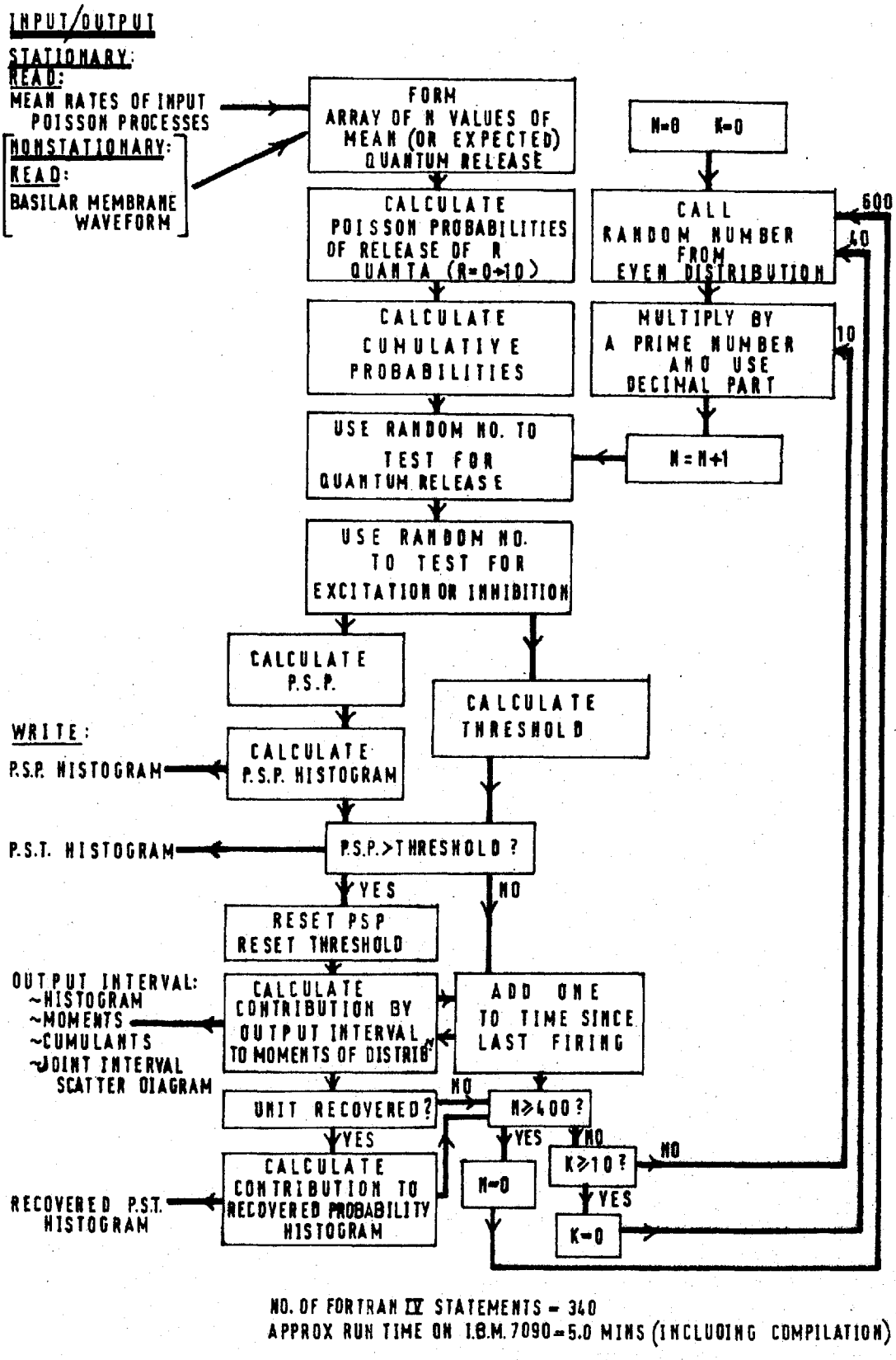

NO. OF FORTRAN IV STATEMENTS = 340
APPROX RUN TIME ON I.B.M. 7090 = 5.0 MINS (INCLUDING COMPILATION)

Figure 28 Simplified block diagram of digital computer programme for the simulation of Johannesma's model neuron.

Each computer run required some 240,000 random numbers, generated from 24,000 machine-store numbers by multiplying each by a series of primes. Approximately 5 hours of IBM 7090 computing time have been used to simulate spontaneous neural activity.

The generation of a Poisson event sequence from an evenly distributed set of random numbers, such as is available in most large, general purpose, digital computers, is fairly straightforward. In a stationary situation this may be done by taking the negative logarithm of successive numbers between 0 and 1 and using it to indicate the next interval in the process. However if the process is non-stationary such a scheme leads to difficulties, since it effectively gives the process a memory, which is not a feature of a rate-modulated Poisson process. (If the next interval chosen is by chance a long one, and the rate of the process changes in the meantime, there is no satisfactory way of proceeding). The alternative method, used here, is to use each random number to test for the number of Poisson events in each programme sampling instant, by using the well-known formula for the probability (p_k) of k events in a time δt:-

$$p_k = \frac{(\bar{\mu})^k . e^{-\bar{\mu}}}{k!} \quad , \quad \text{where} \quad \bar{\mu} = \lambda . \delta t$$

$\bar{\mu}$ = expected or mean no. of events in time δt

λ = mean rate of process

Provided that δt is chosen sufficiently small, it can always

be arranged that there is a negligible probability of more than, say, 10 events in each δt. In that case the random number is used to test for 0 or 1, or 2, or 3 .... or 10 events. (In fact, if $\bar{\mu} < 3.0$, the probability of more than 10 events is well below 1%). If it is desired to generate a non-stationary process it is necessary to ensure that the sampling interval δt is sufficiently small that the process can be considered stationary within it; the relevant value of $\bar{\mu}$ can then be assigned to each sampling interval and a random number used to test for input events in each time bin.

5.3.4 Comparisons between analysis and simulation

Johannesma's analysis gives expressions for the moments and cumulants of the output interval distribution in terms of the input parameters. The evaluation of these involves numerical approximation procedures on a digital computer and considerable programming effort, and only a few results of this work are yet available. However, the agreement between those theoretical results already obtained and the simulations gives confidence in the theoretical work, so that it seems reasonable to base further conclusions on the simulations alone.

In Figure 29 are shown some theoretical predictions relating the mean output (firing) frequency to the mean value of the input. Both quantities are normalised by the time constant of decay τ, and the input step sizes are normalised by the threshold level. Shown in the lower plot are some corresponding results of digital computer simulations. The normalised input and output parameters are given by:-

$$M = m\tau = \tau(n_e.e + n_i.i)$$

and $N = n\tau$, where n = mean output rate.

The parameter C is defined:-

$$C = \frac{S^2}{M} ,$$

where S^2 is the normalised a.c. component of the input:-

Thus $$S^2 = \tau(n_e.e^2 + n_i.i^2)$$

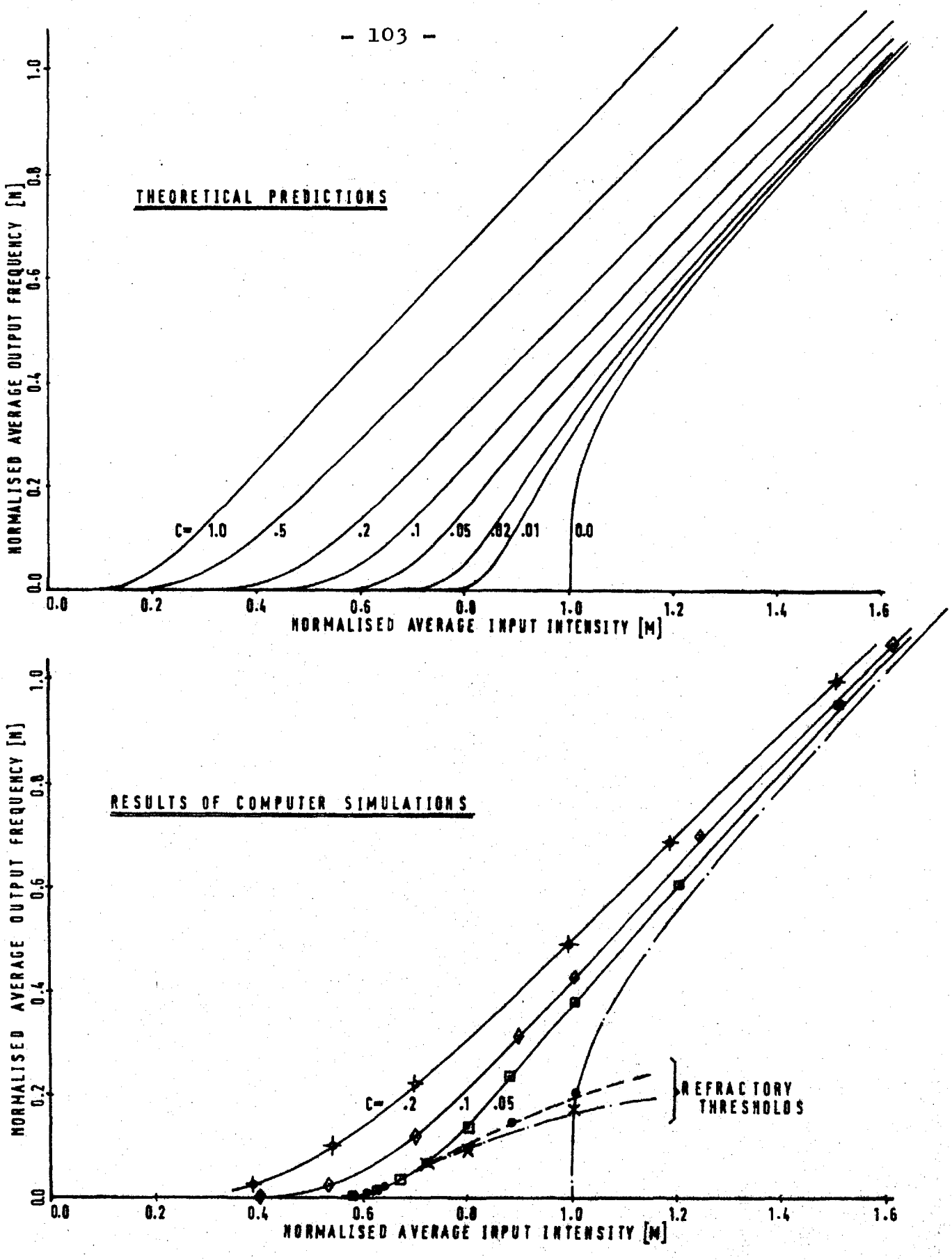

Figure 29 Predicted and simulated curves showing mean input versus mean output for various values of the parameter C. For an explanation of the symbols used in the lower graph, see Figure 31.

$$\therefore \quad C = \frac{S^2}{M} = \frac{n_e.e^2 + n_i.i^2}{n_e.e + n_i.i}$$

The simulations used an excitatory Poisson process for the input, with no inhibition. In this particular case:-

$$C = \frac{n_e.e^2}{n_e.e} = e$$

Thus the curves also represent the results for purely excitatory Poisson inputs of step size = C. It will be noticed that one of the theoretical curves is for C = 0, corresponding to a deterministic input (infinitely high input frequency and infinitely small step size). In such a case no output firings can occur until the equilibrium level of the P.S.P. reaches threshold; this in fact occurs when M = 1.0, and for slightly larger mean inputs there is a very sharp increase in output rate. With a stochastic input, substantial output rates may be obtained even when the equilibrium level of the P.S.P. is well below the threshold. This effect is more noticeable for larger step sizes, when the input is more stochastic.

A close comparison of the simulation results with the predictions for the relevant value of the parameter C shows that the two sets of curves are in close agreement for C = 0.05 and C = 0.10, showing that the restriction of the validity of Johannesma's analysis to "small" step sizes is unlikely to be a restriction in any real physiological sense (step sizes in many real neuronal synapses are typically only 1 or 2% of threshold).

Also shown with the simulation results of Figure 29 are the theoretical result for C = 0 (for comparison purposes) and some simulations in which threshold refractory

effects were included. Such properties are not treated in Johannesma's analysis, but it is interesting to see their effect on the mean output rate. As might be expected, at very low output frequencies the refractory properties of the threshold have no noticeable effect, but as the mean output interval becomes comparable with the resetting time of the threshold the output firing rate is reduced. (A key to the type of threshold properties assumed is shown in Figure 31, where similar symbols are used). In the case of an absolute refractory period of duration 5τ, the normalised output frequency (N) must asymptote to a value of 0.2 as the input level becomes large. With a relative refractory period only, the output frequency would be expected to increase indefinitely with increasing input. These points are corroborated by the simulation results. In discussing such results, typical values of physiological parameters should be borne in mind. For example, if time constants of the order 2 msec. are considered, then N = 1.0 corresponds to an output firing rate of 500 spikes per second, and N = 0.4 to 200 spikes per second. Thus most real physiological conditions are covered by the range $0 < N < 0.4$.

In Figure 30 is shown another set of theoretical predictions, each curve this time representing a constant value of the parameter S. Plotted on the same graph are some results of computer simulations with S = 0.2, which fit the relevant theoretical curve with considerable accuracy. The results do not represent simple Poisson input processes of constant step size and variable rate (as in Figure 29), but an input of constant variance and variable mean; in the simulations this was achieved by using an input composed of

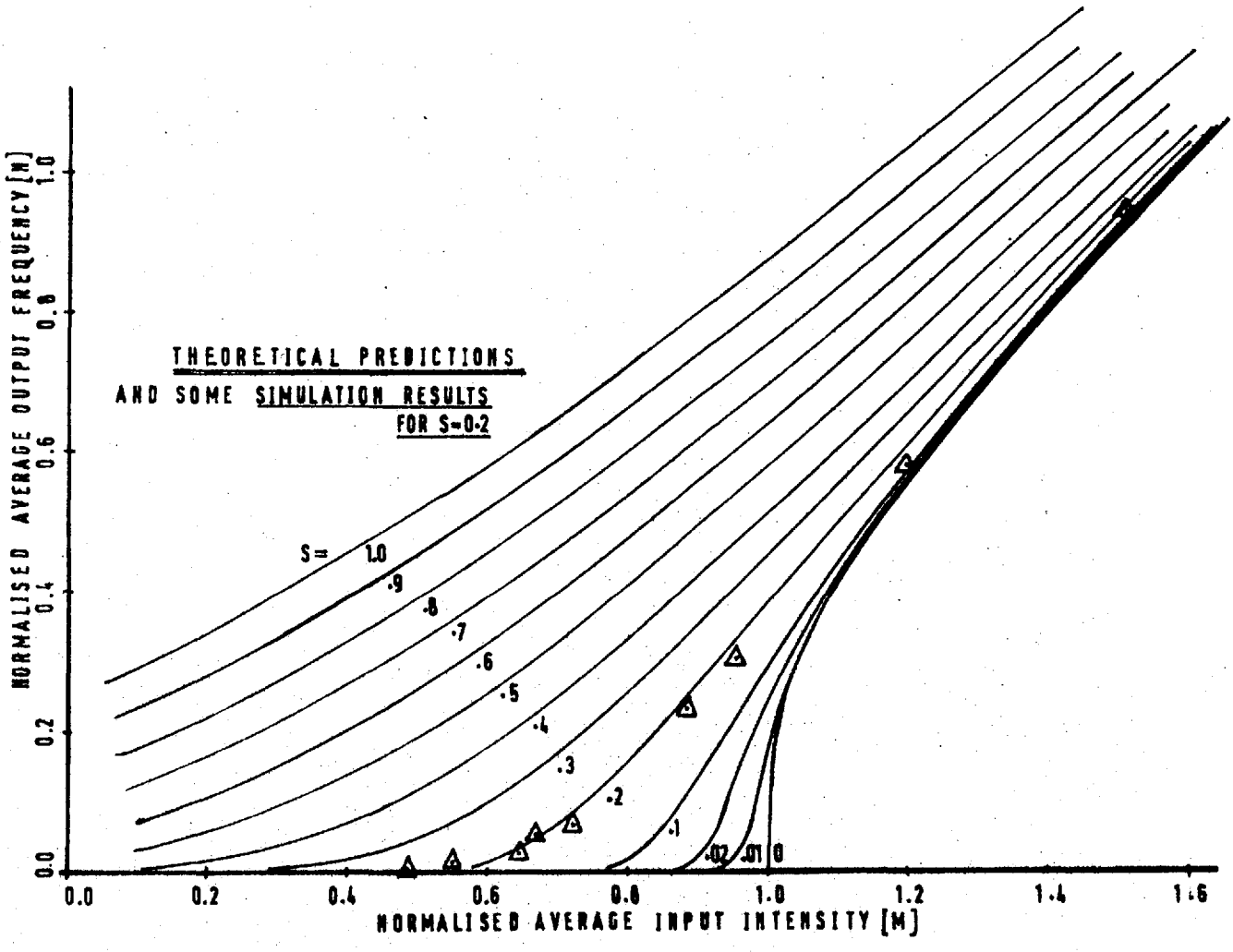

Figure 30 Input-output relations for various values of the parameter S. Full lines represent theoretical predictions, symbols the result of computer simulations for S = 0.2.

a constant Poisson process plus a d.c. term, the latter being set to different values in the various computer runs. It is interesting to note that these characteristics are somewhat less linear than those of Figure 29, supporting the general proposition that the more stochastic the input process, the more linear are the input-output relations of the model.

It is now necessary to leave the theoretical aspects and to concentrate on further results of the computer simulations, with some hope that they will be later corrobor-

ated by theory. Figure 31, plotted on a log-log scale, shows further characteristics of the output interval sequence. In this case the mean output interval is plotted against the standard deviation of intervals, both quantities being normalised by the time constant of decay, τ. The various symbols denote the use of different step sizes, time constants and resetting properties; also drawn is a line of unit slope which is the locus of Poisson processes (in which mean and standard deviation of intervals are always equal). It is thus of interest to note that when the output mean interval is high (i.e. the mean output rate is low), the output distribution tends to satisfy this necessary (but not sufficient) condition for a Poisson process, regardless of the type of threshold properties assumed. The fact that the standard deviation is always slightly less than the mean presumably reflects the absence of any very short intervals; this makes the output distribution more symmetrical than the pure exponential form relevant to a Poisson process, thus reducing its standard deviation. At low values of mean output interval the results are rather different. In such cases, the P.S.P. equilibrium level is above threshold, giving a relatively determinate crossing of the threshold level, and output distributions which therefore tend more to the Gaussian than the Poisson shape. This is reflected in the lower values of σ. The precise form of the output distribution now also becomes increasingly dependent on the threshold characteristics.

The two extreme cases of large and small mean output interval are illustrated diagrammatically in Figure 32, in

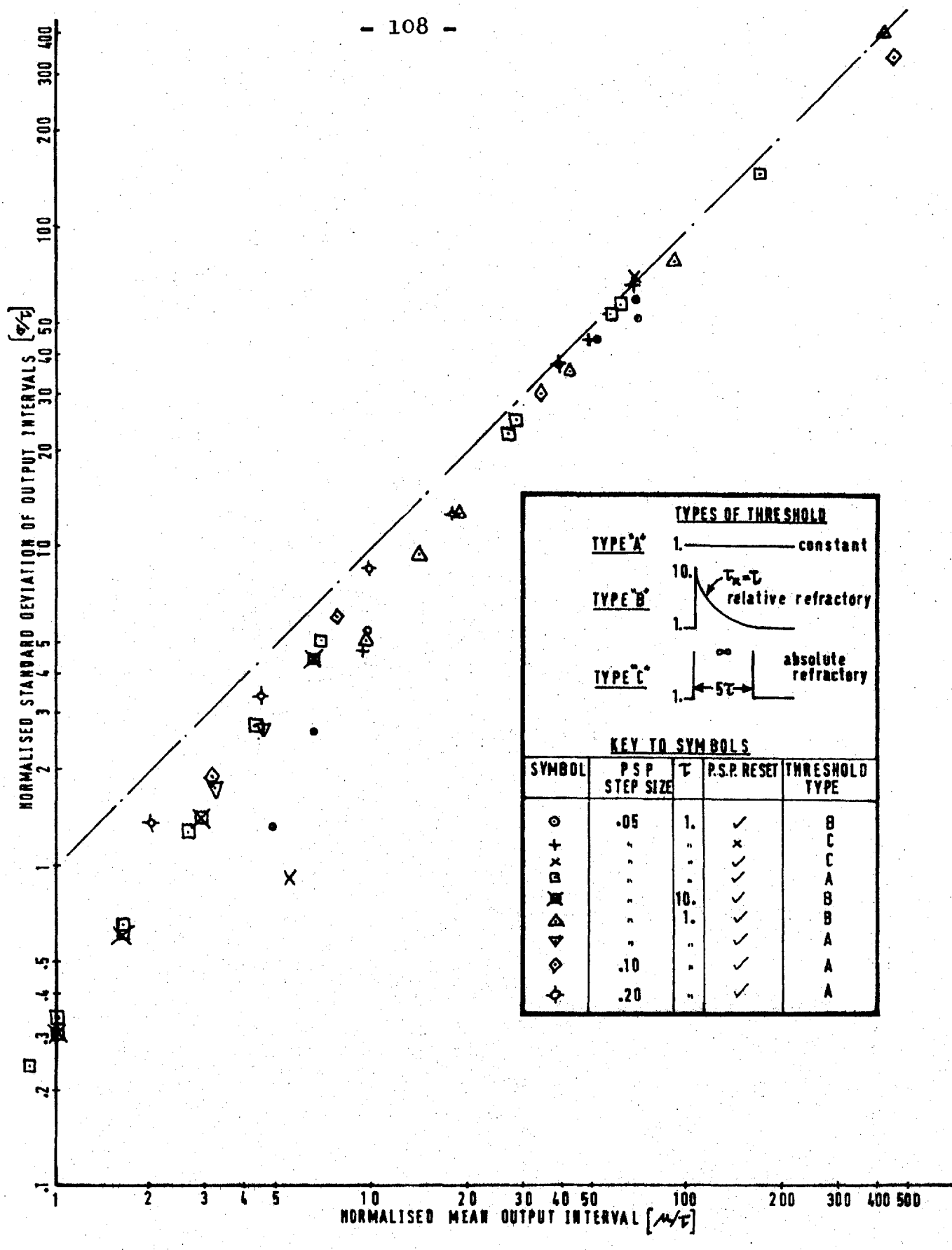

Figure 31 Computer simulation results. Mean versus standard deviation of output intervals, for some 40 simulation runs. The key shows the P.S.P. step size (normalised by the threshold level), the decay time constant and the type of resetting of P.S.P. and threshold, relevant to each symbol. A line of unit slope is also drawn on the graph, representing the locus of Poisson output processes.

which typical P.S.P. trajectories are shown.

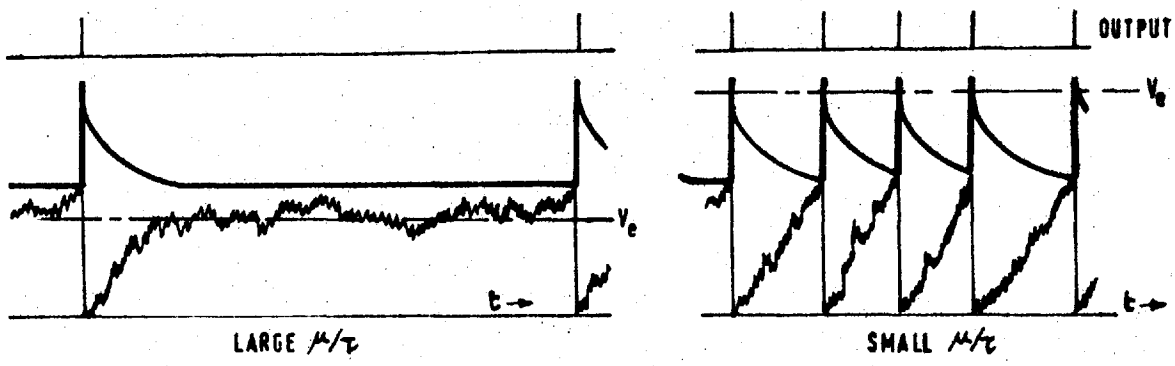

Figure 32 Typical P.S.P. trajectories. Large mean output interval, with P.S.P. equilibrium level below threshold (left); small mean output interval, with P.S.P. equilibrium level above threshold (right).

In the left-hand part of the figure, the P.S.P. equilibrium (V_e) is below threshold level and is generally reached after a few time constants; thereafter the P.S.P. makes random excursions towards threshold. It is not difficult to imagine that the probability of such an excursion reaching threshold is constant for all subsequent time increments, satisfying the condition required for the generation of a Poisson process and an exponential tail in the output interval histogram. In the other case illustrated in the figure, the mean output interval is small, since the P.S.P. equilibrium is above threshold (and is never in fact reached). The output firing sequence is much more regular and its precise distribution will depend on the threshold refrectory details. Figure 31 has already shown these effects to be noticeable when the normalised mean output interval, μ/τ, is less than about 10.0.

These matters are further illustrated by Figures 33 and 34, which show interval histograms and joint interval scatter

diagrams from two computer simulations, the results being plotted directly by a Calcomp incremental X-Y plotter attached to the computer. In Figure 33 are shown the results of a run in which the mean output interval was 17.5τ, and which would therefore be expected to produce an output interval distribution of basically exponential form. This is borne out by the plot, and the joint interval scatter diagram is also typical of an uncorrelated Poisson process with a dead time (i.e. an absence of very short intervals). Figure 34 shows similar characteristics for a computer run in which the mean output interval was 1.66τ, and there was a relative refractory period (type B, see Figure 31). In this case, the interval histogram is much more symmetrical, denoting a more regular output, and the scatter diagram is more typical of a Gaussian interval sequence (in which the lines of constant joint probability are circles).

Having discussed mean and standard deviation of the output intervals, higher order measures such as the normalised cumulants, or γ coefficients (see Appendix A), are now of interest. Figure 35 shows the variation of γ_1 (skew) and γ_2 (excess) as a function of normalised output rate (N), again derived from the computer simulations. At low values of output rate (and thus large mean output interval), γ_1 is approximately equal to the value of 2.0 expected in a Poisson process, and γ_2 is near to the expected value of 6.0. There are large sampling errors in both measures, due mainly to the small number of output intervals (typically 200-300) at these low values of N. As N increases, the values of both coefficients become more reliable and fall steadily towards zero, in a manner consistent with the fact that the distri-

butions are more symmetrical. At these higher output rates, sampling errors in the estimates are less serious and systematic differences between the various symbols tend to reflect the effects caused by different types of threshold. Johannesma[32] has reviewed the relationships between such coefficients and the various other possible ways of describing the form of distributions (e.g. by orthogonal polynomials, or by analytic functions such as the gamma distribution); in particular he has shown that, if a distribution is to be fitted by a gamma function, then a necessary condition is that:-

$$2\gamma_2 = 3\gamma_1^2$$

(Note that this relationship holds for the two extreme cases of a gamma distribution. In the Poisson case $\gamma_1 = 2$ and $\gamma_2 = 6$, and in the Gaussian distribution $\gamma_1 = \gamma_2 = 0$). In Figure 35, the curve drawn on the γ_1 graph represents a best fit by eye through the points, assuming the curve to be asymptotic to the abcissa for $N \rightarrow \infty$. Assuming the above expression to hold, another curve has been calculated for γ_2, and superimposed on the lower graph. The fact that the simulation results tend to lie close to this second curve suggests that the output interval histograms may be fairly closely fitted by an appropriate gamma function. This ties in interestingly with the findings of Stein[59] (see Section 5.2.1).

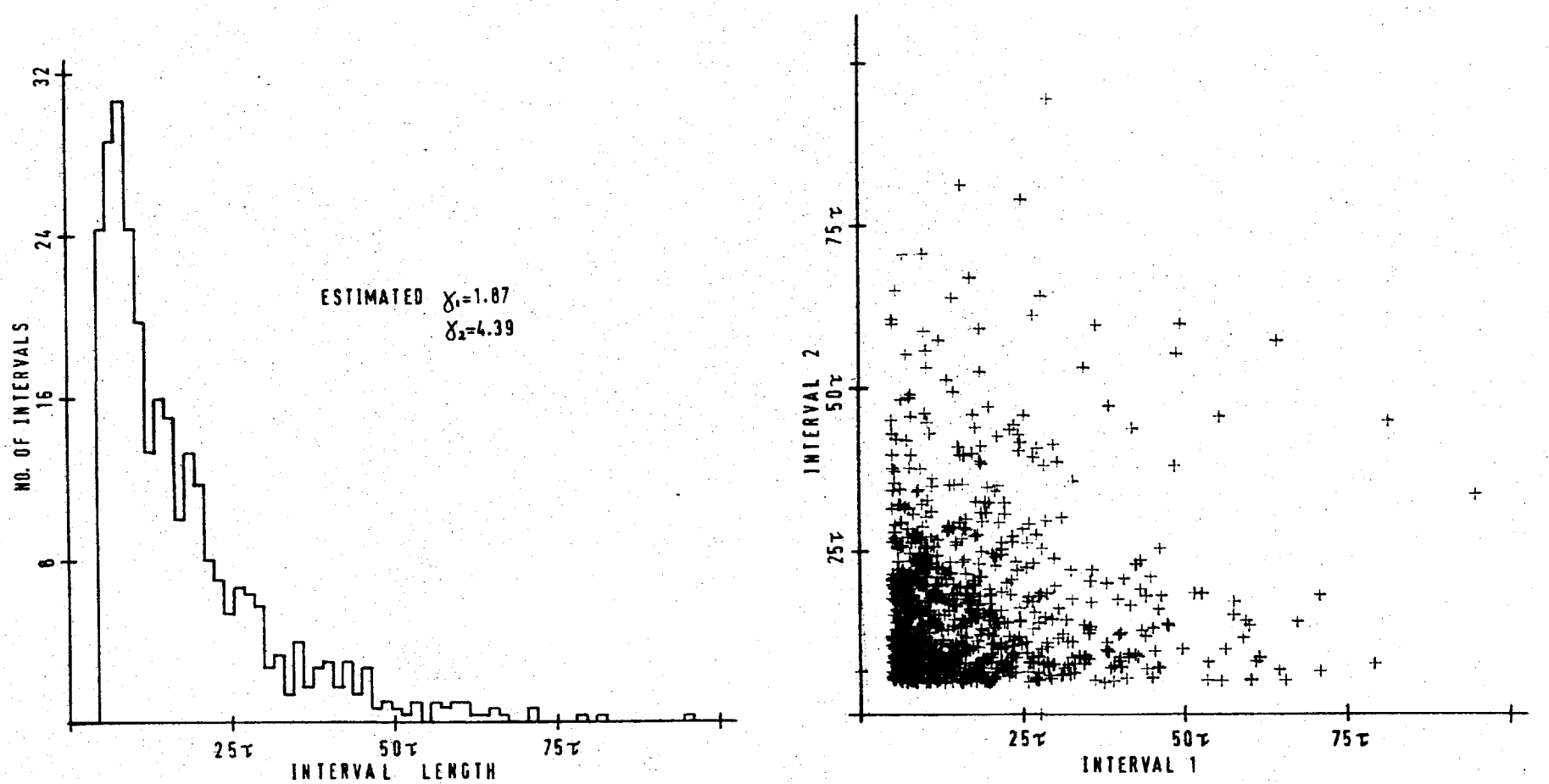

Figure 33 Results of digital computer simulation in which the mean output interval $\mu = 17.5\tau$. Interval histogram (left) and joint interval scatter diagram (right).

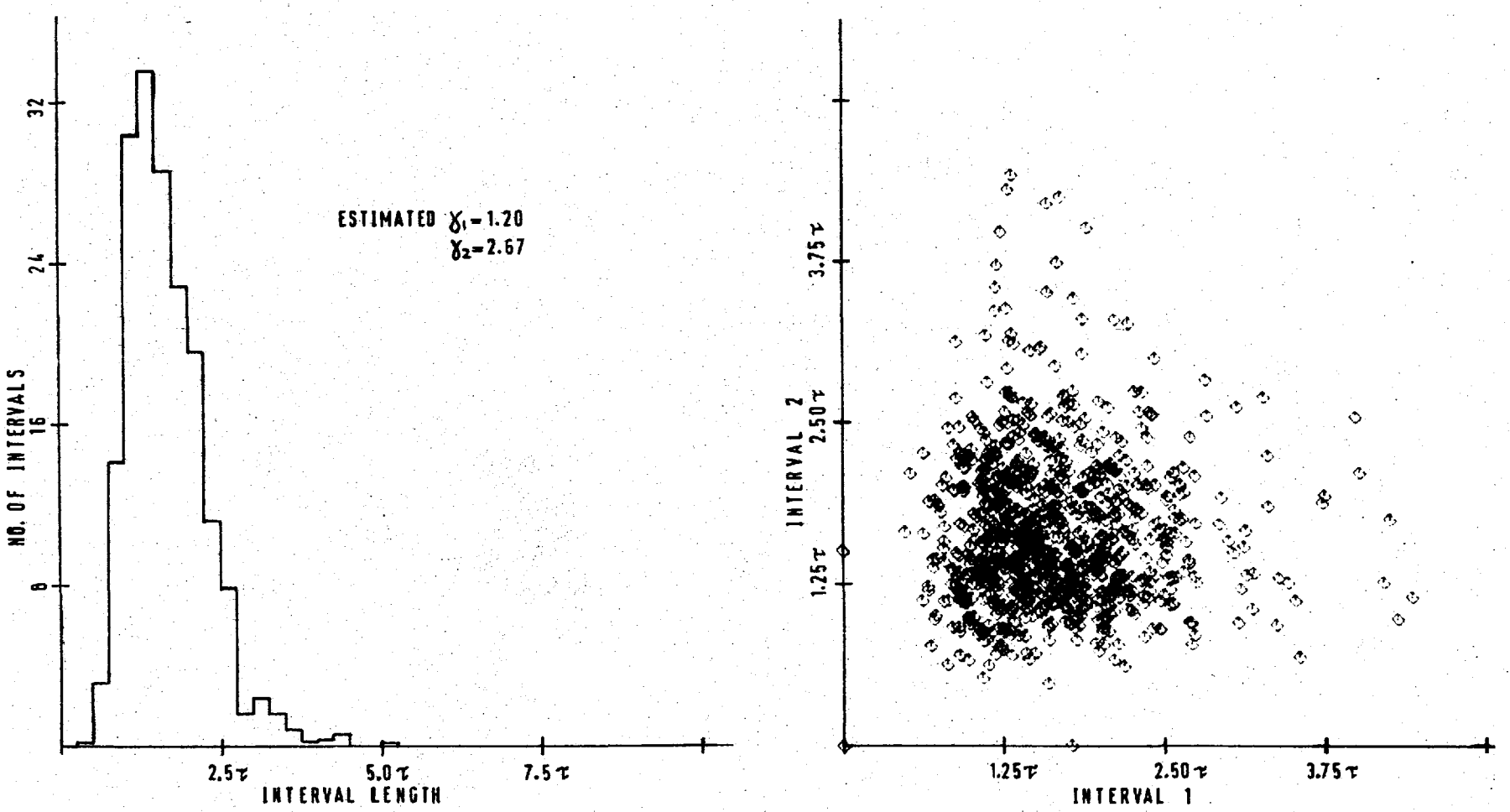

Figure 34 Results of digital computer simulation in which the mean output interval $\mu = 1.66\tau$. Interval histogram (left) and joint interval scatter diagram (right).

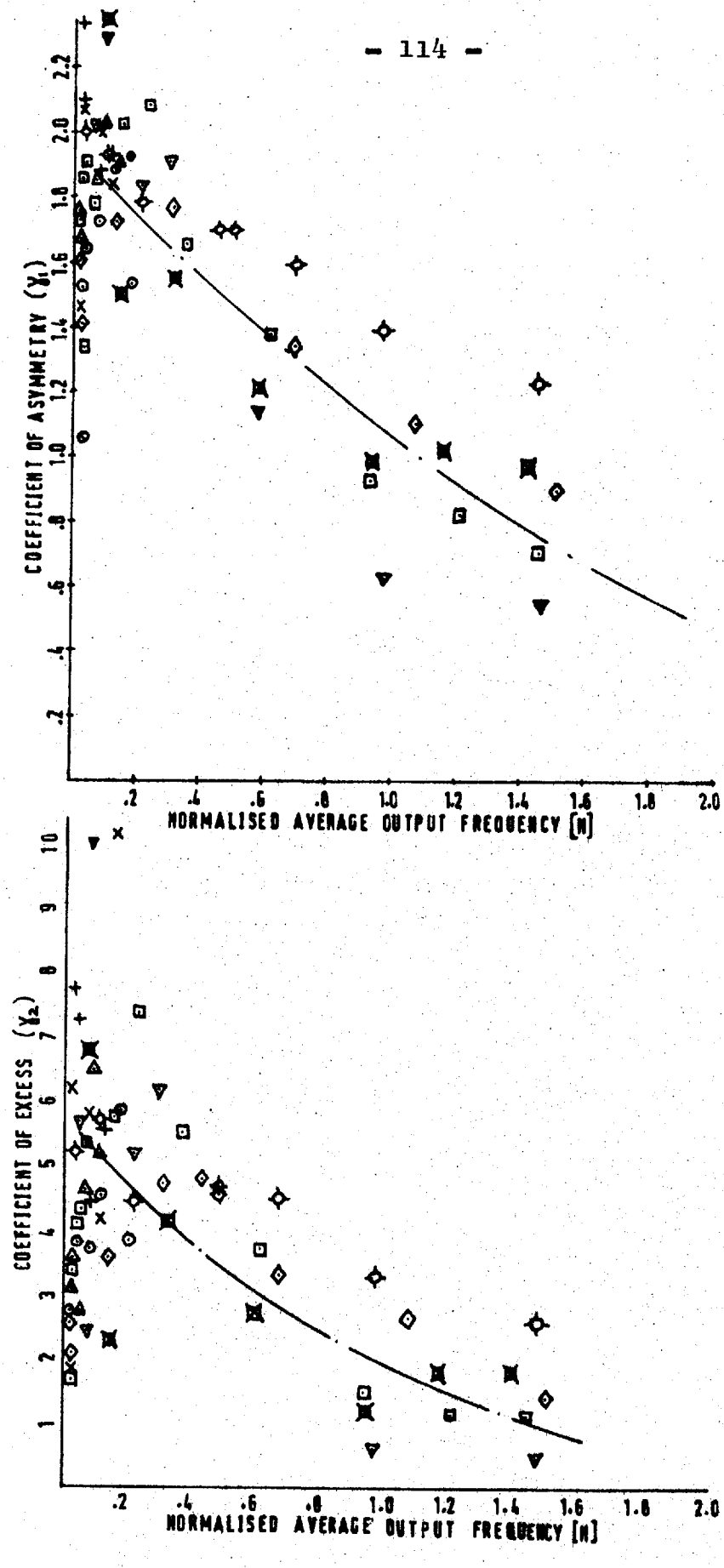

Figure 35 Computer simulation results. Coefficients of asymmetry and excess of the output interval distribution plotted against normalised output rate. A curve is fitted by eye to the upper graph; for an explanation of the curve in the lower graph, refer to the text.

5.3.5 Applicability of the model to spontaneous activity in first-order auditory neurons

A number of points emerge from the foregoing sections, suggesting that it is difficult to justify a model of this type for the simulation of spontaneous activity in first order auditory neurons.

Perhaps the most important issue concerns the exponential form of the distributions which is apparently always observed in the experimental situation (see Figure 10). The model is able to produce a wide range of distribution shapes, and it is difficult to see why the parameters should be restricted in the real physiological system so as to produce only the exponential variety. Only in the case where the P.S.P. quickly establishes itself at its equilibrium level, somewhere below threshold, and then makes random excursions towards the threshold, is an output distribution of predominantly exponential form realised. It seems hard to imagine why an assumed random liberation of chemical quanta across an afferent hair cell junction should not sometimes cause a P.S.P. equilibrium level near to or above threshold. In this context it is very interesting to note that in the cochlear nucleus, units exhibit a wide range of spontaneous interval distributions, and are by no means restricted to the exponential form[47]. The present model would seem an attractive one for simulating the activity of such neurons.

The simulations further show that there is no limit to the output firing rate of the model, unless an absolute refractory period is assumed. In first order auditory neurons in cat, spontaneous rates in excess of about 110 spikes per second are not observed, which might seem to indicate an

absolute refractory period of some 9 milliseconds. From a physiological viewpoint such a value seems too large, but there is a further objection to it provided by the modes of the experimental interval histograms (see Figure 12). These are generally between 4 and 7 milliseconds, regardless of mean rate, and therefore clearly rule out the possibility of absolute refractory effects lasting more than about 2 or 3 milliseconds. These factors therefore seem mutually contradictory.

Figure 36 shows the variation of mode with output frequency, derived from the computer simulations.

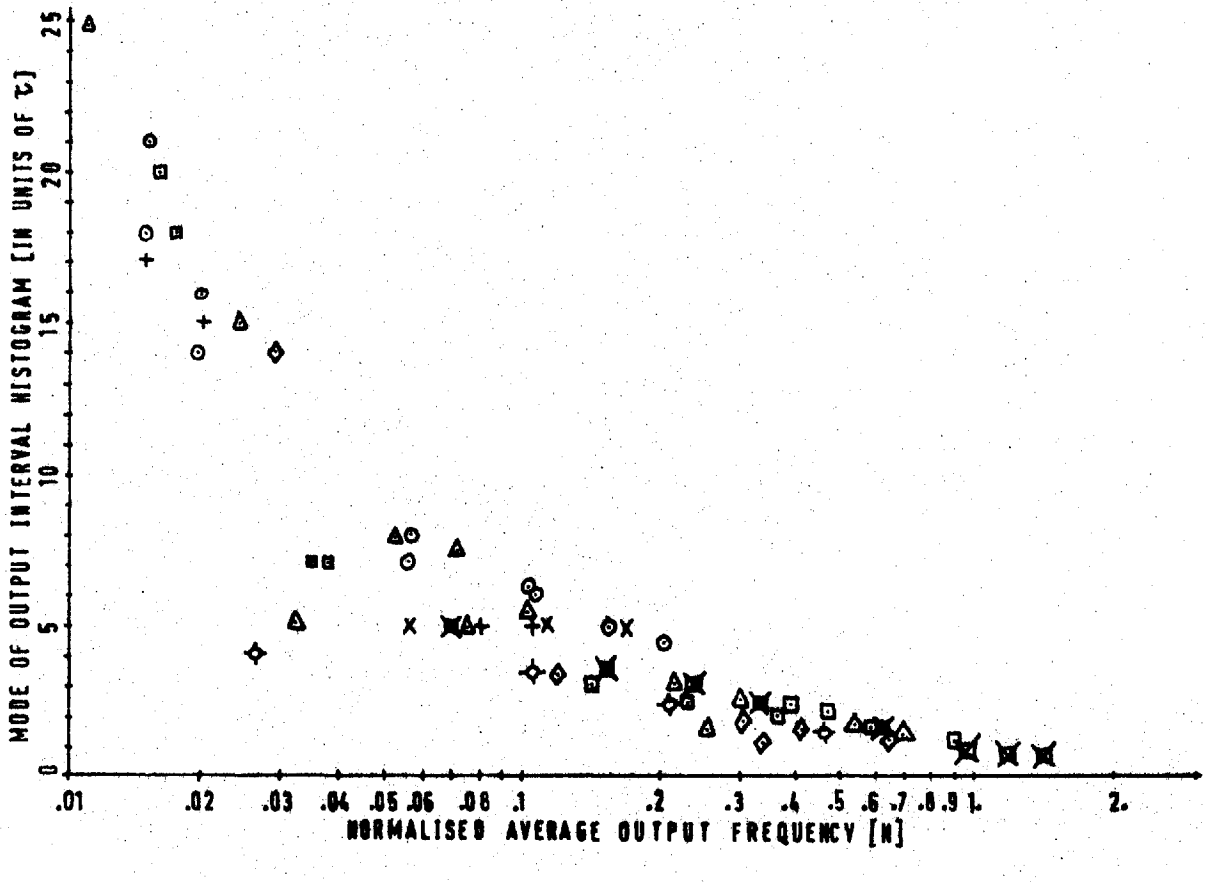

Figure 36 Results of computer simulation. The mode of the output interval histograms, plotted as a function of the normalised mean output rate.

Although there are considerable sampling errors at low output rates, the main trend of the graph is clear. It shows a clear correlation between mean output rate and histogram mode, for a variety of assumptions about the threshold refractory properties. This is in marked contrast to the relative lack of correlation between the two parameters which is actually observed (see Figure 12). If spontaneous rates in auditory fibres between zero and 100 spikes per second, with a decay time constant of, say, 2 milliseconds are considered, this implies values of N between zero and 0.2; reference to Figure 36 shows that in this range a very clear change of mode with mean rate is observed in the model.

The results from the computer model allow a visualisation of what is perhaps the only combination of input and threshold parameters which might produce output distributions of basically exponential shape, with mode independent of mean. The necessary conditions appear to be:-

(a) The P.S.P. equilibrium level must be below threshold.

(b) There must be an absolute refractory period followed by a very short relative refractory period.

(c) The P.S.P. time constant must be very short (probably less than 1 millisecond) for two reasons. If the P.S.P. level is reset to zero on firing, it must have time to regain its equilibrium level before the threshold returns to its resting value; if not reset, the P.S.P. values immediately before and after the firing must be uncorrelated, to avoid serial correlation of output intervals.

Such conditions are illustrated in Figure 37. A sudden

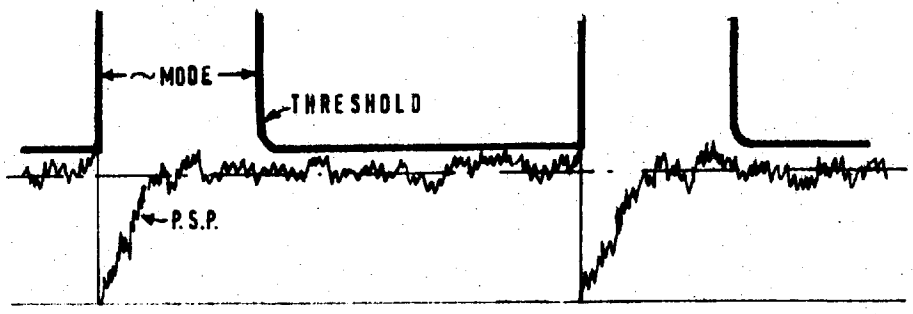

Figure 37 Typical inferred time course for P.S.P. and threshold waveforms, required to reproduce the spontaneous activity of first-order auditory neurons.

return of the threshold to its resting level after, say, 5 milliseconds would be expected to give rise to a 5 millisecond mode, regardless of the level of the P.S.P. equilibrium (which must, however, be below threshold). From a physiological viewpoint, such a system is believed to be very unlikely.

These difficulties do not seem peculiar to Johannesma's model of stationary neural activity. One of the most obvious problems, that of the variation of mode with mean output interval, seems certain to occur in any model which specifies relative refractory effects. Any quantal model in which the P.S.P. rises towards some equilibrium level will tend to produce regular output sequences if the equilibrium is above threshold. As already noted in Section 4.3, Weiss' model of the peripheral auditory system specified a continuous waveform of membrane noise for the generation of spontaneous activity. Although such a scheme does not suffer from the latter difficulty for the same reasons, the noise waveform must have considerable bandwidth if regularity and serial correlation in the output intervals is to be avoided. Furthermore it is possible to produce mean output rates

greatly in excess of those observed in first order auditory neurons, by minor alterations to the variance of the noise. In view of difficulties which arise with both quantal and membrane noise models, it seems that there may be other explanations for the characteristics of measured spontaneous activity in the acoustic nerve of cat.

5.4 Cochlear innervation and spontaneous neural activity

5.4.1 A proposition

Although the use of a simple chemical transmitter model to represent the spontaneous neural activity in the cochlea of the cat may be possible, the results of the foregoing sections suggest that unreasonable restrictions would have to be imposed on the values of the various model parameters. Even allowing such restrictions, some aspects of the measured spontaneous activity seem mutually contradictory. In view of these difficulties, considered to be present to some extent in all existing models, the possibility that the known anatomical details of the organ of Corti are responsible for the observed effects deserves careful consideration.

The proposition now put forward is that the branching of cochlear nerve fibres, into several or many terminations which attach themselves to the hair cells, is responsible for the observed form of the spontaneous activity, by virtue of an effect known as the superposition of point processes.

Consider an afferent nerve fibre in the organ of Corti, either of the radial or spiral type and putting out a number of terminations to hair cells. A fibre of each type is illustrated diagrammatically in Figure 38; the radial fibre terminates on a number of local hair cells, and the spiral fibre travels for some distance before terminating on cells in the outer rows (see also Figure 6). The following discussion applies equally well to either type of fibre.

Spontaneous activity has always been measured by inserting a microelectrode at some point (such as H in Figure 38)

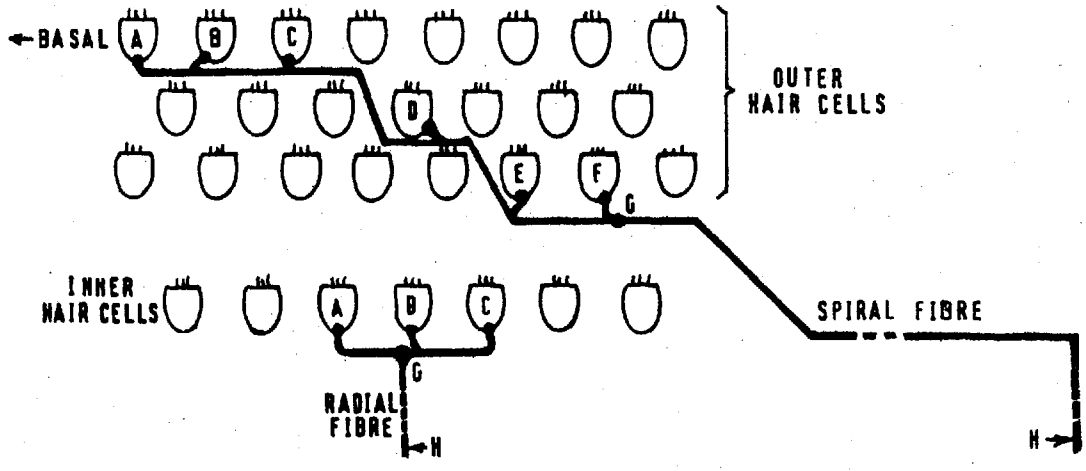

Figure 38 Diagram showing typical terminations of radial and spiral cochlear fibres.

in the auditory nerve. It is proposed that the process observed at H is a superposition of a number of essentially independent processes generated at the sites of connection of the branching fibre to the various hair cells (A, B, C, D, E, F ....). This assumes that the fibre between such sites and the node G can support action potentials, and that a number of independent random spike trains converge upon G.

It is well known that the superposition of a number of independent point processes tends to produce a final sequence with Poisson characteristics[61]. Intuitively this may be understood by considering the difficulty of estimating the time of occurrence of the next spike in the final process, given the time of the previous one. Such prediction becomes increasingly difficult as the number of contributing processes increases, even given their individual interval distributions. In the limit it is only possible to assign a fixed probability of occurrence to each and every time increment δt; this is the condition for a Poisson process.

In the case of a branching cochlear fibre, there would not be a very large number of contributing processes; between 2 and 10 terminations seems to be a typical figure[11]. It therefore seems important to examine the results of superposing a limited number of independent processes.

One other issue arises, concerning serial correlation in the final process. Although the contributing processes may not display any such correlation (in other words there are no constraints between successive intervals), it is possible that the final process will do so. This possibility may be understood by reference to a much simplified example, in which only two processes are superposed, illustrated by Figure 39.

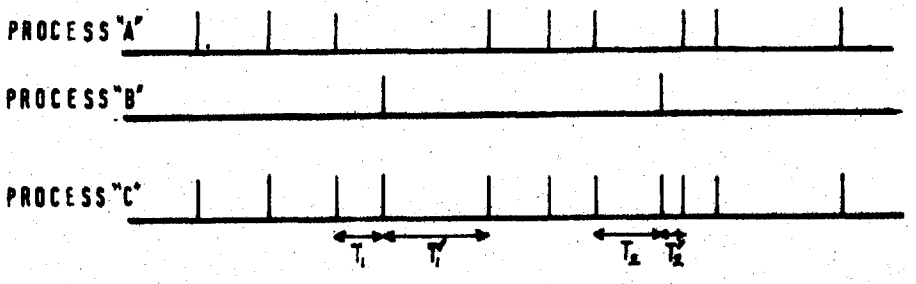

Figure 39 The superposition of two independent point processes. Serial correlation between intervals tends to be present in the final process (C), even when there is none in the contributing processes (A and B).

In this example, events from process B, "injected" into process A to form the superposed process C, tend to produce pairs of consecutive intervals in the final process which are shorter than the mean interval. Such pairs are illustrated by T_1, T_1' and T_2, T_2' in the figure. Thus when a short interval occurs it tends to be followed by another, giving rise to serial correlation. In view of the

fact that no substantial correlation is reported in the physiological measurements, it seems important to bear such effects in mind in any critical examination of the present proposition.

In spite of such reservations, the proposition seems attractive for two main reasons. Firstly, the individual contributing processes need not be Poisson-distributed; indeed, the more dissimilar are the individual distributions, the nearer to Poisson will be the observed process in the acoustic nerve. Thus the full range of interval histogram shapes generated by Johannesma's model (and observed, for example, in the cochlear nucleus[47]) are now allowable as outputs from the individual generators A - F. Equally important, the mode of the final interval histogram will be independent of the modes of the contributing distributions, and will depend almost entirely upon the refractory properties of the fibre between G and H (see Figure 38). These refractory properties could reasonably be expected to reduce strongly the probability of any intervals less than a few milliseconds in the final sequence, regardless of the latter's mean rate.

5.4.2 Computer simulations and results

A digital computer programme has been written to assess the effects of superposing a limited number of independent point processes, in order to examine the proposition in the light of known cochlear neuroanatomy.

A simplified block diagram of the programme is shown in Figure 40. In this scheme, the final process is made up of a sample of 2000 events, contributed by R independent processes, each of Q events; thus Q x R = 2000. The individual processes were generated by deriving the appropriate cumulative distribution function from the interval distribution, and testing the former with a succession of evenly-distributed random numbers between 0 and 1. In this way successive intervals were generated and stored. Finally a sorting routine was used to generate and store the superimposed process.

Two cases have been considered. In the first, the contributing processes all had similar Gaussian interval distributions with standard deviation equal to 25% of the mean. In Figure 41 are shown semilogarithmic plots of the final interval distributions, for R contributing processes (R = 2, 4, 8 and 10). Some averaging of the abcissa values allows the tails of the distributions to be shown more clearly. Against each curve is shown the number of contributing processes and also estimates of the coefficients γ_1 and γ_2. As R increases there is clear evidence of the increasingly exponential form of the histograms. When R = 10 the plot looks reasonably exponential, although lack of information about the incidence of long intervals makes this rather difficult to judge. Interestingly, however, the

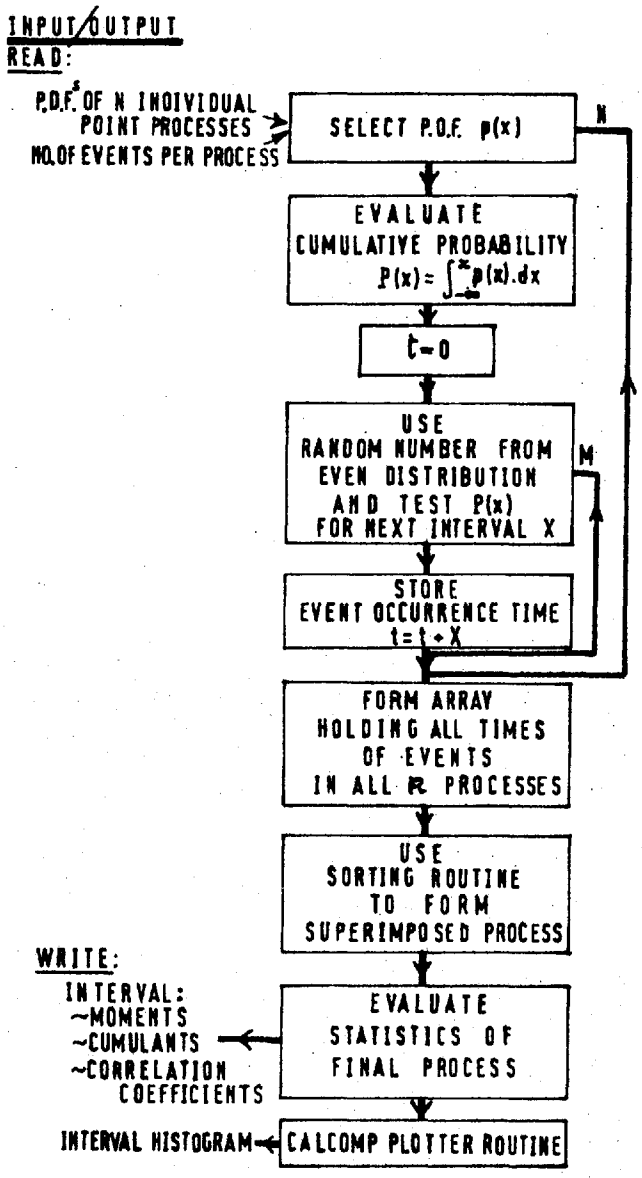

Figure 40 Simplified block diagram of a digital computer programme used to investigate the superposition of a limited number of indpendent point processes.

estimates of γ_1 and γ_2 are still considerably below the values of 2.0 and 6.0 expected for a true exponential distribution. This may well be due to a lack of very long intervals, which have an important effect on the values of the coefficients. Such difficulties point to the value of such coefficients for making any objective assessment of the

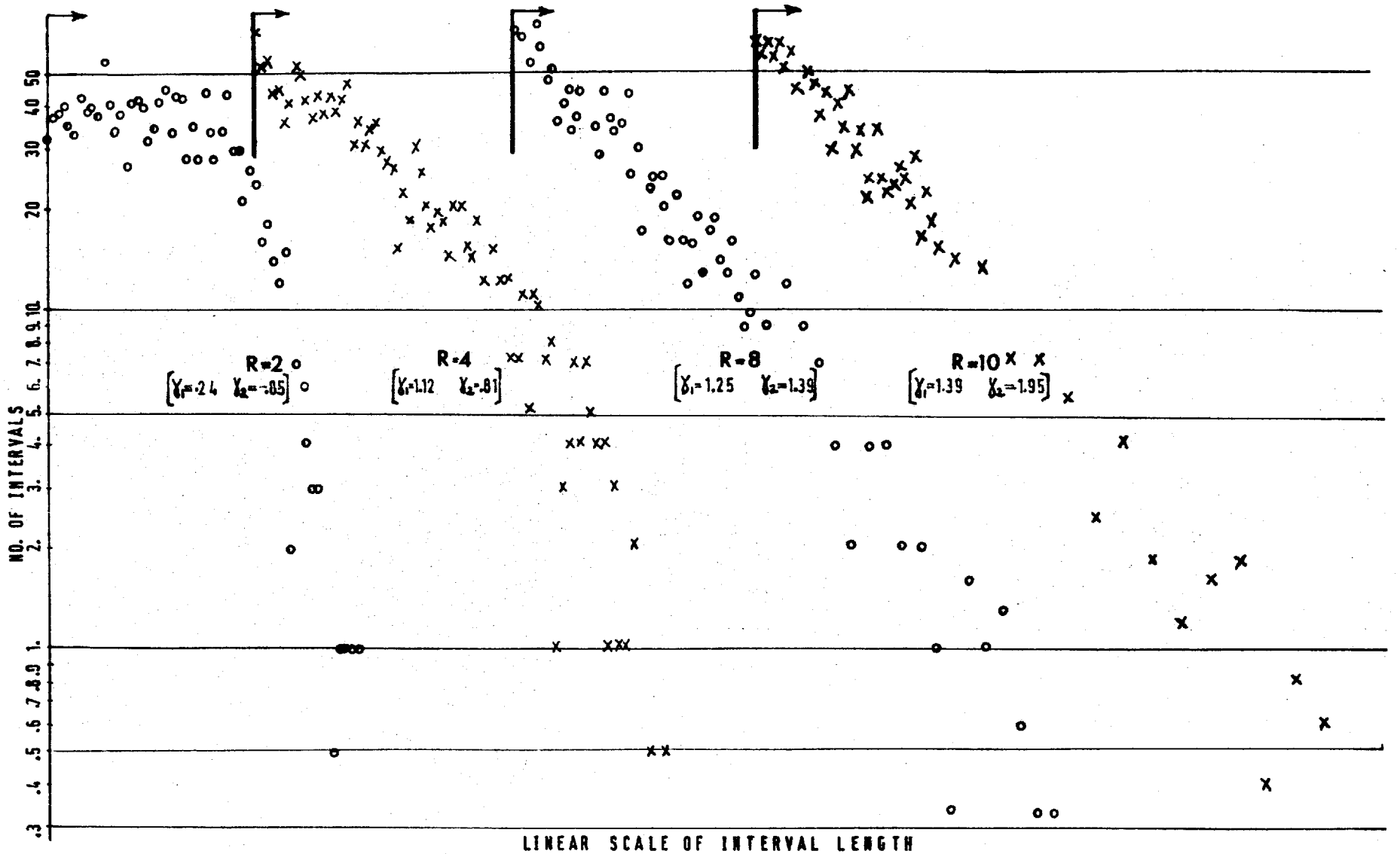

Figure 41 Interval histograms of a process formed by superimposing 2, 4, 8 or 10 indpendent Gaussian processes (σ = 0.25 x mean).

shape of a distribution, (see also Appendix A).

The more regular the contributing processes, the more of them must be superposed before a Poisson process is approximated. Gaussian distributions with a small standard deviation therefore form a difficult case. In Figure 42 are shown similar results for individual distributions of Gamma form, with R = 2, 4 and 8. It is at once clear that the long tail of the basic distributions gives a greater probability of long intervals in the final process, so that, even when R = 4, the resulting interval histogram appears close to exponential. It is also interesting to note that the estimates of γ_1 and γ_2 show evidence of approaching the values of 2.0 and 6.0 more rapidly than in the previous case.

In this context it is also interesting to consider a practical case of the superposition of 5 point processes, investigated by Stagg* in his work on muscle spindle activity in cat. The upper part of Figure 43 shows the interval histograms of 5 individual spike sequences, believed to be independent, and of very variable shape. Below is a semi-logarithmic plot of the superposed interval histogram, which forms a striking example of the effect. In this case not more than 5 contributing processes are required to produce a final sequence of visually exponential form.

Finally, the computed values for the first five serial correlation coefficients of the final process are shown in Figure 44, for the case of the superposed Gaussian distributions already discussed (see Figure 41).

* Stagg, D. Unpublished work.

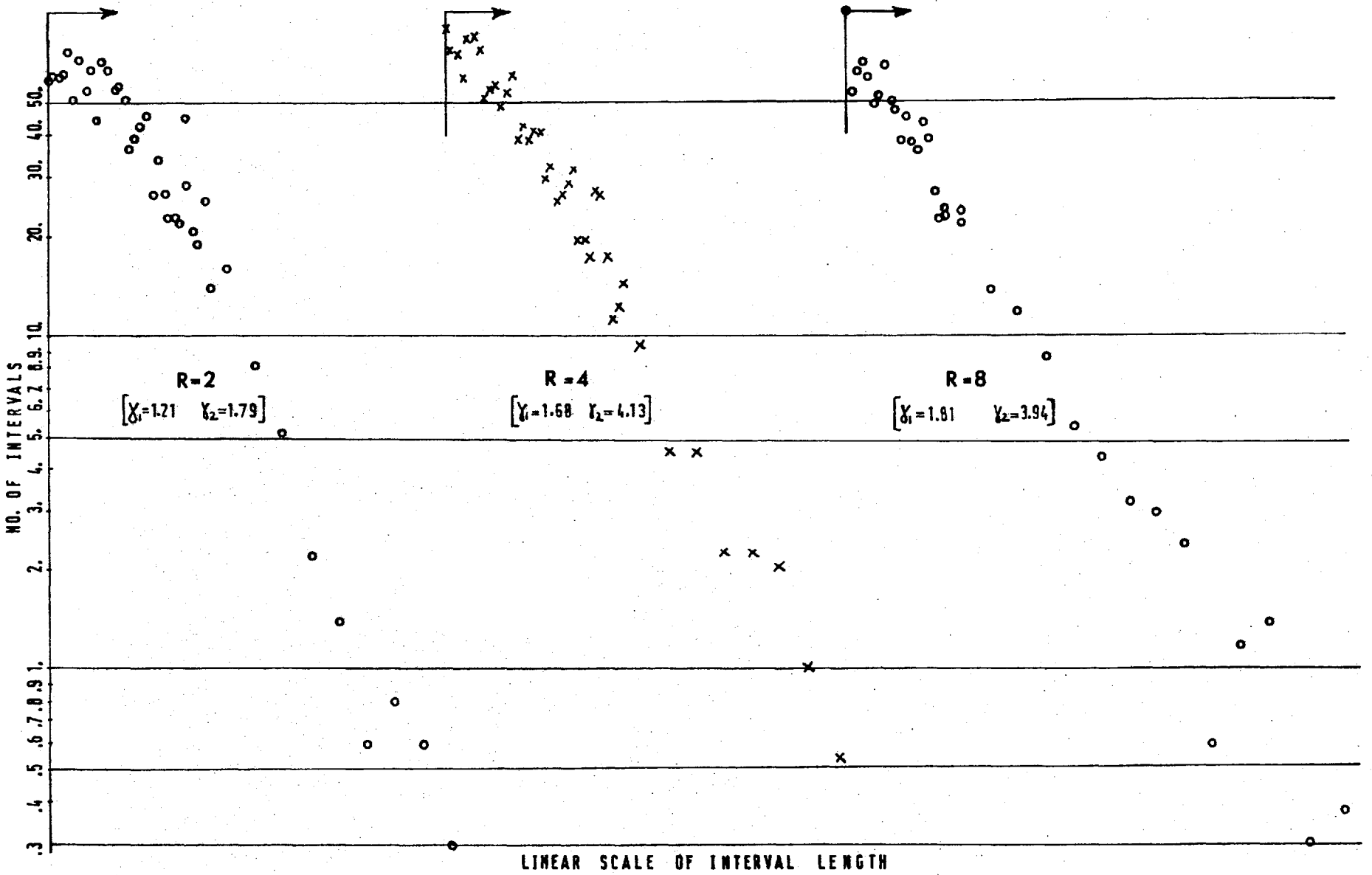

Figure 42 Interval histogram of a process formed by superposing 2, 4 or 8 independent Gamma processes having interval distributions of the form $p(x) = xe^{-x}$.

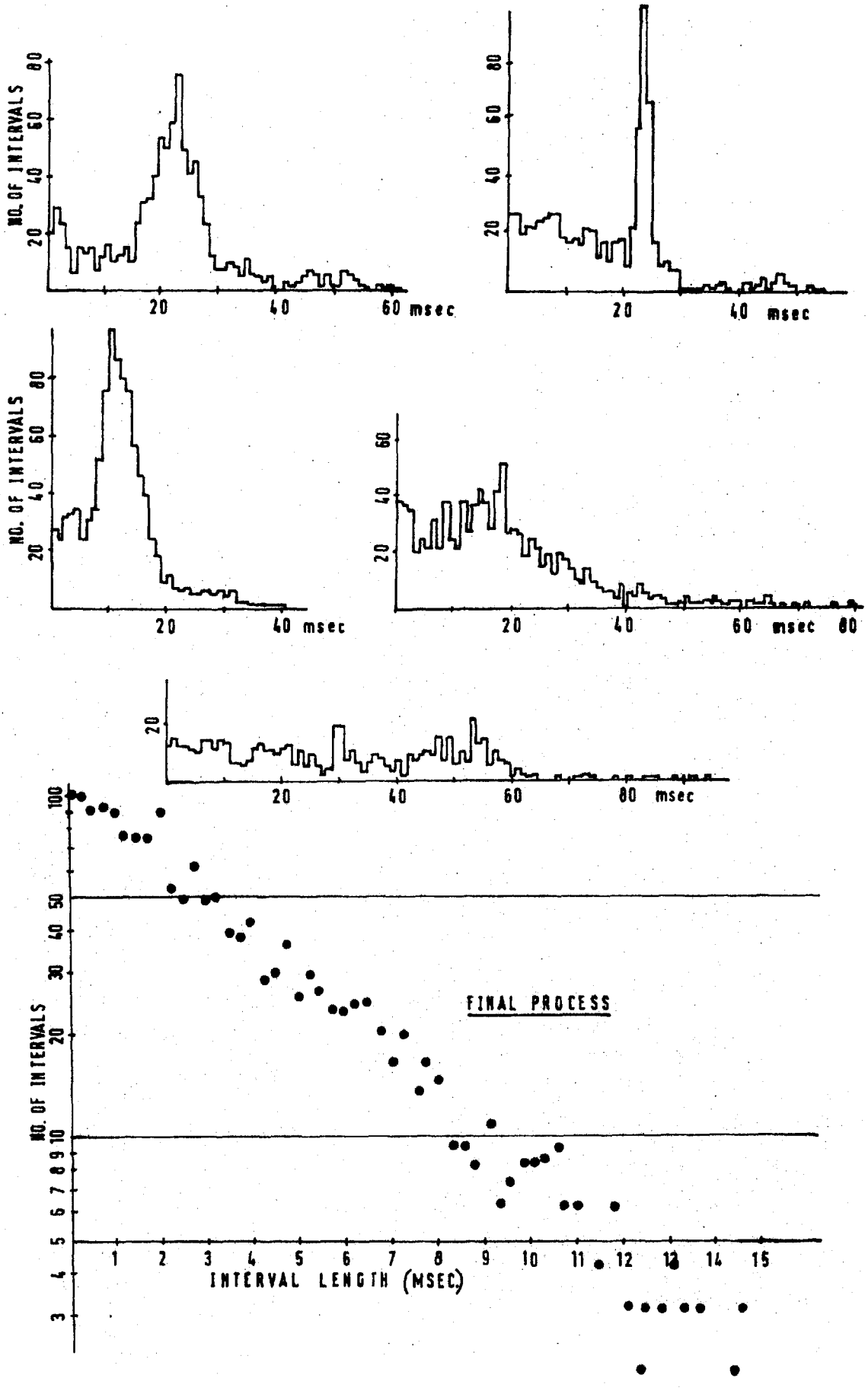

Figure 43 The superposition of 5 point processes of varying characteristics. Above are shown the individual interval histograms and below is a semilogarithmic plot of the final histogram (after D. Stagg, unpublished work).

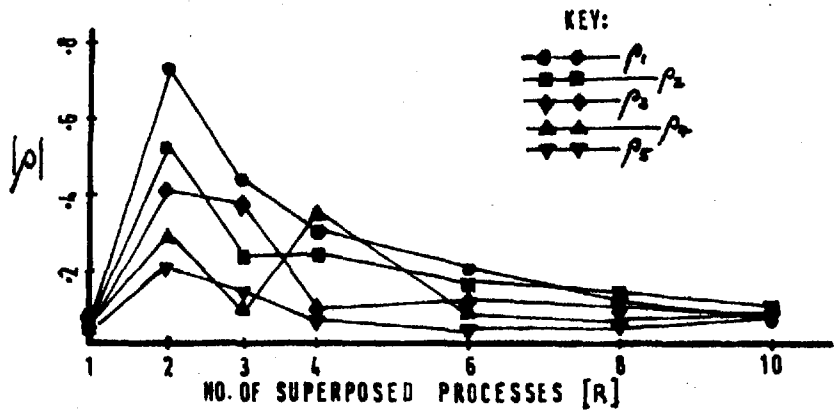

Figure 44 Computed magnitudes of the first five serial correlation coefficients of the superposed process, as a function of the number of contributing Gaussian processes (σ = 0.25 x mean).

The first of these coefficients, ρ_1, is a measure of serial constraints between adjacent intervals in the final process; ρ_2 describes constraints between intervals two apart, and so on. The absolute magnitude of these coefficients must lie between 0 and 1. It is clear from the figure that the coefficients, nominally zero for the single process (R = 1), become substantial when two processes are superposed (R = 2) and slowly decline as R becomes larger. When R = 10 they have become statistically insignificant; reference to Figure 41 suggests that some 10 contributing processes are also necessary for a visually exponential interval distribution of the superposed process. The tie-up between these two measures is intuitively attractive. In the case of the Gamma-distributed basic processes, none of the computed estimates of any of the five correlation coefficients was ever significant, even for R = 2. This result no doubt reflects the stronger tendency for the final process to approach a Poisson sequence in this case.

5.5 Discussion

Much of this section has been devoted to the analysis and computer simulation of Johannesma's model, which clarifies considerably the input-output relations of quantal models for stationary neural activity. Although such detailed studies as this may seem superfluous in the initial stages, it appears that the resulting insight sometimes allows useful propositions about real physiological systems. The present proposal about spontaneous activity in first-order auditory neurons is based on physiological evidence which, although it now appears highly relevant, at first seemed almost trivial.

If this point is accepted, then it follows that even apparently minor characteristics of neural recordings may have great significance. In this context it is interesting to note that measured interval histograms, even though appearing exponential to the eye, may have γ coefficients which differ considerably from the values expected of a truly exponential curve; and although serial correlation may be visually assessed by means of a joint interval scatter diagram, there is perhaps no substitute for objective measures such as correlation coefficients. Such measures of activity in first order auditory neurons would be of great interest.

The concept that the superposition of point processes is the effect responsible for observed spontaneous activity in cochlear fibres of the cat seems very attractive. Results from the computer simulations suggest that multiple innervation of hair cells by a nerve fibre would be sufficient to account for the observed effects if at least 4 to 8

terminations were put out by each cochlear fibre. The precise number of terminations required would however depend on the range and type of contributing distributions.

Like the earlier proposition of van Bergeijk (see Section 4.1), this one requires that independent action potentials are generated in the various terminal branches of the cochlear fibres. There is perhaps an alternative, not however considered very likely: if the fibre is not directly excitable at its terminations, then it must be capable of carrying random fluctuations of membrane potential from the individual terminations to some distant trigger zone, where they cause independent action potentials to be generated. This matter of the location of the trigger zone, or initial segment, has not however yet been resolved (see Section 2.5).

The proposition has interesting implications for the rates of spontaneous action potentials generated at or close to the individual hair cell-nerve ending junction. Although it puts no restrictions on the form of the contributing distributions, the fact that at least 4 to 8 terminations are indicated for each fibre and that the maximum measured spontaneous firing rates are about 110 spikes per second, suggests that the rates of the contributing processes may always be less than 10 or 20 spikes per second. This would presumably put less demand on the supply of chemical transmitter at a single afferent synapse than would higher spike rates, and would help to counter the objection that there is no clear anatomical evidence for abundant supplies of such transmitter (see Section 2.6).

An important result of the proposition must be that the interval histograms measured in the acoustic nerve do not

reflect the details of spontaneous activity in the individual fibre terminations. Existing recordings cannot therefore be expected to provide evidence either for or against chemical transmission at the afferent hair cell junction. It seems that only stimulated activity can provide clues to the mechanisms operating in this region.

6. BASILAR MEMBRANE ACTIVITY AND PERIPHERAL AUDITORY PROCESSING

6.1 Calculation of basilar membrane response

6.1.1 Computer programme

In order to be able to model stimulus conditions in the peripheral auditory system, it is necessary to estimate the response of the basilar membrane to the various acoustic signals of interest. In the work described here, the basilar membrane impulse response formula of Flanagan[15,16], derived from physical measurements by von Bekesy[1] (see Section 2.1), has been used to calculate the response of the membrane to a variety of simple acoustic stimuli. Of particular interest in the present context are the click and tone burst responses, because of the wide use of these signals in physiological recordings (see Section 2.7.2), and the response to low-pass filtered clicks, because of their application in binaural listening experiments (see Section 3). Computations have been carried out using an IBM 7090 digital computer.

Simplified block diagrams of the computer programme, and the system which it models, are shown in Figure 45. The computer evaluates basilar membrane responses to signals fed via a typical (high quality) headphone. This allows the response to different types of signal to be evaluated for a real physical situation, although, in fact, the inclusion of the headphone characteristics has been shown to have only marginal effects on the calculated response of medial and apical basilar membrane regions. The programme makes allowance for the frequency response of the middle ear, but not for that of the outer ear; it is therefore assumed to

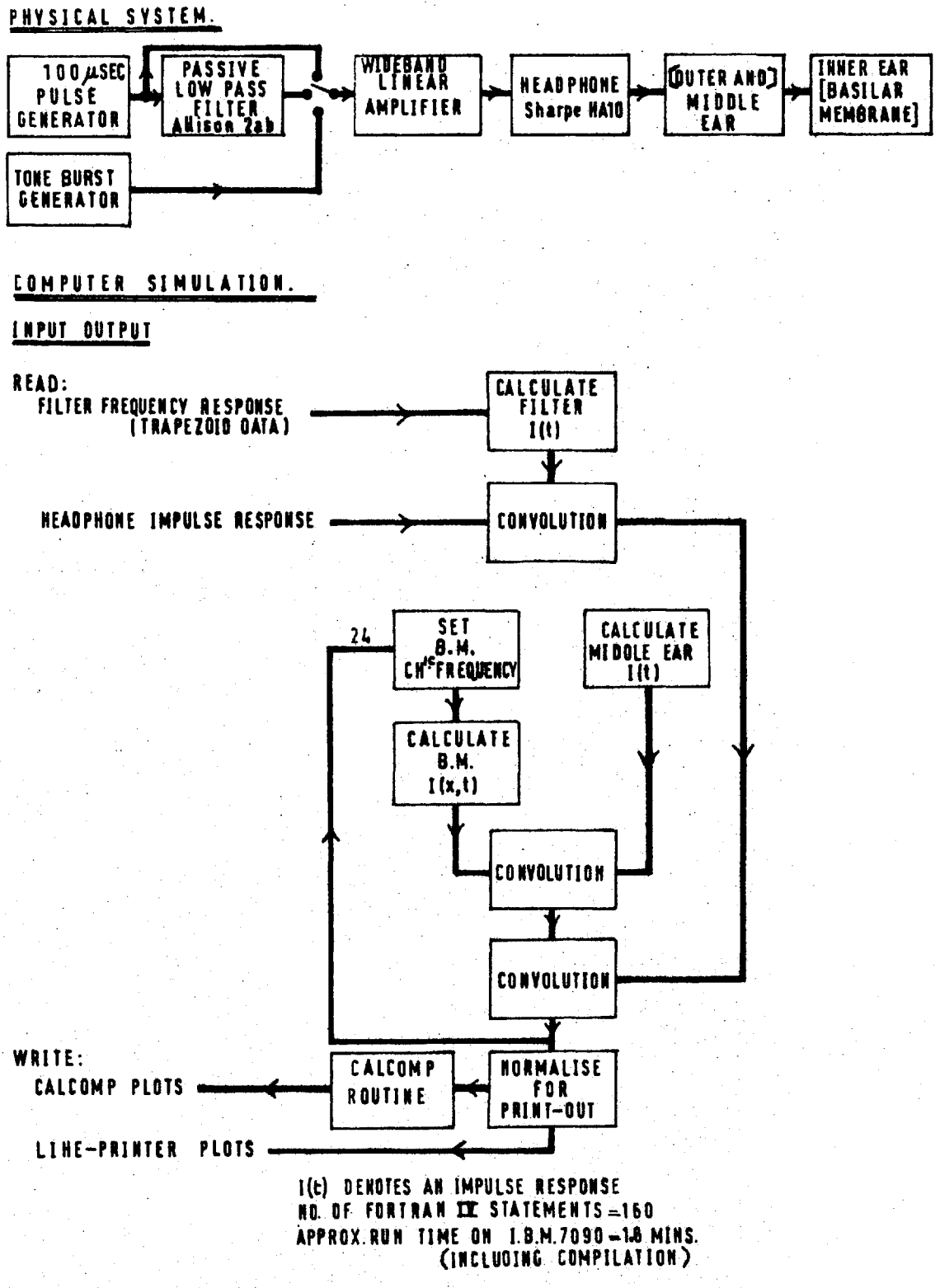

Figure 45 A simplified block diagram of a digital computer programme to calculate basilar membrane responses, and, above, the physical system which it models.

be valid for signal frequency components up to about 1.5 KHz. It uses a basic sampling frequency of 16 KHz.

Computation of basilar membrane displacements is carried out for a series of 24 points on the membrane, having C.F. values between 150 Hz and 1650 Hz, by using the impulse responses of the various parts of the system together with a convolution procedure. This method, although not as economical in computing time as the fast Fourier Transform technique[23] used in conjunction with the various frequency responses, is nevertheless convenient for the time-limited signals considered. It uses about 1.8 minutes on an IBM 7090 computer for the calculation of one set of 24 responses.

The impulse response of the headphone was measured directly and used as data for the programme. That of the low-pass filter was computed from its measured frequency response (at a particular filter setting), using a graphical technique described by Solodovnikov[56], (in this method, the real part of the frequency response is expressed as the sum of trapezoids, the impulse response of each of which is a simple analytic function). The impulse responses of the middle ear and basilar membrane were taken directly from Flanagan's analysis[15,16] (denoted by him as $g(t)$ and $f_1(t)$ respectively). The sensitivity characteristic of the membrane, which peaks at about 1200 Hz, was also included.

6.1.2 Results

Figure 46 shows the calculated responses of 24 points on the basilar membrane to an impulsive stimulus. The top curve shows the acoustic pressure waveform produced by the headphone. Each of the responses is labelled according to the C.F. of the membrane locus considered, and the time axis is divided into 1 millisecond intervals. The C.F. values are in geometric progression, representing points spaced approximately evenly along the membrane. The initial delay in each response corresponds to the delay of the disturbance in passing from the stapes to the membrane point considered. Peaks of given polarity in any one response are successively attenuated by some 20 dB, and are separated from one another by a time interval closely equal to the inverse of the C.F. In this latter respect they parallel in an important way the neural response to an acoustic click (see Section 2.7.2).

Shown in Figures 47 and 48 are computed responses to low-pass filtered transients, with filter cut-off frequencies of 800 Hz and 400 Hz respectively. It is clear that a major effect of filtering is progressively to shift the locus of maximum displacement to more apical cochlear regions, as would be expected from the reduction of high frequency energy in the stimulus. In each case the response curve showing the maximum excursion has been marked by a heavier line. In order to give a better indication of the degree of tuning, the region of the cochlea which responds to within an arbitrary 2 dB of this maximum is also indicated by a thickening of the vertical axis. The fall-off in response magnitude is seen to be somewhat sharper towards the apical side, but the tuning is in all cases rather broad.

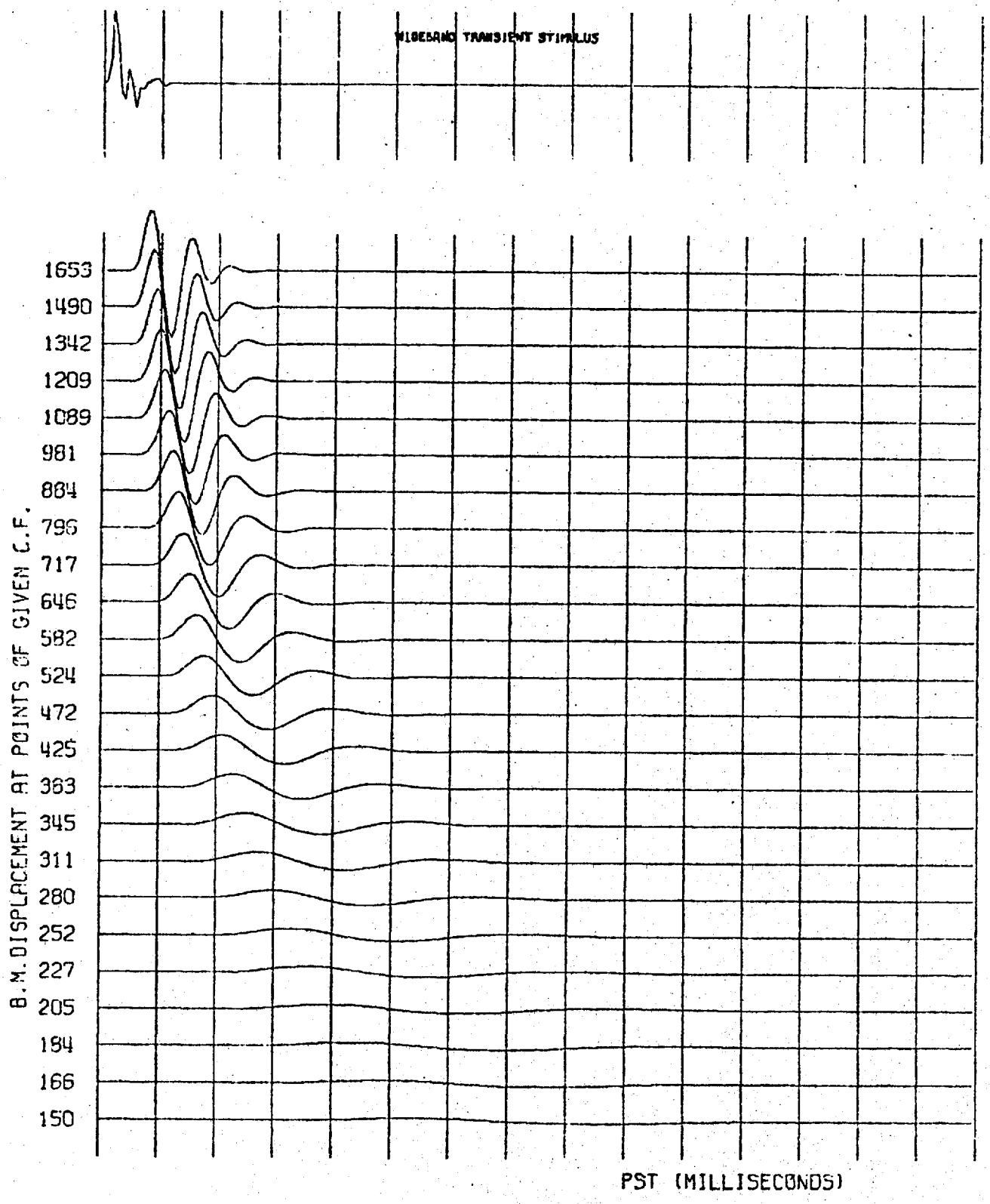

Figure 46 Computed displacement responses of a number of points on the basilar membrane, to an impulse delivered to the headphone. Above is shown the acoustic pressure waveform forming the input to the outer ear.

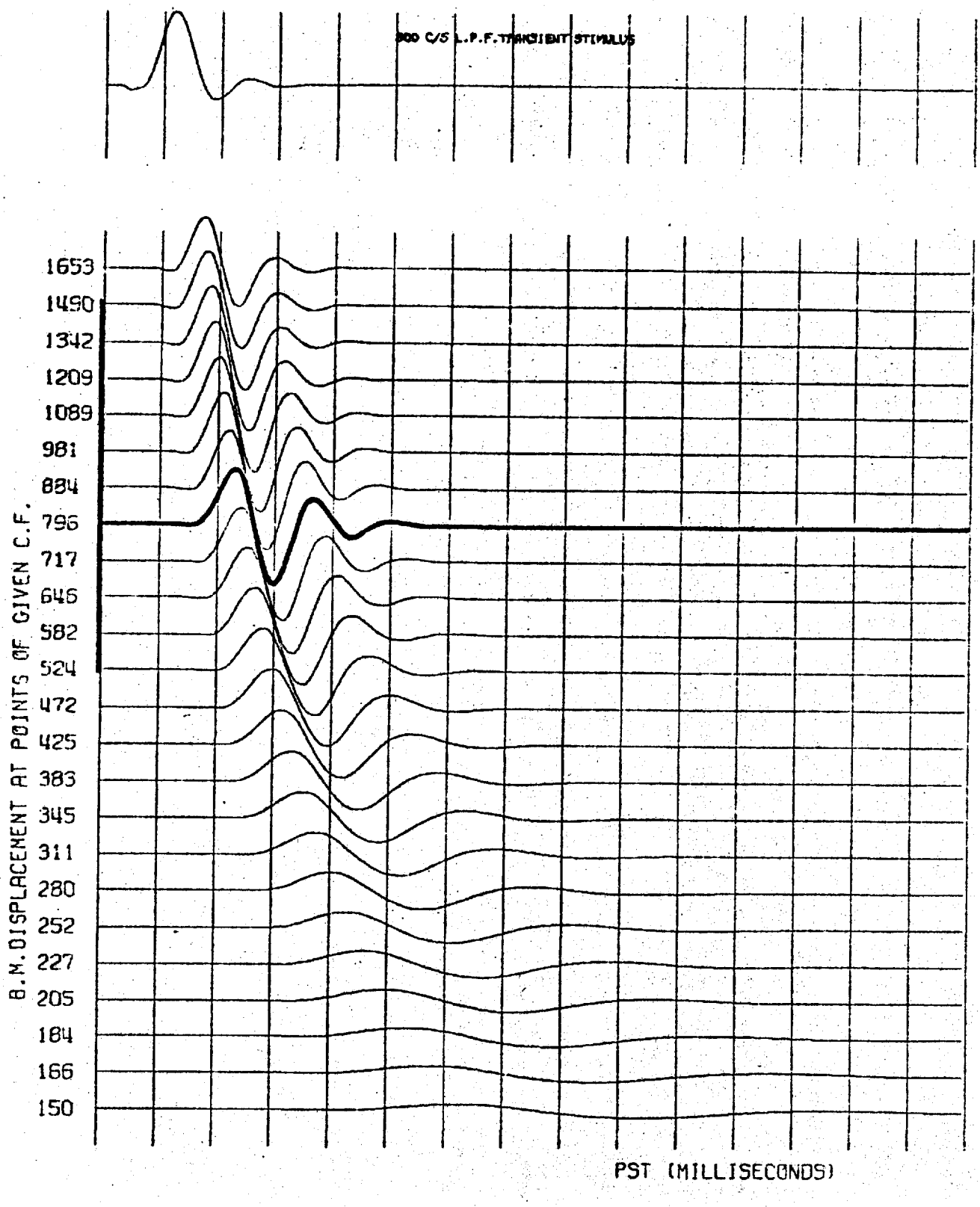

Figure 47 Computed displacement responses of 24 points along the basilar membrane in response to a low-pass filtered transient (Allison 2AB passive filter set to 0-800 Hz passband). The maximum response is indicated by a thicker line, and the region responding to within an arbitrary 2 dB of this maximum is indicated by a broadening of the vertical axis. Above is shown the acoustic pressure waveform delivered by the headphone.

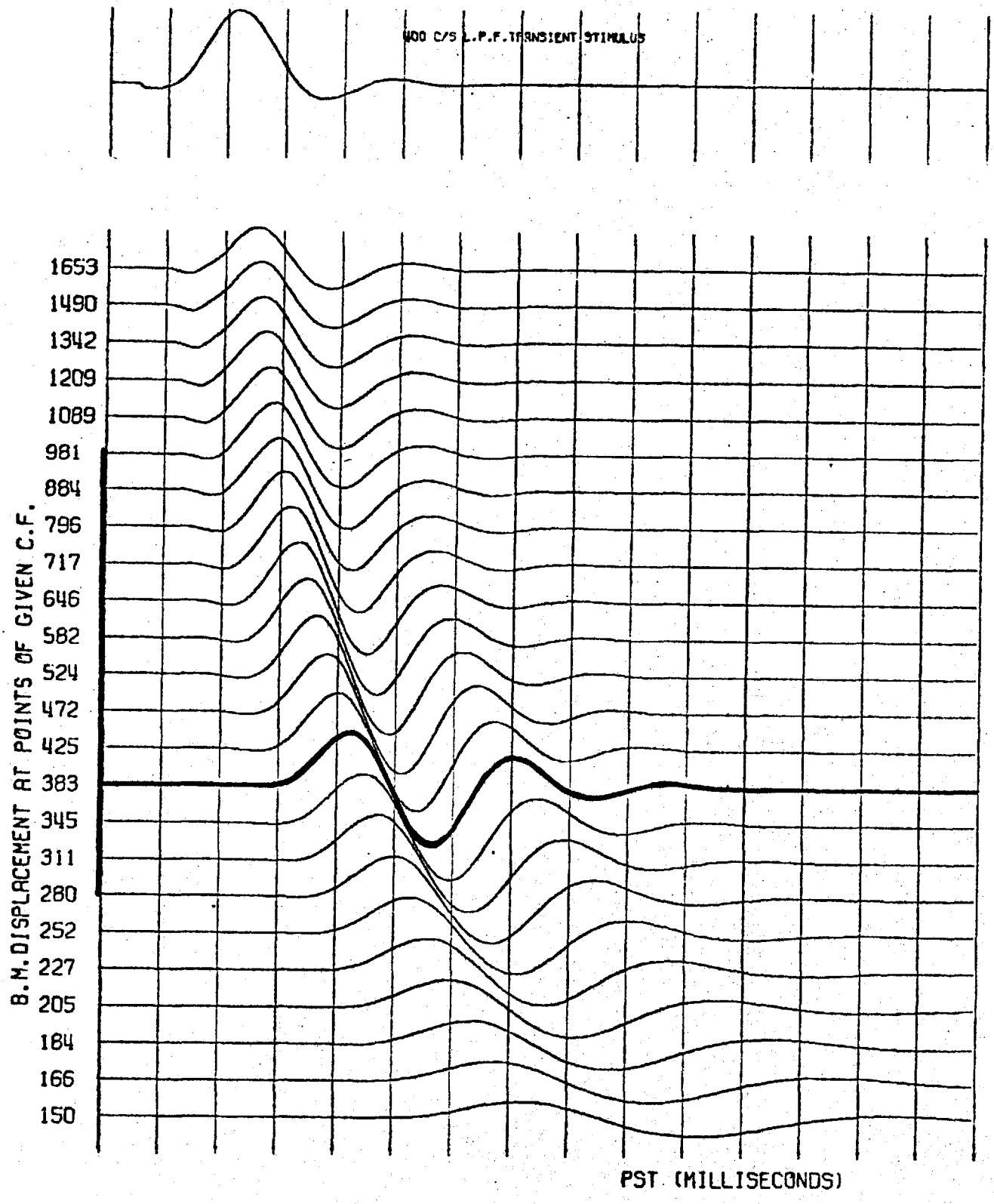

Figure 48 Computed displacement responses of 24 points along the basilar membrane in response to a low-pass filtered transient (Allison 2AB filter set to 0-400 Hz passband). The maximum response locus, and region responding to within an arbitrary 2 dB of this maximum, are again indicated by thicker lines. Above is shown the acoustic pressure waveform delivered by the headphone.

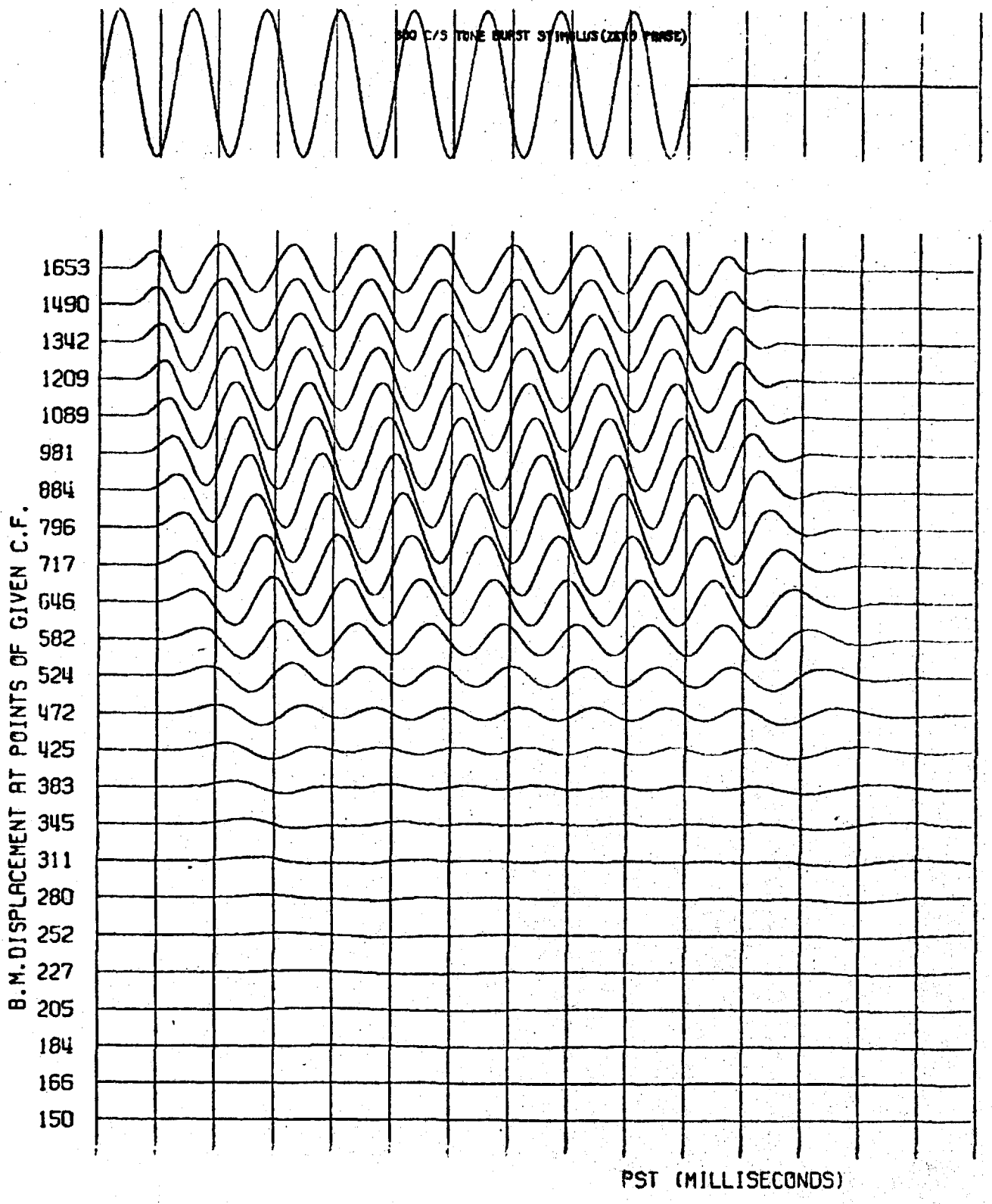

Figure 49 Computed basilar membrane response to an 800 Hz tone burst. The acoustic pressure waveform is shown above.

The basilar membrane response to an 800 Hz tone burst, switched on at zero phase, is shown in Figure 49. This plot is of interest because the neural responses to such stimuli have been studied in some detail (see Section 2.7.2). As would be expected, the 800 Hz region of the cochlear responds maximally in this case. The fall-off in response magnitude in more apical regions is rapid; beyond about the 500 Hz point, the transient responses due to the start and end of the tone burst are more pronounced than the steady response to the tone itself.

6.1.3 Discussion

The computed membrane responses to low-pass filtered transients are interesting in view of the simpler listening situations to which such signals give rise in binaural listening experiements (see Section 3.1). Although the displacement responses of membrane points having C.F. values above 1700 Hz have not been computed, the magnitude of such responses must be considerable in the case of a wideband transient stimulus, if the measured data on the frequency response of the ear is accurate. However, in the case of, for example, the 800 Hz low-pass transient (see Figure 47) the response magnitude falls off considerably between the points of C.F. = 796 Hz and 1653 Hz, and would presumably continue to do so in more basal regions. It therefore seems reasonable to assume that the dominance of a low-pitched impulsive image in binaural experiments using repetitive low-pass transients, and the effective elimination of the high-pitched image which gives rise to confusion in experiments with wideband transient signals, reflects the changed pattern of cochlear activity

in the two cases.

Figures 47 and 48 show that even filtered transients are represented over considerable distances along the basilar membrane. Such results suggest that there is little localisation of the mechanical response to such signals, and make it difficult to argue that the low-pitched impulsive binaural image arises by virtue of crosscomparisons of neural activity in fibres innervating well-defined regions of the two cochleae. There is however the possibility that the limited tuning displayed by the mechanical system may be enhanced by the complex innervation scheme; this point will be investigated in the following section.

It is interesting to note that the shape of the responses of the more apical membrane points is broadly similar for wideband and filtered transient stimuli, and that the main effect of filtering is to alter the relative magnitude of the response in various cochlear regions. Thus the response of the point of C.F. = 796 Hz to a wideband transient is broadly similar in shape to its response to an 800 Hz low-pass transient. This conclusion is considered to justify the discussion of binaural time-intensity trading with filtered transients in terms of neural responses to wideband transients (see Section 3.4).

6.2 Signal processing by cochlear nerve fibres

6.2.1 Introductory comments

Recent evidence concerning details of cochlear neuroanatomy has already been reviewed in Section 2.5. As far as spiral innervation is concerned, it now seems likely that spiral fibres put out terminations to the outer hair cells only towards the end of a basalward spiral course. Another view of spiral innervation, until recently rather generally held, is that such fibres put out large numbers of terminations along their spiral course, and that they travel in both apical and basal directions. Before attempting detailed modelling of stimulus activity at the mechanical-neural interface, it seems worthwhile to put the anatomical evidence temporarily on one side, and to examine the matter from an engineering viewpoint. It is possible that such an approach might provide independent evidence for or against particular innervation details.

The question arises as to the type of signal processing which might be expected in a spiralling cochlear fibre. If it merely terminates on hair cells after a long spiral course, there seem few interesting possibilities. In such a case, the cable properties of the fibre would be expected to impose a low-pass filtering (with attenuation), thus tending to smooth out the faster variations in signals sampled by the fibre terminations. There is however evidence that many cochlear nerve fibres are sensitive to basilar membrane vibration frequencies up to several KHz (see, for example, the PST histograms of Figure 13), so that any substantial low-pass filtering of this sort seems improbable.

If a spiralling fibre were to put out terminations all

along its spiral course, the possibilities seem more interesting. In this case there would be strong analogies with the comb filtering techniques well-known in electrical engineering. A comb filter achieves its filtering action by summing a number of delayed and weighted versions of a signal; a simple realisation of such a device is a delay line with a number of tappings leading to a summing junction. Such an analogy would lead one to expect a filtering action by the spiralling fibre, the details of which would depend upon the fibre properties and the location of its initial segment, or trigger zone.

6.2.2 Computer simulation of spiral cochlear fibres

A computer programme has been written to investigate possible filtering action by spiralling fibres, which are assumed to put out a number of terminations to hair cells along their spiral course. Although the analogy between such a scheme and comb-filtering may be valid in principle, there are complications in the cochlear situation which would make a theoretical approach very cumbersome. The basilar membrane is not merely a delay line, but has complex filtering properties of its own. Secondly, any realistic description must include nerve fibre properties, and cannot therefore regard the fibre terminations as simple tapping points on a delay line.

The types of fibre considered are shown diagrammatically in Figure 50.

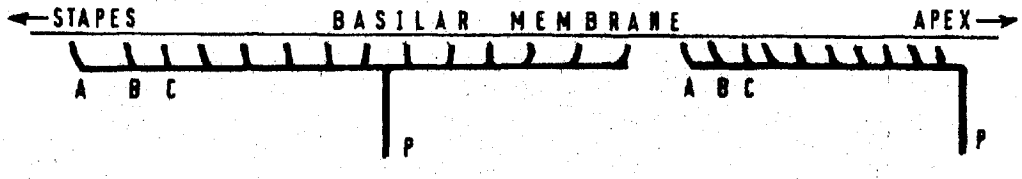

Figure 50 Diagrammatic representation of two cochlear fibres, putting out terminations along the length of their spiral course.

On the left of the figure is shown a fibre which spirals in both basal and apical directions, putting out terminations (A, B, C .....) to the hair cells; on the right a fibre is shown spiralling only in a basalward direction. Initially, it is assumed that such fibres are not excitable along their spiral course, and that all spread of activity from the hair cell terminals to a central trigger zone (P) is of the passive

electrotonic kind. It seems of interest to investigate the resulting waveforms at point P, which, if they exceed some threshold level, might be assumed to cause the generation of action potentials.

Figure 51 shows a simplified block diagram of the digital computer programme used to explore fibre polarisation waveforms at point P, due to the summation of contributions arriving from the various termination sites, suitably attenuated and delayed by the nerve fibre properties.

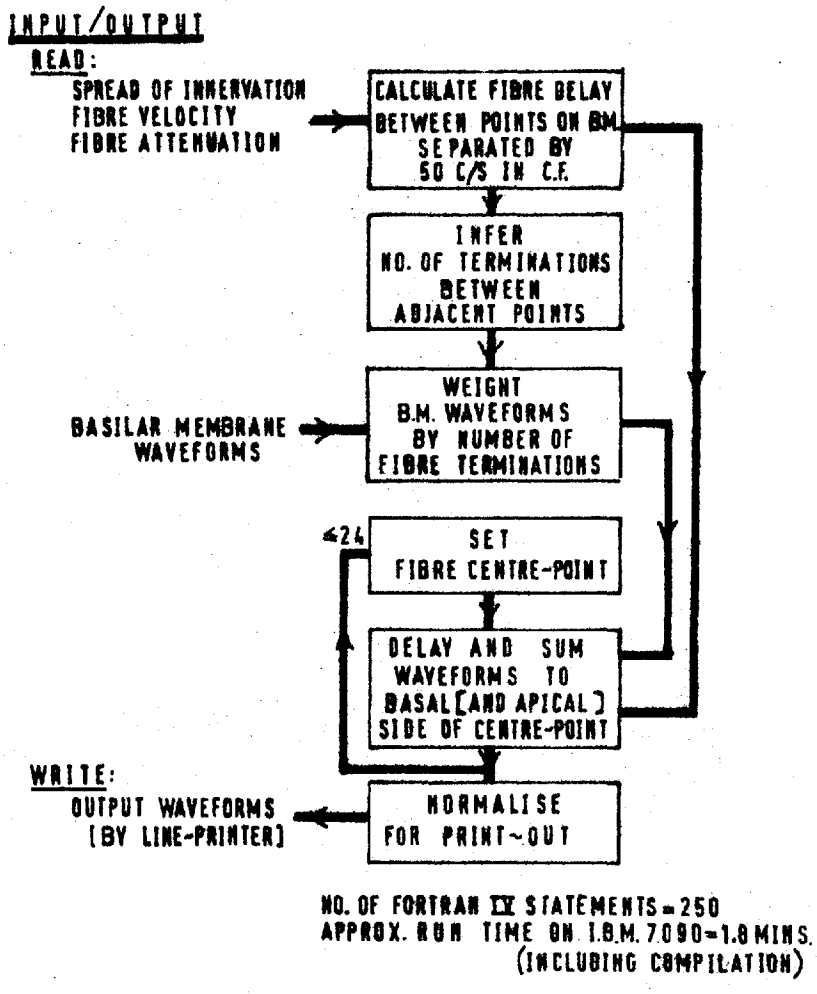

Figure 51 Simplified block diagram of a computer programme to simulate effects of cochlear spiral innervation.

The programme evaluates such waveforms for up to 24 spiral fibres innervating medial and apical cochlear regions. A

"500 Hz fibre" is the description now given to a fibre which enters the organ of Corti opposite the basilar membrane point of C.F. = 500 Hz; thus the quoted frequency refers to the position of the point P. (It does not follow that the spiral fibre will necessarily respond maximally to this sinusoidal frequency).

The programme makes further assumptions about the innervation. Firstly, it assumes a constant density of termination on hair cells lying along a spiral course, and that changes in polarisation of the fibre at any one of its terminations are proportional to the instantaneous value of local basilar membrane displacement. The spiral fibres are assumed to have delay and attenuation properties, but to cause no low-pass filtering of the signals conveyed by them; this simplification may be considered an important weakness of the simulation. On the other hand, if this scheme were to show any interesting results, it would be possible to modify the programme to include more complex effects.

6.2.3 Results

The results were plotted using the normal computer line printer and have been subsequently traced. Because the line printer can only move in relatively large steps, there are slight resolution errors in the plots (overcome in other cases by the use of a Calcomp X-Y plotter). All sets of curves are normalised to give the same maximum excursion somewhere on the plot.

Figure 52 shows the net stimulus at points P due to a low-pass filtered transient signal, for a number of fibres spiralling both basally and apically over distances of 2.5

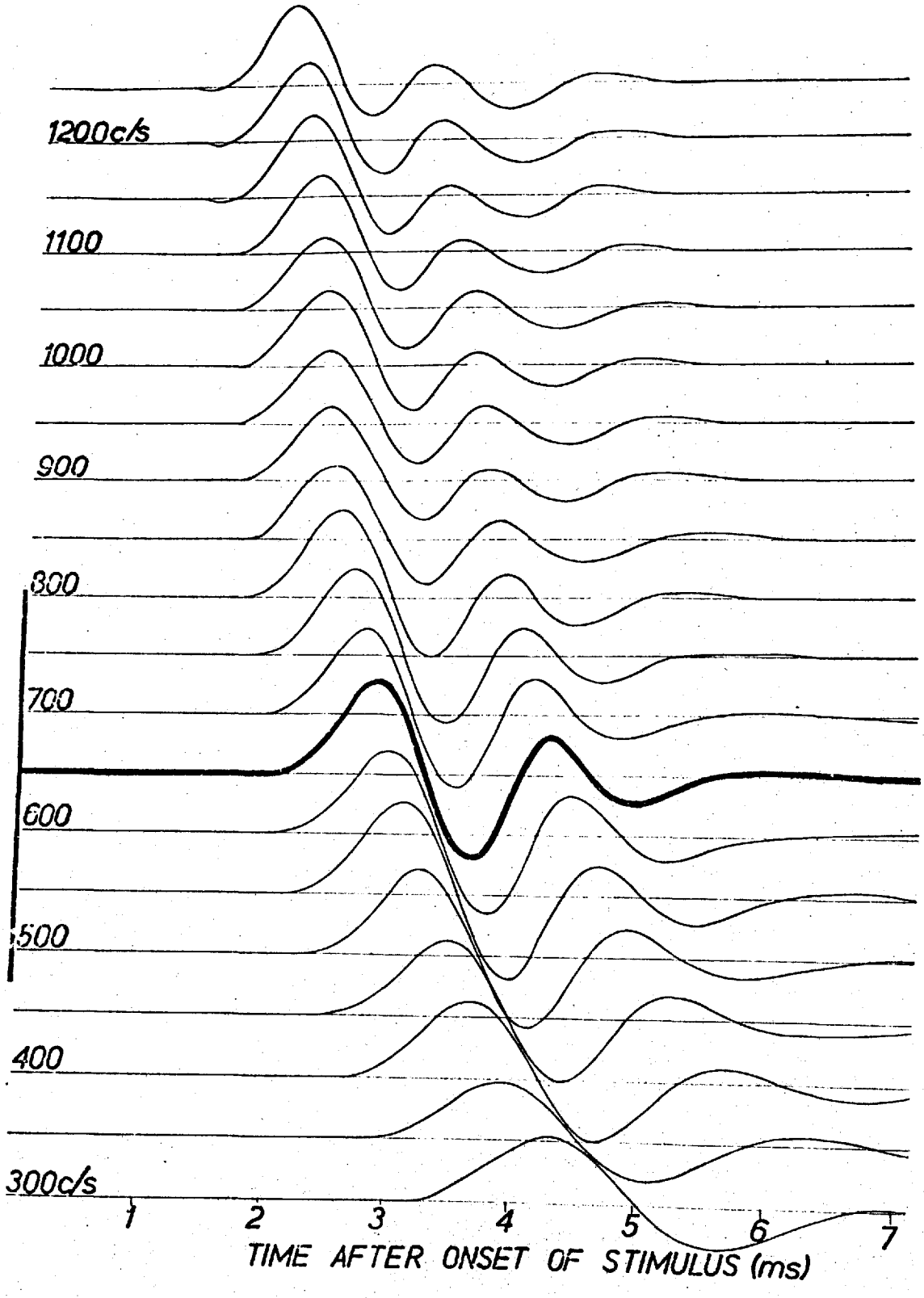

Figure 52 Computed excitation waveforms at trigger zone (P) of 20 spiralling cochlear fibres, in response to a low-pass filtered acoustic transient (Allison 2AB filter set to 0-800 Hz passband). The frequencies denote basilar membrane points opposite which the various fibres enter the organ of Corti. Fibre parameters: extent of spiral course = 2.5 mm. to either side of point P (see Figure 50); fibre velocity = 2 m/s; attenuation constant = 5 mm.

millimetres. Fibre velocity is assumed to be 2 metres per second, and attenuation constant 5 millimetres. Several matters are of interest. The maximum response now occurs in the fibre centred on the 650 Hz region of the basilar membrane, but, more importantly, the region in which the response is within the arbitrary 2 dB of this maximum is reduced in extent compared with Figure 47, in which the basilar membrane displacement patterns were shown. The reduction in relative response is most noticeable in the higher frequency fibres, as would be expected if the action of spiralling fibres were analogous to that of low-pass comb filters. There does seem, in other words, some evidence for a sharpening in cochlear tuning by such an innervation scheme.

The results shown above in Figure 52 were selected from a number of computer runs, using various combinations of fibre parameters, because they seem to display the most interesting effects. More typical, however, are the waveforms shown in Figure 53, representing the responses due to a similar stimulus, with fibre parameters unchanged except for the velocity of propagation, here set to 1 metre per second. This plot shows a break-up of the smooth oscillatory waveforms seen in Figure 52, especially in the higher frequency fibres. Any reasonable theory for the generation of action potentials must presumably equate the peaks of neural PST histograms with the peaks of the nerve fibre stimulus waveforms. Since Kiang's work (see Figure 13) shows that the various PST histogram peaks in response to such transient stimuli are invariably separated from one another by constant intervals, such a break-up in the waveforms seems improbable.

Such difficulties occur quite generally, when what are

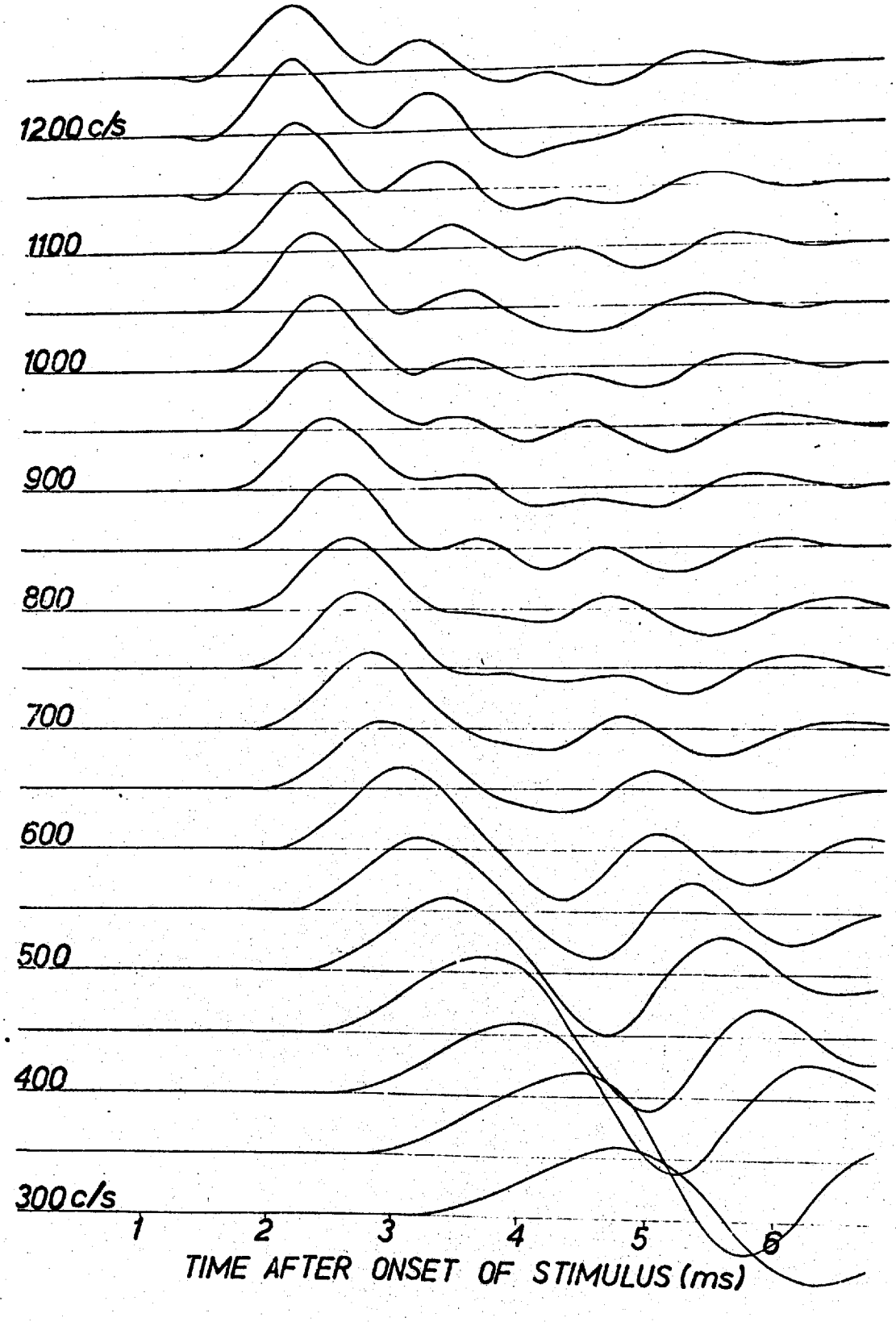

Figure 53 Computed excitation waveforms of 20 spiralling cochlear fibres. All conditions identical to those of Figure 52, except for the assumed fibre velocity, here set to 1 m/s.

believed to be reasonable values for the fibre parameters are chosen. They can generally be reduced by using smaller values for the spiralling distance, or larger values for fibre velocity; however, such changes reduce the evidence for the sharpening of cochlear tuning noticed in Figure 52. Even when the parameters are set to give reasonable results with one type of stimulus (e.g. a low-pass filtered transient), the response to a different stimulus (e.g. a wideband transient) often shows a break-up of the smoothly oscillatory waveforms.

6.2.4 Discussion

The possibilities for subthreshold signal processing by spiral cochlear fibres, analogous to the action of comb filters, seem unpromising. It appears that a careful choice of fibre parameters can give rise to a somewhat increased localisation of acoustic nerve activity (compare Figure 52 with Figure 47). However, if the parameters are varied slightly (but kept within what are believed to be realistic physiological ranges), the resulting waveforms break up and lose their smoothly oscillatory form. Such effects seem unlikely in practice, in view of the electrophysiological recordings of Kiang (see Section 2.7.2).

At the beginning of the present enquiry, it was believed that spiral fibres which put out terminations along their course might produce a latency/intensity effect in the neural activity measured in the acoustic nerve. Assuming for the moment that such fibres are excitable along their length, the following arguments seemed to apply. With a transient stimulus of high intensity, the excitation of the most basal point of the fibre (which, because of the travelling wave properties of the basilar membrane, would be stimulated first)

would be sufficient to cause a local action potential. The spike would then travel along the fibre towards the acoustic nerve trunk. At lower stimulus intensities the spatio-temporal summation of contributions of many, more apical, fibre terminations would be required to generate a spike. The latter would therefore tend to occur at some later time (post-stimulus) and at a more apical fibre locus. The main objection to such a scheme for the explanation of timing-intensity (or ITD/IAD) phenomena would be that latency changes in the individual peaks of a click PST histogram would be expected, whereas such effects are not visible in the recordings of Kiang.

In spite of this difficulty, some simulations have been carried out on the digital computer. The results are not reported here in detail because they seem essentially negative; and in any event the proposition about timing-intensity effects put forward in Section 3.4 now seems far more attractive. It is however of interest to outline the main results of these simulations, in which the net excitation waveforms at various points along a single spiral fibre were calculated, in response to a transient acoustic stimulus.

The results suggested that the maximum excitation effects anywhere along such a fibre were only some 2 to 4 times greater than those at its extreme basal end. This would presumably allow only a very limited dynamic range for any timing-intensity effect such as that described. Furthermore, the spike conduction velocity of the fibres would have to be greater than the travelling wave velocity on the basilar membrane, if any postulated timing/intensity ratio was to be of the right polarity (i.e. a reduction in neural latency must result

from an increase in stimulus intensity). Physiologically such a restriction seems debatable, since travelling wave velocities on the basilar membrane are of the order of a few metres per second. Finally, the simulations suffered from the same difficulties as the previous ones in which inexcitable fibres were simulated; the values of fibre parameters had to be severely restricted if there was to be no break-up in the computed waveforms.

In view of all these results, it seems unlikely that any plausible subthreshold processing could be achieved by spiral nerve fibres putting out terminations to the outer hair cells all along their spiral course. In particular, there are no clues to the suppression of the earlier peaks of click PST histograms of neural activity at low intensities. It is not believed that alteration of the computer programmes to include the filtering properties of fibres in more detail would affect these basic conclusions. It is finally tempting to argue that such results provide independent evidence against such patterns of nerve fibre termination; but in any case it is difficult to visualise any substantial signal processing being achieved by such innervation schemes.

On the other hand it is not easy to understand the reasons (if any) why fibres should spiral for long distances before finally terminating on outer hair cells. If the stimulus spreads electrotonically from such terminations to some distant trigger zone, it presumably undergoes considerable attenuation, with consequent loss of system sensitivity. It is also probable that the fibres would impose low-pass filtering, which, if substantial, would be difficult to reconcile with the measured click histograms of Kiang.

Equally, it would be hard to imagine any reasons for a long spiral course, if spikes were assumed to be generated at the fibre terminations on the hair cells. Useful signal processing could not apparently be achieved by the mere passage of spikes along a spiral fibre, before entering the habenula perforata. And although the proposition of Section 5.4.1 (concerning the statistics of spontaneous activity in the acoustic nerve) seems to imply the superposition of a number of independent spike trains generated at the different fibre terminations, such a condition could be satisfied equally well by a simpler radial innervation scheme (with each fibre terminating radially on a number of hair cells). Such matters therefore remain, for the present, unresolved.

7. ELECTRICAL MODELS FOR COCHLEAR NEURAL TRANSDUCTION

7.1 Electrical synaptic transmission

The proposition that the observed spontaneous activity in first-order auditory neurons may be explained on the basis of multiple innervation of hair cells by cochlear nerve fibres has already been put forward in Section 5.4.1. This proposition, if accepted, has the corollary that the measured spontaneous activity gives no indication of the precise mechanisms operating at the individual afferent hair cell junction, and clues to this process must therefore be sought in the recordings of stimulus conditions.

The effective suppression of the earlier peaks of a click PST histogram at low intensities is an effect of great interest (see Sections 2.8 and 3.4). However, it seems clear that it cannot also be ascribed to the multiple innervation of hair cells by cochlear fibres, because the effect is present at stimulus intensities near threshold, even in units displaying low spontaneous rates. At such intensities the total amount of stimulus-locked activity is very small, and there is unlikely to be any substantial interference between spikes arriving from the various terminals of a single fibre. A PST histogram recorded in the acoustic nerve is therefore assumed to represent equally well the activity at a single hair cell termination, at least near threshold.

The question arises whether an explanation of these interesting effects is possible in terms of known electrical properties of nerve and synapse, without the need to specify an intermediate chemical transmitter effect. Although there is substantial evidence[8] for chemical transmission at many types of nervous system synapse, there are also well-documented

instances of purely electrical synaptic transmission. These have recently challenged the growing support for the generality of chemical systems[66]. In some work on the giant motor synapse of the crayfish, Furshpan and Potter[19] produced strong evidence for purely electrical activity, by demonstrating substantial transmission in both directions across the synaptic junction (in the normal chemical system transmission is only possible one way, because chemical is only stored in one of the synaptic terminals). By inserting electrodes in both presynaptic and postsynaptic fibres, they were able to demonstrate effects which could be explained purely on the basis of a synaptic rectifier element, responding only to the potential difference across the synapse, regardless of how this was produced. The explanation was sufficient to account quantitatively for the transmission of electrotonic stimuli as well as action potentials. The relatively large size of the presynaptic fibre was considered to be important in assuring transmission; furthermore, the resistance per unit area of the synapse was approximately 15% of that of the presynaptic nerve membrane, making the synaptic junction a low resistance path to the passage of current in the conducting direction. This is in marked contrast to the normal electrical isolation provided by a chemically-transmitting synapse.

Robertson, Bodenheimer and Stage[50] investigated Mauthner cells in the brains of goldfish and found various types of distinctive synaptic contact which, they believed, did not conform in structure to a chemical system. In particular there was no good evidence of regular synaptic clefts, or of substantial inclusions of the synaptic vesicles generally thought to contain chemical transmitter substance. Although their evidence is less quantitative than that of Furshpan

and Potter, it supports the possibility of electrical transmission.

Such work may or may not be relevant to the afferent junction between hair cell and nerve in the cochlea, but it suggests that chemical transmission is not indispensable in synaptic systems. It might, for example, be imagined that the electrical activity of the hair cells (responding to local basilar membrane vibrations) would be transferred to the afferent nerve endings via rectifying synaptic contacts of the type reported by Furshpan and Potter. This would cause nerve fibres to be stimulated by electrical pulses corresponding to alternate half-cycles of basilar membrane vibration. A leaky integration of such pulses by the capacitive-resistive properties of nerve might then be envisaged; this could give rise to a facilitation effect during a transient stimulus, whereby the nerve depolarisation produced by the earlier rarefaction half-cycles of membrane movement would enhance the effects of later half-cycles, from the point of view of spike generation. At higher stimulus intensities, the first half-cycle would itself be sufficient to cause spike generation, and the refractory properties of nerve would reduce the probability of further spikes due to the same stimulus.

Although such a proposition might be attractive at first sight, a quantitative approach soon shows that some additional effects are required if suppression of the first one or two peaks of a click PST histogram is to occur at low stimulus intensities. This follows from the greatly reduced magnitude of successive basilar membrane oscillations; the third peak in response to a click is apparently only 1 or 2% of the first one (see Figure 46). Even allowing for an effective

postsynaptic integration effect by nerve fibre properties, the third peak could hardly cause a great deal more firing than the first, as in fact it does at low and medium intensities (see Figure 14). The next task, therefore, seems to be to examine the known nonlinear properties of nerve in more detail.

7.2 Nonlinear effects in nerve

The most complete account of spike generation and propagation in nerve fibres is that of Hodgkin and Huxley[28], who successfully predicted the detailed form of the action potential in the giant axon of Loligo. This they did by studying the time course of sodium and potassium ion conductances, in response to artificially applied steps in the membrane potential, known as voltage clamps. Their work has stimulated much interest and research into the ionic theory of nerve, which has come to enjoy rather wide acceptance in the detailed explanation of conduction and excitation phenomena[33]. More recently a number of workers (for example Noble[45] and Lewis[39]) have extended the coverage of the theory to include a variety of subthreshold phenomena, thereby emphasising its generality. Although it is not intended to describe the ionic hypothesis in detail, some general remarks seem appropriate.

The theory is basically concerned with the dynamic opposition of two ionic fluxes (sodium and potassium) across the nerve membrane. The net flux of either ion type is the sum of two components, one caused by diffusion down its concentration gradient, the other by a drift down its potential gradient; both components are limited by the resistance of the membrane. The potassium ion concentration is greater inside the nerve membrane, the sodium concentration greater on the outside. At equilibrium (representing the

normal membrane resting potential of some 70 mV, inside negative) the membrane is almost impermeable to sodium ions, whereas its permeability to potassium and a few other ions (particularly chloride) is small but finite, and the equilibrium potential is sufficient just to balance the inward and outward fluxes carried by the various ions.

By a series of voltage clamp experiments, in which they applied and maintained step changes of potential across the membrane, Hodgkin and Huxley were able to deduce the time course of changes in membrane permeability to sodium and potassium ions. They found that such changes were complex functions of both the instantaneous membrane potential and time; this led to their description by simultaneous first-order differential equations with voltage-dependent parameters.

The dangers of drawing parallels between a squid's giant axon held at a temperature of $6^{o}C$ and cochlear nerve fibres cannot be overestimated. However it seems pointless to speculate about unknown nonlinear effects in the cochlea without some reference to those systems which have already been quantitatively investigated. Furthermore, the acceptance of the ionic theory for the explanation of effects in a wide variety of nerve fibres seems to give some justification for such an approach. Fortunately an electronic model of the Hodgkin-Huxley theory is available, which gives some insight into the ionic mechanisms involved, without involving the complex nonlinear methods which would be necessary for simulation by digital computer.

7.3 Lewis' electronic model of nerve membrane

7.3.1 General description

Lewis[40] has described an electronic model of nerve membrane, in which transistor circuits are used to model the ionic equations of Hodgkin and Huxley. Unlike some other recent electronic neural models (for example that of Jenik[31], and Kletzky and Fraioli[38]) which do not pay specific attention to subthreshold phenomena, Lewis' model attempts to describe the detailed time-course of sodium and potassium ionic fluxes both above and below firing threshold. From this point of view it seems suitable for the investigation of possible subthreshold effects in cochlear nerve fibres. The model is designed to reproduce the voltage clamp results of Hodgkin and Huxley; in practice, spike generation may readily be demonstrated, and Noble[45] has suggested that adjustment of parameters allows the simulation of non-excitable nerve. It seems possible, however, that the voltage clamp results do not completely specify the time course of sodium and potassium fluxes for all types of stimuli, and such a danger should be borne in mind in the discussion which follows. Finally, the circuit models only a small patch of nerve membrane, and cannot therefore reproduce electrotonic spread or spike propagation effects.

The model employs active circuits to simulate the passage of sodium and potassium ions across the membrane, and also includes a path for leakage ions (mainly chloride) and the effects of membrane capacitance. The main elements are shown in Figure 54. g_{Na} and g_K are the sodium and potassium conductances respectively, and are complex functions of the membrane potential (V_m) and time. The leakage-ion conductance g_l and the membrane capacitance C (in series with a small

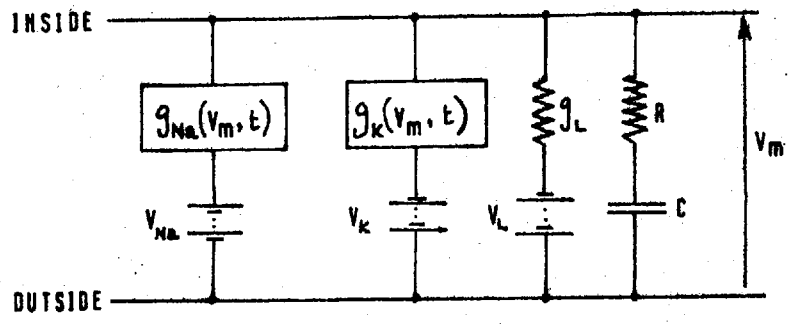

Figure 54 The main elements of Lewis' model of a patch of nerve membrane, designed to reproduce the voltage clamp data obtained by Hodgkin and Huxley from the giant axon of Loligo.

resistor R) are constants. Each conductance element is placed in series with a battery which represents the equilibrium potential for that ion; if the membrane potential at any instant is equal and opposite to the equilibrium potential, then there will be no transmembrane current carried by the ion, regardless of the value of the relevant conductance.

Lewis has described several limitations of his detailed realisation of this system. Firstly, it assumes that changes in sodium ion current are due entirely to changes in g_{Na} and not to changes in V_m. This is justified on the basis that the driving voltage for sodium ions (equal to the difference between V_{Na} and V_m) is large in the normal resting condition, and is not therefore substantially altered by small changes in V_m. This seems a reasonable assumption for subthreshold behaviour, although it is likely to produce errors in the form of any action potential generated by the circuit. Another limitation is that diodes are used to perform multiplication operations in the g_K circuit; these are not very accurate and Lewis later replaced them with more complex multipliers[39]. Finally, the present writer has found

that the circuit does not reproduce the changes in g_{Na} during voltage clamps (as observed by Hodgkin and Huxley) with great accuracy, and has found it necessary to introduce several minor modifications.

7.3.2 Response of the model to voltage clamps

An appreciation of the main features of the model's response to voltage clamps helps considerably in understanding detailed circuit operation, which will be described in the next section.

Before a voltage clamp is applied, the membrane potential, V_m, is at its normal resting value of about 70 mV (inside negative), and there exists an equilibrium condition in which the three ionic ion currents are in balance. In fact, the sodium ion current, I_{Na}, is normally very small in this condition and the value of V_m settles rather close to the potassium equilibrium potential, V_K. If the membrane is partially depolarised by being clamped to some new voltage level (say - 50 mV), the time-course of the various ionic currents reflects directly upon changes in the ionic conductances (g_{Na} and g_K) since the driving voltages are constant while the clamp is maintained.

It is found that under such conditions the sodium conductance, after a short delay, rises to a peak value which may be hundreds of times greater than its previous resting value, and then declines to a new steady state value which is non-linearly related to the new value of V_m. By contrast, the potassium conductance rises much more slowly to a new, and relatively high, steady-state value. These effects are illustrated in Figure 55, which is traced from oscilloscope photographs taken during voltage clamp tests on the modified

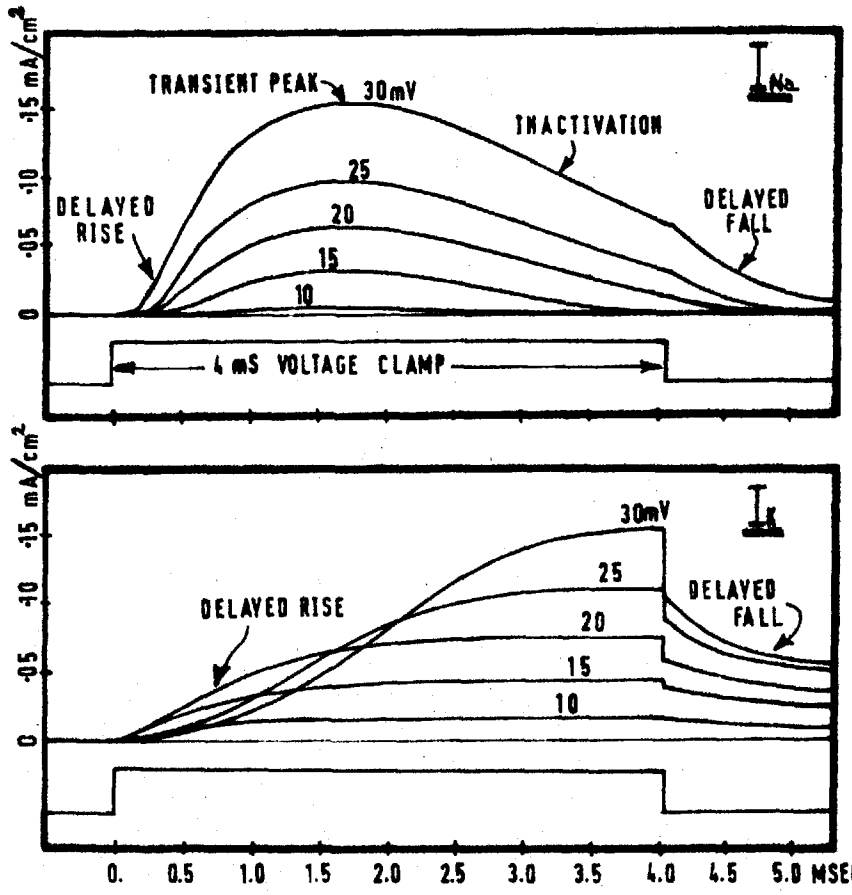

Figure 55 Results of testing a modified version of Lewis' electronic model, showing typical time-course of sodium and potassium ion currents in response to a number of voltage clamps of 4 msec. duration. Against each curve is indicated the magnitude of the imposed depolarisation.

version of Lewis' circuit. Although the figure shows sodium and potassium currents (which are conveniently measured), these are very closely related to the conductances. In the case of sodium, the current is indeed assumed to be a direct measure of conductance, since changes in sodium ion driving voltage are ignored. In the case of potassium, the step change in current seen when the clamp is removed is due to the change in V_m; however, the steady rise and fall of potassium current during constant voltage conditions are

directly proportional to conductance changes. These results parallel very closely the measurements of Hodgkin and Huxley.

The main features of these curves are sufficient to account for spike generation when the membrane potential is no longer artificially clamped. If an initial depolarisation greater than a certain minimum level is induced by, for example, a short current stimulus, the sodium conductance rises and so allows a further inflow of sodium ions. This increases the depolarising effect which produced it, and an explosive reaction occurs which is typical of a positive feedback system. However, a number of factors check the amplitude and duration of the action potential. Firstly, the membrane potential is brought close to the sodium equilibrium potential during the spike, which reduces the sodium driving force; also, sodium inactivation (possibly due to the "clogging" of sodium ion paths through the membrane) occurs. Secondly, the potassium conductance, after its rather long initial delay, rises to a high level, and the resulting outflow of potassium ions produces a negative feedback effect tending to restore the equilibrium potential.

In the case of chemical synaptic transmission, an excitatory chemical quantum is thought to cause a general increase in the postsynaptic membrane's conductance to all ions[8], which, in particular, aids the inflow of sodium because of its relatively large driving potential near equilibrium. If this initial effect is sufficiently large, the loop-gain requirements for spike generation are realised; if not, there is a return to resting conditions. Noble[45] has pointed out that inexcitability in some nerve fibres might be explained by their high value of membrane capacitance, which prevents

initial sodium inflow from having much effect on the membrane potential, thereby inhibiting the feedback mechanism.

7.3.3 Detailed circuit operation

It is not intended to repeat the detailed discussion of the circuit given by Lewis, but only to discuss its more important features and to report various modifications.

The circuit is drawn in detail in Figure 56. It represents 1 cm^2 of nerve membrane, with all voltages and currents 100 times their actual physiological values. At the top of the diagram is a line representing the inside of the nerve membrane, to which are connected the various ionic paths and an input circuit of low source impedance used to supply stimuli (either voltage clamp waveforms, or current stimuli via a 100 KΩ resistor). The right hand end of the line is connected to another follower circuit of high input impedance, the output of which feeds V_m to the g_{Na} and g_K circuits.

Referring to the sodium conductance circuit, there are two paths to the base of transistor no. 1 (T1), one a d.c. path giving the steady-state dependence of g_{Na} on V_m, the other incorporating a 1 μF capacitor and giving transient effects. A modification to Lewis' circuit is the connection of a 0.1 μF capacitor between the base of T1 and earth, giving a delayed rise of g_{Na} under voltage clamp conditions (see Figure 55) which more closely parallels the results obtained by Hodgkin and Huxley. The nonlinearity in the dependence of g_{Na} on V_m is provided by voltage-dependent resistors. The g_{Na} function is already generated at the base of T2, which has an overall amplitude control in its collector circuit. A further modification to Lewis' circuit

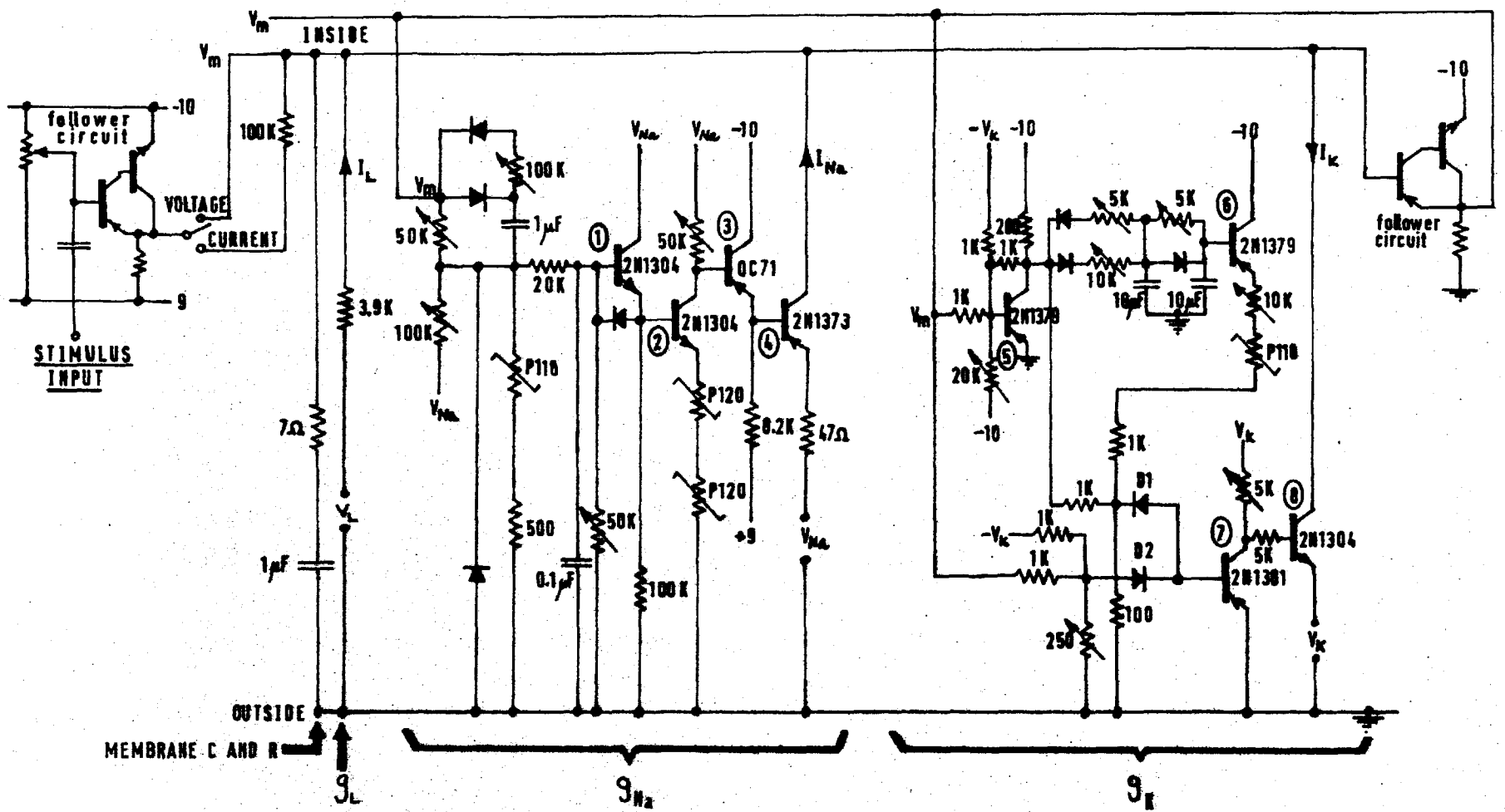

Figure 56 Modified version of Lewis' circuit for the simulation of the Hodgkin-Huxley equations.

is the inclusion of an additional transistor, T3, as a low impedance drive to the base of the final conductance transistor, T4.

In the potassium circuit, the g_K function is generated in the emitter circuit of T6. The output of the summing stage, T5, is equal to $(V_K - V_m)$, and this is added to the conductance function at the cathode of diode D1. The anode of D2 receives a signal equal to $(V_m - V_K)$. Assuming the diodes to be square-law devices, the net current to the base of T7 is approximately equal to the product $g_K \times (V_m - V_K)$, which is the required potassium ion current. Balancing of the diode circuits to achieve this multiplication, a difficult operation which is only possible over limited ranges of g_K, has been found to be simplified by the use of a 250Ω variable resistor as a gain control in the anode of D2.

7.4 The ionic theory in relation to cochlear neural transduction

There are two main reasons why the ionic theory seems attractive in the context of cochlear nerve fibres. Firstly, it is well-documented and has found a rather wide application in the description of subthreshold and superthreshold effects in a variety of nerve fibres. Secondly, it displays complex nonlinearities; and, in particular, the delayed rise of sodium conductance upon application of a depolarising clamp (see Figure 55) seems in some intuitive way to parallel what may well be a delay effect in click PST histograms, in which later peaks are generally far more prominent than would be expected on the basis of presumed basilar membrane activity.

This parallel suggests that the first, and largest, basilar membrane rarefaction peak in response to a click stimulus may cause an initial depolarisation of local cochlear nerve fibres which, at low and medium stimulus intensities, is generally insufficient to cause spike generation. However it activates the sodium conductance mechanism, which reaches a peak transient value coincident with some later basilar membrane rarefaction movement. Even though this movement is much smaller, its effectiveness is thereby greatly enhanced. In such an explanation, the delayed rise in sodium conductance becomes the crucial factor; detailed changes in the potassium circuit would be relatively unimportant, although the later rise of potassium conductance would presumably have a dampening effect on the effectiveness of later basilar membrane activity.

In more detail, there seem two ways in which such a scheme might operate, assuming that basilar membrane activity

causes an intermediate polarisation of hair cells (see Section 2.6). A hair cell could either be imagined to control the membrane potential of afferent nerve terminals attached to it, or it might cause a controlled current to be forced into those terminals. In other words, the hair cell could be considered as either a voltage or current source, depending upon the relative impedance characteristics of hair cell and nerve fibre.

The first alternative may seem less attractive because it precludes the generation of a local action potential in the nerve terminal, and must rely on electrotonic spread of activity to some distant trigger zone, presumably with consequent attenuation and loss of timing resolution. However, the proposition is explored more critically in Figure 57, which shows the response of the sodium conductance circuit of the electronic model to periodic voltage stimuli of limited duration. Once again, these results were traced directly from oscilloscope photographs. The stimulus waveforms were obtained from standard signal generators controlled by an F.E.T. switching circuit, and show the imposed variations of membrane voltage about its resting level of about - 70 mV (with depolarisation shown as positive).

With such stimulus waveforms it is easy to show that no measurable changes in g_{Na} (or g_K) occur until peak depolarisations of some 10 or 15 mV are imposed. Therefore at low stimulus intensities the various ionic currents are linearly related to the stimulus. When the stimulus is sufficient to cause peak depolarisations of above about 15 mV, successive peaks of the sodium conductance waveform are enhanced by the delayed effects due to previous peaks;

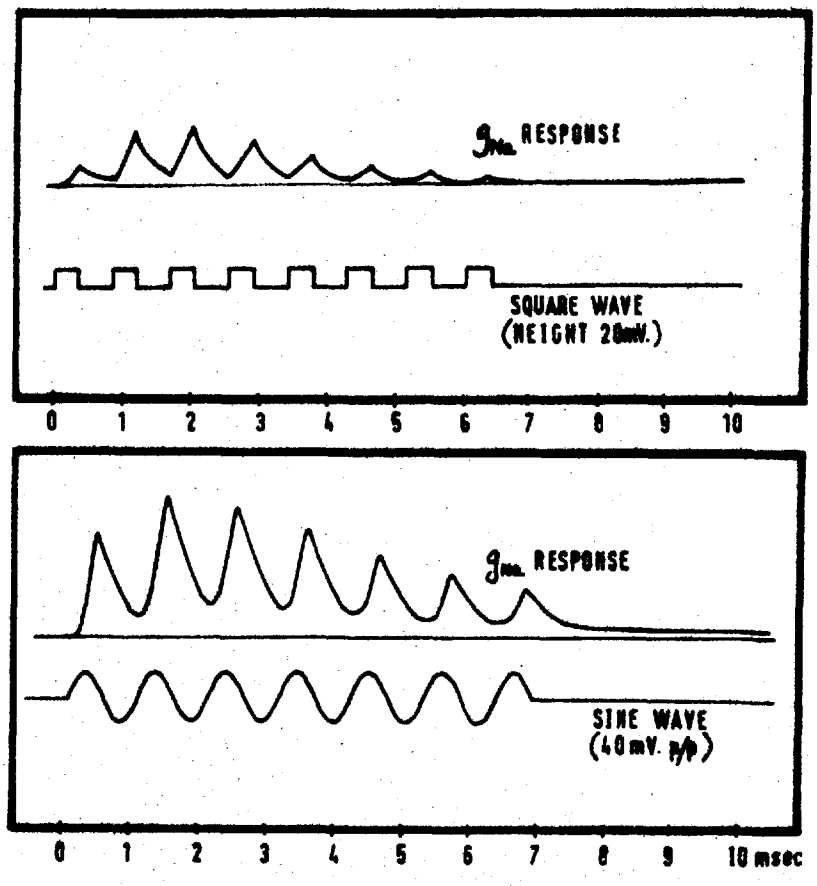

Figure 57 Typical responses of the sodium conductance circuit of the electronic model, to periodic voltage stimuli of limited duration. Above is shown the response to a train of 8 depolarising pulses; and, below, the response to a switched sinusoid.

after a few milliseconds, however, the effects of sodium inactivation become important, and the response declines. Hyperpolarising half-cycles have little or no effect on the sodium conductance mechanism; thus, although it is not shown, the response to the rectified version of the sinusoidal stimulus was found to be similar to the one illustrated. It is interesting to note that the peaks of the responses follow an envelope similar to the time-course of g_{Na} during the normal type of voltage clamps (shown in Figure 55). This reflects the fact that the magnitude of such responses is

largely governed by sodium inactivation, a characteristic of the nerve and not of the stimulus.

The stimulating waveform of real interest in the present context is the heavily damped oscillation of the basilar membrane in response to a transient acoustic stimulus. Although such a waveform has not been used to test the circuit model, it is quite clear from Figure 57 that, unless the model parameters were drastically revised, no dramatic enhancement of sodium ion inflow could be expected during the second or third rarefaction half-cycles of membrane activity. A further objection is that considerably longer delays in the rise of sodium conductance would be required; in the case of a cochlear fibre of C.F. = 200 Hz, a delay of perhaps 5 or 6 milliseconds would be appropriate. The rise in potassium conductance would have to hold off for even longer. It seems most unlikely that cochlear fibres, much finer than the giant axon studied by Hodgkin and Huxley, would display timing delays of this order of magnitude.

Some of the same difficulties must apply to the second possibility, which is that the hair cells inject pulses of current into the nerve terminals in response to local basilar membrane rarefaction movements. In this case the potential of the nerve membrane would not be determined, and spikes might presumably be generated at the nerve terminals. Figure 58 shows the effects on the nerve membrane potential of injecting periodic current stimuli of limited duration. In the upper part of the figure a train of 8 short depolarising pulses causes the membrane potential to rise, and then either to decay again, or, in the case of a stronger stimulus, to exceed the threshold for spike generation. Below threshold, the membrane capacitance, together with the various ionic

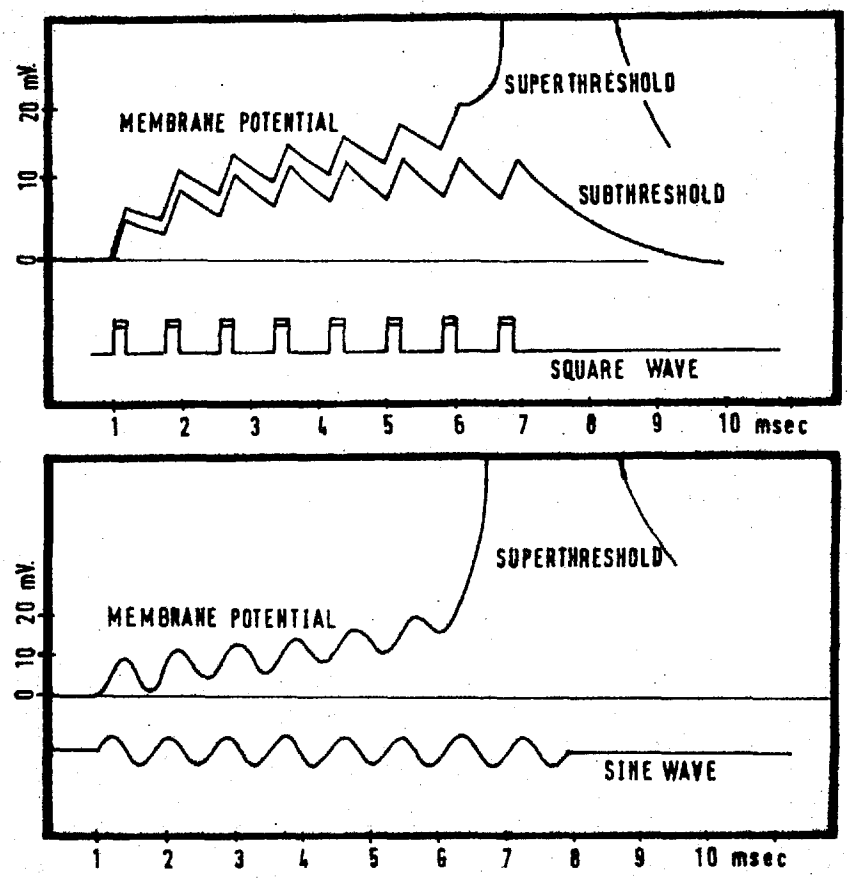

Figure 58 Typical membrane potential responses of the electronic model to periodic current stimuli of limited duration. Above are shown responses to a subthreshold and superthreshold stimulus consisting of 8 unipolar current pulses. Below is a single superthreshold response to a switched sinusoidal current stimulus.

conductance paths, performs a leaky integration of the current stimulus. At threshold, the regenerative action of the sodium conductance mechanism, which has previously had only a very limited effect, causes a violent increase in membrane potential and a spike is generated. In the case of a bipolar current stimulus the integration effect tends to keep the membrane potential oscillating around its resting value, unless, as shown in the lower part of Figure 58, individual depolarising half-cycles are sufficient to cause membrane voltage changes

of more than about 10 mV. In this case the regenerative effect is again set in motion, producing a drift of membrane voltage towards threshold.

These results clearly demonstrate that a unipolar, or rectified, current stimulus is much more effective in generating action potentials. In the context of cochlear fibres, such rectificatification seems essential to any proposition based upon current control in nerve terminals by hair cells. If there were no such rectifier action, the basilar membrane response to a condensation click would apparently cause an initial hyperpolarisation of nerve terminals which would severely suppress the sodium regenerative effect. There is evidence in neurophysiological recordings (see Section 2.7.2) that an initial condensation movement of the basilar membrane actually enhances nerve firing during subsequent rarefaction movements. Even if a rectifying junction exists, there are again no dramatic effects in Figure 58 which would cause later peaks of click PST histograms to be greatly enhanced, bearing in mind the relatively small basilar membrane movements presumed to cause them.

7.5 Discussion

The results reported in this section appear rather negative. Unless there is a drastic revision of the parameters of the ionic model of Hodgkin and Huxley, it is difficult to believe that such a model could begin to account for the complex effects visible in click PST histograms of first order auditory neurons.

It could be argued that to use the characteristics of the giant axon in Loligo for a discussion of auditory neurons is in any case naïve, and that if the complexities of sodium and potassium ion fluxes in nerve are in fact responsible for some of the observed effects, then a drastic revision of the Hodgkin-Huxley parameters would certainly be expected. There seems, however, to be a further reason, in addition to those already discussed, why a proposition based on known electrical properties of nerve and synapse is unacceptable.

Reference to Figure 13 suggests that, for units in the cat's auditory nerve having C.F. values less than about 4 KHz, there is an approximately equal number of peaks visible in each click PST histogram. Furthermore the effective suppression of the earlier peaks of these histograms does not depend noticeably on the C.F. of the fibre. These points strongly suggest that the time-course of any mechanism responsible for such effects must be directly related to the C.F. of the unit considered. As far as is known, there is no evidence that the time-course of any ionic effects in a nerve terminal would occur approximately 15 times faster in a fibre innervating the 3000 Hz region of the cochlea, compared with one innervating the 200 Hz region. Such considerations seem finally to rule out any proposition based on known electrical effects in nerve.

8. CHEMICAL TRANSMITTER MODELS FOR COCHLEAR NEURAL TRANSDUCTION

8.1 Introductory comments

In view of the difficulties of explaining certain important characteristics of the firing patterns of first order auditory neurons in terms of electrical properties of nerve and synapse, it now seems appropriate to explore possible chemical transmitter effects at the junction between hair cell and afferent nerve ending in the cochlea.

Before beginning such an investigation, the relationship between chemical synaptic transmission and the previously discussed ionic theory of nerve should perhaps be summarised. This may be appreciated by reference to Figures 25 and 26, which represent the chemical transmitter models for stationary neural activity of Stein and Johannesma. In such models, it is generally assumed that each quantum of a given chemical transmitter substance, released across the synaptic cleft, gives rise to a fixed step in the postsynaptic membrane potential (V_m). In terms of the ionic theory, however, each such quantum is believed to cause a fixed step-change in conductance of the membrane to one or more types of ion[8,42]; on such a basis, the resulting potential change would be expected to depend upon the driving potentials of these ions, which in turn depend upon the instantaneous level of V_m. As already noted in Section 7.3.1, the driving potential for sodium ions is not substantially altered by subthreshold changes in membrane potential; therefore the size of excitatory steps in V_m (due to step changes in sodium conductance caused by excitatory chemical quanta) will in practice be largely independent of V_m. On the other hand,

an inhibitory chemical transmitter (causing step changes in potassium conductance) will give rise to steps in membrane potential which depend markedly on the latter's instantaneous level. This occurs because the driving potential for potassium ions increases very substantially as the membrane is depolarised.

It is clear that quantal models such as those of Stein and Johannesma do not take details of the ionic theory into account; they neither allow for changes in ionic driving potentials nor for the complexities of the ionic conductance mechanisms. In short, they consider the subthreshold activity of nerve to be linear and to be characterised by step changes in V_m of constant magnitude. On the basis that the ionic theory is believed to offer no ready explanations for the neural effects of interest in this study, it is now proposed to adopt such simplifying assumptions about the postsynaptic membrane (i.e. the cochlear nerve-ending), and to use such models for the investigation of effects due to assumed variations in the rate of release of a chemical transmitter.

8.2 Evidence from other chemical synaptic systems

The random release of chemical transmitter substance at the afferent hair cell-nerve ending junction has already been suggested (see Section 5) as an attractive hypothesis for the explanation of spontaneous spike generation in first-order auditory neurons. Assuming that modulation of such a chemical release might be an important effect of basilar membrane activity, it is of interest to consider relevant evidence from other chemical transmitter systems.

It is well established that the arrival of a propagated action potential at a presynaptic terminal causes a large temporary increase in the rate of release of chemical transmitter. Some 200-300 quanta are thought to be liberated across a synaptic cleft by a typical incoming spike, in perhaps 1-2 milliseconds[8]. This increased chemical liberation does not, however, depend upon all-or-none spike activity, but may also be produced by graded potentials. For example, Katz and Miledi[34], in studies on the giant synapse in the stellate ganglion of squid, have described the relation between an applied presynaptic depolarisation and the peak level of the resulting PSP, considered to be a direct measure of the number of quanta released. They found that the logarithm of the peak PSP value was linearly related to the applied polarisation, up to a certain "saturation" limit (a 12 mV. increase in presynaptic depolarisation gave rise to a ten-fold increase in the peak postsynaptic response). Katz[36] has related such results more specifically to the frequency of liberation of chemical quanta, showing that in muscle of the rat diaphragm the logarithm of the liberation frequency is linearly related to the polarisation of the presynaptic terminal.

Depolarisation from the resting level was found to increase the frequency and hyperpolarisation to decrease it.

This and other evidence[8] supports the view that, in a number of chemical transmitter systems, polarisation and quantal liberation are logarithmically related in a way which greatly enhances the effects of large depolarising signals. Although the precise mechanisms involved are unknown, there is strong evidence[6,8,29] that calcium ions perform a vital role by entering the presynaptic terminal during depolarisation. It is also possible that the co-operative action of 4 such calcium ions is needed at each "release-site" before the liberation of a chemical quantum across the synaptic cleft can occur.[35]

In addition to the evidence for reduction in the rate of quantal release during hyperpolarisation of a presynaptic terminal, it seems that a hyperpolarising stimulus may also cause "mobilisation" of chemical transmitter, which then moves up to the synaptic boundary ready for release during subsequent depolarisation. Eccles[8] has reviewed such effects, and concludes that hyperpolarising currents seem to provide a powerful force mobilising the chemical quanta. More recently, Katz and Miledi[34] have described how, in the stellate ganglion of squid, an initial hyperpolarisation of a presynaptic membrane greatly enhances the transmitter release due to a subsequent depolarisation. Because this effect is matched by raising the external calcium ion concentration, they suggest that hyperpolarisation may in some way facilitate the entry of calcium ions during subsequent depolarisation. A detailed analysis of facilitation effects at the neuromuscular junction of the frog has led Mallart

and Martin[41] to suggest that there may be two separate mechanisms at work. The first, which is short-term, is described as a "residual change in excitability" of the transmitter release mechanism. The second and longer-term effect (occupying some 60-200 msec.) is thought of as producing an increase in transmitter release of different origin, perhaps as a result of additional transmitter mobilisation; and there is evidence of a coincident hyper-polarisation of the presynaptic terminal.

It is clear from such evidence that documented chemical synapses display a number of complex effects. Once again, the risks of applying such findings to a study of cochlear synapses must be great; on the other hand, they provide some clues as to the types of mechanism which may be expected in a system involving the synthesis and liberation of chemical transmitter substance.

One aspect of this evidence is disappointing. All references to the variation of transmitter release rate with presynaptic polarisation point to a logarithmic relationship which greatly enhances the postsynaptic effect of a large depolarising signal, compared with that of a small one. If such effects were to be paralleled at the afferent synapses in the organ of Corti, large depolarisations of the hair cells (presumed to be caused by large basilar membrane rarefaction movements) would cause more than proportional transmitter release. Such a scheme could not be expected to enhance the probability of firing during the later (and smaller) basilar membrane rarefaction movements caused by a click stimulus.

8.3 Digital computer simulations

8.3.1 Simple relationships between stimulus and chemical release

Some initial digital computer simulations, in which the rate of release of chemical transmitter substance was varied in sympathy with a stimulus waveform, are now reported. The use of a computer programme for the simulation of spontaneous activity in first order auditory neurons has already been described (see Section 5.3.3 and Figure 28). The programme was however written to accept nonstationary inputs and to generate the various statistics appropriate to stimulus conditions, such as PST histograms and estimates of recovered probability (see Section 2.7.3).

One of the main aims of this work is to achieve realistic simulations of the click PST histograms recorded in cat by Kiang (see Section 2.7.2). In this context, integration effects by the postsynaptic membrane (the cochlear nerve ending) seem likely to be significant. If an initial release of transmitter substance, caused, for example, by the first basilar membrane rarefaction movement in response to an acoustic click, does not actually cause the PSP to reach firing threshold, its effect may nevertheless linger and enhance the chances of spike generation during later rarefaction half cycles. Such an effect seems, however, to rely on certain other assumptions. For example, suppose that ongoing (spontaneous) release of a chemical transmitter at a hair cell junction were to be increased by local rarefaction movements of the basilar membrane, and suppressed by condensation movements. An initial rarefaction peak might cause the PSP to move towards threshold without actually

reaching it, but the following condensation movement would tend to return the PSP towards its previous level. Intuitively it may be seen that postsynaptic integration effects are only likely to enhance the later peaks of a click PST histogram if condensation activity of the basilar membrane causes little or no suppression of chemical release. This points to the need for a rectifier action.

Such matters have been explored in a number of digital computer simulations using a model of a chemical synapse like that of Johannesma (see Figure 25), with threshold refractory properties included. These simulations all assumed an excitatory step size of 5% of the distance to threshold, with no inhibitory input. Figure 59 shows the effects of a stimulus consisting of a number of cycles of an 800 Hz. sinusoid. This waveform is not intended to represent a basilar membrane response, but is convenient for assessing the effects of postsynaptic integration because it has a number of identical peaks; variations in the height of peaks of the PST response may therefore be attributed directly to the action of the model. In this simulation the modulation of the quantal rate about its mean spontaneous value (M = 0.64, with τ = 1 msec. See Section 5.3.4) was made proportional to the instantaneous value of the stimulus waveform, with peak changes of $\pm$ 50 %. Thus negative half-cycles of the sinusoid caused a reduction and positive half-cycles caused an increase in the rate of chemical release, compared with the spontaneous rate. This case therefore corresponds to a situation in which no enhancement of the effects of later stimulus peaks due to postsynaptic integration would be expected. This is borne out by the PST histogram, which shows a small

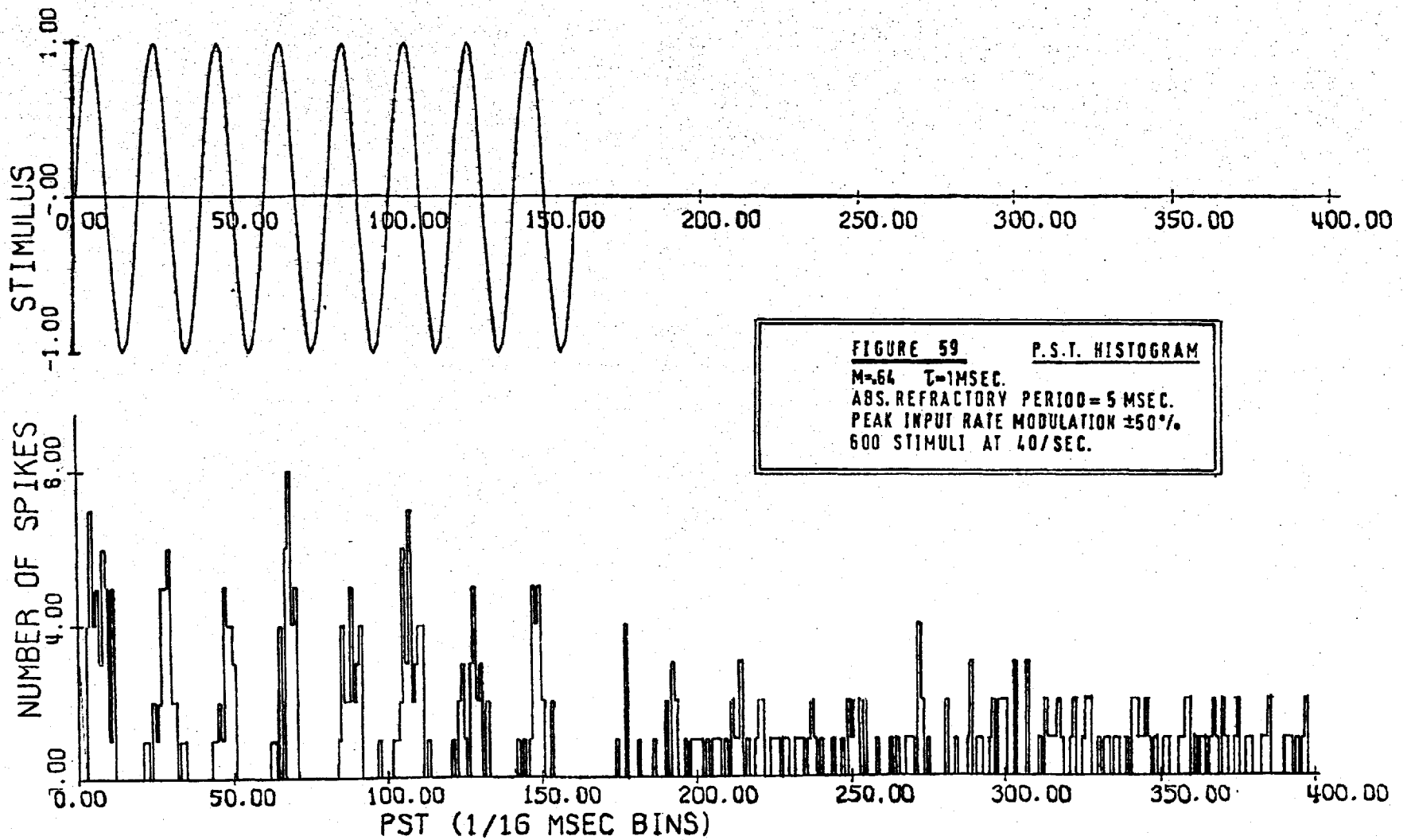

Figure 59 Results of digital computer simulation, showing PST histogram of model neuron in response to a time-limited sinusoidal variation in the rate of chemical liberation. Each of the 600 stimulus presentations was followed by a 15 msec. dead period, during which spontaneous activity continued.

but steady reduction in firing probability during successive positive stimulus half-cycles; this is due to the unit being more often refractory towards the end of the stimulus.

If there is no suppression of the spontaneous liberation of chemical transmitter during negative half-cycles of the stimulus, enhancement of later peaks of the PST histogram occurs. However, this effect is very small unless a time constant of PSP decay (τ) considerably greater than a period of the stimulus waveform (1.25 msec.) is used. Figure 60 shows another simulation, this time assuming such a rectifier action, and with τ = 3 msec. Here there is evidence for a slight increase in the effectiveness of the later positive half-cycles of the stimulus waveform. The effect is more clearly seen in the estimates of recovered probability shown in Figure 61. The recovered probability, again plotted as a function of post-stimulus time, shows a steady increase caused by an effective integration of successive half-cycles of the stimulus. When the stimulus ends, the high level to which the PSP has (on average) been raised gives rise to increased spontaneous firing, which declines after a few time constants. Recovered probability is a valuable measure of the effects of quantal rate variation, since it does not depend upon the detailed assumptions about threshold refractory properties.

The results of these two computer runs are summarised in Figure 62, showing the unconditional and recovered probability estimates for successive positive half-cycles of the stimulus waveforms. Here again, the effectiveness of a rectifier type of action in producing postsynaptic facilitation is clear. These curves are typical of a number of such computer

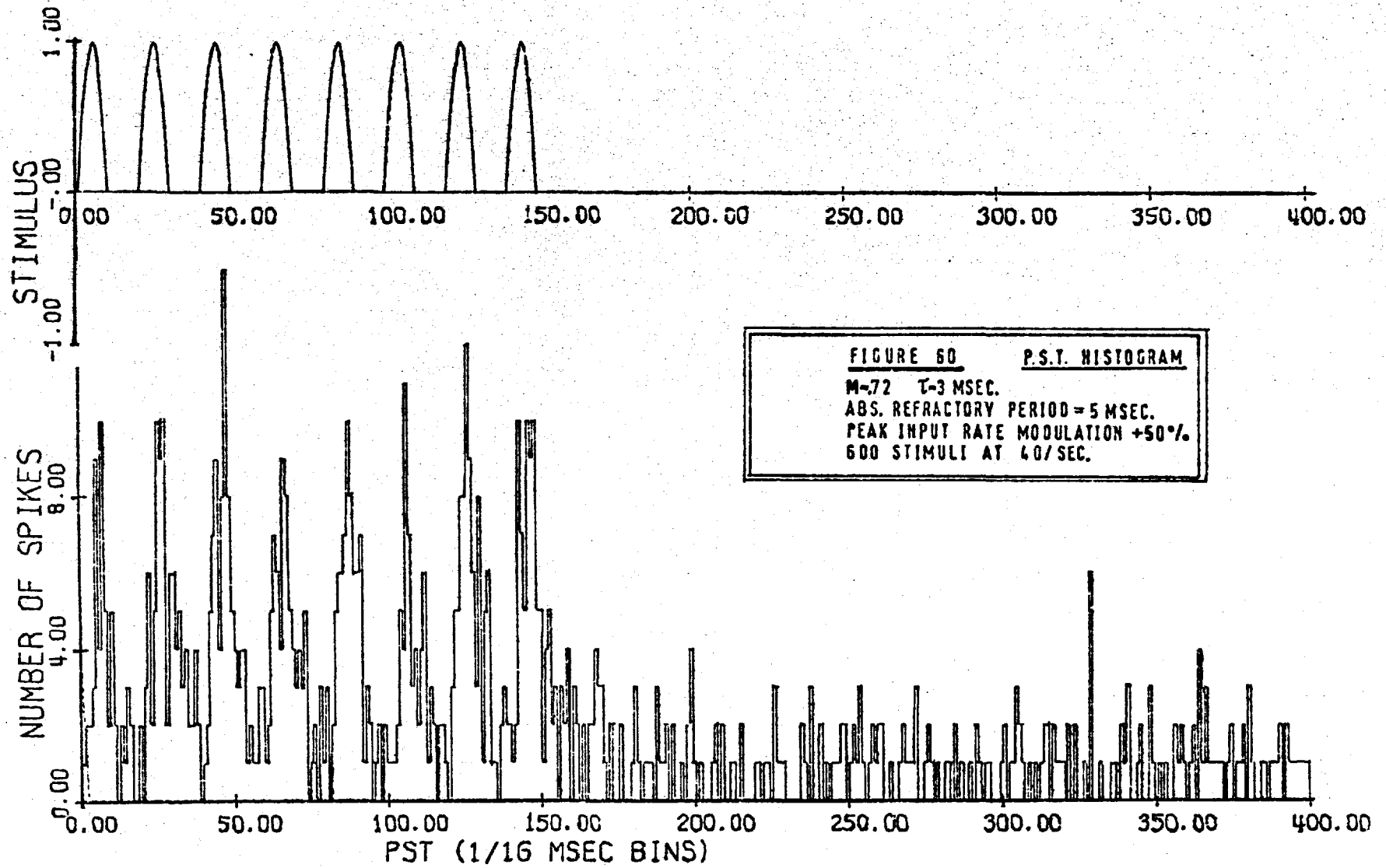

Figure 60 Results of digital computer simulation. In this case negative half-cycles of the stimulus waveform have no effect on the spontaneous quantal rate, and there is slight evidence for an enhancement of the later peaks of the PST histogram.

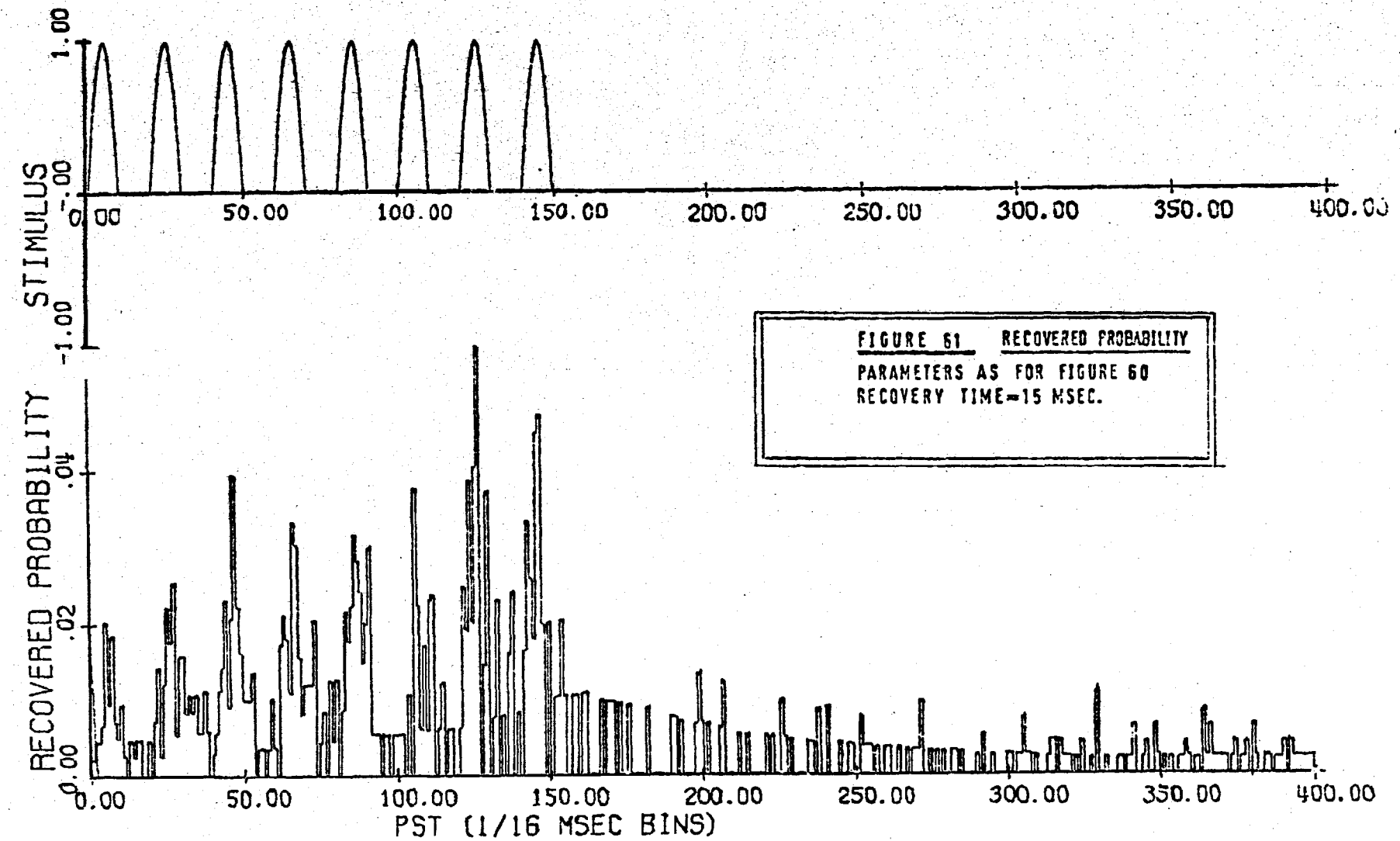

Figure 61 Recovered probability histogram for the computer simulation of Figure 60. The steady rise in recovered probability during successive positive half-cycles of the stimulus is clearly visible. When the stimulus ends, the effects of postsynaptic integration are still visible in the enhanced spontaneous firing.

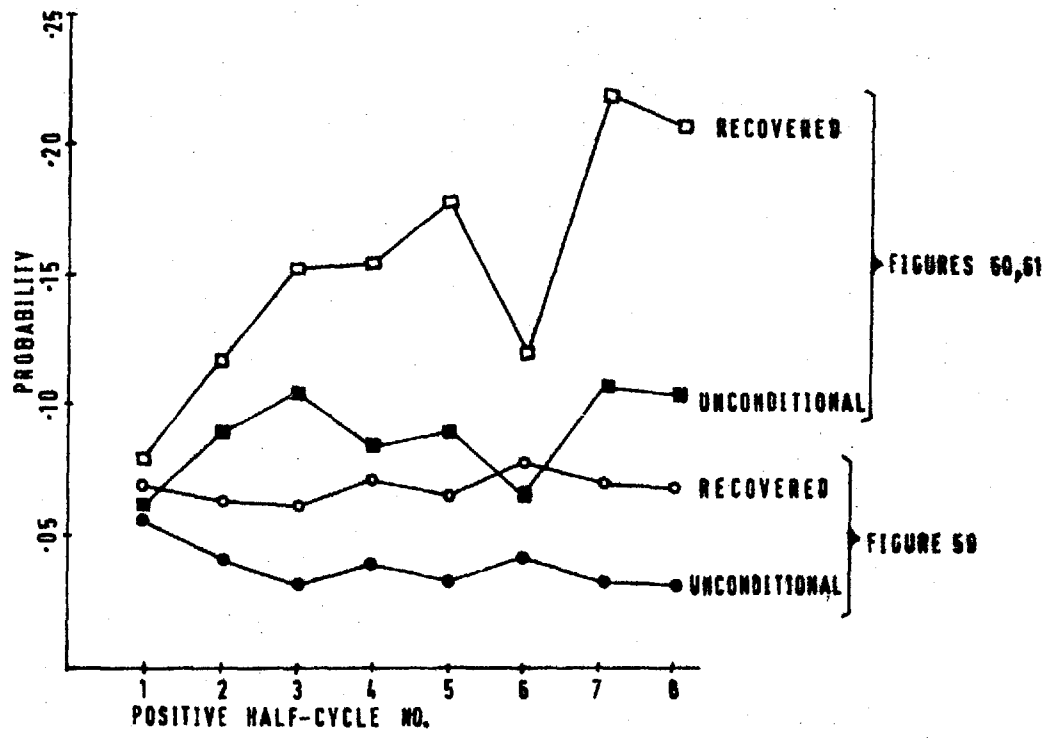

Figure 62 Unconditional and recovered probability estimates associated with the various positive half-cycles of the stimulus waveform, for computer runs shown in Figures 59, and 60/61.

simulations, using different PSP time constants, and modulating the chemical release of model neurons displaying various shapes of spontaneous interval histogram.

Such simulations allow a number of interesting conclusions. Firstly, postsynaptic integration effects of this type can account for very little enhancement of later peaks of a click PST histogram (and indeed for a negligible amount unless time constants of the order of 2 or 3 periods of the stimulus are used). In the case of a fibre of C.F. = 200 Hz. (say), this would require a time constant of some 4 to 10 milliseconds, which is believed to be an unrealistic value for an auditory nerve fibre. Even allowing for such a value, the enhancement of later peaks would be negligible unless a rectifier action were assumed, but, in that case, substantial firing would be expected during condensation half-cycles of

basilar membrane vibration. Gray's work (see Section 2.7.3) has shown that the troughs in click histograms corresponding to condensation movements are not merely caused by refractory effects, because they are also present in recovered probability histograms.

From all these points of view it could not be expected that a linear variation of the rate of chemical release in sympathy with a basilar membrane impulse response waveform would produce any very useful results. That this is in fact the case is shown by Figure 63, which is also typical of a number of other computer runs. The stimulus waveform used here is the basilar membrane impulse response for the point of C.F. = 520 Hz. On the left is shown a typical PST histogram obtained when a 'rectifier' type of action is assumed; i.e. negative half-cycles of the stimulus have no effect on the spontaneous rate of chemical liberation. Even so, there is no obvious enhancement of the later histogram peaks due to an integration effect. On the right is a histogram obtained by assuming positive and negative half-cycles of the stimulus to cause alternate increase and decrease of the spontaneous liberation of transmitter. Here there is some evidence for a trough after the first response peak, but very little for the presence of subsequent peaks.

The shortcomings of this simple model for the simulation of click PST histogram responses may now be summarised:-

(a) Insufficient peaks are visible.

(b) There is no effective suppression of the first one or two peaks at low intensities.

(c) There is no mechanism present which could cause the first rarefaction half-cycle (2C) during a condensation click to produce more firing than the first rarefaction

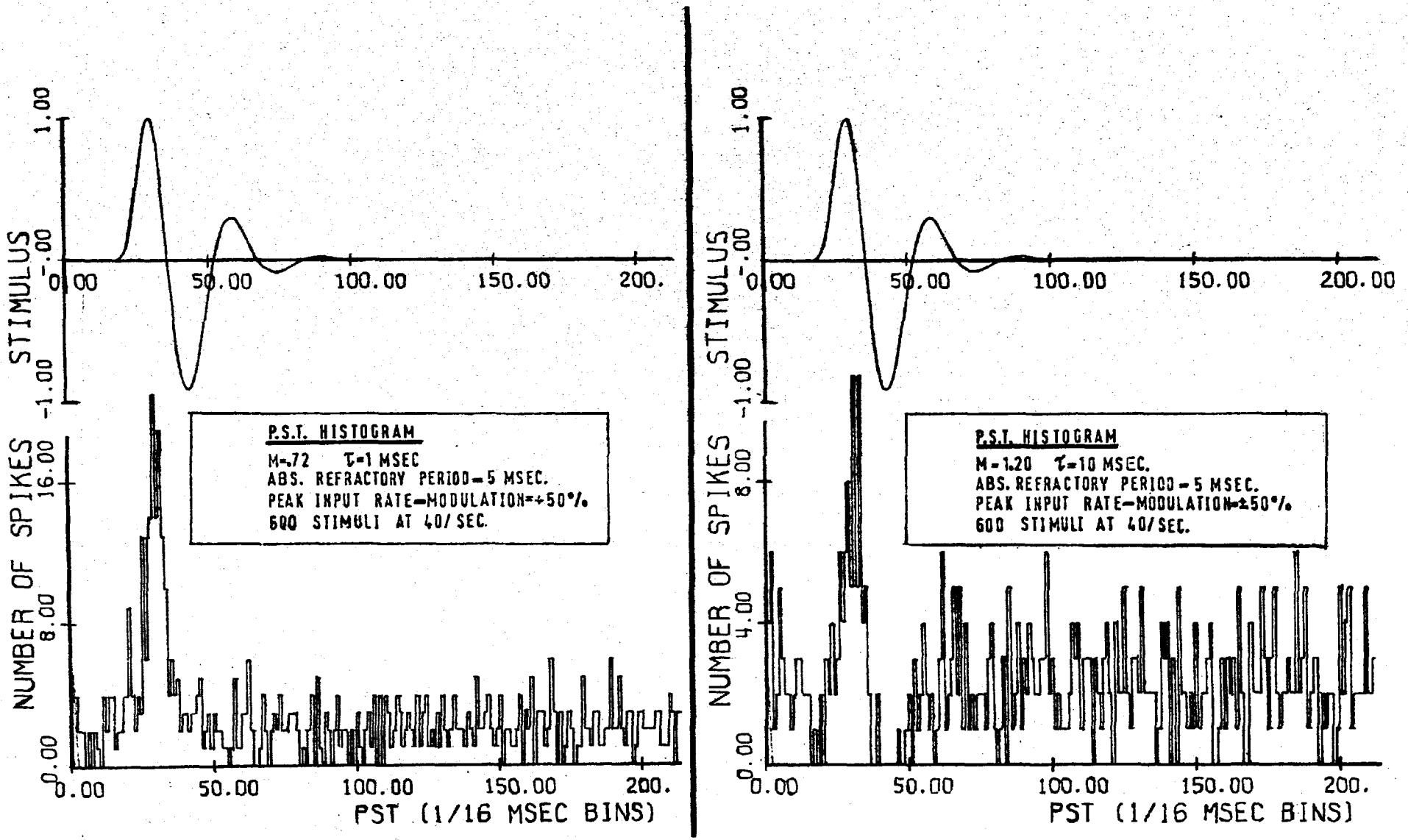

Figure 63 Typical PST histograms formed when the instantaneous rate of chemical transmitter release is linearly related to a basilar membrane impulse response waveform (here for the point of C.F. = 520 Hz.) On the left positive stimuli caused increased transmitter liberation, up to a maximum value 50% above the spontaneous rate, but negative stimuli had no effect. On the right, positive and negative half-cycles of the stimulus waveform caused alternate enhancement and reduction of the spontaneous rate, again with a maximum modulation of 50%. These results are typical of many other computer runs.

half-cycle (1R) during a rarefaction click (see Section 2.7.3)

(d) Even with maximum modulation of the spontaneous rate by the stimulus waveform ($\pm$ 100%), the probability of firing during any one stimulus half-cycle is only of the order 0.2, corresponding to very low stimulus intensities in actual recordings (see Figure 17).

8.3.2 More complex effects

It seems clear that simple linear relationships between the rate of a postulated chemical transmitter release and basilar membrane displacement waveforms cannot produce model responses which parallel physiological recordings from first-order auditory neurons. As has already been mentioned in Section 4.3, Weiss[67] used an arbitrary nonlinear transducer function to produce a number of peaks in the click histograms of his model, although he was not interested in the mechanism of suppression of the earlier ones. Typical click PST histograms from cat (see Figure 13) display some 4 to 8 peaks at medium stimulus intensities; further useful evidence is provided by Gray (see Figure 17), whose analysis suggests that, in a mid-intensity range, there is an approximately linear relationship between firing probability and the logarithm of the stimulus.

These various factors suggest that some form of exponential transducer function might be appropriate, of a type which would greatly enhance the relative neural results of small basilar membrane displacements. (The short review of other chemical transmitter systems already presented shows that such a scheme would be a direct contradiction of the available evidence, if it may be assumed that hair cell polarisation is linearly related to basilar membrane

displacement). A similarly empirical approach suggests, however, that a simple exponential transformation could not produce a suppression of the earlier peaks of a click PST histogram at low intensities. It is therefore interesting to speculate that a transmitter mobilisation effect may be responsible.

Evidence that hyperpolarisation of a presynaptic terminal can produce a so-called "mobilisation" of chemical transmitter has already been reviewed. This additional transmitter, which has presumably been synthesised and stored in the region close to the synaptic boundary, is thought to move up to that boundary as a prelude to release across the synaptic junction. Such action might provide an explanation for two effects of interest, namely the relatively small neural effects of early basilar membrane rarefaction movements in response to a click stimulus, and the relatively great effect of click histogram peak 2C as opposed to peak 1R.

In more detail, suppose that condensation basilar membrane activity (presumed to lead to hair cell hyperpolarisation) causes a mobilisation of extra transmitter substance, which then starts to move up to the synaptic boundary. In the case of a transient stimulus it may not arrive at that boundary until some time after the onset of the stimulus, and would therefore be expected to enhance the neural effects of the later basilar membrane rarefaction movements. If the transient were a rarefaction click, the first rarefaction half-cycle (1R) would not be preceded by any such additional mobilisation; in the case of a condensation click, however, mobilisation caused by the initial membrane condensation movement would be expected to

enhance the effect of the subsequent rarefaction half-cycle (2C). Thus, even though the acoustic clicks were of similar intensity, the neural effects of peak 2C would be greater than those of peak 1R.

Because there is no quantitative evidence available for the description of such effects, it is necessary to make some assumptions if they are to be simulated on a computer (in fact it becomes clear later that the precise details of such assumptions are unimportant in the development of the argument). Consider therefore a hypothetical synaptic region, a section through which is shown in Figure 64.

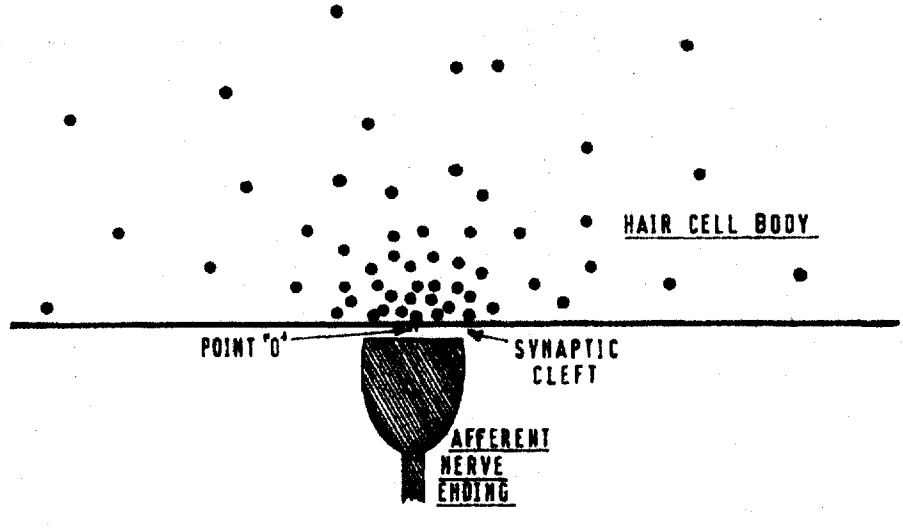

Figure 64 Diagrammatic sectional view of an afferent hair cell synapse, showing a hypothetical chemical transmitter distribution in the presynaptic terminal.

Here the density of stored chemical transmitter is assumed to decline exponentially with distance from'O', the release site. Assuming that, after mobilisation at time t = 0, the transmitter migrates with constant velocity to point O (and is thereafter available for release), it may be shown that the quantity which arrives during a small time interval δt

at some later time t is given by:-

$$q(t).\delta t = 4\pi D\, v^3 t^2 e^{-tv/r}.\delta t$$

which is of the form of a gamma function of second order, where:-

D = transmitter density at point O.

r = radius from O at which density is reduced to $^1/_e$ of its value at O.

v = velocity of migration towards O.

This function is considered typical of a number which might be used to represent the delayed arrival of transmitter at a synaptic boundary, following mobilisation. Although it no doubt involves gross simplifications, it is believed to be adequate for the present purposes.

Various overall schemes for the modelling of spontaneous and stimulated activity at such a synaptic boundary now appear possible. For example, it seems reasonable to postulate a variable chemical transmitter population close to the boundary. (In the discussion which follows, this population, which is considered available for instantaneous release by suitable polarisation of the hair cell, is referred to as the "synaptic population"). In the absence of stimuli, each quantum in this synaptic population might be considered to have a small but finite probability of release in each time increment δt. Such spontaneous liberation would be balanced by spontaneous mobilisation of relatively distant transmitter which, moving up to the boundary, would tend to keep the synaptic population constant. A stimulus could then have two distinct effects: hyperpolarisation of the hair cell would cause an increase in mobilisation and (after a time delay) a rise in the

synaptic population at the boundary; and the alternate half-cycles of hair cell hyperpolarisation and depolarisation could be assumed to modulate the release probability of whatever transmitter population was instantaneously available for liberation.

This scheme, selected from other apparently plausible ones, has been simulated in some 15 runs on the digital computer. In order to produce a number of peaks in the click PST histograms, the release probability (p) of each chemical quantum in the synaptic population was assumed to be simply related to the logarithm of the instantaneous basilar membrane displacement (x) as follows:-

$$p = p_s(1 + K \log x), \quad 1 < x < \infty$$

$$p = p_s, \quad -1 < x < 1$$

$$p = p_s(1 + K \log(-x))^{-1}, \quad -\infty < x < -1$$

where: p_s = spontaneous probability of release

K = constant.

Thus positive values of x correspond to basilar membrane rarefaction movements, negative values to condensation movements, and values between $\pm$ 1 are considered subthreshold and have no effect. Each basilar membrane condensation movement was also considered to cause additional transmitter mobilisation proportional to the logarithm of the instantaneous condensation displacement. The subsequent arrival of this transmitter at the synaptic boundary was calculated by a short subroutine of the main computer programme; this involved convoluting the previously discussed transmitter arrival function (treated as an impulse response) with the logarithm of the condensation displacement waveform. The

transmitter mobilised in this way was considered to augment that generated spontaneously.

In some initial computer runs the mobilisation of additional chemical transmitter was suppressed, in order to give a clearer idea of the effects of the assumed logarithmic relationship between basilar membrane activity and probability of release of the available synaptic population. Figure 65 shows the results of such a computation, representing the response of a unit of C.F. = 520 Hz. to an acoustic click of medium intensity. At the top of the figure is shown the variation in rate of the Poisson release of chemical transmitter, due to the relevant basilar membrane impulse response. The first membrane rarefaction peak causes the rate to rise to some 4 times its spontaneous level (the latter being represented as unity) and condensation movements cause corresponding reductions. Since the mobilisation of transmitter is here assumed to be unaided by the stimulus, there is a steady run-down in the synaptic population. This run-down, which is of course more rapid during rarefaction half-cycles, is responsible for the unsymmetrical peaks of the release waveform and for a temporary reduction in spontaneous activity following the stimulus. There is evidence for 3 or 4 separate peaks in the PST and recovered probability histograms. However, further simulations have confirmed that the PST responses are stereotyped at all stimulus intensity levels (presumed to cause different degrees of modulation of the quantal rate), in the sense that the first histogram peak is always the greatest.

It is true that, when additional mobilisation of transmitter by the stimulus is assumed, a very careful choice of the various model parameters can give rise to

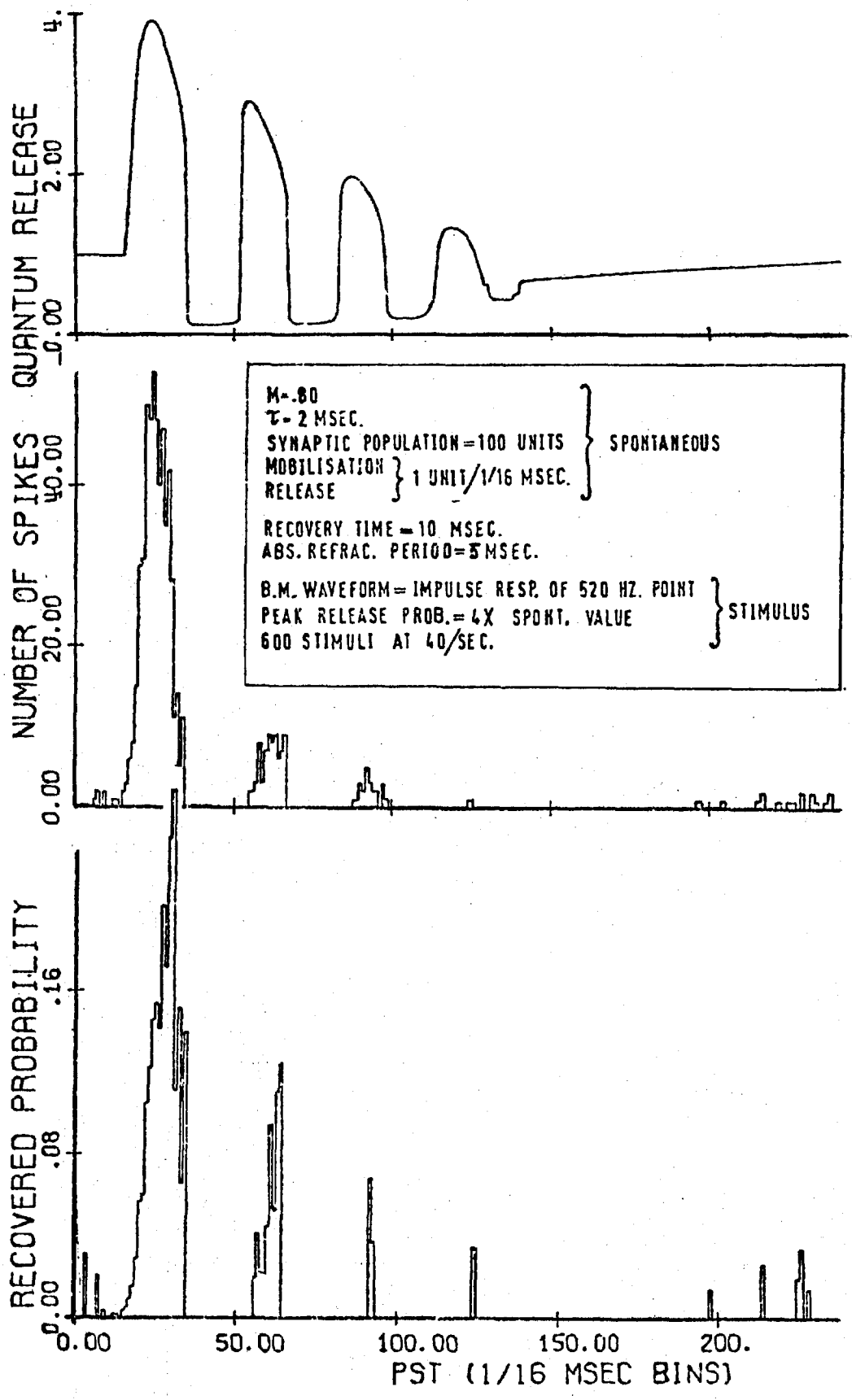

Figure 65 Computer simulation result, representing the response of a first-order auditory neuron to a click of medium intensity. C.F. of unit = 520 Hz. Above is shown the variation in rate of the Poisson process representing chemical release (normalised to the spontaneous rate). A logarithmic transformation between basilar membrane displacement and rate is assumed, but there is no additional transmitter mobilisation due to the stimulus.

click PST histograms resembling those measured in the cat's auditory nerve. However, some 15 computer runs using a range of parameters and simulating fibres of various characteristic frequencies show that results rather unlike those of Kiang are much more probable. Of these, Figure 66 illustrates a typical case. This simulation was essentially similar to that shown in Figure 65, except that condensation membrane movements were assumed to cause enhanced mobilisation of chemical transmitter. The time scale of the function representing the subsequent arrival of this transmitter at the synaptic boundary was chosen empirically. Such results are quite unlike the histograms recorded by Kiang in two main respects: firstly, although the later peaks of the histogram are relatively enhanced, the peaks as a whole do not follow a smooth envelope (compare with Figures 13 and 14); and, secondly, unless the quantity of stimulus-mobilised transmitter balances the additional transmitter released, there is inevitably a build-up or run-down in the population at the synaptic boundary, reflected in enhanced or reduced spontaneous activity following the stimulus.

Such critical results highlight the following very restrictive assumptions which are required if the model is to produce responses with the desired characteristics:-

(a) The ratio between the synaptic population present during spontaneous activity (and therefore available for release during the first half-cycle of membrane movement caused by a rarefaction click) and the additional amount mobilised by a stimulus must be such that the peaks of simulated click PST histograms follow a smooth envelope at all intensities and in all fibres.

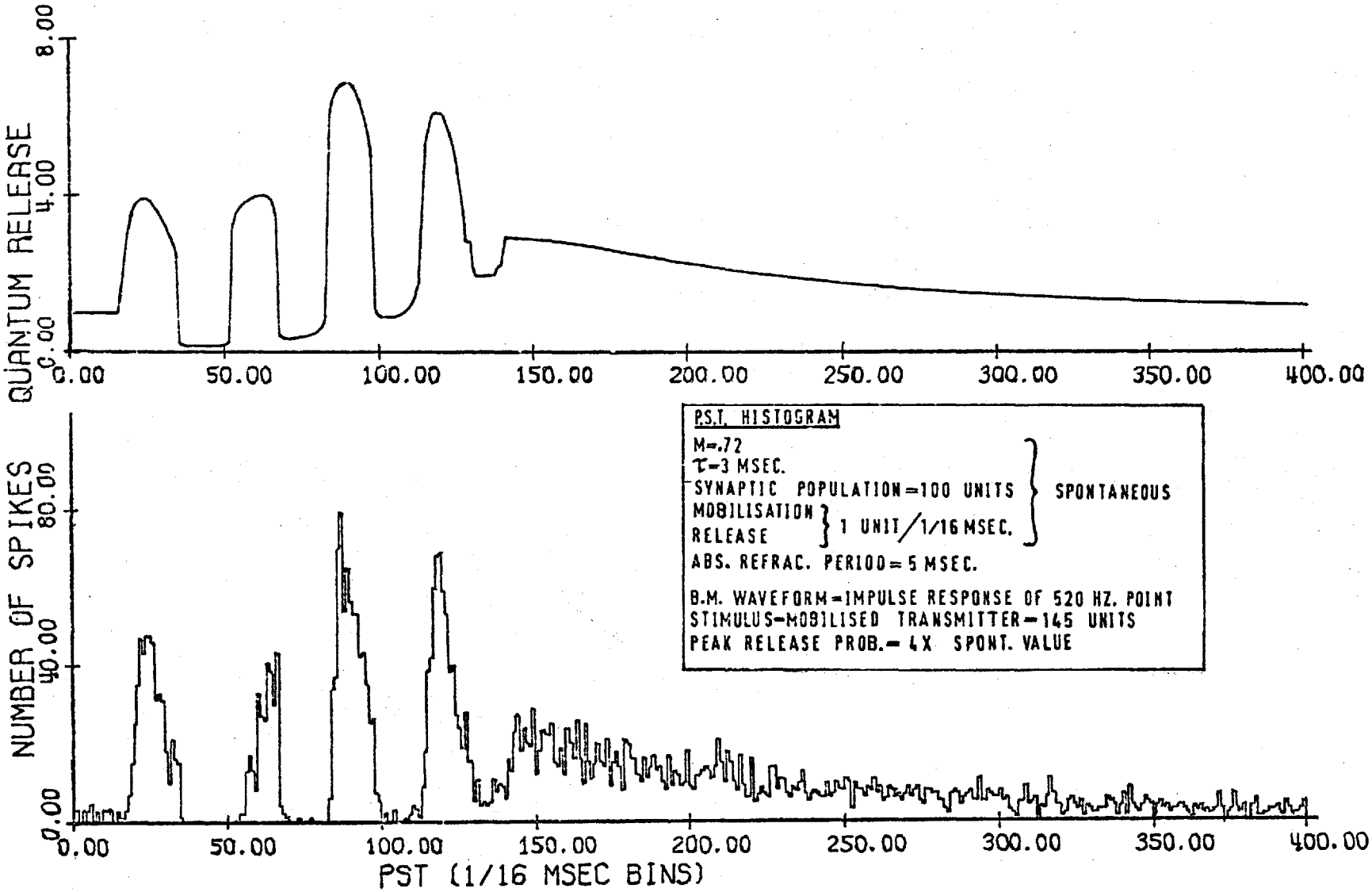

Figure 66 Computer simulation. Apart from the assumption of additional transmitter mobilisation by the stimulus, this run was essentially like the one shown in Figure 65. It illustrates the difficulty of choosing model parameters which produce a realistic neural response.

(b) Mobilisation and release caused by a stimulus must approximately balance each other, in all nerve fibres and at all intensities.

(c) The time-course of the mobilisation effect must be approximately inversely proportional to the C.F. of the fibre concerned; this implies that chemical mobilisation occurs about 15 times slower in a hair cell in the 200 Hz. region of the cochlea than in a hair cell in the 3KHz. region.

8.4 Discussion

It is obviously impossible to explore in detail all the models of chemical synapses which might seem plausible, and relevant to the cochlear neural transduction process; in terms of computing time alone, this would be an enormous task. However, it is believed that the simulations undertaken have shown the main effects to be expected in quantal threshold models with non-stationary stochastic inputs (a situation for which, as far as is known, no theoretical analysis exists). Whilst these investigations may not be exhaustive, it seems unlikely that any really important details have been missed. From the viewpoint of cochlear transduction the typical results reported in this section seem sufficient to illustrate the difficulties inherent in any proposition based upon known effects in chemical synapses.

Various other schemes, different in detail from the one described, might seem to have an equal or better chance of reproducing the intensity effects visible in the click responses of first order auditory neurons measured by Kiang. For example, it might be argued that the assumption of a synaptic population, available for release during spontaneous activity and increased during stimulus conditions by the arrival of additional mobilised transmitter, is unnecessarily complicated. On the other hand if such a synaptic population were not available and all chemical effects were subject to a mobilisation delay, it would be difficult to account for any firing at all during the first half-cycle of basilar membrane activity due to a rarefaction click. In fact it is believed that any alternative scheme which depends upon the concepts of transmitter mobilisation and release must encounter one or more difficulties of the

type already discussed.

Quite apart from problems caused by detailed assumptions, there remain two apparently fundamental issues. The first of these concerns the relationship between chemical release rate and presumed hair cell polarisation; the production of a number of peaks in the click PST histograms of the model requires an assumption which is in direct conflict with the evidence from other chemical synapses. And finally there is the difficulty over the time-course of the phenomenon which gives rise to the intensity effects of interest, for this seems clearly related to the region of the organ of Corti in which a particular fibre terminates.

9 STIMULATED NEURAL ACTIVITY AND COCHLEAR INNERVATION

9.1 A proposition

The results of Sections 7 and 8 suggest that it would be difficult to account for details of click PST histograms on the basis of mechanisms in the single hair cell-nerve ending junction. Perhaps the most fundamental difficulty relates to the time-course of the required effects, which clearly depends on the cochlear region in which a particular nerve fibre terminates. It is therefore interesting to speculate that the complex pattern of cochlear innervation may provide an explanation.

In the region below the inner hair cells the various types of afferent and efferent fibre are in close proximity (see Section 2.5). In particular, radial afferent fibres (which innervate local inner hair cells) lie adjacent to spiral afferent fibres (which cross to the outer hair cell rows and then travel for some distance before terminating). At any particular locus beneath the inner hair cells the time-course of the envelope of (say) click responses in these two types of fibre, although different in detail, might be expected to be broadly similar in duration because the two groups are stimulated by broadly similar basilar membrane activity. This argument, together with the fact that there are still no definite theories for the relative functions of inner and outer hair cells, seems to allow the following proposition based on the details of cochlear innervation.

It is proposed that the activity of radial afferent fibres (innervating the inner hair cells) is mediated by signals arriving from the outer hair cells along spiral nerve fibres. Thus the spiral fibres, which are believed to travel basally before terminating, are considered to convey a signal

representing the activity of a number of outer hair cells to a more apical region. The proposed controlling action of such a signal on the activity of the radial fibres could presumably occur in the region under the inner hair cells, where the various types of afferent (and efferent) fibres are in close contact.

Whereas, in Section 6.2, the low-pass filtering properties of spiralling fibres were ignored, it is now proposed that such properties play an important role, and that there is therefore considerable "smearing" of the signals generated by the outer hair cells as these signals pass along the fibres. The waveform of electrotonic activity in such a fibre when it reaches the region below the inner hair cells (hereafter referred to as the control waveform) would therefore be a smoothed representation of basilar membrane activity in some more basal cochlear region. It is now proposed that this control waveform fulfils some essential role in the transduction process of radial afferent fibres (innervating the inner hair cells) and that, in the absence of such a waveform, firings in such fibres would be unlikely, or even impossible. In more detail,the activity of an inner hair cell, responding to local basilar membrane vibration, is proposed to determine the detailed timing of (say) chemical transmitter release across its afferent synapses; however, the amount (or effectiveness) of such transmitter would be determined by this other, essentially parallel, activity in spiral nerve fibres.

In the case of a click stimulus, the signal input to a spiral fibre would presumably be closely related to the impulse response of the basilar membrane in the region where the fibre terminates, as shown in Figure 67.

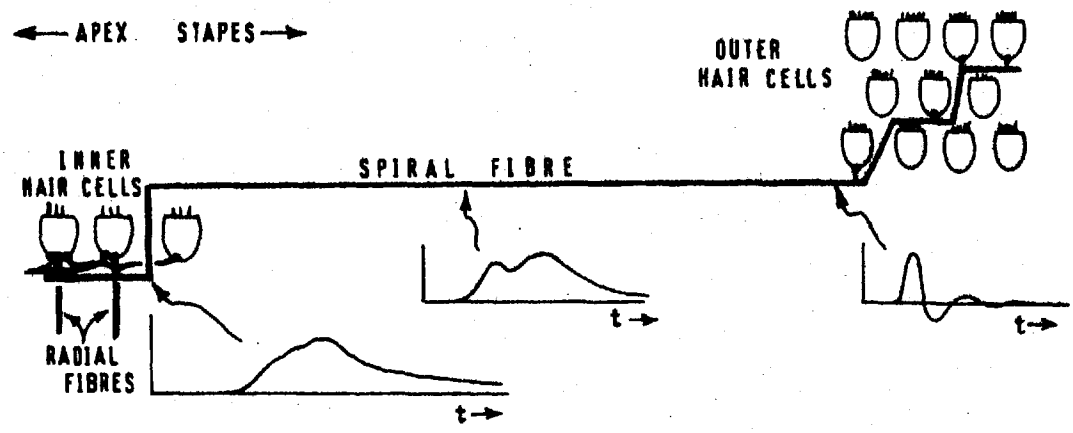

Figure 67 Illustration of the proposed electrotonic waveforms at various points along a spiral cochlear fibre in response to an acoustic click. The substantial attenuation to be expected as the signal travels apically along the fibre is not indicated.

Here the time-course of the fibre impulse response is assumed to be long compared with that of its input (the outer hair cell signal), so that the waveform which finally reaches the region under the inner hair cells is broadly similar to the fibre impulse response. As discussed in Sections 7 and 8, the form of measured click PST histograms suggests the action of a facilitating or control mechanism which has a time-course related to the cochlear region innervated by a particular fibre. In terms of the present proposal, a control waveform having this property might be expected if there were a systematic variation in the lengths of spiral fibres in different cochlear regions.

Such proposals, which are believed to differ rather fundamentally from existing hypotheses about the roles of the various hair cell rows and fibre groups, give the outer hair cells an essentially controlling function over the activity in radial afferent fibres. The immediate attraction of such a scheme is that it seems to provide a simple and potentially

feasible explanation of the click PST histogram effects observed by Kiang, without requiring elaborate assumptions about variations in hair cell or nerve ending properties in different cochlear regions.

One variation of the scheme might usefully be mentioned at this stage. If the outer hair cells were to perform a rectification (full- or half-wave) of the basilar membrane displacement waveform, and if the time-course of the impulse response of the spiral fibre were relatively short, the spiral fibre waveform in the region under the inner hair cells would be expected to be a smoothed version of the fibre input, as shown in Figure 68. In this case, the time-course of the

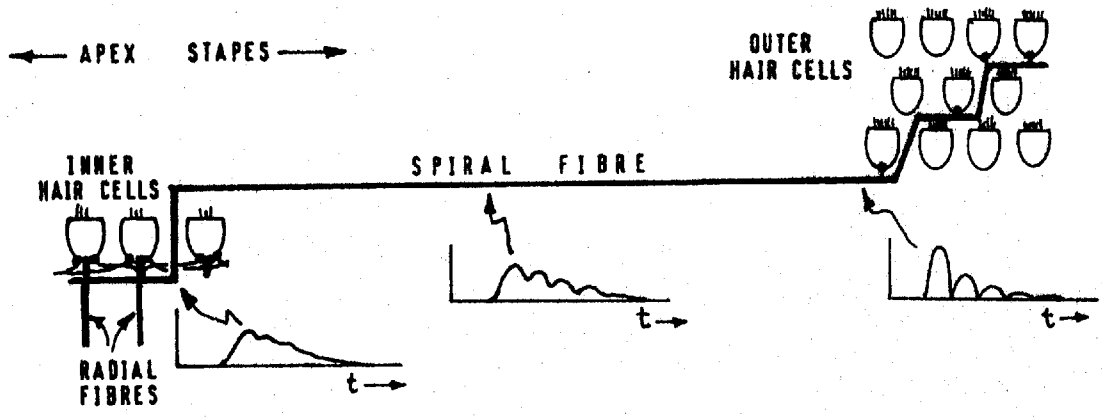

Figure 68 Illustration of a different scheme in which the electrotonic waveform at the apical end of a spiralling fibre is a smoothed version of more basal (rectified) basilar membrane activity. In this case the time-course of the control waveform is essentially that of the basilar membrane activity.

control waveform would be directly related to the cochlear region concerned, without requiring assumptions about systematic variations in the lengths of spiral fibres. It would, however, seem necessary to assume some sort of rectifying action by the outer hair cells in this case; furthermore, the time-course of the control waveform might

be too short, in view of the fact that 6 or 8 peaks are visible in a typical click PST histogram. On the other hand, the scheme previously illustrated in Figure 67 should work equally well with such rectifying action by the outer hair cells, and such an assumption might be necessary in the case of continuous signals. However, it is not at this stage considered either appropriate, or necessary, to postulate details of the outer hair cell transduction.

Before considering the implications of these schemes in detail, it is necessary to assess the cable properties of spiral cochlear fibres, to see whether (in suitable computer simulations) realistic click PST histograms can in fact be generated on the basis of such proposals.

9.2 Filtering properties of spiral cochlear fibres

Although the electrical characteristics of spiral cochlear fibres are unknown, it seems of interest to estimate their likely filtering properties by making use of measurements made on other unmyelinated nerve fibres. The following calculations represent an attempt to define the subthreshold properties of spiral fibres, for the purpose of computer simulation of the schemes already illustrated qualitatively by Figures 67 and 68.

References to subthreshold propagation in nerve[33,44] generally treat electrotonic spread in unmyelinated fibres as a linear passive process, without introducing the complexities of ionic mechanisms. Such a model is illustrated in Figure 69, where the fibre is represented as a cable having axoplasm resistance r_i, membrane resistance r_m, and membrane capacitance c_m, all per unit length. The resistance of the medium surrounding the fibre is assumed to be negligible.

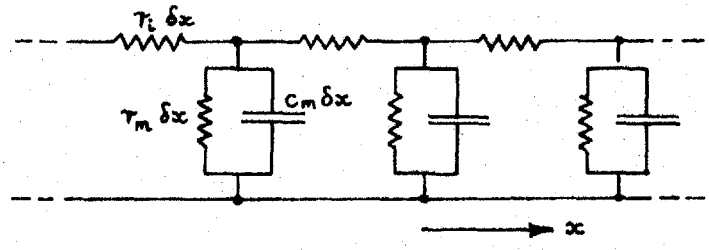

Figure 69 A simple RC cable model of a length of unmyelinated nerve fibre.

The propagation constant, γ, of such a cable is given by:-

$$\gamma = \sqrt{(1 + j\omega c_m r_m)\,\frac{r_i}{r_m}}$$

$$= \alpha + j\beta$$

where α = attenuation constant

and β = phase constant.

Consider typical values for an unmyelinated fibre of diameter 1μ (similar to spiral cochlea fibres). If the specific conductance of the membrane (G) is 0.5 mmhos per cm^2, and the specific resistance of the axoplasm (R) is 200 ohms. cm, (Katz[33]), then:-

$$r_m = \frac{1}{G\pi d} = 6.4 \times 10^6 \text{ ohms/cm.}$$

$$\text{and} \quad r_i = \frac{4R}{\pi d^2} = 2.5 \times 10^{10} \text{ ohms/cm.}$$

If the usual value of $1\mu F/cm^2$ is accepted for the specific membrane capacitance, then:-

$$c_m = 3.1 \times 10^{-10} \text{ farads/cm.}$$

At low frequencies, such a fibre acts as a simple resistive cable; this is approximately true when the phase shift along the fibre is small, or when:-

$$\omega c_m r_m \ll 1$$

for example,

$$\text{put } \omega c_m r_m = 0.1$$

$$\therefore \omega = 50$$

$$\therefore f = \omega/2\pi \simeq 8 \text{ Hz.}$$

Thus at frequencies lower than about 8 Hz. such a fibre behaves as a simple attenuator, with:-

$$\gamma = \sqrt{\frac{r_i}{r_m}} = 62 \text{ nepers/cm.}$$

and a length constant:-

$$\lambda = \frac{1}{\gamma} = 0.16 \text{ mm.}$$

At higher frequencies the shunting effect due to the membrane capacitance becomes progressively greater until, finally, the membrane resistance may be ignored. In this case:-

/over..

$$\gamma = \sqrt{j\omega c_m r_i}$$

$$\text{giving } \alpha = \beta = \sqrt{\frac{\omega c_m r_i}{2}},$$

and a frequency-dependent length constant:-

$$\lambda = \sqrt{\frac{2}{\omega c_m r_i}}$$

The response of such a cable, at a distance x from the site of application (at time t = 0) of a voltage step E, is given by:-

$$V(t) = E(1 - \text{erf } {}^{x}/_{2} \cdot \sqrt{\frac{r_i c_m}{t}}),$$

and the differential of this function with respect to time is the fibre impulse response, which, by tabulating values of the error function, may be shown to peak at a time $\bar{t}$ given by:-

$$\frac{x}{2}\sqrt{\frac{r_i c_m}{\bar{t}}} \simeq 1.24$$

$$\therefore \bar{t} = 0.162\ r_i c_m x^2.$$

If a fibre length of 1 mm. is assumed, with values for r_i and c_m as before:-

$$\bar{t} = 12.5 \text{ msec.}$$

With a fibre of length 0.5 mm., the impulse response peaks after about 3 msec. Such responses are illustrated approximately to scale in Figure 70, normalised to give the same maximum value.

On the basis of these calculations, it seems very likely that signals propagated along spiral cochlear fibres are subjected to substantial low-pass filtering. In the simplified case when the shunting effects due to membrane resistance are ignored, indications are that fibres about 1

millimetre long would have impulse responses of time-course comparable with that illustrated in Figure 67. Furthermore the time at which any particular feature of the waveform (for example, the peak of the response) occurs is expected to be proportional to the square of the fibre length.

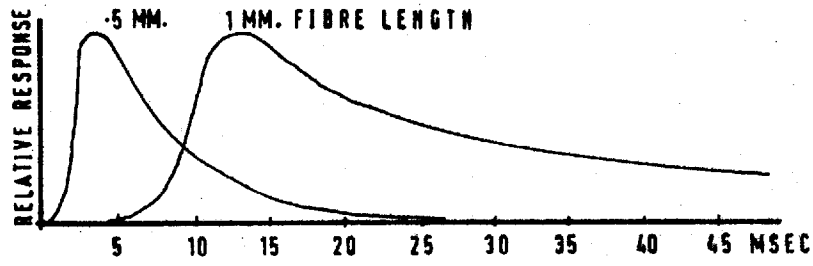

Figure 70 Impulse responses of unmyelinated nerve fibres of diameter 1μ, calculated by assuming the shunting effect due to membrane resistance to be small compared with that due to membrane capacitance.

9.3 Digital computer simulations

Some digital computer simulations have been carried out to test these proposals, again using the basic programme illustrated in Figure 28. In this case, however, the local basilar membrane activity was considered to control only the timing of stochastic release of a chemical transmitter across an inner hair cell synapse. The mean amount released (or alternatively, the quantitative effect of any release on the polarisation of the afferent nerve terminal) was assumed to be determined solely by the control waveform arriving along a spiral fibre.

Initially the effects of rarefaction click stimuli of various intensities on a radial afferent fibre of C.F. = 333 Hz. were considered. The control waveform was assumed to be the impulse response of an RC cable (corresponding to the situation illustrated in Figure 67), adjusted in time scale so as to reach its peak value after about 4 msec., and therefore presumably corresponding to a spiral fibre approximately 0.5 mm. long. The average amount of transmitter released across the synaptic junction during any one rarefaction half-cycle of local basilar membrane vibration was assumed to be directly proportional to the instantaneous value of the control waveform; during local membrane condensation activity the transmitter release was assumed to be substantially suppressed.

The PST histograms obtained are shown in Figure 71, together with the waveforms of transmitter release. In this particular case the chemical release waveform was arbitrarily assumed to be made up from a number of half-cycles of a sinusoid, so as to give a smooth curve. During rarefaction

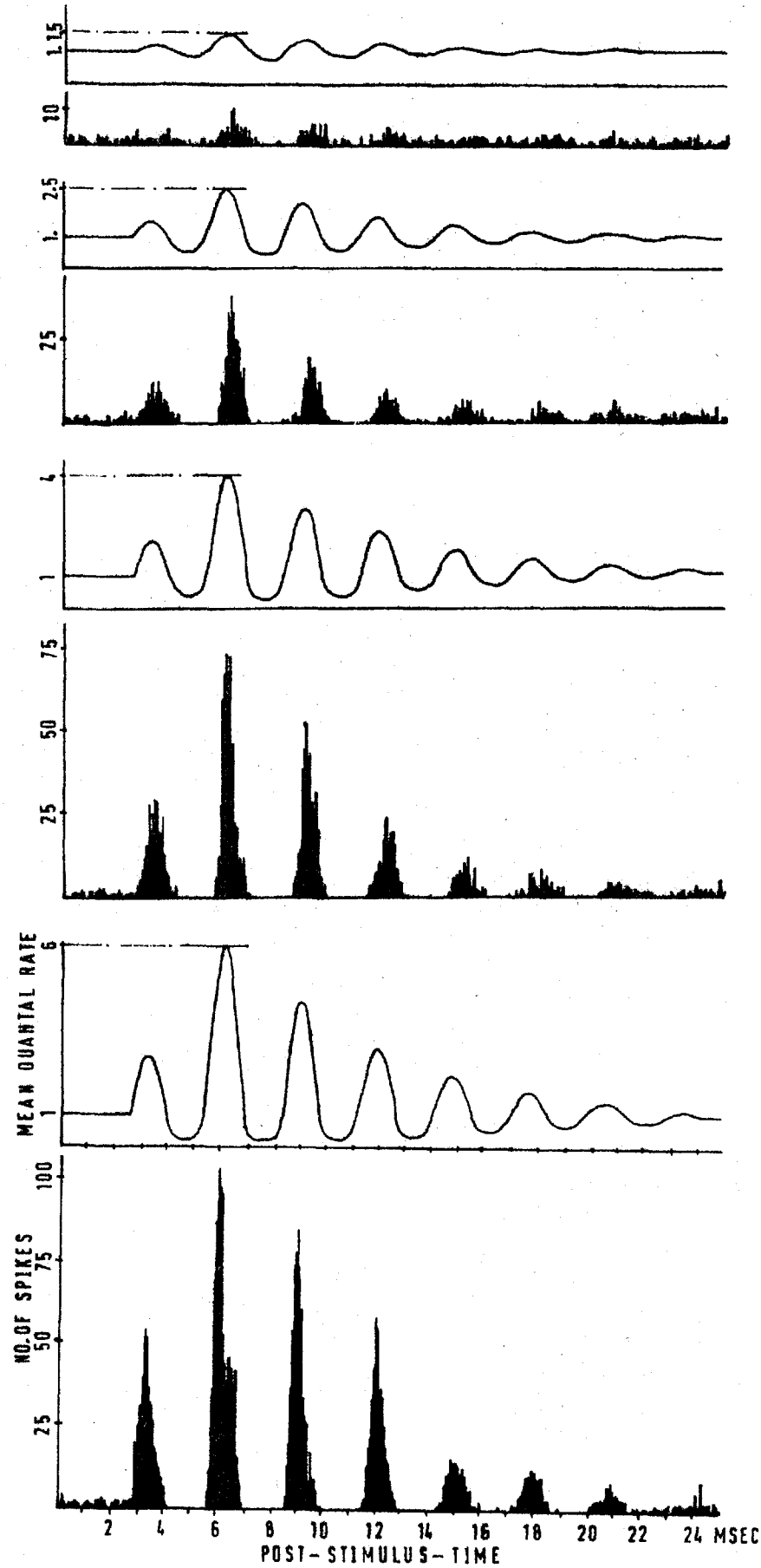

Figure 71 Digital computer simulations. PST histograms and transmitter release waveforms relevant to a radial afferent fibre of C.F. = 333 Hz. Rarefaction clicks at 4 stimulus intensities. A control waveform representing the impulse response of a spiral afferent fibre was used to determine the mean transmitter release during successive rarefaction half-cycles of local basilar membrane activity. (τ = 2 msec., M = 0.72 (spontaneous), threshold = constant, 600 stimuli).

half-cycles of basilar membrane activity each half-sinusoid, of height proportional to the instantaneous value of the control waveform, was added to unity (representing an ongoing spontaneous rate of chemical release), to give the chemical release rate. During condensation membrane activity the spontaneous rate was reduced by dividing it by the instantaneous value of a half-sinusoid (again having a peak value proportional to the instantaneous value of the control waveform). The construction of this release waveform is certainly arbitrary, but it seems that the precise details of it are unimportant in determining the broad features of these PST histograms, which would be produced by any release waveforms of the same general form.

These results seem to parallel closely those of Kiang (see Figure 13). In particular, a number of histogram peaks are now visible and the first one becomes relatively greater with increasing stimulus intensity. It is also clear that the histogram peaks tend to follow a smooth envelope, reflecting the fact that the quantal rate is now determined by a smooth control waveform (compare with Figure 66). On the other hand, a simple calculation of the shift in centre of gravity of the histograms with intensity shows that it is in the opposite direction to that calculated from the physiological recordings in cat; an increase in peak quantal rate modulation is accompanied by an increase in the mean time, post-stimulus, of stimulated neural firings. This is probably due to the assumption of a constant threshold in these simulations, causing no effective reduction in the size of later histogram peaks due to refractory effects.

This latter difficulty may be simply overcome by incorporating threshold refractory properties. However, rather than use much computer time in an attempt to match the desired centre of gravity shifts exactly, some further simulations were carried out assuming severe refractory properties (an absolute refractory period of 15 msec.); these demonstrate that effects of the desired type are readily obtained. In Figure 72 are illustrated some further computer results, this time representing the responses of a radial fibre of C.F. = 1 KHz. to rarefaction and condensation clicks at 6 intensity levels. In the case of condensation clicks, the first effect of the stimulus is assumed to be a suppression of spontaneous chemical release and this causes an initial trough in the PST response. The waveforms of assumed chemical release rate are not shown in each case, but typical ones for rarefaction and condensation clicks are illustrated at the bottom of the Figure. The ratio between the peak release rate (determined by the control waveform, here adjusted to peak after about 1.5 msec.) and the spontaneous rate is denoted by Q, and the value of Q relevant to each pair of responses is indicated.

In this case there is clear evidence for a dramatic increase in the size of early histogram peaks as intensity is raised. The shift in histogram centre of gravity is now in the expected direction and is shown more clearly by Figure 73. The centre of gravity in each case was estimated from the height and latency of the individual histogram peaks, so as to allow comparison with similar estimates made on physiological records (see Figure 20). There is clear evidence of a steady shift of histogram centre of gravity with intensity.

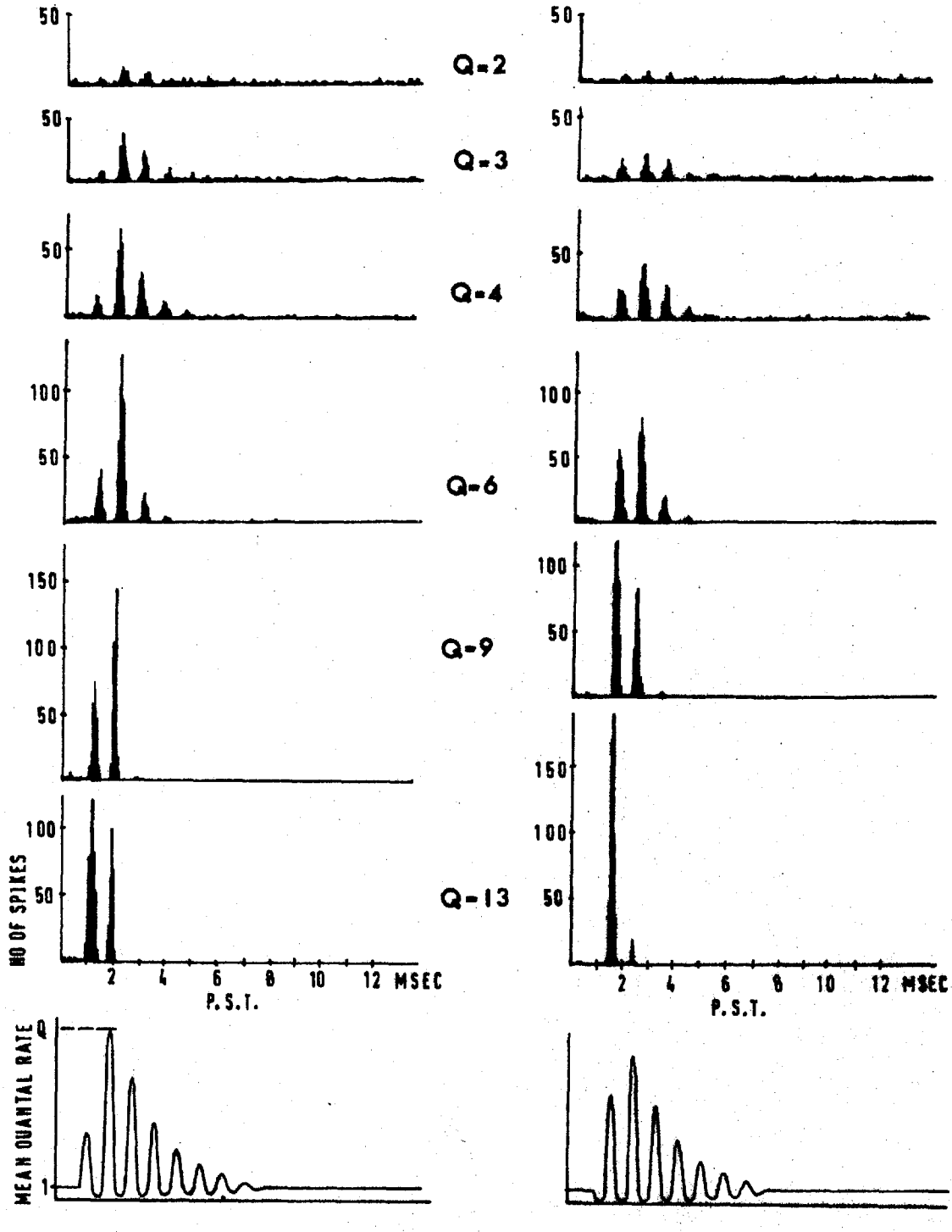

Figure 72 Digital computer simulations. PST histograms representing the response of a radial fibre to rarefaction clicks (left) and condensation clicks (right). A typical example of the transmitter release waveform is shown below each intensity series, and the normalised peak release due to each stimulus (Q) is indicated against each pair of responses. (τ = 2 msec., M = 0.72 (spontaneous), abs.ref. period = 15 msec., 600 stimuli).

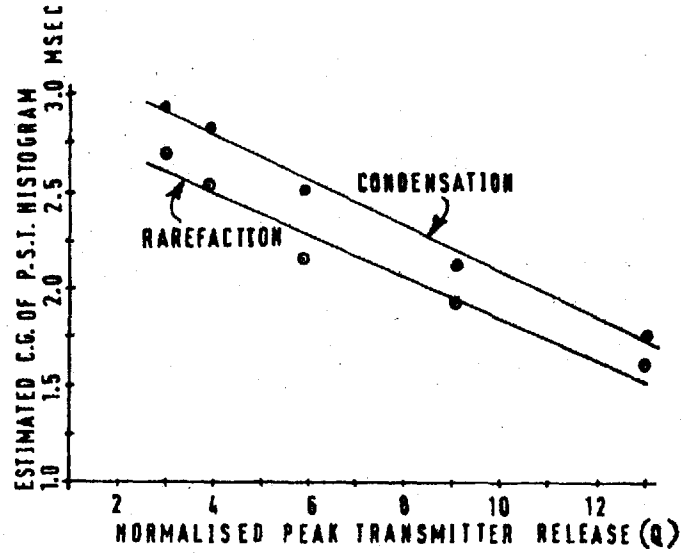

Figure 73 Estimated shifts in the centre of gravity of the PST histograms illustrated in Figure 72, as a function of the normalised peak transmitter release (Q).

Such effects as centre of gravity shift in the simulated histograms therefore depend to a large extent on assumed threshold refractory properties. Such complications may be usefully eliminated by considering recovered probabilities. Shown in Figure 74 are estimates of recovered probability relevant to whole peaks of the histograms of Figures 71 and 72, plotted as a function of the peak transmitter release caused by the stimulus. These results, which indicate a systematic rise in recovered probability from peaks 1R to 2C to 3R at all intensities, and a gradual reduction for subsequent peaks, seem to parallel importantly the equivalent estimates for first order auditory neurons in cat (see Figure 17).

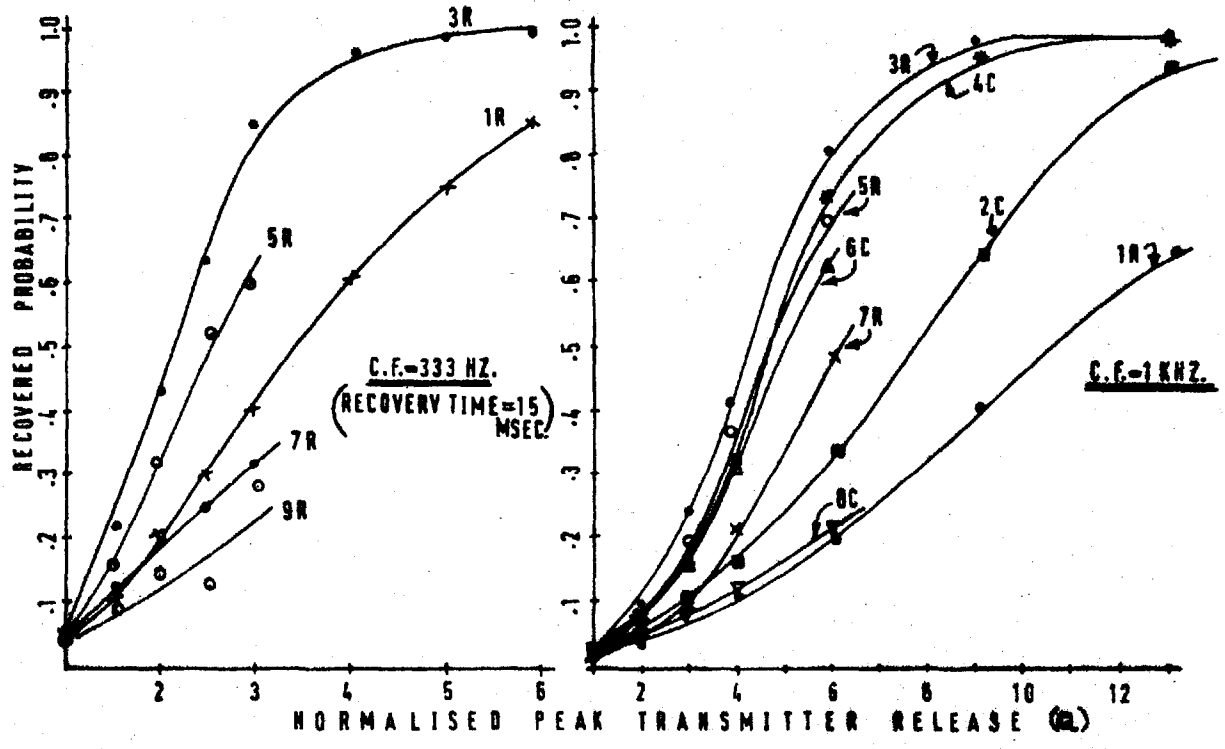

Figure 74 Estimates of recovered probability for whole peaks of the histograms illustrated in Figures 71 and 72 (together with estimates from other computer runs not illustrated). A redundant 'C' or 'R' is used to indicate peaks due to condensation or rarefaction clicks, and to allow an easy comparison with the results of Gray (see Figure 17).

The broad similarity between the recovered probability curves obtained in the physiological situation and from these computer simulations makes it possible to estimate the dynamic signal range represented by the simulations of Figures 71 and 72 as about 30-50 dB. The centre of gravity shifts shown in Figure 73 also occur over this dynamic range, and therefore represent a timing-intensity ratio of some 35 μsec./dB, which is of the same order as the physiological estimates, (see Figure 20).

9.4 Discussion

The results of computer simulations reported in this section seem very encouraging, and appear to support the proposal of a controlling action by outer hair cells and spiral fibres on radial fibre activity. In particular, the assumption of a control waveform arriving along spiral fibres from the outer hair cells obviates the need for restrictive assumptions about mechanisms in the single hair cell and nerve ending, and provides what is believed to be both a novel and plausible explanation of the roles of outer and inner hair cell rows.

In the simulations described here, the output of a single spiral cochlear fibre, stimulated at its basal terminations by outer hair cell activity, was assumed to be responsible for the controlling action at an inner hair cell synapse. Although specific assumptions are always necessary for the purposes of digital computer modelling, they may, from a physiological viewpoint, be unnecessarily restrictive. In this case, a number of alternative schemes (one of which has already been illustrated in Figure 68) might be expected to give broadly similar results to those described. For example, it appears quite feasible that firings in any one radial afferent fibre are controlled by activity in a number of spiral fibres, possibly having a range of lengths. In the case of a transient acoustic stimulus, it seems possible to envisage a wave of such control activity travelling from base to apex of the cochlea, and reflecting at any one locus the net effect of activity in a number of spiral fibres. However, such a hypothesis would imply functional connection between any one radial fibre and a

number of spiral fibres, a question which has not yet been settled by anatomical investigation.

Similarly, the assumption that interaction between radial and spiral fibres occurs in the region below the inner hair cells may be unnecessarily restrictive. The central projections of spiral fibres have not yet been systematically mapped, and it therefore remains possible that they affect radial afferents at some more central site - for example, close to the cell bodies in the spiral ganglion. Finally, the present proposition, in its most general form, does not seem to depend exclusively on electrotonic activity in spiral fibres. The wave of control activity, mentioned above, might equally well arise as a net result of spike activity in a large number of spiral fibres (presumably of variable length). In this case, however, it would seem the more necessary to postulate functional connection between any one radial afferent and a large number of spiral fibres. To summarise, the computer simulations seem to demonstrate the validity of the general proposition that spiral fibre activity exerts control over radial afferent fibres, but it is possible to envisage a number of detailed schemes for the generation of a suitable control waveform.

Such proposals pose a number of important questions about the course of spiral fibres. The view that their function is to exert control over radial afferent fibres implies that they do not also convey spike activity in the acoustic nerve (at least, not activity of the kind reviewed in section 2.7). On the other hand, if spiral fibres are not represented in the nerve trunk, their central terminations seem likely to be in the region of the spiral ganglion,

since they are known to enter the organ of Corti via the habenula perforata (see Figure 7). It would clearly be very interesting to have further information about the course of such fibres in this region.

Although the waveforms of transmitter release used in the simulations were arbitrarily composed of a number of half-sinusoids, of peak value determined by the control waveform (see Figures 71 and 72), it seems unlikely that such details are important in determining the main features of simulated PST histograms. All that is required is that the mean effect of quantal release during any one local basilar membrane rarefaction movement is determined by a control waveform of suitable type. From this point of view it seems possible to regard the inner hair cell synapse as an ON-OFF switch, controlling only the detailed timing of transmitter release; for this purpose a very restricted inner hair cell dynamic range would be quite appropriate.

The assumptions necessary to reproduce the differences between rarefaction and condensation click responses should perhaps be elaborated. According to the present proposition, the relatively great neural response to basilar membrane rarefaction 2C (due to a condensation click) compared with that of rarefaction 1R (due to a rarefaction click) is caused by the greater instantaneous value of the control waveform in the former case. In other words, the control waveform arriving along the spiral fibre(s) has had time, in the case of the condensation stimulus, to get nearer to its peak value by the time the first local membrane rarefaction occurs. A simple consideration of the waveforms involved suggests that this relative time-advance of the control waveform could only occur in one of two ways; either

the outer hair cells perform some sort of effective full-wave rectification of basilar membrane activity, or they react only to condensation movements. In the simulations illustrated in Figure 72, a full-wave rectification is implied, because the timing of the control waveform (measured with respect to the onset of the acoustic stimulus) was assumed to be unaffected by a change of stimulus polarity.

The general proposition which has been put forward seems to be supported by considerable evidence than that obtained from computer simulations. Such evidence may now be usefully summarised:-

(a) A majority of afferent fibres in the acoustic nerve have now been traced to terminations on the inner hair cells. It is proposed that most, if not all, of the published neural recordings from the acoustic nerve have been taken from such radial afferent fibres (see section 2.5).

(b) There is substantial anatomical evidence for interaction between spiral and radial afferent fibres in the densely-packed region below the inner hair cells (see section 2.5).

(c) Spiral fibres are now believed to terminate only after completing their spiral run, and, assuming that such spiralling is a characteristic of some functional significance, it seems reasonable to postulate some important role for the fibre properties. It is difficult to imagine that attenuation would be functionally useful; it would certainly not add to system sensitivity. Therefore presumed low-pass filtering seems likely to be an effect of interest (see section 2.5).

(d) There is no evidence in published neurophysiological records from the acoustic nerve of systematic groupings in fibre firing characteristics which might be thought to reflect spiral (as opposed to radial) fibre innervation.

(e) There are marked differences between the number, type, and arrangement of hairs on inner and outer hair cells, for which no satisfactory explanations have so far been given (see Figure 5). In view of the present proposition, it is tempting to speculate that the outer hair cells, having a relatively large number of hairs of graded height, might supply a control signal of wide dynamic range to the radial afferent fibres. Such a dynamic range might be explained by the activation of an increasing number of hairs by the tectorial membrane as signal intensity rises, and also by the connection of any one spiral fibre to hair cells of (presumably) different sensitivity in the various outer rows (see Figure 6). On the other hand, an inner hair cell, believed to have a smaller number of hairs of uniform size, would merely be required to act as a switch, responding to local basilar membrane vibrations and determining the detailed timing of events (e.g. quantal release) at its afferent synapses. The dynamic range of the inner hair cell could therefore be much smaller, and could well be correlated with the relative simplicity of its hair arrangement (see section 2.3).

(f) There are no known systematic variations in individual hair cell or afferent nerve terminal dimensions, or properties, which depend on position along the cochlear partition and which might be assumed to account for the observed magnitudes of the various peaks of click PST histograms.

(g) Such proposals may also help to explain the neural response to tone bursts at the C.F. of a fibre. Although the basilar membrane response to such a stimulus (see, for example, Figure 49) appears to reach its steady-state after little more than one cycle of the stimulus, typical PST histograms of fibre activity show a relatively slow increase in the heights of successive peaks following the start of the response, (see Figure 15). This could apparently be explained by the relatively slow rise of the proposed control waveform which would, once again, be expected to determine the quantitative effect of successive membrane rarefactions.

The most striking result of the present proposition, in terms of realistic modelling of the neural responses measured by Kiang, is that it can apparently account with great simplicity for the major effects of interest. It is only necessary to assume a simple switching action by inner hair cells, and a parallel controlling action by outer hair cells and spiral fibres. With such assumptions three main classes of difficulty encountered in earlier sections of this study are apparently resolved. Firstly, the range of model parameters no longer needs to be severely restricted for the production of realistic click PST histograms. Secondly, the assumption of an exponential relationship between hair cell polarisation and chemical transmitter release rate (which finds no support in the available evidence) is no longer necessary, since the form of the proposed control waveform is itself such as to produce a number of peaks in the simulated click PST histograms. Finally, and perhaps most importantly, the need for a facilitation or control mechanism having a time course related to the cochlear region

considered is plausibly satisfied by such proposals. For example, the scheme investigated in the computer simulations (and illustrated by Figure 67) implies a systematic variation in the length of spiral fibres along the cochlear partition. Although such a variation has not been reported, this could be due to the fact that the courses of individual spiral fibres have not yet been systematically mapped. In any case, since timing effects in such a fibre are expected to vary as the square of its length, a 3 : 1 or 4 : 1 variation in length along the cochlear partition would seem adequate to account for the full range of click responses reported by Kiang (see Figure 13).

10 DISCUSSION AND CONCLUSIONS

10.1 Modelling the peripheral auditory system; a reappraisal

The proposition of section 9, that outer hair cells act as controllers of the activity in radial afferent fibres, may qualify considerably other ideas about the relationships between cochlear structure and nerve fibre activity. It now seems appropriate, therefore, to re-examine the propositions and conclusions of earlier sections in the light of such ideas.

A simple quantal (chemical) model for the spontaneous activity in first-order auditory neurons was examined in some detail in section 5. It became clear that severe restrictions had to be placed on the choice of parameters of such a threshold model, if it was to generate spontaneous activity similar to that observed in cat, and a proposition based upon the superposition of point processes was then suggested. Although multiple innervation of cochlear hair cells by afferent nerve fibres seemed to fulfil the required anatomical conditions for such a superposition effect, it has subsequently been proposed that neural activity measured in the acoustic nerve derives from radial afferent fibres. These are currently believed to innervate few, and possibly only one, inner hair cell (see Figure 7). A superposition scheme based on cochlear multiple innervation therefore seems less plausible, although it is possible that there are other ways in which a superposition effect might arise. For example, if spiral afferent fibres have, as proposed, an important control function, it seems possible that random noise activity in such fibres may cause (or be an essential prerequisite for) the generation of random spikes in radial

afferent fibres. If several or many spiral fibres each cause independent generation of random spikes in one radial afferent fibre, a superposition effect might be expected to give rise to an observed Poisson process in the radial fibre when it reaches the acoustic nerve (subject only to its refractory properties). But it is argued that whether or not such a scheme proves to be supported by future investigation, the results of section 5 illustrate clearly the type of restrictions which must apply to models of spontaneous spike generation in the cochlea.

It is also interesting to recall the results of section 6, in which possible signal processing by spiral fibres was considered. At that stage, it was assumed that spiral afferent fibres are represented in the acoustic nerve, and that they therefore display the typical neural activity reported by Kiang (as reviewed in section 2). For this reason it seemed difficult to assume any substantial smearing of electrotonic signals due to the cable properties of such fibres, and the only properties considered were those of delay and attenuation. The results suggested that any significant signal processing by such a system (such as an effective sharpening of cochlear tuning) was unlikely. The proposition of section 9, however, adopts a radically different view of spiral fibre properties, suggesting that, if such fibres are no longer assumed to form part of the acoustic nerve, those low-pass filtering properties which had earlier seemed an embarrassment may now be considered of great functional importance. On this very different basis, signal processing by spiral fibres again appears to be a very significant possibility.

It cannot be claimed that sections 7 and 8, in which possible electrical and chemical transmission effects at individual afferent synapses were examined, are exhaustive. The great difficulty of quantitative discussion of the details of the cochlear neural transduction - and particularly of attempts at digital computer simulation - lies in the present lack of physiological evidence. It would, of course, be possible to invent mechanisms for the explanation of the details of neural activity, but in the present work a preliminary attempt has been made to relate such details to cochlear physiology. All that can be claimed is that this initial study suggests no ready explanations for certain neural effects in terms of known properties of nerve or synapse. The proposition of a controlling action by spiral fibres (and outer hair cells) on the activity of the afferent radial fibre arose at this stage, and although it may be controversial, it seems to enjoy considerable support from recent anatomical evidence. If accepted, it could well resolve a number of unanswered questions on the relative function of inner and outer hair cells and of the complex pattern of cochlear innervation.

The present study, starting from the proposition that the details of neural PST histograms measured in the cat's auditory nerve could account for certain binaural listening phenomena, then adopted the view that these details might also be important clues to the cochlear transduction process. However, the neural effects of interest are now proposed to be largely a product of the cochlear innervation scheme, and not of the mechanisms of the individual hair cell - nerve ending function; this may well apply to spontaneous as well

as stimulated activity. Indeed it now seems that the complexities of the innervation do not allow details of activity at individual afferent synapses to be deduced from spike recordings in the acoustic nerve; this applies particularly to the outer hair cell junctions, where it remains unclear whether the transmission is likely to be electrical or chemical.

In the case of the synapse between inner hair cell and radial afferent fibre, anatomical evidence points more positively to a chemical transmitter system (see section 2.6), and the proposition of section 9 seems marginally to support the same conclusion. For, although it is difficult to suggest the precise mechanism by which spiral fibres might control the activity in radial fibres, it seems that they must fulfil some essential step in the spike generation process. In this context it is interesting to note that effective chemical transmission is now believed to depend upon complex intermediate steps (such as inflow of calcium ions to the presynaptic terminal, see section 8.2), which might perhaps be controlled by spiral fibre activity.

Sections 8 and 9 described models for stimulated activity in cochlear neurons, in which the stochastic nature of their responses was attributed to the assumed probabilistic release of a chemical transmitter substance; this was represented by a Poisson process, in which the instantaneous release rate was controlled by the stimulus. Although there are other possible ways of incorporating the stochastic nature of the responses (such as by assuming chance fluctuations in nerve membrane potential, see section 5.1), there seems, so far, to be no reason for abandoning the

present hypothesis. It might be possible to test it more comprehensively by investigating variations of recovered probability on a much finer time scale, both in digital computer simulations and in the recordings of nerve fibre activity; such work would however be very expensive in computing time and, as yet, there is not much physiological evidence available. It therefore seems possible that further anatomical and physiological investigations of the hair cell and nerve ending would be more rewarding. On the other hand the present study emphasises the need for clarification of a number of basic issues - such as the overall roles of inner and outer hair cells and of the innervation pattern - which seem more important at this stage than the details of activity at single cochlear synapses. A clarification of these basic issues would almost certainly allow a more logical approach towards the investigation of cochlear synaptic transmission, based on a better understanding of the relationship between cochlear neuroanatomy and recordings from single fibres in the acoustic nerve.

10.2 The significance of time-intensity trading in binaural listening

One of the main interests of this work has been to investigate further the phenomenon of time-intensity trading in binaural listening, and to enquire whether or not the main subjective effects of IAD may be correlated with activity in the peripheral auditory system. Since this task requires a clearer appreciation of the detailed ways in which intensity is coded at the periphery, it has led to a careful examination of possible transducer mechanisms in the cochlea. As a result of this approach, it is now argued that a plausible explanation of the main time-intensity trading effect is indeed available on the basis of cochlear neural activity, if electrophysiological recordings recently obtained from single fibres in the cat's auditory nerve are relevant to the human.

The proposition put forward in section 3.4 seeks to explain the substantial perceived shifts in lateral position of fused binaural images, under the influence of IAD, in terms of a shift in the centre of gravity of the PST histograms of afferent nerve fibres innervating the cochlear region of interest. Such a proposal, by its very nature, must emphasise transient acoustic signals and argues that the amplitude of such signals is effectively coded into neural latency at the periphery by virtue of a complex interaction between the damped oscillatory response of the basilar membrane, the detailed nature of the mechanical-to-neural transduction, and the refractory properties of auditory nerve fibres. In addition to this coding of signal amplitude into effective neural latency, amplitude is

undoubtedly also represented in terms of a total population of responding neurons, and it seems not unreasonable to postulate that both types of clue may affect a final subjective judgement of the lateral position of a binaural image.

At this stage it is of interest to mention other possible peripheral mechanisms which might account for the main IAD/ITD trading effects. Perhaps the simplest of these would be a straightforward amplitude-to-time conversion caused by the threshold properties of an auditory neuron. If basilar membrane displacement is considered the essential stimulus for a nerve fibre, then the time taken for a particular displacement half-cycle to reach a level sufficient to cause stimulation would be expected to vary inversely with stimulus intensity. Such a mechanism would be expected to apply to any type of signal and would therefore place no particular emphasis on acoustic transients. However, a simple consideration of a pure tone stimulus shows that the magnitude of such an effect would be very small except near threshold, and at all intensities very much less than the figure of 20-30 μsec./dB reported in section 3. For example, if a sensation level of zero is considered to correspond to membrane displacements which just reach a neural firing threshold, then the trading ratio for a 800 Hz. tone at a mean level of, say, 30 dB S.L. would, on this basis, be expected to be about 0.8 μsec./dB. Although such a calculation assumes a deterministic threshold device and is therefore liable to considerable error, it is clear that the maximum time advance of a neuron's response to a particular membrane rarefaction movement would be of the

order $^1/_4$ cycle of the stimulus waveform, over the whole dynamic range; this figure is also mentioned by Kiang [37] when discussing latency changes with intensity of individual peaks of a click PST histogram. For a 800 Hz. tone, such considerations would yield a mean trading ratio of about 4 μsec./dB over a dynamic range of 80 dB. It thus seems impossible to account for the larger reported trading ratios on the basis of a simple threshold conversion effect.

A very different mechanism might be envisaged, which would direct attention not to mean latency changes with amplitude in the response of individual auditory fibres, but which would instead concentrate on the earliest response, post-stimulus, arising anywhere in the cochlea. Such a mechanism could perhaps be visualised most simply for a transient stimulus, although it might also be expected to apply to continuous signals such as tones. For example, in the case of a wideband transient near threshold, neural responses would presumably arise only in well-defined cochlear regions (see section 6). At a higher intensity more basal fibres would be stimulated, and at an earlier time post-stimulus. If the mechanism responsible for binaural fusion were to pay attention to the earliest stimulus-locked response, regardless of its cochlear region of origin, a monaural increase in amplitude might be interpreted as equivalent to a time-advance of the signal to that ear. However, such a scheme presents a number of difficulties: there is substantial evidence that binaural images are formed by crosscomparisons of neural signals from corresponding regions of the two cochleae (see section 3.1), whereas such a mechanism would require a unilateral shift of

attention to a more basal site; furthermore, the rather broad representation of signals on the basilar membrane (see, for example, section 6) implies that even modest increases in intensity would in many cases be sufficient to shift the site of earliest neural response very considerably. Approximate calculations suggest that trading ratios of the order 100-300 μsec./dB could be expected on this basis.

It is therefore argued that the present proposition about time-intensity trading provides the most plausible explanation for the phenomenon which has so far been put forward. There is substantial evidence [63] that the main impulsive image perceived with transient stimuli arises by virtue of neural activity in the medial or apical cochlea, and if this is the case there seems no other peripheral mechanism which could simply account for the magnitude of the trading ratio reported.

The binaural experiments described in section 3 used low-pass-filtered transients, so as to allow the subject to concentrate on the main impulsive image of low-pitched character. The various other images, tonal and impulsive, which are known to arise with repetitive transients and tones, have not been investigated here. It seems relevant, however, to review briefly the results obtained by other experimenters in their investigations of binaural trading ratios, and to see whether or not a consistent picture emerges.

Reports of binaural trading ratios are somewhat variable, although the ratios have traditionally fallen into two groups. The first of these, generally reported when pure tones have been used, occupies the approximate range

1-3 μsec./dB. The second group, usually reported for transient signals, falls in the range 20-60 μsec./dB, with considerably higher values occasionally reported. Thus Shaxby and Gage [54A], in an early paper, reported a mean value of 1.7 μsec./dB for pure tones at 500, 800, and 1200 Hz., whereas Deatherage and Hirsh [5B] found trading ratios for low-pass transients (filter cut-off = 2.4 KHz.) which were dependent on the absolute level of the test and varied between about 20 and 100 μsec./dB. The latter authors believed that the trading ratio for transients arose by virtue of basal cochlear activity, and suggested that the effect was consistent with latency-intensity effects observed in the whole-nerve action potential (N_1) measured at the round window. In some experiments using high-pass clicks (filter cut-off set to 2 KHz.), David, Guttman and van Bergeijk [5A] found similar trading ratio values to those of Deatherage and Hirsh.

Whitworth and Jeffress[71A] carried out some experiments with tonal signals which suggested that subjects were able to distinguish two images, one apparently trading at about 1 μsec./dB and the other at about 25 μsec./dB. The first they called the "time" image since it was not substantially affected by IAD, and the other the "intensity image". Their experimental method was to ask the subject to compare the perceived lateral position of the signal (having ITD and IAD parameters set by the experimenter) with that of a reference tone (having an ITD control set by the subject). Signal and reference tones were alternately presented to the subject, and interchanged every 0.8 second. They reported that the "time" image was not perceived by subjects

with high frequency hearing losses, but suggested that a simple amplitude-to-time conversion by the threshold properties of auditory fibres would adequately account for its low trading ratio. In a recent paper, Hafter and Jeffress [25A] have reported trading ratios obtained with tone burst signals, of durations between 1000 msec. and 10 msec. and low-pass filtered to 850 Hz. A reference burst of the same duration as the signal was again used as a pointer, with a rest period of some 300-450 msec. between presentation of signal and reference. Although they described the 1000 msec. tone burst signal as subjectively "tonal" in character and the 10 msec. burst as "impulsive", subjects again reported two images in all cases, with trading ratios of about 5 and 35 μsec./dB respectively. Hafter and Jeffress then investigated the use of high-pass filtered transients and found that subjects again reported two binaural images, this time trading at about 25 and 100 μsec./dB. They again referred to these as time and intensity images, although it seems doubtful whether, as this implies, the image trading at 25 μsec./dB should be placed in the same category as the other time images described. Like other authors, they argued that latency changes in the whole-nerve action potential (N_1) could account for the trading ratio of the intensity image, and that the ratio relevant to the time image could arise by virtue of an amplitude-time conversion effect due to fibre threshold properties.

Although no attempt has been made in this study to investigate images other than that trading at about

30 μsec./dB, the proposition put forward about centre of gravity shifts in neural PST histograms certainly suggests a rather different interpretation of these various experimental findings. Most importantly, it is argued that the dominant image, which has a trading ratio of about 30 μsec./dB (which is assumed to correspond to the intensity image described by other workers), arises by virtue of medial or apical cochlear activity, whereas other authors have related it to basal responses and the whole-nerve action potential. There seems to be powerful supporting evidence for the present view from binaural experiments by Toole and Savers [63], who masked the basal cochlea with high-pass filtered noise and showed that the main impulsive image arising with transient signals was a medial (or apical) effect. Furthermore, Whitworth and Jeffress [71A] have reported that subjects with high frequency hearing loss were able to track the intensity image, whereas they could not perceive the time image. Finally, the fact that an image trading at about 30 μsec./dB has been reported when using high-pass clicks does not necessarily contradict the present proposition, since the filter cut-off frequency employed (2 KHz.) may well not have precluded substantial basilar membrane activity in, say, the 1500 Hz. region.

The evidence, already reviewed, for the presence of an intensity image with tonal signals is perhaps more puzzling, although the experimental technique employed may have introduced some effects which would not be found when using continuous tones. It seems quite possible that the use of a reference "pointer" tone, alternately presented with the signal, may have provided the subject with the necessary

clues for a judgement based on the centre of gravity effect. In other words, the transient effects at the onset of the tone bursts might be sufficient evidence for the perception of an intensity image which trades at about 30 μsec./dB. It seems possible that the subjects would have failed to report and track an intensity image, had they been presented with more truly continuous tones having a rise-time at the instant of switching which allowed them no clues to transient effects.

The consistent evidence for the presence of the so-called time images might perhaps be explained in a number of ways. The consensus of opinion expressed by other authors is that such images arise by virtue of activity in the basal cochlear region and that a straightforward amplitude-to-time conversion by neural threshold properties would be sufficient to account for the small trading ratio involved. Such an explanation does indeed seem plausible, although a number of further points are perhaps worth making. Firstly, if such images originate basally and in response to transient stimuli, it might also be reasonable to postulate a centre of gravity effect; however, the close spacing in time of successive membrane rarefactions in the basal region and the correspondingly limited duration of the PST response would ensure that any such effect gave rise only to a very small trading ratio - perhaps of the magnitude reported (indeed the magnitude of the reported ratios is often so small that it is tempting to believe that such time images are essentially unaffected by IAD - but that the simultaneous presence of an intensity image with a substantial trading ratio confuses or biases the subject's

judgements about the time image). It also seems quite possible that time images do not always arise in the basal cochlea, but that, if a subject is asked to search for extra images, he may manage to resolve a single intensity image into one or more time images with small or negligible trading ratios. For example, with low-pass repetitive transient stimuli a subject will normally perceive a single intensity image, the lateral position of which, it is here argued, reflects the centre of gravity of the relevant neural PST histograms. Such an image will trade at, say, 30 μsec./dB. However, if a trained subject is then asked to search for other images he may manage to separate out so-called "multiple" images, corresponding to individual membrane rarefaction movements (and thus to individual peaks of the relevant neural PST histograms). Such an effect has already been described in section 3.5; it reflects not so much the existence of images separately represented in terms of peripheral activity, but rather the fact that the brain is presumably able to process the neural information reaching it in a number of different ways .

Finally, the possibility that intensity itself (represented in a total population of responding cochlear neurons) influences final judgements about the lateral position of a binaural image should not be overlooked. In some experiments with pure tones, Sayers and Toole [52] produced some experimental evidence, that increased intensity on one side merely gave rise to a bias of lateralisation judgements towards that side; this matter has been further discussed in a recent paper by Sayers and Lynn [51A]. Other authors [43A] have reported electrophysiological evidence that

some units in the superior olivary complex are essentially intensity-sensitive, and it seems quite possible that such units affect final lateralisation judgements.

10.3 The prediction of effects due to more complex acoustic signals; suggestions for further work

The proposition that the form of click PST histograms measured in the acoustic nerve of the cat can account for the main aspects of time-intensity trading in binaural listening experiments with repetitive acoustic transients cannot, by itself, be expected to give insight into the likely effects of other types of stimulus. Such insight almost certainly requires an appreciation of the underlying physiological mechanisms, and for this reason a major part of the present study has been concerned with the modelling of likely transducer mechanisms in the cochlea.

The proposals of section 9 seek to explain the centre of gravity shifts in click PST histograms with intensity on the basis of a controlling action by outer hair cells and spiral afferent cochlear fibres on radial fibre activity. If such a description were accurate it would be of considerable importance, because it specifies quite detailed physiological mechanisms, and should therefore give the sort of insight into the overall function of the cochlea which is required for the successful prediction of responses to other types of signal.

For example, in addition to the emphasis which such proposals put on the importance of transients in the localisation of sounds, the type of mechanism envisaged in section 9 suggests that the envelope of basilar membrane activity would be very strongly represented in the control waveform arriving along spiral cochlear fibres. (Envelope detection would result from the proposed rectifying action by outer hair cells, followed by low-pass filtering as the

signal passes along a spiral fibre). In this context, it is interesting to recall such experimental results as those of Leakey, Sayers, and Cherry [38A] who used binaurally presented tones of about 4 KHz., amplitude modulated with either low frequency (e.g. 200 Hz.) tones, or noise. They found that their subjects were able to report binaural images which behaved exactly as if they were due to the modulating signals alone - even though such frequencies were not represented in the spectrum of the modulated carrier, and their subjects were not able to report image lateralisation with pure tones of frequency above about 1500 Hz. They concluded that the binaural fusion mechanism was apparently able to operate on the envelope of the modulated carrier.

In more general terms, it would be attractive to be able to predict the response of a first-order auditory neuron to other, more complex, signals; for example, speech recognition studies might benefit considerably from an understanding of the way in which such signals are coded in the cochlea. Although it seems necessary to examine the proposition about the controlling action of spiral fibres on radial afferent fibres in more detail, (presumably by further anatomical and electrophysiological investigation) before it could be used for the confident prediction of more complex neural responses, it is already possible to suggest the broad outlines of a scheme which might be used for such prediction.

A stochastic threshold model would presumably be uneconomic in most cases, since the large number of repetitions of the stimulus required for a reliable prediction would involve lengthy computations (the simulations

described in this work used some 5 minutes on an IBM 7090 computer to model 15 seconds of the activity of a single neuron). A faster scheme might involve estimating neural firing probability directly from basilar membrane activity; the statistical analysis by Gray (see section 2.7.3), and the simulations of section 9, suggest that there is a fairly simple relationship between stimulus intensity and the recovered probability of firing of a cochlear fibre during any one basilar membrane rarefaction movement. It should therefore be possible to make reasonable estimates of recovered probability for an afferent fibre of known C.F., relevant to successive membrane rarefactions. The complications introduced by neural refractory properties would then have to be included. Although such a scheme would only produce probability estimates, it should provide a useful idea of the averaged response of an ensemble of nerve fibres innervating a particular cochlear region.

A possible scheme of this type is illustrated in Figure 75. Two distinct processes are considered to be involved in the release of a chemical transmitter across an afferent synapse and in the resulting depolarisation of a nerve terminal. Above and on the right, local basilar membrane activity (computed from the acoustic pressure waveform) is assumed to cause a switching action by the inner hair cell transducer mechanism, which allows chemical transmitter to be released only during membrane rarefaction movements. On the left, membrane activity at a more basal site stimulates outer hair cells, which deliver a signal to a spiral fibre. The cable properties of the spiral fibre cause this signal to be (attenuated and) low-pass filtered,

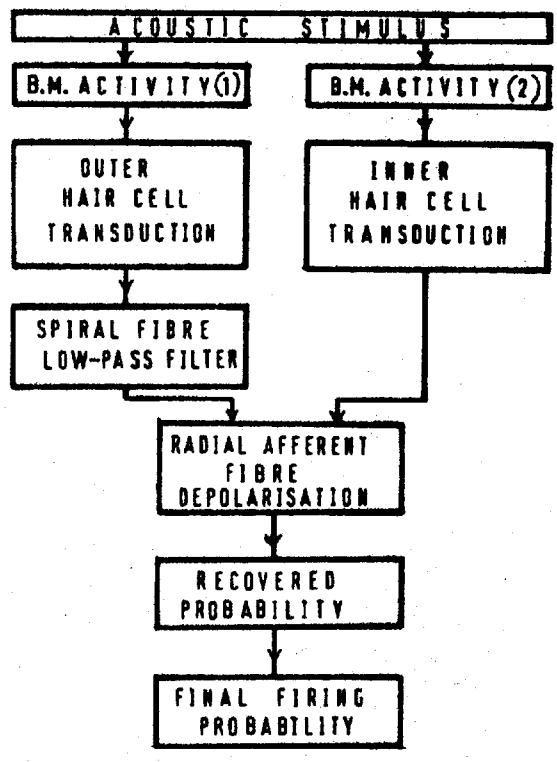

Figure 75 Block diagram of a scheme for the computation of the response of a radial afferent cochlear fibre to any acoustic stimulus. The function of the various blocks is described in the text.

thus generating the control waveform which determines the amount (or quantitative effect) of the transmitter release at the inner hair cell synapse. This transmitter release is assumed to be simply related to the recovered probability of firing during the corresponding local membrane rarefaction movement. Finally it is assumed that recovered probability can be converted into unconditional firing probability, using some algorithm which takes account of neural refractory properties.

Whether or not transmitter release is determined in this manner will presumably be clarified by future

investigations. In any case, there remain two questions. Firstly, it needs to be shown that transmitter release, however caused, may be simply related to recovered probability; and secondly, it is not clear that a simple computational scheme can be devised for estimating unconditional firing probability from recovered probability. These two points will now be briefly discussed.

In section 9, recovered probability estimates for the various peaks of simulated click PST histograms were obtained (see Figure 74), arising from the use of known transmitter release waveforms. It is therefore possible to use the results of these simulations to plot the total transmitter release during any one membrane rarefaction movement (which is proportional to the corresponding area under the transmitter release curve) against the recovered probability estimate for that rarefaction. Two effects might be expected to militate against a simple relationship between transmitter release and recovered probability. Firstly, the recovered probability relevant to a particular rarefaction should depend to some extent on previous transmitter release, because of postsynaptic integration - although the earlier simulations of section 8 suggested that this is likely to be only a small effect. Secondly, it is not clear whether different spontaneous firing rates, probably reflecting different values of the PSP equilibrium level in the absence of a stimulus, might substantially affect the probability that a particular burst of stimulated transmitter release causes firing threshold to be exceeded.

However, the limited results plotted in Figure 76 suggest that these effects are relatively minor, and that a simple function might in fact be used to relate recovered probability to transmitter release, regardless of the C F. of the fibre, its spontaneous rate, or preceding basilar membrane activity.

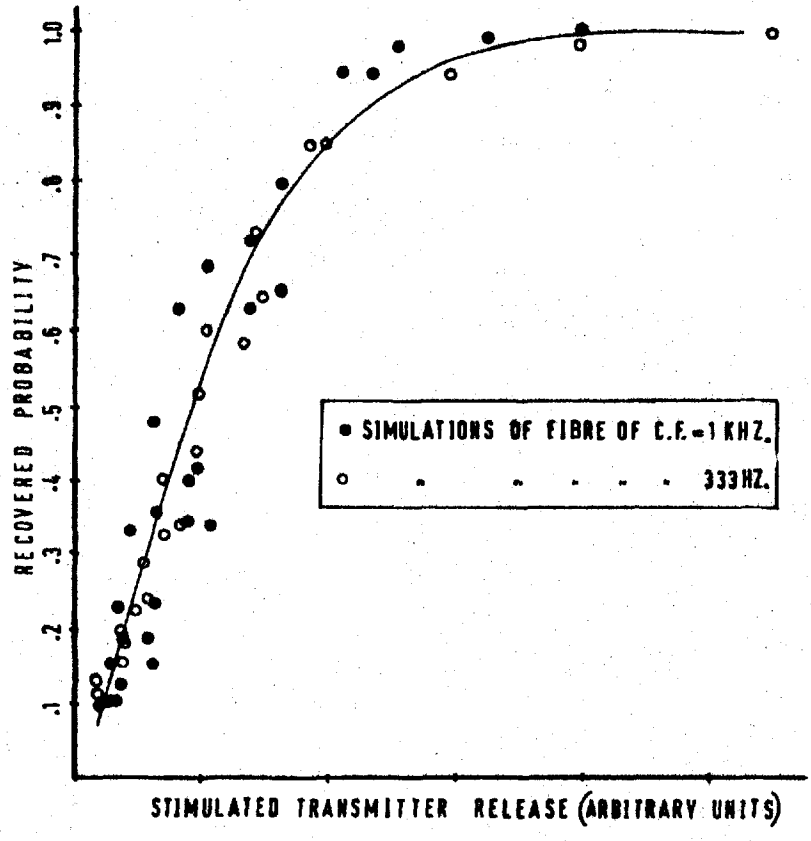

Figure 76 Estimates of recovered probability for the various peaks of the simulated PST histograms of Figures 71 and 72, as a function of the total stimulated transmitter release caused by the relevant basilar membrane rarefaction.

The plotted points represent various peaks of the simulated histograms of Figures 71 and 72 (1R, 2C, 3R ... 8C in the case of the 1 KHz. fibre, and 1R, 3R, 5R, 7R in the case of the 333 Hz. fibre), and there are no clear

systematic variations between the earlier and later histogram peaks, or between the two different fibres. All points lie reasonably close to a smooth curve, which could be represented by a simple analytic function. As a first approximation it therefore appears that transmitter release could be simply transformed into a recovered probability value, relevant to one basilar membrane rarefaction half-cycle.

Various assumptions might be made about the refractory properties of a first-order cochlear neuron, in order to try to relate unconditional firing probability to recovered probability. For example, it might be assumed that:-

$$p(t).\delta t = p_r(t).\, F(t - t').\, \delta t$$

where $p(t)$ is the unconditional probability density

$p_r(t)$ is the recovered probability density

and $F(t - t')$ is a multiplier between zero and unity representing the refractory properties of the neuron recovering from its previous firing at t'. F may be thought of as a sensitivity function, which reduces the firing probability and depends for its magnitude only on the time since the last firing.

In order to simplify the analysis of this situation, consider the activity of an initially-recovered fibre, for which the recovered probability of firing during a succession of small subsequent time increments has been estimated. Let these recovered probability values be r_1, r_2, r_3 ... etc., and the corresponding values of unconditional firing probability be p_1, p_2, p_3 ... etc. Since the unit is assumed to be initially in a recovered condition:-

$$p_1 = r_1$$

The probability of firing during the next time increment is made up of two parts; either the unit has fired during the first time increment, or it has not. Thus:-

$$p_2 = (1 - p_1)\, r_2 + p_1 r_2 F_1 = r_2[1 - p_1(1 - F_1)],$$

where F_1 denotes the value of the sensitivity function due to a firing during the previous time bin. The probability of firing during the third time increment is more complex but may be evaluated by considering the various possibilities, which are:-

(a) the unit is "recovered"

or (b) it fired during time increment 1

or (c) " " " " " 2

or (d) " " " " " 1 and 2

This yields:-

$$p_3 = (1 - p_1)(1 - p_2)r_3 + p_1(1 - p_2).r_3F_2 + \\ + p_2(1 - p_1)r_3F_1 + p_1p_2r_3F_1$$

which reduces to:-

$$p_3 = r_3[1 - (1 - p_2)p_1(1 - F_2) - p_2(1 - F_1)]$$

Similar considerations yield the result for p_4 :-

$$p_4 = r_4[1 - (1 - p_3)(1 - p_2).p_1.(1 - F_3) \\ - (1 - p_3)p_2(1 - F_2) - p_3(1 - F_1)]$$

and the general relation:-

$$p_n = r_n[1 - \sum_{K=1}^{n-1} [(1 - p_{n-1})(1 - p_{n-2}) \ldots \\ \ldots (1 - p_{K+1})].p_K.(1 - F_{n-K})]$$

Since any practical application of such results almost certainly involves a digital computer, it is interesting to note that an exponential form for the sensitivity function F allows a considerable simplification in computation. For example, let the function F be of the form

$$F(T) = 1 - e^{-T/\tau}$$

where T = time since last firing

τ = time constant of recovery.

Note that if T = 0, F = 0 (unit absolutely refractory)

$T \rightarrow \infty$, $F \rightarrow 1$ (unit recovered)

In this case successive values of the function (1 - F), required for the computation, will be related by a constant α. Thus:-

$$\frac{1 - F_K}{1 - F_{K-1}} = \alpha = (1 - F_1), \text{ for } \delta t \ll \tau$$

Consider now the practical computation of successive values of firing probability p_1, p_2, p_3 ... etc., assuming the unit to be initially recovered:-

$$p_1 = r_1(1)$$

$$p_2 = r_2(1 - [p_1\alpha])$$

$$p_3 = r_3(1 - [p_1\alpha^2(1 - p_2) + p_2\alpha])$$

$$p_4 = r_4(1 - [p_1\alpha^3(1 - p_2)(1 - p_3) + p_2\alpha^2(1 - p_3) + p_3\alpha])$$

etc.

It is seen that a new value p_n may always be formed by multiplying each term within the square brackets of the expression for p_{n-1} by a factor $\alpha(1 - p_{n-1})$; a new term equal to αp_{n-1} is added to the result; the total is then subtracted from unity and the final result multiplied by r_n.

Thus if in a digital computation a "running score" is kept of the terms within the square brackets, this may be updated each time by a simple multiplier. Three or four more simple arithmetic operations would then allow derivation of the next value of unconditional probability. In this special case the derivation of final firing probability from recovered probability estimates would seem to be quite an economic proposition in terms of computing time.

11 A FINAL REVIEW

This final survey is intended to serve as a reference to the main material, ideas and conclusions of the foregoing sections of this work.

In the introductory section, the recent trend of developments in the study of signal processing in the peripheral auditory system was outlined, and the importance of binaural listening as an experimental technique was emphasised. The particular problem of the subjective effects of interaural amplitude difference (IAD) in binaural listening was suggested to be of great interest, not only because of the effects themselves, but also because the understanding of them was seen to reflect importantly on the coding of signal amplitude at the periphery, and therefore presumably also on the details of the mechanical-neural transduction in the cochlea.

A brief review of cochlea anatomy and physiology followed in section 2. Necessarily restricted in scope, this section concentrated on those aspects of the cochlea likely to be most relevant to a study of its main transducer action. For this reason, much of the section was concerned with recent evidence on the junction between hair cells and afferent nerve endings in the cochlea, and with the complex pattern of cochlear innervation. Finally the important evidence on firing patterns of individual fibres in the cat's auditory nerve in response to simple acoustic stimuli, as recently reported by Kiang [37], was reviewed.

Section 3 opened with a brief review of binaural hearing phenomena, paying particular attention to the

previous papers by Sayers and Toole [52,53,62,63], in which these authors discussed the relationships between peripheral auditory system activity and perceptual effects in binaural headphone listening. Attention was then focussed on the largely unsolved problems relating to the effects of IAD in such conditions, and in particular to the so-called ITD/IAD trading phenomenon, whereby, within certain ranges of the experimental parameters, perceived lateral shifts in a binaural image caused by ITD may be offset by the introduction of IAD. Some new listening experiments were then reported which are believed to clarify the extent of this trading relationship between ITD and IAD, relevant to the dominant image of impulsive character which is perceived most easily by subjects when presented with binaural repetitive low-pass-filtered transients. The characteristics and extent of the ITD/IAD trading of this image suggested a proposition, then put forward, which seeks to explain the main subjective effects in terms of peripheral neural activity. It was then shown that, if the details of neural activity measured by Kiang [37] in single fibres of the cat's auditory nerve (in response to transient stimuli) are relevant to the human listening situation, the proposition would receive powerful quantitative support from such physiological data. Some further listening experiments were then reported which produced results consistent with the proposition.

The view that the main effects of IAD in binaural listening may be correlated with the details of activity in the acoustic nerve, suggested a careful study of the mechanical-neural transduction process in the cochlea. For,

although there are striking parallels between presumed basilar membrane vibrations and firing patterns in acoustic nerve fibres (at least in the case of relatively simple acoustic signals), there are also important details which cannot be explained on the basis of existing models of the cochlea transducer. Before beginning such a study, however, previous models of the peripheral auditory system were reviewed in section 4. Particular attention was paid to the work of Weiss [67], whose digital computer model has reproduced some of the main aspects of neural responses in the acoustic nerve. It was pointed out, however, that none of these existing models takes any detailed account of the complex pattern of cochlear innervation, whereas this pattern seems almost certainly of great significance in the neural coding of auditory stimuli.

The view that details of cochlear neural responses are not only critical for the understanding of the cochlear transducer, but are also closely implicated in certain aspects of aural perception, suggested that all available clues to the underlying mechanisms should be carefully explored. One possibly important clue is the statistical data on spontaneous firings in auditory nerve fibres, which have been reported in some detail by Kiang. A stochastic threshold model of spontaneous activity in such fibres, most simply interpreted as representing an assumed random liberation of a chemical transmitter substance across an afferent cochlear synapse (i.e. hair cell - nerve ending junction), was investigated in detail in section 5. Also described was a parallel theoretical analysis of such a system by Johannesma [32], who has done much to clarify the

effects of the various input parameters on the statistics of the output (spike) sequence. Satisfactory agreement was reported between aspects of this analysis and digital computer simulations. The results of such simulations suggested that the details of spontaneous activity in first-order auditory neurons could not be accounted for by a simple stochastic threshold model of this type, and a proposition based upon a point process superposition effect was then put forward and discussed. It was argued that if an auditory nerve fibre terminates on a number of hair cells, and random spikes are generated at each termination by (say) spontaneous liberation of a chemical transmitter, then the effective superposition of these independent point sequences could account for the statistics of the spontaneous activity observed in fibres of the acoustic nerve. Some further digital computer simulations indicated that somewhere between 4 and 10 terminations per nerve fibre would be required, if the physiological data was to be paralleled. Because multiple terminations of afferent fibres only apparently occur in the outer hair cell rows, this proposition seemed to apply only to spiral afferent fibres; however, at this stage the relative roles of the various fibre groups in the cochlea were not further considered.

The remainder of the work was devoted to the study of stimulated activity in cochlear nerve fibres, and in particular to their response to transient stimuli. Section 6 described the calculation (by digital computer) of basilar membrane displacement patterns in response to any given acoustic stimulus, using as data the physiological

measurements of basilar membrane frequency response by von Bekesy [1]. Calculated membrane response patterns for stimuli of particular interest were then presented. Finally, possible signal processing by spiral afferent cochlear fibres was investigated by computer operations on basilar membrane response waveforms, treating the fibre as a cable (having delay-line and attenuation properties) which puts out terminations (or sampling points) to the basilar membrane at various points. The results of this approach suggested that the possibility of any substantial signal processing by such fibre connections was small, and that - perhaps more importantly in the present context - there were apparently no explanations for those details of cochlear neural responses which are proposed to be of such significance in the coding of signal amplitude.

In section 7, an attempt was made to explain these important details of the peripheral neural response on the basis of possible electrical transmission effects at the afferent cochlear synapse, (the evidence for chemical transmission being by no means conclusive). Although the difficulties of a quantitative discussion of an unknown system are very great, the documented electrical properties of synapse, and nerve (as described by Hodgkin and Huxley [28]), were investigated and extended to a discussion of the single afferent cochlear synapse. In spite of the grave assumptions implicit in such an approach, some apparently fundamental objections to such a scheme were discovered. Firstly, the time course of the mechanisms in the hair cell and nerve ending would have to be very different from those measured experimentally in other systems. But, more important,

considerable systematic variations in the electrical properties of hair cell and nerve along the cochlear partition would seem to be required for the successful simulation of the neural recordings of Kiang.

Possible chemical transmitter models for the realistic simulation of Kiang's data were next explored, in section 8. Stochastic threshold systems having non-stationary inputs (representing in this case the stimulated release of a chemical transmitter substance across an afferent cochlear synapse) have so far not been investigated theoretically, and clearly involve problems of great analytical complexity. Digital computer simulations were therefore used to investigate possible effects in a chemical transmitter system - including postsynaptic integration and effects due to assumed neural refractory properties. Once again, the results indicated that the measured data of Kiang were unlikely to be paralleled by such a model. Firstly, the evidence from other chemical synaptic systems suggested that unlikely assumptions (concerning the variations in rate of release of chemical transmitter in response to a stimulus) were needed in order to simulate realistic neural responses. Also, extremely restricted ranges of model parameters were implied, if model responses quite unlike those of Kiang were to be avoided. And once again, a systematic variation in the properties of the postulated chemical synapse along the length of the cochlea seemed to be required, whereas there is no known physiological evidence for such assumptions.

Such difficulties suggested that a radically different approach was required if Kiang's measurements were to be realistically simulated in all their important details.

So far, attempts had been made to explain such details on the basis of the likely properties of the afferent hair cell - nerve ending junction, but in section 9 a new proposition based upon the complex pattern of cochlear innervation was presented. This proposal is believed to differ radically from existing hypotheses about the roles of the various hair cell rows and nerve fibre groups in the cochlea. It postulates a "control" waveform, generated by the passage along a spiral fibre of electrical activity originating in outer hair cells, which has a major controlling effect on spike activity in radial afferent fibres (which terminate on the inner hair cell row). In other words, activity in such radial fibres is modulated by a signal of relatively great dynamic range which arrives along spiral fibres; the site of such modulating action was conveniently thought of as the region below the inner hair cells, or perhaps closer to the spiral ganglion. It was argued that this concept of the relative functions of outer and inner hair cells, and of the various fibre groups, allowed the neural data of Kiang to be readily simulated. The severe restrictions on the values of the model parameters, which had been found necessary in the models of sections 7 and 8, were no longer required, and quite simple assumptions were adequate to explain the dependence of the effects of interest on the cochlear region innervated by a particular nerve fibre. These arguments were illustrated by further digital computer simulations, showing that realistic results could be generated by such a model, and that the effects of intensity paralleled convincingly those seen in actual neural recordings.

Section 10 contained a reappraisal of certain aspects of earlier sections. It was suggested that the earlier proposal which sought to explain observed spontaneous activity of cochlear fibres on the basis of a superposition effect due to multiple innervation, had now to be modified. This seemed necessary in view of the proposition of section 9 about a controlling action by outer hair cells and spiral fibres on radial afferent fibre activity; a corollary of this later proposition must be that the activity measured in single fibres in the acoustic nerve is that of radial afferents, which are believed to innervate few (and perhaps only one) hair cell in the inner row. However, an alternative scheme was suggested which would also be expected to cause an effective superposition effect; and it was argued that the results of section 5, whether or not they represented a detailed explanation of spontaneous activity in the cochlea, were valuable in showing the type of models which could account for such activity. The next part of section 10 discussed ITD/IAD trading ratios in binaural listening, and attempted to correlate the results of the present study with those of other workers. In particular, it was argued that the dominant impulsive image perceived by a subject when presented with binaural repetitive low-pass-filtered transients (and which seems to be the image mainly involved in the subjective phenomenon of time-intensity trading) arises by virtue of medial or apical cochlear activity, and is due to the transients in an acoustic signal; other workers have generally considered this image to arise in the basal cochlea. Finally, the implications of the proposed functions of the various hair cell rows and fibre groups

were considered in more detail, a preliminary attempt being made to formulate an algorithm for the prediction of single fibre activity in response to more complex signals (such as speech sounds).

In conclusion, it is believed that this study, by paying close attention to the details of published data on cochlear neural activity, has suggested a new and plausible explanation for the major effects of IAD in binaural listening, and has thereby helped to clarify the nature of amplitude coding in the peripheral auditory system. A detailed investigation of possible neural transducer mechanisms in the cochlea has indicated that there are considerable difficulties in considering that the fine details of acoustic nerve firing patterns are due to mechanisms operating in the single afferent synapse (between hair cell and nerve ending). On the other hand, the complex pattern of cochlear innervation (which has been largely ignored in previous models of the peripheral auditory system) is believed to provide the basis for relatively simple and attractive explanations for the neural responses to simple auditory stimuli, obtained from single fibres in the cat's auditory nerve. If future work supports such explanations, they seem certain to have important implications for the basic understanding of cochlear function.

APPENDIX A. MOMENTS AND CUMULANTS OF A DISTRIBUTION

Visual methods are often used to assess the shape of a curve or distribution, or to compare distributions obtained by direct measurement (e.g. neural interval histograms) with those produced by, say, digital computer models of the real physical system. For example, a plot on semilogarithmic paper of a typical interval distribution of spontaneous activity in a first-order auditory neuron in cat shows the distribution to be more or less exponential, with a dead time due to neural refractory effects. Visual assessments of this type are rather subjective, and lead to the use of such phrases as "approximately exponential", or "having a tail faster (or slower) than exponential", in the literature. Although, in many cases, it may not be easy to fit a particular distribution by a simple analytic function, there would be advantages in using more objective measures. Such measures should allow more accurate assessment of the differences between electrophysiological records and the results of model simulations.

Johannesma[32] has reviewed various alternative ways of describing the shape of a distribution, such as by its moments or cumulants, or by orthogonal polynomials; he has also listed their various properties. In the present work, emphasis is put on the description of interval distributions by their cumulants, which can be simply calculated during a digital computer simulation, and which are directly involved in Johannesma's theoretical analysis of stationary neural activity (see Section 5.3.1). Since cumulants are not widely known, some of their properties are now listed:-

(a) The cumulants (K_n) are simply related to the moments (M_n) of a distribution.

Thus:-

$$K_1 = M_1 = \text{mean}$$

$$K_2 = M_2 - M_1^2 = \text{variance}$$

$$K_3 = M_3 - 3M_1M_2 + 2M_1^3 = \text{third central moment}$$

$$K_4 = M_4 - 3M_2^2 - 4M_1M_3 + 12M_1^2M_2 - 6M_1^4$$

etc.

(b) The cumulants are also simply related to the coefficients of a power series expansion of the logarithm of the characteristic function $P(x)$ of the distribution. Thus:-

$$\log_e P(x) = \sum_{n=1}^{\infty} K_n \cdot \frac{(-x)^n}{n!}$$

(c) They are also related to the coefficients of expansions of the distribution in terms of orthogonal polynomials.

(d) Cumulants play a fundamental role in the description of the filtered Poisson process (shot noise).

(e) Unbiased estimators are available for obtaining the values of cumulants from experimental results.

(f) The importance of the n^{th} cumulant, in the description of a physical process, in general decreases as n increases. It seems that, in practice, the first 4 or 5 cumulants can give a rather good description of a probability distribution of fairly simple shape (e.g. unimodal, with smooth extremities.)

The first 3 cumulants are thus identical to the first three central moments; higher order cumulants are related to, but not identical with, higher order moments. Because it is often useful to compare the shapes of two distributions

without regard to their scale, cumulants of order >2 are sometimes normalised by the second cumulant (i.e. variance) to yield the so-called γ coefficients. Thus:-

$$\frac{K_3}{(K_2)^{3/2}} = \gamma_1 = \text{coefficient of asymmetry}$$

$$\frac{K_4}{(K_2)^2} = \gamma_2 = \text{coefficient of excess}$$

etc.

It is interesting to assess values of the cumulants and coefficients of well-known distributions. For example, consider the exponential distribution, which represents the interval distribution of a Poisson process:-

$$p(t) = \lambda e^{-\lambda t}$$

the characteristic function $P(x)$ is given by:-

$$P(x) = \int_o^\infty \lambda . e^{-\lambda t} . e^{-xt} . dt = \frac{\lambda}{x+\lambda}$$

the cumulants may be derived by expanding the logarithm of $P(x)$ in powers of x:-

$$\log_e P(x) = \log_e \left(\frac{\lambda}{x+\lambda}\right) = -\log \left({}^{x}/_{\lambda} + 1\right)$$

$$= -\left[{}^{x}/_{\lambda} - \frac{1}{2}\left(\frac{x}{\lambda}\right)^2 + \frac{1}{3}\left(\frac{x}{\lambda}\right)^3 - \ldots\right] = \sum_{n=1}^{\infty} \frac{(-x)^n}{n!} . K_n$$

equating powers of x yields:-

$$K_1 = {}^{1}/_{\lambda} = \text{mean}; \quad K_2 = \frac{1}{\lambda^2} = \text{variance}; \quad K_3 = \frac{2}{\lambda^3}; \quad K_4 = \frac{6}{\lambda^4}$$

etc.

and $\gamma_1 = 2$; $\gamma_2 = 6$; $\gamma_3 = 24$ etc.

In the case of a Gaussian distribution, the probability density function is of the form:-

$$p(t) = \frac{1}{\sigma\sqrt{2\pi}} \cdot e^{-\frac{(t-m)^2}{2\sigma^2}}$$

and the characteristic function may be shown to be:-

$$P(x) = e^{(-mx + \frac{\sigma^2 x^2}{2})}$$

$$\therefore \log_e P(x) = -mx + \frac{\sigma^2 x^2}{2}$$

giving $K_1 = m$ = mean; $K_2 = \sigma^2$ = variance.

All higher order cumulants, and all γ coefficients, are zero, regardless of the mean or variance of the distribution.

Such results give some insight into the description of the shape of a distribution by its γ coefficients. The higher order coefficients pay increasing attention to the tails of a distribution, with odd-order coefficients also reflecting lack of symmetry. In any practical situation (either a computer simulation or a physical measurement) sampling errors in the tails of a histogram will tend to make estimates of higher order cumulants and γ coefficients increasingly unreliable. The Gaussian distribution is in a sense the "reference" for such measures of simple unimodal distributions; for example, the Poisson distribution, having $\gamma_1 = 2$ and $\gamma_2 = 6$, is both more asymmetrical and more long-tailed than the Gaussian, when both are normalised by their respective variances.

It would indeed be valuable if future accounts of the recordings of stationary neural activity were accompanied by estimates of, say, the cumulants of any distributions. This would enable more meaningful comparisons to be made between such results and those of digital computer models.

BIBLIOGRAPHY

1. BÉKÉSY, G.von. 1960. Experiments in hearing (McGraw Hill)

2. BÉKÉSY, G.von. 1966. Pressure and shearing forces as Stimuli of labyrinthine epithelium. Arch. Otolaryngol. 84, p.122

3. BREDBERG, G., ENGSTROM, H., ADES, H.W. 1965. Cellular pattern and nerve supply of the human organ of Corti. Arch. Otolaryngol. 82, p.462

4. BULLOCK, T.H., HORRIDGE, G.A. 1965. Structure and function in the nervous systems of invertebrates: Vol. 1 (Freeman)

5. COX, D.R., SMITH, W.L. 1954. On the superposition of renewal processes. Biometrika. 41, p.91

5A. DAVID, E.E., GUTTMAN, N., VAN BERGEIJK, W.A. 1959. Binaural interaction of high frequency stimuli. J. Acoust.Soc.Amer. 31, p.774

5B. DEATHERAGE, B.H., HIRSH, I.J. 1959. Auditory localisation of clicks. J.Acoust.Soc.Amer. 31, p.486

6. DODGE, F.A., RAHAMIMOFF, R. 1967. Co-operative action of calcium ions in transmitter release at the neuro-muscular junction. J.Physiol. 193, p.419

7. DOHLMAN, G.F. 1960. in: Neural mechanisms of the auditory and vestibular systems. Editor G. Rasmussen (Charles Thomas)

8. ECCLES, J.C. 1964. Physiology of synapses (Springer)

9. ENGSTROM, H. 1960. in: Neural mechanisms of the auditory and vestibular systems. Editor G. Rasmussen (Charles Thomas)

10. ENGSTROM, H., ADES, H.W., HAWKINS, J.E. 1962. Structure and functions of the sensory hairs of the inner ear. J.Acoust.Soc.Amer. 34, p.1356

11. ENGSTROM, H., ADES, H.W., ANDERSSON, A. 1966. Structural pattern of the organ of Corti (Almqvist

11. (continued)

and Wiksell)

12. ENGSTROM, H., ADES, H.W., BREDBERG, G. 1966. Cyto-architecture of the mammalian organ of Corti. Internat.Audiol. (Leyden) 5, p.86

13. ENGSTROM, H. 1967. The morphology of the normal sensory cells. Acta Otolaryngologica (Appendix to Feb.-Mar.)

14. FETZ, E.E., GERSTEIN, G.L. 1963. An RC model for spontaneous activity of single neurons. M.I.T. Q.P.R. No. 71, p.249

15. FLANAGAN, J.L. 1960. Models for approximating basilar membrane displacement. Bell System Tech.J. 39, p.1163

16. FLANAGAN, J.L. 1962. Models for approximating basilar membrane displacement. Part II. Bell System Tech.J. 41, p.959

17. FLANAGAN, J.L. 1965. Speech analysis, synthesis and perception (Springer)

18. FLOCK, A., KIMURA, R., LUNDQUIST, P., WERSALL, J. 1962. Morphological basis of directional sensitivity of the outer hair cells in the organ of Corti. J.Acoust.Soc. Amer. 34, p.1351

19. FURSHPAN, E.J., POTTER, D.D. 1959. Transmission at the giant motor synapse of the crayfish. J.Physiol. 145, p.289

20. FURUKAWA, T., ISHII, Y. 1967. Effects of static bending of sensory hairs on sound reception in the goldfish. Jap.J.Physiol. 17, p.572

21. GEISLER, C.D., GOLDBERG, J.M. 1966. A stochastic model of the repetitive activity of neurons. Biophys.J. 6, p.53

22. GEISLER, C.D. 1968. A model of the peripheral auditory system responding to low frequency tones. Biophys.J. 8, p.1

23. GENTLEMAN, W.M., SANDE, G. 1966. Fast Fourier transforms - for fun and profit. Proc.Fall Joint Computer Conf. p.563

24. GERSTEIN, G.L., MANDELBROT, B. 1964. Random walk models for the spike activity of a single neuron. Biophys.J. 4, p.41

25. GRAY, P.R. 1966. A statistical analysis of electrophysiological data from auditory nerve fibers in cat. M.I.T. (R.L.E.) Tech.Rep.No.451

25A. HAFTER, E.R., JEFFRESS, L.A. 1968. Two-image lateralisation of tones and clicks. J.Acoust.Soc.Amer. 44, p.563

26. HALL, J.L. 1964. Binaural interaction in the accessory superior olivary nucleus of the cat - an electrophysiological study of single neurons. M.I.T. (R.L.E.) Tech.Rep.No.416

27. HARMAN, L.D., LEWIS, E.R. 1966. Neural modelling. Physiol. Reviews 46, p.515

28. HODGKIN, A.L., HUXLEY, A.F. 1952. A quantitative description of membrane current and its application to conduction and excitation in nerve. J.Physiol. 117, p.500

29. HUBBARD, J.I., JONES, S.F., LANDAU, E.M. 1968. On the mechanism by which calcium and magnesium affect the release of transmitter by nerve impulses. J.Physiol. 196, p.75

30. ISHII, T., MURAKAMI, Y., BALOGH, K. 1967. Acetylcholinesterase activity in the efferent nerve fibres of the human inner ear. Ann.Otol.Rhinol.Laryngol. 76, p.69

31. JENIK, F. 1962. Pulse processing by neuron models. Proceedings of the Ojai symposium. Editor R.F. Reiss (Stanford)

32. JOHANNESMA, P.I. 1967. Diffusion models for the stochastic activity of neurons. Presented at International School on neuronic networks, Ravello, June 1967.

33. KATZ, B. 1966. Nerve, muscle and synapse (McGraw Hill)

34. KATZ, B., MILEDI, R. 1967. A study of synaptic transmission in the absence of nerve impulses. J.Physiol. 192, p.407

35. KATZ, B., MILEDI, R. 1968. The role of calcium in neuromuscular facilitation. J.Physiol. 195, p.481

36. KATZ, B. 1962. The transmission of impulses from nerve to muscle and the subcellular unit of synaptic action. Proc.Roy.Soc. B. 155, p.455

37. KIANG, N.Y-S. 1965. Discharge patterns of single fibers in the cat's auditory nerve. M.I.T. Research monograph No. 35

38. KLETZKY, E.J., FRAIOLI, A.J. 1967. An electronic neuron model for sensory system studies. Proc.Int.Electronics Conf., Toronto.

39. LEWIS, E.R. 1965. Neuroelectric potentials derived from an extended version of the Hodgkin-Huxley model. J.Theoret.Biol. 10, p.125

40. LEWIS, E.R. 1962. An electronic model of the neuron based on the dynamics of potassium and sodium ion fluxes. Proceedings of the Ojai Symposium. Editor R.F. Reiss (Stanford)

41. MALLART, A., MARTIN, A.R. 1967. An analysis of facilitation of transmitter release at the neuromuscular junction of the frog. J.Physiol. 193, p. 679

42. MARTIN, A.R. 1966. Quantal nature of synaptic transmission. Physiol. Reviews 46, p.57

43. MOUNIER-KUHN, P., HAGUENAUER, J.P. 1966. Variations de l'activité cholinesterasique dans les cellules ciliées de l'organe de Corti après exposition à des sons de fréquence basse ou elevée. Acta Otolaryngologica. 63, p.297

43A. MOUSHEGIAN, G., RUPERT, A.L., LANGFORD, T.L. 1967. Stimulus coding by medial superior olivary neurons. J.Neurophysiol. 30, p.1239

44. NASTUK, W.L. 1963. Physical techniques in biological research. Vol. VI (Academic Press)

45. NOBLE, D. 1966. Application of Hodgkin-Huxley equations to excitable tissues. Physiol.Reviews. 46, p.1

46. PERKEL, D.H., GERSTEIN, G.L., MOORE, G.P. 1967. Neuronal spike trains and stochastic point processes. Biophys.J. 7, p.391

47. PFEIFFER, R.R., KIANG, N.Y-S. 1965. Spike discharge patterns of spontaneous and continuously stimulated activity in the cochlear nucleus of anaesthetised cats. Biophys.J. 5, p.301

48. RALL, W. 1962. Theoretical significance of dendritic trees for neuronal input-output relations. Proceedings of Ojai Symposium. Editor R.F. Reiss (Stanford)

49. ROBERTS, T.D.M. 1966. Basic ideas in neurophysiology (Butterworth)

50. ROBERTSON, J.D., BODENHEIMER, T.F., STAGE, D.E. 1963. The ultrastructure of Mauthner cell synapses and nodes in goldfish brains. J.Cell Biol. 19, p.159

51. RUCH, T.C., FULTON, J.F. 1960. Medical physiology and biophysics (Saunders)

51A. SAYERS, B.McA., LYNN, P.A. 1968. Interaural amplitude effects in binaural hearing. J.Acoust.Soc.Amer. 44, p. 973

52. SAYERS, B.McA., TOOLE, F.E. 1964. Acoustic image lateralisation judgements with pure tones. J.Acoust. Soc.Amer. 36, p.923

53. SAYERS, B.McA., TOOLE, F.E. 1964. Acoustic image lateralisation judgements with binaural transients. J.Acoust.Soc.Amer. 36, p.1199

54. SAYERS, B.McA. 1965. Physical aspects of auditory perception. First Internat.Cong. on Med.Physics, Harrogate p.83 (Taylor and Francis)

54A. SHAXBY, J.H., GAGE, F.H. 1932. MRC Special Report, Serial No. 166, p.1

55. SIEBERT, W.M., GRAY, P.R. 1963. Random process model for the firing pattern of single auditory neurons. M.I.T. Q.P.R. No. 71 p.241

56. SOLODOVNIKOV, V. 1960. Statistical dynamics of linear automatic control systems (Van Nostrand)

57. SPOENDLIN, H.H., GACEK, R.R. 1963. Electronmicroscopic study of the efferent and afferent innervation of the organ of Corti in cat. Ann.Otol.Rhinol.Laryngol. 72, p.660

58. SPOENDLIN, H.H. 1967. The innervation of the organ of Corti. J.Laryngol.Otol. 81, p.733

59. STEIN, R.B. 1965. A theoretical model of neuronal variability. Biophys.J. 5, p.173

60. TASAKI, I., DAVIS, H., ELDREDGE, D.H. 1954. Explorations of cochlear potentials in guinea pig with a microelectrode. J.Acoust.Soc.Amer. 26, p.765

61. TEN HOOPEN, M., REUVER, H.A. 1966. The superposition of random sequences of events. Biometrika 53, p.383

62. TOOLE, F.E., SAYERS, B.McA. 1965. Lateralisation judgements and the nature of binaural acoustic images. J.Acoust.Soc.Amer. 37, p.319

63. TOOLE, F.E., SAYERS, B.McA. 1965. Inferences of neural activity associated with binaural acoustic images. J.Acoust.Soc. Amer. 38, p.769

64. TRINCKER, D. 1962. The transformation of mechanical stimulus into nervous excitation by the labyrinthine receptors. Symp.Soc.Exper.Biol. 16, p.289

65. VAN BERGEIJK, W.A. 1961. Studies with artificial neurons II: analog of the external spiral innervation of the cochlea. Kybernetik 1, p.102

66. WEI, L.Y. 1968. Electric dipole theory of chemical synaptic transmission. Biophys.J. 8, p.396

67. WEISS, T.F. 1964. A model for firing patterns of auditory nerve fibers. M.I.T. (R.L.E.) Tech.Rep. No. 418

68. WEVER, E.G. 1949. Theory of hearing (Wiley)

69. WEVER, E.G. 1966. Electrical potentials of the cochlea. Physiol. Reviews 46, p.102

70. WHITFIELD, I.C., ROSS, H.F. 1965. Cochlea microphonic and summating potentials and the output of individual hair cell generators. J.Acoust.Soc.Amer. 38, p.126

71. WHITFIELD, I.C. 1967. The auditory pathway (Arnold)

71A. WHITWORTH, R.H., JEFFRESS, L.A. 1961. Time versus Intensity in the localisation of tones. J.Acoust. Soc.Amer. 33, p.925

72. WOLKEN, J.J. 1956. A molecular morphology of Euglena Gracilis var. bacillaris. J.Protozool. 3, p.211